

QC
918
B29N9+

Cornell University Library	
THE GIFT OF	
Carnegie Institution of	
Washington	
ENGINEERING LIBRARY	
A.201826	23/3/06

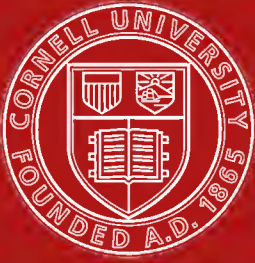
Cornell University Library
QC 918.B29N9

The nucleation of the uncontaminated atm



3 1924 004 124 925

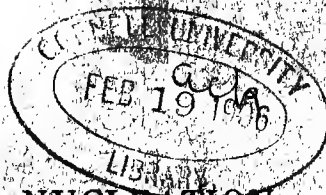
engr



Cornell University Library

The original of this book is in
the Cornell University Library.

There are no known copyright restrictions in
the United States on the use of the text.



THE NUCLEATION OF THE UNCONTAMINATED ATMOSPHERE

BY CARL BARUS

Hazard Professor of Physics, Brown University



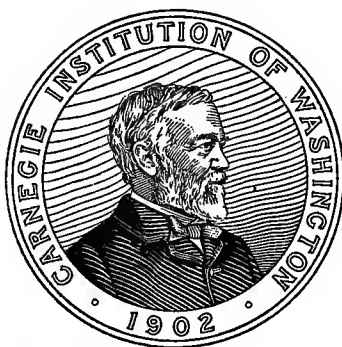
WASHINGTON, D. C.:

Published by the Carnegie Institution of Washington

January, 1906.

THE NUCLEATION OF THE UNCONTAMINATED ATMOSPHERE

BY CARL BARUS
Hazard Professor of Physics, Brown University



WASHINGTON, D. C.:
Published by the Carnegie Institution of Washington
January, 1906.

T 6 T

CARNEGIE INSTITUTION OF WASHINGTON
PUBLICATION NO. 40

FROM THE PRESS OF
THE HENRY E. WILKENS PRINTING CO.
WASHINGTON, D. C.

PREFACE.

The object primarily in view when the present experiments were begun was a continuous record of the nucleation of the atmosphere in a locality relatively free from the habitations of man, and therefore free from nucleations of local and artificial origin. In other words, it was to be determined whether below the fog-limit of dust-free air, *i. e.*, below the least exhaustion at which filtered air condenses without foreign nuclei, the atmosphere contains any nucleation whatever beyond that introduced from terrestrial sources and coming chiefly from the originally ionized products of combustion. An investigation of this kind seemed well worth while, after it had been shown¹ that the nucleation of the atmosphere, even above cities, obeys certain clear-cut laws, showing a marked tendency to reach an enormously developed and sharp maximum in December and a flat but very low minimum in June. The former at least does not in general coincide with the period of maximum cold, and the possibility that some effect from without was superimposed on the local effect seemed sufficiently probable to warrant special inquiry. This was carried out as detailed in Chapters IV and V of the present memoir, in two series of observations, made with similar apparatus, simultaneously at Providence and at Block Island. The two stations, lying about 70 kilometers apart, pass through practically the same meteorological variations of wind and weather; while Block Island, surrounded by a body of water whose smallest radius is nearly 20 kilometers from the center of the island, while one-half of it fronts the ocean, is in the winter at least nearly free from local effect. Leaving the detailed discussion of the results to the chapters specified, it is noteworthy that the average monthly nucleations at both points of observation show the same law of change, though the actual fluctuation at Providence is naturally less salient. The data found at each station prove that the tendency to pass through maxima in December, observed at Providence in 1902-03 and 1903-04, has again unmistakably asserted itself. In addition to this, however, the observations at both stations developed a new and surprisingly pronounced maximum in February as the chief feature in the nucleations of the last winter. Predominating in each of the series of results over the earlier maximum, and holding

¹ Barus : Smithsonian Contributions, Vol. XXXIV, 1905.

for *different* bodies of air, the February maximum at least can not be of local origin; and it is thus in a measure probable that the December maximum also is due to non-local causes. But whether these are the aggregated effects of remote terrestrial sources, or whether they represent an actual invasion of the atmosphere on the part of some cosmic agency, remains to be seen.

The air to be treated in the present series of experiments is, therefore, continually approaching a state of purity so far as foreign admixtures are concerned. Hence the properties of dust-free air, or in practice of filtered air, became increasingly important. It may be proved by aid of the inclosed steam-jet¹ that even dust-free air must be an aggregate of nuclei, whose number grows rapidly larger as their diameter decreases, with a maximum for molecular dimensions; or that size is distributed among the molecules and quasi-molecules of dust-free air in a way somewhat recalling the distribution of velocity among molecules, and that among particles larger and smaller the air molecule represents a condition of maximum occurrence. The fog-limit of dust-free air is thus a variable quantity, depending eventually on the details of the method of filtration, or other process for rendering the air dust-free. In fact, as the fog-limit rises, the coronas for a given exhaustion above the fog-limit increase in aperture, up to a limit. It should always be remembered that the particles or nuclei here in question are very small, even in comparison with ions.

With the object of meeting the state of things in question, systematically, the data in Chapters I, II, and III were investigated, while Chapter VI contains a summary of the work as a whole. The method employed is believed to be a new departure, inasmuch as all results are expressed in terms of the number of nuclei observed per cubic centimeter, so that the nucleations produced are the criteria throughout. To offer conditions sufficiently varied for the experimental work, the nucleation of dust-free air is in these chapters *coarsened* by ionizing it, either by the X-rays or by a weak sample of radium acting through a sealed tube. It thus appears that the ions or fleeting nuclei resulting are also pronouncedly of all sizes within limits and that the increment of nucleation between two definite degrees of exhaustion (*i. e.*, degrees of sudden cooling) above the fog-limit but not too far from it, is greater as the radiation applied from without is more intense. Virtually the gradation of particles is thus more fine-grained or more nearly continuous with the efficient nuclei lying within closer limits of size, as the ionization is more intense.

¹Barus: Bulletin U. S. Weather Bureau, No. 12, 1895

Throughout the whole research the important bearing of the solutional or water nucleus¹ on the phenomena of condensation is manifest. If the nucleus is soluble in water, vapor pressure decreases with the continued evaporation of the fog particle, until the decrement of vapor pressure due to increased concentration of the solution is equal to the increment due to increased curvature. The result is a persistent solutional nucleus (water nucleus), necessarily larger than the original nucleus of solute. A great variety of puzzling phenomena like the alternations of efficient nuclei in successive otherwise identical exhaustions, the persistence of fleeting nuclei or ions on solution, the lowered fog-limit of an evaporated corona, etc., thus find a satisfactory explanation.

The final general result to be referred to here is the readiness with which nuclei are produced by the gamma-rays, even after penetrating a centimeter or more of lead, together with the distinction which is thus drawn, experimentally, between these rays and the X-rays. The latter show small penetration, but are so phenomenally active in producing secondary radiation that to a wooden fog-chamber the distance effect for a radius of over six meters between bulb and fog-chamber is relatively negligible. The effect of the gamma-rays, on the contrary, in spite of the remarkable penetration evidenced, for instance, by the nucleation produced, is nearly vanishing when tested by the same nucleation at a distance of but 50 centimeters. Again, within the fog-chamber the distribution of nuclei along the axis is in both cases uniform for all distances (50 cm.) within the range of observation, except when the X-radiation is sufficiently intense to produce persistent nuclei. In this case the curiously pronounced distribution detailed in Chapter I is observed, which seems to show either that the nucleation originates in the walls of the vessel or that, in consequence of secondary radiation, the density of ionization near the walls is such as to promote rapid growth of nuclei in those parts to abnormal sizes. The nuclei in question are over 200 times more persistent than the ions, and if they decay by breaking into like fragments one may estimate that the former are 5 or 6 times larger in diameter than the latter. Persistent nuclei produced by the X-rays require, in fact, but a vanishing pressure difference to induce condensation. They have, moreover, the property of increasing in number if left without interference for a short time after radiation ceases.

In view of the interest which thus attaches to dust-free or filtered air, the nuclear systems of which are throughout small as compared with

¹ Barus : Structure of the nucleus, Smithsonian Contributions, No. 1373, 1903.

the much coarser ions, and show rapidly increasing numbers with decreasing size until the molecular dimensions are reached or even surpassed in degrees of smallness, I have undertaken and have now in progress, under the auspices of the Carnegie Institution of Washington, a systematic research on the properties of filtered air. The fact that the nucleation responds to very penetrating rays, like the gamma-rays of radium, adds additional interest to the inquiry.

In conclusion, it gives me pleasure to acknowledge my indebtedness to Mr. Robinson Pierce, jr., for the efficiency and patience with which he conducted the measurements of nucleation at Block Island, placed in his charge under the very trying mid-winter conditions there encountered. His results are given in Chapter IV. I am further indebted to Miss Lillie L. Scholfield, by whose skill in drawing and experience in editorial work I have materially profited.

My thanks are due finally to the Chief of the U. S. Weather Bureau, for his kindness in placing suitable quarters for observation in the Weather Bureau Building at Block Island at our disposal, and to Mr. Day, the officer in charge of the station, for many courtesies throughout the work.

CARL BARUS.

BROWN UNIVERSITY, *Providence, R. I., July, 1905.*

CONTENTS.

CHAPTER I.—*Results with an Objective Method of Showing Distributions of Nuclei Produced by the X-rays or Other Radiation.*

	PAGE
1. Introductory	I
2. Apparatus	I
3. Vertical radiation at one end of the trough, entering through wood....	2
4. Axial radiation entering one end of the trough.....	3
5. The same continued for larger pressure differences.....	4
6. Condensation of dust-free moist air in the absence of X-ray nuclei. Fog limit	4
7. Possibility of producing nuclei by sudden intense exhaustion.....	5
8. Successively increasing times of exposure to X-radiation.....	6
9. Symmetrically graded sizes or numbers of fog particles.....	7
10. Possible origin of nuclei at the walls of the receiver.....	9
11. Absorption of ions at the walls of the receiver.....	10
12. Summary	10
13. Tentative experiments with lead screens, inside and outside the fog chamber	11
14. The same continued, with change of apparatus.....	13
15. Conclusion	16

CHAPTER II.—*Numbers and Gradations of Size of the Efficient Nuclei in Dust-Free Air, Energized or not by X-Ray or Other Radiation.*

EXPERIMENTS WITH DUST-FREE AIR NOT ADDITIONALLY ENERGIZED.

16. Apparatus	17
17. Manipulation. Fog limit.....	18
18. Alternations of large and small coronas (periodicity).....	18
19. Effect of lapse of time on the nucleation of dust-free air imprisoned in the fog chamber.....	21
20. Effect of pressure difference on exhaustion.....	22
21. Remarks on the tables.....	25
22. Blurred coronas.....	27
23. Time effect.....	27
24. Oscillations at variable pressure differences.....	27
25. Nucleations at varying pressure differences.....	27
26. Fog limits.....	28
27. Oscillations at fixed pressure differences.....	29
28. Undersaturation	29
29. Undersaturation continued.....	30
30. Nucleation	31

EXPERIMENTS WITH DUST-FREE AIR ENERGIZED BY RADIUM.

31. Effect of radium in hermetically sealed glass tube.....	32
32. Remarks on the tables.....	35
33. Data for nucleation.....	36
34. Fog limits raised by weaker ionization.....	37

	PAGE
35. Nucleation	38
36. Radium in sealed aluminum tube.....	39

EXPERIMENTS WITH DUST-FREE AIR ENERGIZED BY THE X-RAYS.

37. Persistence of nuclei due to X-rays in the lapse of time.....	41
38. Fog limits for nuclei produced by X-rays.....	42
39. Sudden exhaustion in the absence of condensation.....	43
40. X-ray nuclei at different high pressure differences.....	45

CHAPTER III.—*Critical Conditions in the Formation of Ions and of Nuclei.*

41. Apparatus. X-ray bulbs.....	47
42. Fog chambers. Filters with saturator.....	48
43. Notation	49

EFFECT OF LARGE PRESSURE DIFFERENCES.

44. Nuclei in dust-free air, not energized.....	49
45. Dust-free air energized by the X-rays from a distance.....	51
46. The same continued. Rays not cut off during condensation.....	53

GENERATION AND DECAY OF NUCLEI.

47. Fleeting nuclei.....	54
48. Persistent nuclei.....	57
49. Persistence of fleeting nuclei after solution.....	60
50. Enlargement of nuclei in dust-free non-energized air.....	62
51. Occurrence of water nuclei.....	63
52. Cause of periodicity.....	64
53. Rain	64
54. Persistent nuclei in general.....	65
55. Graduation of size of fleeting nuclei. Fog limits.....	66
56. Secondary generation.....	69

NUCLEATION DUE TO RAYS PENETRATING FROM A DISTANCE OR THROUGH DENSE MEDIA.

57. Effect of distance of the X-ray bulb from the free wooden fog chamber.	71
58. Generation and decay for radiation from $D = 200$ cm.....	73
59. Electrical effect for different distances.....	75
60. Apparent penetration of the X-rays coming from 600 cm.....	75
61. Apparent penetration of the X-rays coming from 200 cm. and from 6 to 7 cm.....	78
62. Generation through lead plate and through iron.....	79

FOG CHAMBERS INCLOSED IN CASKETS.

63. Wood fog chamber in lead casket. Penetration.....	80
64. The same continued. Radiation from a distance.....	81
65. Glass fog chamber. Radiation from a distance.....	84
66. Radiation from a distance. Glass fog chamber in lead case.....	84

CONTENTS.

IX

NUCLEATION DUE TO GAMMA RAYS.

	PAGE
67. Lead-cased wood fog chamber. Penetration.....	85
68. The same continued.....	85
69. The same continued. Effect of distance.....	87
70. Glass fog chamber. Penetration.....	88
71. The same continued. Radiation from a distance.....	89
72. Distribution of nucleation along the axis, within the fog chamber.....	90
73. General remarks.....	90

CHAPTER IV.—*The Nucleation of the Atmosphere at Block Island, by Robinson Pierce, Jr.*

74. Introductory.....	91
75. Apparatus.....	91
76. Observations.....	101
77. Remarks on the tables. Wood fog chamber.....	101
78. Continued. Brass fog chamber.....	102
79. Summary and comparisons.....	103
80. Tentative inferences.....	107
81. Average daily nucleations at Block Island.....	109
82. Average monthly nucleations at Block Island.....	110

CHAPTER V.—*The Contemporaneous Nucleations of the Atmosphere at Providence and at Block Island.*

83. Introductory.....	111
84. Observations.....	111
85. Comparison of the data for Providence and for Block Island.....	120
86. Average daily nucleations.....	127
87. Average monthly nucleations.....	128
88. Conclusion.....	130

CHAPTER VI.—*Summary and Conclusions.*

89. Introductory.....	132
90. Notation.....	133
91. Fleeting nuclei. Ions.....	133
92. Fog limits of fleeting nuclei.....	134
93. Persistent nuclei.....	135
94. Fleeting nuclei become persistent on solution. Origin of Rain.....	137
95. Solutional enlargement of the nuclei of dust-free air.....	138
96. Water nuclei. Solutional nuclei in general.....	140
97. Alterations of large and small coronas. Periodic distributions of efficient nuclei in dust-free air.....	141
98. Cause of periodicity.....	141
99. Persistence in general.....	141
100. Secondary generation.....	141
101. Space surrounding the X-ray tube a plenum of radiations.....	142
102. Lead-cased fog chamber.....	143
103. Possibility of two kinds of radiation from the X-ray tube.....	145

	PAGE
104. Nucleation due to gamma-rays.....	145
105. Distribution of nucleation within the fog chamber. Radium.....	146
106. The same continued. X-rays.....	146
107. Origin of persistent X-ray nuclei.....	147
108. Order of size of persistent X-ray nuclei.....	148
109. Ordinary nuclei.....	149
110. Ordinary dust-free air an aggregate of nuclei.....	149
111. Nucleation of filtered air.....	150
112. Nucleation of atmospheric air not filtered. Dust contents at Providence.....	151
113. The same continued. Dust contents of atmosphere at Providence and Block Island compared.....	152

LIST OF ILLUSTRATIONS.

	PAGE
FIG. 1. Fog chamber with appurtenances and X-ray bulb, X.....	2
2-6. Diagram of a succession of distorted coronas.....	7
7. Computed curves.....	8
8-10. Forms of lead screens.....	11
11-12. Fog chambers with screens and X-ray bulb.....	14
13. Fog chamber with axial and oblique radiation.....	15
14-18. Graphs showing the alternations of the apertures (s) of corona in non-energized dust-free air.....	21
19. Decay of the nuclei examined in the lapse of hours.....	21
20-25. Change of apertures (s) of coronas and number of efficient nuclei (n) varying with the different pressure differences for the cases of superior and inferior coronas.....	26
26. Number of efficient nuclei (n) obtained in successive exhaus- tions of dust-free air energized by radium.....	34
27-30. Change of aperture (s) of coronas and nucleations (n) vary- ing with the pressure differences in cases of dust-free air energized or not by radium (in sealed glass).....	34
31-32. Decay of the nuclei produced by radium after the removal of the tube from the fog chamber.....	34
33-34. Apertures of coronas (s) and nucleations (n) varying with the pressure differences, for the case of dust-free air energized by radium acting from different distances.....	36
35-37. Decay curves found after the removal of the radium from the fog chamber.....	36
38-39. Apertures (s) and nucleations (n) varying with the pressure differences for the case of persistent nuclei produced in dust- free air by the X-rays.....	43
40. Filter with wet sponge tube (saturator).....	48
41. Rectangular wood fog chamber.....	48
42. Cylindrical glass fog chamber.....	48
43. Rectangular fog chamber.....	49
44. Cylindrical fog chamber.....	49
45-51. Illustrating Tables 29, 32, 33, 34, 35, 36.....	51
52-55. Illustrating Tables 30, 31.....	54
56-62. Illustrating Tables 37, 38.....	62
63-68. Illustrating Tables 39, 40, 41.....	65
69-78. Illustrating Tables 43, 44, 45, 49, 50, 53, 54.....	73
79-82. Illustrating Table 47.....	76
83-87. Illustrating Tables 47, 51, 53, 54.....	82
88-90. Illustrating Table 56.....	88

	PAGE
FIG. 91-92. Graphs showing the current nucleations.....	104, 105
93. Chart showing the average daily nucleations at Block Island, in hundreds per cubic centimeter, from December to May, 1904-05.....	106
94. Location of the stations at Providence and at Block Island..	106
95-101. Daily record of the nucleations of Providence and of Block Island in thousands of nuclei per cubic centimeter from November, 1904, to May, 1905.....	120-125
102. Average daily nucleations in thousands per cubic centimeter at Providence and at Block Island from November, 1904, to May, 1905.....	127
103. Average monthly nucleations at Providence and at Block Island, in thousands per cubic centimeter, from October, 1902, to May, 1905.....	128
104. Average monthly nucleations from November, 1904 to May, 1905, at Providence in ten thousands per cubic centimeter, and at Block Island in thousands per cubic centimeter, showing the probable run of the curves in the absence of the February maximum and the coincidence of the maxima and the minima.....	129

CHAPTER I.

RESULTS WITH AN OBJECTIVE METHOD OF SHOWING DISTRIBUTIONS OF NUCLEI PRODUCED BY X-RAYS, FOR INSTANCE.*

1. Introductory.—By passing the X-rays into one end of a long rectangular (virtually tubular) condensation chamber and observing the effect produced after successive different intervals of time by the condensation method, evidence, with a possible bearing on the origin of these nuclei, was obtained. The coronas are distorted and at first occur on the bulb side of the apparatus only. The distribution of nuclei is inferred from the form of the corona.

The experiments described were all made with strictly dust-free air, as both the method of precipitation and of filtration were applied prior to each experiment. Furthermore, as the exhaustions necessitated the use of short lengths of rubber tubing ($\frac{1}{2}$, $\frac{3}{4}$, and 1 inch in bore in the different cases), the amount of sudden cooling obtained does not directly correspond with the pressure difference, δp , owing to the resistance of the tube to the flow of air. The data, δp , thus refer to a given type of apparatus, but they are satisfactory as relations, so long as this is not changed. Furthermore, the pressure difference was so adjusted as to entrap all X-ray nuclei, to the exclusion of the normal, quasi-molecular nuclei of dust-free air, or at least of such nuclei for which a packed-cotton filter is no barrier.

2. Apparatus.—The method was purposely reduced to extreme simplicity, and the apparatus is shown in figure 1. *AB* is the long rectangular condensation chamber of wood impregnated with resinous cement. The front and rear faces are plate glass, through which the coronas may be observed. The other sides are lined within with thick cotton cloth, kept wet, and there is a layer of water at the bottom to insure complete saturation of air. *C* is a stopcock leading to an efficient filter (not shown). Supersaturation is produced by sudden exhaustion at the *B* end of the apparatus, while the *A* end receives the radiation from the X-ray bulb, *X*. A large vacuum chamber was placed in connection with the exhaust pipe shown, through a wide stopcock, the details of which need not be explained. The X-rays used were not very penetrating, and were obtained from a soft bulb actuated by

* Much of the experimental part of this chapter was carried out by Mr. Robinson Pierce, jr., and myself, conjointly.

a small induction coil (4" spark) and 3 to 5 storage cells. Two filters of solidly packed cotton were used, one 7 inches and the other 16 inches long. They were about equally efficient.

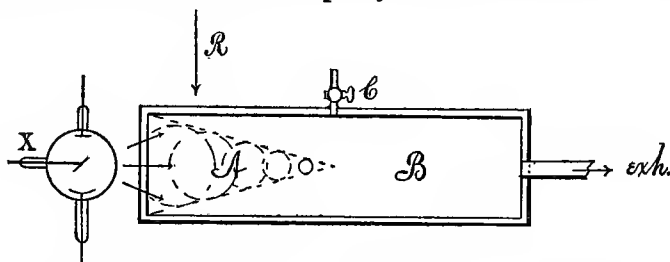


FIG. 1.—Fog chamber, *AB*, with appurtenances and X-ray bulb, *X*.

3. Vertical radiation at one end of the trough, entering through wood.—In the preliminary experiments the bulb was placed so as to radiate into the trough in the position shown at *R*, and kept in action 5 minutes. The effect was then observed by condensation at the pressure difference, $\delta p = 17$ cm., much below the fog limit of dust-free air (section 6). Two results were noted: In the first place, while the coronas obtained with the X-rays in bulky apparatus are usually of the smaller or normal type, the coronas seen in this shallow apparatus were often enormous, transcending the middle green-blue-purple corona (nucleation, $n = 100,000$ per cubic centimeter). Even after two or three subsequent exhaustions, filtered air being added prior to each, large coronas were still in evidence. In the second place, the coronas, and hence the nuclei, were observed chiefly on the *A* side of the apparatus, under the bulb. Fearing that there might be some direct effect due to induced high potentials, the X-ray bulb was raised 10 and 20 cm. above the trough, with results naturally smaller in magnitude, but of the same kind. The following data may be given:

TABLE 1.—Number of nuclei, n , in thousands per cm.³. $\delta p = 17$ cm. Temperature about 20° . Angular aperture $\phi = s/30$.

Time of radiation.....	Bulb near trough (2 cm.).						Bulb 10 cm. above trough.				Bulb 20 cm. above trough.	
	5 min.		5 min.		5 min.		6 min.		5 min.		6 min.	
Coronas on—	<i>s</i>	<i>n</i>	<i>s</i>	<i>n</i>	<i>s</i>	<i>n</i>	<i>s</i>	<i>n</i>	<i>s</i>	<i>n</i>	<i>s</i>	<i>n</i>
First exhaustion.....	(*)	(*)	(*)	3.9	20.5	3.5	15	2.7	6.6
Second exhaustion.....	5.9	68	6.5	100	2.7	6.6	2.7	6.6	1.9	2.2
Third exhaustion.....	5.9	68

* Immense, but too diffuse for measurement.

In all cases the first coronas were accompanied by dense rain and fogs, frequently in horizontal strata, so that sharp measurements of

aperture are generally out of the question. Moreover, the first condensation is accompanied by turbulent displacement of fog particles and the contents of the receiver are thoroughly stirred up. After filling with filtered air and exhausting again, the coronas are therefore nearly uniform and alike on both sides. In the above table the nucleation produced decreases about as the inverse square of distance, but as the bulb is essentially variable in intensity such a result is not trustworthy.

4. Axial radiation entering one end of trough.—Seeing that it is possible to retain the nuclei on one side of the trough, subsequent experiments were conducted with the X-ray bulb placed as shown at *X* in the figure. Moreover, a smaller interval of radiation was selected to more and more fully exclude the displacement of nuclei by diffusion. The angular diameters (about $s/30$) of the coronas were measured with two goniometers, one on each side (A and B) of the trough, the distance of the coronal centers from the bulb being about 20 cm. and 47 cm., respectively. The following table summarizes the results obtained, remembering that all initial coronas are coarse and blurred and accompanied by copious rain and fog, so that the diameters must be estimated :

TABLE 2.—Number of nuclei in thousands per cm.³. $\delta\phi = 17$ cm.; angular diameter, $\phi = s/30$.

Time of radiation.	Corona on first exhaustion.				Corona on second exhaustion.			
	A side.		B side.		A side.		B side.	
	<i>s</i>	<i>n</i>	<i>s</i>	<i>n</i>	<i>s</i>	<i>n</i>	<i>s</i>	<i>n</i>
2.5 minutes.....	4.5	32	2.2	3.3
3.5 minutes.....	4.5	32	2.2	3.3	3.2	11	3.0	9.3
2 minutes.....	4.0	22	2.0	2.5
2 minutes.....	2.5	5.2	0	0

The second coronas are obtained after refilling with filtered air, and it is noteworthy that after the rains of the foggy first coronas fall out (which they do rapidly), there are abundant nuclei left for the next corona. As stated, the nuclei are now uniformly distributed and the coronas persistent, while in the first exhaustion, apparently, certain larger particles captured all the moisture and removed it in a rainy precipitate. The smaller particles are therefore evaporated into water nuclei (as will be shown below), while the initial temperature of the fog chamber is being rapidly regained.

It is to be observed, moreover, that the nucleations on the A and the B sides in these cases are on the average as 9:1, or in a larger ratio,

while the ratio of distances is below 1:2, because the absorption of the wood is equivalent to a removal of the bulb; hence the density of distribution falls off faster than the inverse cube. The contrast is even greater, because in the 2 or 3 minutes of radiation some nucleation must arrive on the B side by convection and diffusion.

We were originally of the opinion that there is marked absorption of the nucleating power of X-rays, by the successive vertical layers of air from left to right, but it is best not to prejudice the case here.

5. Continued for larger pressure differences.—Several questions now present themselves for immediate decision; viz, whether all the X-ray nuclei have been caught and in how far the exhaustions are below the point of spontaneous condensation of moist air. Accordingly larger pressure differences were applied. Table 3 gives a few examples.

TABLE 3.—Nucleations, n , in thousands per cm.³. Time of exposure to X-rays, 3.5 minutes. Angular aperture $\phi = s/30$.

$\delta p =$	17 ^{cm}		21 ^{cm}		31 ^{cm}	
Side	A	B	A	B	A	B
$s =$	4.6	1.8	3.9	2.1	2.8	2.5
$10^{-3}n =$	35	1.9	27	3.5	11	7.8
Ratio	18:1		7.7:1		1.4:1	

Hence above $\delta p = 21$ cm. for this apparatus, nuclei show themselves on both sides, and the question arises to what extent the normal air nuclei (of dust-free air) have been captured. At $\delta p = 31$ cm. the fog particles condensed on X-ray nuclei probably drop out at once and the persistent corona observed is precipitated on the normal air nuclei stated. At all events, the gradual evanescence of the X-ray effect as δp increases is noteworthy.

6. Condensation dust-free of moist air in the absence of X-ray nuclei—Fog limit.—With the object of finding the pressure difference of exhaustion, δp , corresponding to the lower limit of spontaneous condensation of moist air without foreign nuclei, experiments were first tried with a cock $\frac{3}{4}$ inch in bore, in the exhaustion tube. The results were identical on the A and the B sides, as follows:

TABLE 4.—Spontaneous condensation in saturated air. Angular aperture $\phi = s/30$.

$\delta p =$	24 ^{cm}	31 ^{cm}
$s =$	2.2	2.7
Repeated, $s =$	2.4	3.2
“ $s =$	2.1	—
Do., large filter, $s =$	2.2	3.5
Do. $s =$	1.9	—
Air over night, $s =$	2.0	—
Mean, $\left\{ \begin{array}{l} s = \\ n = \end{array} \right.$	2.1	3.1
	3,500	15,500
	$\delta p_0 = 22^{\text{cm}}, n = 0$	

This indicates that at a pressure difference of about $\delta p_0 = 22$ cm. for the given apparatus and dust-free moist air, spontaneous condensation with vanishing coronas begins on sudden cooling and that thereafter the coronas increase regularly. This pressure, δp_0 , will be usually referred to as the "fog limit."

In corroboration with the preceding, similar experiments were tried with an instantaneous valve, opened with a hammer, and having a clear bore of over 1 inch. The results shown in table 5 were identical on both sides, but unexpectedly irregular, the only explanation for which might seem attributable to a possibly unequal degree of suddenness in opening the valve. But this is not the case; for alternations of large and small coronas in dust-free air, such as are here imperfectly shown, may be kept up indefinitely if strictly identical conditions are retained. Effectively, the large fog particles emit more nuclei, the smaller fewer nuclei for the next condensation in order, everything else remaining the same. The importance of these oscillations about the mean aperture, whether the emission is ionized or not, can not be called in question, as I shall show in Chapter II.

TABLE 5.—Spontaneous condensation of saturated air. Angular diameter $\phi = s/30$.

Press. diff., $\delta p =$		19 ^{cm}	19.4 ^{cm}	21.4 ^{cm}	24 ^{cm}
Repeated,	$s =$	2.3	3.4	3.3	4.4
	$s =$	0	2.1	2.0	2.5
	$s =$	0	0	3.0	4.3
	$s =$	0	0	2.0	3.5
	$s =$	—	0	3.5	3.3
	$s =$	—	—	2.2	3.3
Mean,	$s =$	0	0	2.7	3.6
	$n =$	0	0	7,600	21,000
		$\delta p_0 < 20^{\text{cm}}, n = 0$			

For $\delta p = 19.4$ and below, therefore, no nuclei appeared after thorough cleaning. For $\delta p = 20$ cm. and above, *i. e.*, at a somewhat lower pressure difference than before in consequence of more rapid exhaustion, spontaneous condensation begins. The large coronas are blurred. Hence in neither case will air nuclei be caught at $\delta p = 17$ cm., in the given apparatus.

7. Possibility of producing nuclei by sudden intense exhaustion.*—The condensation of the moist air in the absence of foreign nuclei may be considered as due to the spontaneous nucleation of the air, the available nuclei increasing in abundance as with increasing pressure

* Investigations on the spontaneous condensation of moist air were first suggested by myself, in Bull. U. S. Weather Bureau, No. 12, 1893, pp. 13 and 48. They have since been fully treated in the masterly work of C. T. R. Wilson, Trans. Royal Soc. Lond., vol. 189, pp. 265, 307, 1897; *ibid.*, vol. 192, pp. 403-453, 1899.

differences the sizes of captured nuclei are smaller, until the air molecule itself is approached. It follows, then, that normal dust-free air always contains unstable systems.

Hence the question may well be asked whether very sudden and intense exhaustion may not itself possibly be productive of nuclei. Thus, if an unstable molecular configuration is just about to break down, it is conceivable that the tendency to break down is accentuated by the violent treatment in question.

We made some experiments on this subject, by looking for the presence of ionization under these conditions, using a pressure difference, $\delta p > 30$ cm., by placing a gold-leaf electrometer, properly insulated, in the condensation chamber. The loss of charge in damp air is at first surprisingly small; nevertheless the experiments are very difficult and we were unable to come to a conclusion.

8. Successively increasing times of exposure to X-radiation.—After this digression, experiments were resumed with the apparatus, as shown in figure 1. The pressure difference, $\delta p = 17$ cm., was used throughout, as this is well within the lower limit of spontaneous condensation for the given receiver, while coronas may be obtained with X-ray nuclei for pressure differences even lower than $\delta p = 10$ cm. Such coronas are vague, however, until the rain nuclei are thrown out, and on second exhaustion ($n = 39,000$, $s = 4.8$ were usual values after 4 minutes of exposure to the radiation) they are naturally faint.

The immediate incentive to the work of the present section was given by the occurrence of elliptic distortions of coronas, as shown in the following tables:

TABLE 6.—Distorted coronas, Increasing times of exposure to X-rays. $\delta p = 17$ cm. Coronal center 19 cm. (A side) and 46 cm. (B side) from bulb. Angular aperture $\phi = s/30$.

Time, Side,	2 min.	
	A	B
First exhaustion,	$s = 4.5$, elliptic, strong.	1.0? faint, circular.
Second exhaustion,	$s = 2.7$, circular.	2.4 circular.
First exhaustion,	$s = 4.6$, elliptic, strong.	0.0
First exhaustion,	$s = 4.6$, elliptic, strong.	0.0

TABLE 7.—Preceding table continued.

Time, Side,	1 min.		2 min.		3 min.	
	A	B	A	B	A	B
$s =$	3.1, round, strong.	0	4.1, elliptic, strong.	0	5.8, ellipse, larger and distorted.	0

On second exhaustion, after refilling with filtered air, the coronas were nearly identical on both sides.

A series of observations was now systematically carried out, unfortunately with somewhat weaker radiation. After 1, 2, and 3 minutes of exposure, respectively, the coronas on the A side were round to roundish (*cf.* figs. 2 and 3), of gradually increasing strength and density, and with rainy precipitation and fog usually marked. There was nothing on the B side even after 6 minutes of exposure. After 4 minutes (*cf.* fig. 4), the corona became spindle-shaped, $s=5.4$ cm. in major axis, accompanied by rain from horizontal layers of fog.



FIGS. 2-6.—A succession of distorted coronas.

After 6 minutes of exposure to the X-rays, the coronas underwent remarkable distortion, becoming gourd-shaped (fig. 5), often with a long, serpentine neck dipping into the B side of the condensation chamber. The length of figure on the goniometer was about 6.8 cm., the outline being orange and the field within greenish. Rain and fog abounded. The coronas on second exhaustion (after adding filtered air) were green-blue-purple, $s=4.9$, $n=42,000$, and white-red-green, $s=4.5$, $n=32,000$, on the A and B sides, respectively. The experiment was repeated, with like results.

After 8 and 11 minutes of exposure, both the A and the B sides became the seat of the now wedge-shaped corona (*cf.* fig. 6), greenish within and orange in outline. There was much rain and fog.

Figures 2-6 are seen immediately after the exhaustion. A moment later there is a storm-like disturbance in the condensation chamber, accompanied by rain and fog. Hence the distribution of nuclei found on exhaustion is incompatible with a persistent distribution of fog particles. In fact, the first coronas usually fall out rapidly, showing the occurrence chiefly of large fog particles in spite of the corona. The second coronas are circular and persistent, whence a nearly uniform distribution of nuclei may be inferred.

9. Symmetrically graded sizes or numbers of fog particles.—Since the coronas obtained all show an unmistakable tendency to horizontal symmetry with reference to the longitudinal axis of the condensation chamber, the nuclei to which the coronas are due must either originate in, or else be absorbed by, the top and bottom of the apparatus. Nuclei originating or lost at the front and rear faces are nearly uniformly distributed normal to the line of sight and produce circular

coronas. Nuclei originating or lost at the left-hand end of the chamber will additionally distort the corona, and such distortion is clearly in evidence, apart from the one-sided position of the coronas.

Mere inspection of the coronas (figs. 2-6) shows that they are larger for fog particles near the axis, and smaller for particles near the top and bottom of the condensation chamber. Hence it is next necessary to explain that the details of the distorted coronas observed actually correspond with a gradation of the number of *effective* or available nuclei, from the axis outward on all sides. In the case of linearly graded fog particles increasing in diameter, δ , from bottom to top, it appears that the equation of the apertures, s , of the loci* of like color of the corona is

$$s = -\frac{\delta_0}{a \sin \phi} \left(1 - \sqrt{1 + \frac{2 a s_0 \sin \phi}{\delta_0}} \right),$$

where s_0 is the aperture for the particles of diameter, δ_0 , in the horizon or plane of sight, and δ the angle in polar coordinates between the radius vector to the part of the corona in question and the horizontal, the origin being at the center of the corona. Finally $\delta = \delta_0 - ah$. Such coronas when the gradation becomes marked are *campanulate* in outline, finally becoming basin-shaped.

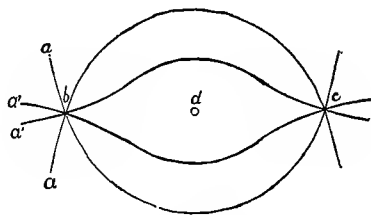


FIG. 7.—Computed curves.

In the present case, however, there are two symmetrical distributions of this kind, *i. e.*, increasing diameters of fog particles from the axis of the chamber toward the top and the bottom. Hence pairs of intersecting curves, two examples of which are given in figure 7 ($a' > a$), show the coronas to be anticipated, if the remote parts beyond b and c of the corona are ignored and only the stronger curves surrounding the spot of light, d , admitted. In other words,

* Barus: Am. Journ. Sci. (4), XIII, p. 309, 1902.

as the distance, b c , varying with the number of axial nuclei and the distribution constant, a , increases, all the figures, 2, 3, 4, 5, 6, may be logically evolved.

On the left-end face, moreover, there would be special interference with the distribution of nuclei giving rise to the corresponding distortion seen in the coronas. Further distortion due to the decrease from left to right of the intensity of the radiation must also be apparent, and the gradient of distribution will be slightly altered by diffusion. One may note that if anything issues from the walls of the vessel, it comes as abundantly out of the water below as out of the wet cloth above.

10. Possible origin of nuclei at walls of receiver.—As has already been suggested, the observed gradation of fog particles may result from the (real or virtual) evolution of effective nuclei at the top and the bottom of the apparatus, in consequence of the impact of X-rays on those parts. There is much electric evidence against such an explanation; nevertheless it is worth a brief examination, particularly as it includes the effect of secondary radiation to be discussed below (Chapter III).

The enormous coronas which have been obtained with the above (shallow) apparatus, as compared with the small coronas seen in the cases of more bulky apparatus, is in keeping with this view. Again, the rapid decrease of the nucleating power of the X-rays might to some extent be associated with the increasing obliquity of the rays, but no evidence of this was found.

The observed distortion of coronas is clearly due to a gradation of nuclei, either as to size or number, or both. If efficient nuclei issue from the top and bottom, they must be present in greatest number near those parts of the apparatus, and consequently the largest diameter of coronas should apparently be found there. But if the largest number of effective nuclei is present near the top and bottom, the tendency to growth by cohesion will also be most marked in those regions. Hence, with this admission, the largest nuclei must be looked for nearest the top and bottom, while the gradation in size decreases regularly toward the axis. The large nuclei, therefore, may be sufficiently numerous near the walls to capture all the available moisture on condensation, leaving the small nuclei without a load of water and unable to appreciably descend. Hence the marked rain effect, the rapidity with which the first coronas usually drop out, the turbulent motion which succeeds condensation, the occurrence of large persistent coronas

on second exhaustion even after the first coronas have quite dropped out, etc., are all in a measure accounted for.

Finally, one may note that secondary radiation (the importance of which I at first underestimated) issuing from the top and the bottom of the condensation chamber would accentuate the present effect, or even wholly replace it.

Thus it seems not unreasonable to infer that nuclei are produced by the impinging X-rays in much the same way in which they are produced by high temperature (ignition), or by high potential; and the question arises whether the nuclei thus put in evidence may not be associated with the electrons to which the cohesions between the molecules may be ascribed.

11. Absorption of ions at walls of receiver.—If the nuclei due to the ionization of air by the X-rays are absorbed at the walls of the receiver* a diffusion gradient will be established, resulting in a decreasing number of nuclei from the axis outward, a distribution the reverse of the preceding. The observed distortion will therefore here be due to a gradation in the numbers of nuclei.

One difficulty in the present instance seems at first sight to be fatal; for no reason is suggested why the coronas on second and third exhaustion do not eventually show flower-like distortion, which they never do. In other words, it is here tacitly assumed that only the nuclei in the nascent state, as it were, are appreciably diffusible, while the nucleus is relatively a fixture. It will be shown in Chapter III, however, that on second and third exhaustion all the nuclei have probably been converted into solutional water nuclei by evaporation, so that the difficulty in question is not serious.

12. Summary.—To decide between these hypotheses it is necessary to guide the X-rays by screens, suitably placed both on the inside and the outside of the apparatus; but these experiments will, in the succeeding chapters, lead to results much too diffuse and complicated in character to be summarized at present.

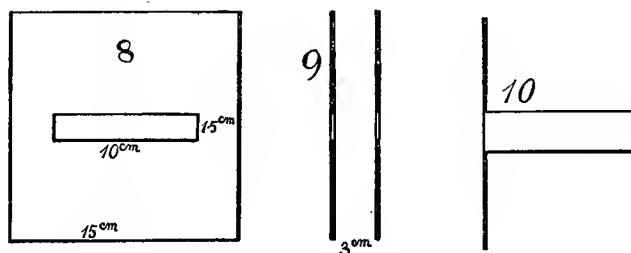
Here there is room only for a final remark. Whenever nucleation and ionization are associated as the outcome of any process (physical or chemical), the former is generated proportionally to the latter, in such a way that each is produced at its own rate depending on inci-

*A number of similar cases have been worked out in Smithsonian Contributions, No. 1309, 1901, "Experiments with ionized air;" and *ibid.*, No. 1373, Chapter V, 1903.

dental conditions. This is best worked out with water nuclei. The subsequent life-history of the nucleation and the ionization is distinct, nuclei, when produced by intense radiation as above, being surprisingly persistent, ions by contrast characteristically fleeting. Hence it seems to me to be best in keeping with all the data in hand to regard the nucleation as the product which owes its growth or origin to the expulsion of the corpuscles representing the concomitant ionization. Ignition and high potential nuclei, X-ray and radiation nuclei in general, phosphorus and water nuclei, produced throughout in strictly dust-free air, all admit of this account of their occurrence and properties. There is no observable case of a process producing ionization without nucleation, although there are many cases of nucleation free from ionization.

13. Tentative experiments with lead screens, inside and outside of the fog chamber.—These experiments were made in large number; but owing to the variability of the X-ray bulb and the action of the coil, as well as the difficulty of realizing truly geometric conditions with X-radiation, they are not satisfactorily conclusive. It will be seen in the following chapters that results like the present can not in any case be more than preliminary in character.

The screens were lead plates with holes cut in them, or lead tubes soldered to the edges of the holes normal to the plate. They were placed between the X-ray bulb and the A end of the fog chamber to guide the radiation.



FIGS. 8-10.—Forms of lead screens.

In case of the observations 1 to 6, the screen was in the shape of figure 8, with a horizontal slit 10 cm. long and 1.5 cm. wide, stretching nearly across the end of the fog chamber. Often screens of this kind were adjusted 2 to 3 cm. apart, as shown in figure 9. The screen was earthed and the bulb placed as near it as practicable.

12 NUCLEATION OF THE UNCONTAMINATED ATMOSPHERE.

TABLE 8.—Miscellaneous experiments, chiefly with screens. Long fog chamber, vol. 13,000 cm.³. δp usually 17–18 cm. Coil with 4 cells. Observations at middle of chamber, 29 cm. from end.

No.	Exposure.	Corona.	s.	Screen.	Remarks.
	<i>Min.</i>				
1	10	Round.....		Lead, with slit.....	Corona strong; clear.
2	5	do.....		do.....	Corona very small.
3	11	Oval?.....	3.6	do.....	Corona not sharp.
4	10	do.....	0.0	Same, doubled.....	No corona.
5	7	Oval.....	4.0	Screen removed.....	
6	10	Round.....	3.0	Double-slitted screen..	
7	14	0.0	Lead, with tube, 2.5 cm. diameter, 8 cm. long.	
8	7	Oval.....	6.1	Screen removed.....	On both A and B sides.
9	12	0.0	Lead, with tube (axial)	Corona just visible.
10	11	0.0	Do., tube directed to bottom.	
11	11	0.0	Tube axial.....	Just visible; forms gradually.
12	14	0.0	Do., bulb plate normal.	
13	13	Clear.....	(?)	Tube directed to glass.	Small corona.
14	10	Oval.....	5.0	Screen off.....	Large diffuse corona; strata.
15	20	Round.....	4.0	Lead, with tube, 3.5 cm. diameter, 4 cm. long.	Strong corona; larger in middle of apparatus.
16	11	do.....	3.0	do.....	Clear corona; little fog.
17	11	do.....	3.0	do.....	Clear corona, oval on A side.
18	10	0.0	do.....	Coil works badly.
19	10	(?)	do.....	Coil works badly (?).
20	10	Round.....	(?)	do.....	Corona just appears.
21	11	do.....	(?)	do.....	Small coronas throughout chamber.
Recent results,* with more powerful coil (6 cells) $\delta p = 16.7$.					
22	3	Distorted; fog and streamers.	A side full.....	Disk of lead 3 cm. in diameter over center.	Second corona— $s_2 = 3.4$.
23	5	Campanulate.....	do.....	do.....	$s_2 = 4.2$.
24	5	Streamers.....	do.....	do.....	$s_2 = \text{large}$.
25	5	Round.....	3.6	Hole (2.5 cm.) in lead plate.	$s_2 = 1.9$.
26	5	do.....	2.4	do.....	$s_2 = 1.1$.
27	3	Streamers†.....	A and B sides full.	Screen off.....	$s_2 = 5.9$.
		$\delta p =$	18.5	Six cells.....	$s_3 = 2.6$.
28	4	Fine oval.....	6.4	Lead tube axial.....	Corona on both sides.
29	4	Round.....	2.5	Lead tube at top.....	
30	4	Roundish.....	4.5	Lead tube axial.....	
31	4	Round.....	3.5	Lead tube at top.....	
32	4	Open on top....	1.6	Lead tube at bottom..	Corona horseshoe-shaped.
33	4	Roundish.....	3.0	Lead tube axial.....	
34	4	do.....	3.5	do.....	Coil improved.

* All lead screens earthed.

† Campanulate on B side.

Since the front and rear faces of the fog chamber can only contribute a distribution of nuclei corresponding to round coronas with the given line of sight, while the lead cuts off most of the efficient radiation from the top and bottom, round coronas should appear if the nuclei come out of the walls. This was, in fact, the case in the first and second experiments, where clear, round, strong coronas were observed; the third observation, however, leaves the question in doubt.

Similarly conflicting results were obtained with the screen (fig. 9), the radiation being weaker in view of the greater distance of the bulb from the fog chamber and the more efficient screening. With the lead plates removed, the usual phenomena (oval coronas) appear; but throughout, the contrast is not sharp enough for definite decision.

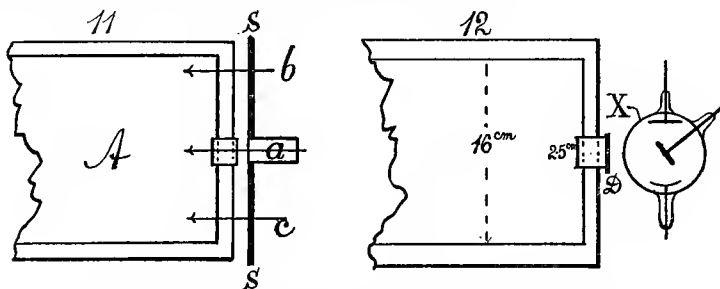
Long lead screens placed horizontally within the fog chamber opposite the slit in the external screen, as at *A* in figure 11, did not stop the radiation. Elliptic coronas were observed around the trace of the screen as a minor axis, precisely as if the internal screen were absent. Hence either diffusion or secondary radiation must be very active throughout the exposure.

In experiments 7 to 21 the lead screen, figure 10, was a broad flange on a lead tube, 2.5 cm. in diameter and 4 cm. or 8 cm. long. The X-radiation was usually directed axially, sometimes obliquely, against the walls. With the tube 8 cm. long measurable coronas were not obtained, no matter whether the rays passed axially through the fog chamber or not. In the absence of the lead screen, or when the lead screen was replaced by a thin continuous aluminum screen, the nuclei often filled the chamber on the *A* and the *B* sides and the coronas were large. This would again be accepted as evidence favoring the view that the nuclei come out of the walls; but when the radiation is directed against these walls through the tube there is no appreciable increment. Thus the experiments remain inconclusive.

The work was now continued by cutting down the tube to 4 cm. in length. The strong coronas obtained were clear and round, with very little fog. At times they seemed to be largest in the middle of the apparatus. Slight oval distortion appeared on the *A* side near the bulb only. The general absence of distortion when the impact of X-rays is cut off from the top and the bottom again is favorable to an origin of nuclei in those parts. Failure of the experiments 18 to 21 is attributable to the spark gap of the coil; but here coronas were often seen throughout the length of the fog chamber, very gradually decreasing in size from *A* to *B*. When the eye was moved rapidly in this direction, the coronas were found to lie within a triangle, symmetrical with respect to the axis of the fog chamber, and the diameter of the coronas vanishes at the apex of the triangle, near the middle of the chamber, as suggested in figure 1.

14. Continued, with change of apparatus.—In these experiments a more powerful coil was used, actuated by six storage cells and a Foucault interrupter. The object first aimed at was a contrast of the rays entering the fog chamber axially with the oblique rays which strike the walls. Accordingly, in experiments 22 to 24 the entrance

of radiation into the axial part of the end of the fog chamber is cut off by a lead disk, D , figure 12, about 2.5 cm. in diameter. In comparison with experiment 27, where the screen was removed, the coronal effect for the disk is somewhat weaker, but throughout of the same nature, with campanulate or spindle-shaped coronas filling more than half of the length. Much rain and fog were present, and crimson-colored streamers stretched horizontally and symmetrically, bow-shaped (convexity outward), from end to end. The first coronas (s_1) are not measurable, but, after the first fog particles have fallen out, the second (s_2) are quite so, being round and clear.



FIGS. 11-12.—Fog chambers with screens and X-ray bulb.

The disk was now removed and a lead screen, S , figure 11, with a hole about 2.5 cm. in diameter, placed over the end of the fog chamber, with the X-ray bulb placed as before. To make the wood more transparent a waxed cork was inserted, giving free entrance to the axial rays. All screens were earthed as usual. Experiments 25 and 26 show the results. The contrast with the preceding is marked. The coronas are round, and in the first exhaustion show apertures (s_1) decidedly smaller than the coronas obtained in the second exhaustions of the preceding cases. True, the amount of radiation entering the fog chamber is much larger for the case of the disk than for the case of the perforated screen; but it nevertheless follows that the axial rays, even if entering under favorable conditions, can not be specially efficient. Rays which have penetrated the fog chamber obliquely and impinge on the top and bottom are responsible for nearly the whole of the dense fog usually observed.

In further experiments, work with the flanged lead tube (2.5 cm. in diameter, 4 cm. long, figure 10, center of bulb 5 to 6 cm. from the end of the fog chamber and about 8 cm. from the inner face) was resumed and successively placed in positions, a (axial), t (radiation grazing the top surface), b (radiation grazing the surface of water below, as seen in figure 11), the screen being moved with the bulb. The experiments

28, 30, 33, and 34 are deficient from the gradual loss of strength of the X-ray bulb; but the data for s in the axial case are nevertheless larger than for the cases where the rays grazed the top or the bottom of the fog chamber. In the latter, the corona is particularly small and open on top, showing the absence of nuclei in the upper strata of the air of the fog chamber. Thus the endeavor to directly call out the nuclei from the top or the bottom of the fog chamber has again failed.

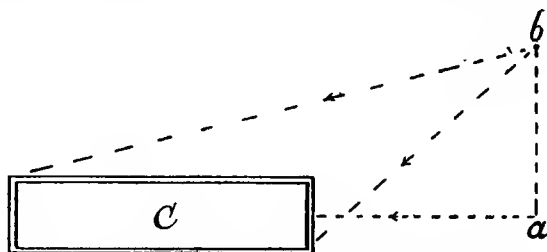


FIG. 13.—Fog chamber with axial and oblique radiation.

A final test on the effect of the walls was made in a somewhat different manner by placing the bulb at a distance of 80 cm. from the chamber C , figure 13, at first axially, as shown at a , and then in the raised position, b . In the first instance the rays pass through the least surface of wood and the incidence within is grazing; in the second (nonaxial), the rays pass through a much larger surface of wood and the incidence is at a large angle. Table 9 shows the results in the two cases to be identical, barring increased distance and the tendency of the bulb to lose efficiency in the lapse of time. In the present case, however, the nuclei are of the fleeting kind discussed in the chapters below, and comparison with the above persistent nuclei is not at once permissible.

TABLE 9.—Comparison of axial and oblique rays $\delta\phi = 23.3$ cm.

Position of bulb.	s .	Remarks.
Axial	3.6	Distance, 80 cm. from bulb to chamber (inside) axially. Raised position 35 cm. above axis. Rays off, $s = 0.0$ (fig. 13). Observations made during exposure to X-rays.
Raised	3.6	
Raised	3.5	
Axial	3.6	Distance, 40 cm.
Raised	* 5.3	
Axial	4.6	
Axial	† 4.0	Distance, † 80 cm. $\delta\phi = 24.8$ cm. Exposure, 3 min.
Raised 35 cm.	† 4.0	
Raised 55 cm.	† 3.8	
Raised 55 cm.	† 3.8	
Axial	3.9	

* Periodicity. Difference due to X-ray bulb.

† Air $s = 1.5$.

‡ $s_2 = 1.0$.

15. Conclusion.—Generally, when the bulb is close to the end of the chamber, the coronas obtained after a short exposure are all roundish, but taper from a large size near the bulb to the vanishing diameter or apex, figure 1, near the middle of the fog chamber, with all intermediate gradations of aperture in corresponding intermediate positions. The pressure difference, δp , applied is thus more and more in excess of the fog limit as the line of sight is nearer the bulb. Beyond the apex the pressure difference used is below the fog limit. Smaller nuclei occur throughout the chamber, but they are probably more and more fleeting in character. The colloidal nuclei of dust-free air are always present. The number of nuclei within the given range of condensation, *i. e.*, above a certain lower limit of diameter, increases with the intensity of the ionization, axially as well as transversely. If the exposure is prolonged and the radiation sufficiently intense, the nuclei are everywhere within the given pressure difference, but the axial excess of efficient nuclei is retained. Beyond this, the endeavor to come to a decision as to the origin of the persistent nuclei on the basis of the above experiments seems as yet premature; for in addition to the hypothesis which refers them to the impact of X-rays on the walls of the vessel, the diffusion hypothesis, the effect of secondary radiation within the vessel (such radiation outside of the vessel produces fleeting nuclei only as will be detailed in Chapter III), etc., there is something to be said in favor of the spontaneous production of water nuclei in the presence of the intense X-radiation arriving at any point from both primary and secondary sources.

CHAPTER II.

NUMBERS AND GRADATIONS OF SIZE OF NUCLEI IN DUST-FREE AIR.

EXPERIMENTS WITH DUST-FREE AIR NOT ADDITIONALLY ENERGIZED.

Alternations of large and small coronas observed in case of identical condensations produced in dust-free air saturated with moisture.

16. Apparatus.—By dust-free air I mean air which has been passed through a packed-cotton filter. My filters are 16 inches long, conical, tapering from about 2 inches in diameter at the large end to about $\frac{1}{2}$ inch at the other. They contain absorbent cotton rammed in from both ends and kept in place by wire. When filtered air is required, the stopcock is only just opened so that influx of dust-free air may be extremely slow.* This insures proper filtration and does not interfere with the saturation of the air in the fog chamber. In this section condensation was produced in a long glass cylinder, 16 inches from end to end and $5\frac{1}{2}$ inches in diameter, placed horizontally and normal to the line of sight. It contained a rectangular framework of copper wire covered with wet cotton cloth, except on the two opposed broadsides through which the coronas were observed. The distance between the bottom (water) and the roof of the rectangular framework was about 9 cm. The provisions for keeping the air saturated are thus ample.

The vacuum chamber was a large boiler of galvanized iron, having a capacity, V , of over 100,000 cc., while the capacity, v , of the condensation chamber is about 6,700 cc., so that the volume ratio, v/V , is but 0.063. The two chambers are connected by about a foot of rubber tubing over 1 inch in bore, usually containing a 1-inch plug gascock. An instantaneous clapper valve of the same dimensions and opened with a hammer was often used for comparison.

Later the glass fog chamber was advantageously replaced by one of waxed wood (see fig. 1, Chapter I), with the opposed sides, through which the coronas were observed, made of plate glass. The internal dimensions in this case were $55 \times 12 \times 20$ cc., and the volume ratio, v/V , in connection with the vacuum chamber, about 0.13. There is difficulty, however, in using a chamber of this kind for the present purposes, where even very small leakage is a serious discrepancy.

* When the rate of filtration is gradually decreased until it all but vanishes, results of special interest are observed which will be detailed elsewhere.

17. Manipulation—Fog limit.—The experiments were conducted as follows: Having selected a suitable pressure difference above that at which condensation in dust-free air just begins (usually termed the "fog limit" in the present paper), the dust-free moist air in the closed condensation chamber at atmospheric pressure is suddenly exhausted and the corona measured. After all fog has subsided the exhaustion cock is closed and the filtered air very slowly admitted. The operations are then repeated, allowing time (about 2 to 3 minutes) for saturation. Under all circumstances the treatment for large and small coronas was identical.

In the given apparatus condensation in dust-free moist air began at the pressure difference, $\delta p = 22.5$, corresponding to the volume expansion of about 1.43. The pressure difference usually applied in the experiments was $\delta p = 31.2$, and the volume expansion 1.72.

18. Alternations of large and small coronas (periodicity of inferior and superior coronas).—The small coronas are usually sharp, but the large coronas appear blurred and filmy, accompanied with much rain. Remembering that all operations are conducted in a way strictly the same, table 10 (pp. 19–20) shows the coronas seen in the successive exhaustions. The angular diameter or aperture is $\sin \phi/2 = s/60$, or nearly $\phi = s/30$. The eye at the goniometer was about 40 cm. from the axis of the condensation chamber (placed as close as possible to insure clearer vision) and the source of light 250 cm. beyond it. Observations were made along the axis of the cylinder, placed horizontally. The number of nuclei per cubic centimeter of the exhausted air will be denoted by n , while N shows the number per cubic centimeter of air at normal pressure. The reduction of n to N where it is not essential will often be omitted.

In the case of 2-minute periods between the exhaustions the periodicity is maintained without exception (fig. 14). For brevity let the smaller coronas be called *inferior*, the larger coronas *superior*. Frequently a very small inferior corona evokes a relatively large superior corona, or larger inferior coronas are followed by smaller superior coronas; but this is not always the case. As a more general rule, if the aperture is intermediate between the inferior and superior coronas, the succeeding corona is of the same size, and oscillation terminates. In part III, for an accidentally more rapid influx than the exceedingly slow influx of filtered air in the earlier parts of table 10, this is initially the case, but the oscillation is soon reestablished. In part IV, the water was shaken so as to wet the glass sides of the chamber, but without effect on the oscillation (fig. 15). In part V of table 10, the original periodicity is again wiped out by accidental influx of much air through

the filter. Periodicity thereafter fails to reappear, as is also the case in parts VI and VII. Similar cases occur in parts VIII, IX, and X. The mean apertures at 25° , 20° , and 11° do not differ sufficiently to indicate a temperature effect above the value of the incidental errors.

TABLE 10.—Periodicity in the condensation of dust-free air. Plug valve. Pressure difference, $\delta p = 31.2$ cm. Temperature = 25° C. Glass clear, no shaking of water needed. Two-minute periods between exhausts. Slow influx. Cylindrical fog chamber, volume ratio $v/V = 0.063$.

Exhaust No.	s.	$n \times 10^{-3}$.	Exhaust No.	s.	$n \times 10^{-3}$.	Exhaust No.	s.	$n \times 10^{-3}$.
Part I.			Part II—Continued.			Part III.		
1	*1.7	2.3	5	2.9	9	†21	3.9	59
2	5.7	73	6	6.4	97	22	3.8	58
3	2.5	6.1	7	3.0	10	23	3.1	47
4	6.4	97	8	6.6	106	24	5.8	88
5	2.9	9.6	9	3.1	11	25	3.1	47
6	6.6	106	10	6.4	97	26	5.2	79
7	3.2	12.6	11	3.2	12.6	27	3.1	47
8	12	6.6	106	28	6.3	96
	†2.9	9	13	3.2	12.6	29	3.4	52
Part II.			14	6.3	93	30	5.9	90
1	2.9	9	15	3.1	11			
2	6.2	90	16	6.6	106			
3	3.4	15	17	3.5	16.7			
4	5.3	59	18	5.5	67			
			19	3.0	10			
			20	6.9	122			

*After 16^h (left over night).

†After 25^m.

‡Accidental rapid influx. Note the rise of inferior coronas.

TABLE 10, continued.—Slow influx; water shaken; fog in glass; 20° C.; $\delta p = 31.2$.

Exhaust No.	s.	$n \times 10^{-3}$.	Exhaust No.	s.	$n \times 10^{-3}$.	Exhaust No.	s.	$n \times 10^{-3}$.
Part IV.			Part V.			Part VI.—Temperature, 11° C. $\delta p = 31.2$.		
*1	1.7	2.3	1	2.3	3.5	†1	4.6	39
2	5.2	56	2	5.7	73	2	4.6	39
3	2.8	7.9	3	3.0	10	3	4.6	39
4	5.3	59	†4	4.1	26	Part VII.—Temperature, 11° C. $\delta p = 29.8$.		
5	2.4	5.0	5	4.2	29	† { 2 3 4	3.9	23
6	5.9	82	6	5.3	59		4.7	42
7	3.0	10	7	5.2	56		4.6	39
8	5.7	73					4.7	42
9	2.9	9.0						
10	5.5	67						
11	2.8	7.9						
12	5.6	70						
13	2.8	7.9						
14	5.4	64						
15	2.8	7.9						

* Left after 15^h.

† Periodicity absent in the first case after accidental influx.

20 NUCLEATION OF THE UNCONTAMINATED ATMOSPHERE.

TABLE 10, continued.—24–25° C. Cylinder. $\delta p = 31.2$. Promiscuous results.

Exhaust No.	s.	$n \times 10^{-3}$.	Exhaust No.	s.	$n \times 10^{-3}$.	Exhaust No.	s.	$n \times 10^{-3}$.
Part VIII.			Part IX.			Part X.		
1	*3.0	10	1	†3.3	14	1	‡3.5	17
2	4.9	49	2	5.3	59	2	5.2	56
3	4.5	36	3	3.0	10	3	2.5	6.1
4	4.7	43	4	5.7	73	4	6.1	85
5	4.7	43	5	2.7	7.9	5	**2.8	7.9
			6	5.7	73	6	5.4	64
			7	2.7	7.9	7	4.2	29
						8	5.2	56
						9	4.8	46
						10	4.9	49
						11	4.9	49
						12	4.8	46

* After 24 hours.

† After 15 hours.

‡ After 2 hours.

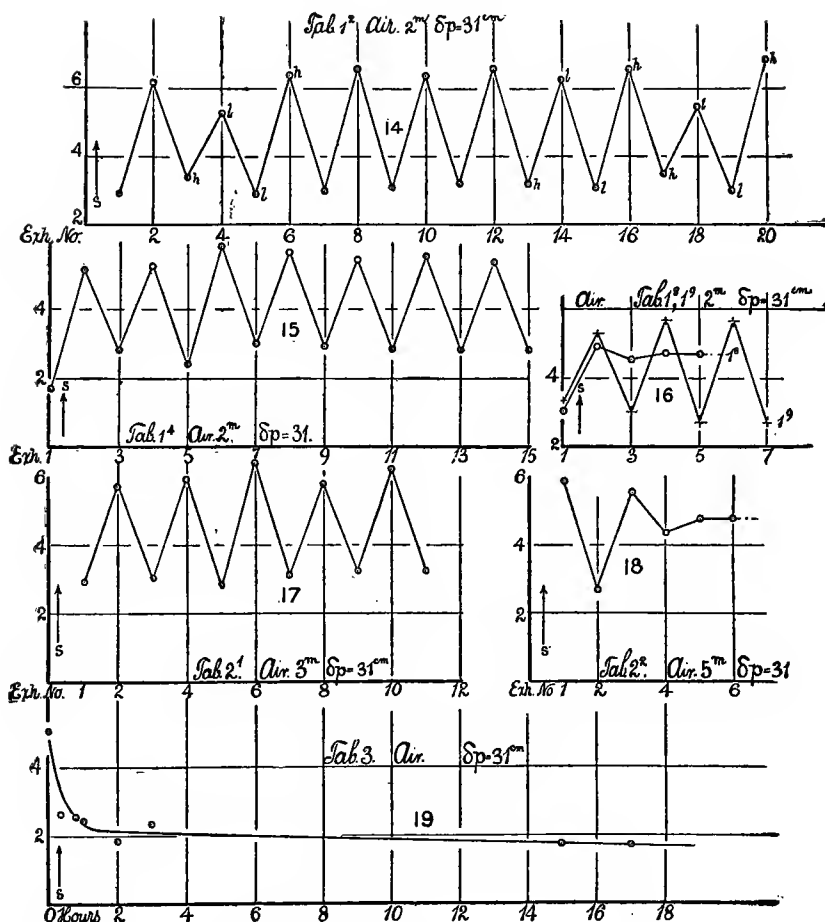
** Apparatus (water) shaken, thereafter glass dull.

In table 11, for 3-minute periods between the exhaustions as a safeguard against partial saturation, the same oscillations reappear (fig. 17). Very small inferior coronas are again followed by the larger superior coronas. On the other hand, the larger superior coronas usually precede larger inferior coronas, as above. The case of 5-minute periods between the exhaustions (fig. 18) begins with marked periodicity, after which, however, contemporaneously with the deposition of fog on the glass between observations, periodicity vanishes.

TABLE 11.—Periodicity in the condensation of dust-free air. Plug valve. $\delta p = 31.2$. Temperature = 25° C.

Exhaust No.	s.	$n \times 10^{-3}$.	Exhaust No.	s.	$n \times 10^{-3}$.	Exhaust No.	s.	$n \times 10^{-3}$.
Three-minute periods between exhaustions.						Five-minute periods (and longer) between exhaustions.		
1	2.9	9	7	3.1	11	1	59	82
2	5.7	73	8	5.8	76	2	2.7	7.9
3	3.0	10	9	3.2	12.6	3	5.6	90
4	5.9	82	10	6.2	90	4	*4.4	46
5	2.8	7.9	11	3.2	12.6	5	*4.8	59
6	6.4	126				6	*3.8	61

* Glass fogged during the interval.



FIGS. 14-18.—Graphs showing the alternations of the apertures (s) of coronas in non-energized dust-free air. The abscissas show the numbers of the successive exhaustions; the ordinates are nearly as the cube roots of the number of efficient nuclei.

FIG. 19.—Decay of the nuclei examined in the lapse of hours.

Table 1, referred to in figs. 14, 15 and 16, will be found as table 10, p. 19.

Table 2, referred to in figs. 17 and 18, will be found as table 11, p. 20.

Table 3, referred to in fig. 19, will be found as table 12, p. 22.

19. Effect of lapse of time on the nucleation of dust-free air imprisoned in the fog chamber.—The 5-minute periods in the preceding table, or figure 18, do not markedly diminish the aperture of the coronas. Larger periods of waiting are very effective, as is seen in table 12, where v/V shows the volume ratio of fog and vacuum chambers. The

measurements refer to an initial large corona of say $s=5$ cm.; but as this can not be measured without destroying the nuclei, the present data merely show the usual occurrence of inferior coronas in the lapse of time (fig. 19). In 15 hours the aperture is reduced to one-third and the nucleation possibly to one-thirtieth. Certain relatively high results at the end of the table seem to be referable to the presence of radium in the laboratory, but no definite statement can be made.

TABLE 12.—Evanescence of nucleation of dust-free air in lapse of time.

Glass fog chamber. $*v/V=0.063$.										Wooden fog chamber. $*v/V=0.13$.			
δp .	Temp.	Time	s.	$n \times 10^{-8}$	Temp.	Time	s.	$n \times 10^{-8}$		δp .	Time	s.	$n \times 10^{-8}$
31.2	°C.	h. m.			°C.	h. m.				°C.	h. m.		
	11	0 0	(4.6)	(70)	20	0 0	(5.5)	(67)		†33.0	0		
		20	2.6	3.9		1 0	2.4	5.0					
	20	0 0	(5.2)	(56)	23	0 0	(5.5)	(67)			24	3.0	10.3
		15 0	1.7	2.3		3 0	2.3	4.1			0	3.4	15.6
	20	0 0	(5.2)	(56)	25	0 0	(5.5)	(67)			0	3.3	14.5
		2 0	1.8	2.4		16 0	1.7	2.3					
	20	0 0	(5.5)	(67)		24	3.0	10					
		0 50	2.5	6.1		15	3.3	14					

* Volume ratio of fog and vacuum chambers. † Vacuum chamber disconnected.

The marked occurrence of inferior coronas in the lapse of time (under conditions, therefore, where the air must be saturated with moisture) seems to be positive proof against the view that these coronas owe their origin to undersaturation. The corona immediately following (second exhaustion) is always a superior corona. One may note that if extremely fine nuclei (colloidal molecules) pass the filter, a time loss like the present would accompany their decay.

20. Effect of pressure difference on exhaustion.—The reason for irregular results in tables 13, 14, and 15 is now apparent, for in these experiments the tendency to periodicity was not yet understood. Nor can it in any case be effectually combatted. After the fog chamber has been cleared of foreign nuclei, which occurs at a pressure difference above 20 cm. of mercury and at about the same volume expansion in both chambers, the effect of further increasing the pressure difference, δp , is an exceedingly rapid increase of the apertures of coronas. The first coronas after the air is made dust-free are usually particularly large. Though this looks like a foreign effect, it is probably due to periodicity.

Very soon, however, the effect of δp ceases to increase the apertures. All the s -curves either pass through a maximum or reach a limiting asymptote, as is particularly marked in case of table 15 (figs. 20 and 21). The fog limit lies a little lower in case of the large chamber (wood, $v/V=0.13$) than in the case of the small chamber (glass, $v/V=0.063$), an anomalous result, since the latter condensation must be the swifter. There does not seem to be any adequate effect for the relative suddenness of condensation in the two cases. The last parts of table 13 contain examples in which, with the same apparatus and apparently under identical conditions (dew on one side of the glass), a steady and thereafter an oscillating aperture is encountered. The last series gives an instance of oscillations which vanish when the water in the fog chamber is shaken from side to side.

TABLE 13.—Effect of pressure difference. Long condensation chamber. $v=55 \times 12 \times 20 = 13,200$ cm.³, for fog chamber; $V=106,000$ cm.³, for vacuum chamber $v/V = \frac{13,200}{106,000} = 0.125$. Instantaneous valve. Goniometer 85 cm. from fog chamber.

δp .	s .	$N \times 10^{-3}$.	δp .	s .	$N \times 10^{-3}$.
Outgoing.			Returning.		
19.6	0.0	0.0	33.0	2.0	5.9
24.2	1.8	3.7	29.2	2.9	19.8
24.2	1.8	3.7	25.8	1.5	3.1
28.3	3.0	21.5	22.7	.9	1.9
32.7	3.0	25.9	20.0	.0	.0
37.4	3.1	33.7			

TABLE 14.—Cylindrical condensation chamber. $v/V=0.06$. Instantaneous valve. Goniometer 85 cm. from fog chamber.

δp .	s .	$N \times 10^{-3}$.	δp .	s .	$N \times 10^{-3}$.
Outgoing.			Outgoing.		
18.8	0.0	0	35.1	2.5	16
20.4	0.0	0	42.6	2.6	24
20.7	0.0	0	52.2	3.5	102
25.6	*4.1	84			

* Initial excess.

24 NUCLEATION OF THE UNCONTAMINATED ATMOSPHERE.

TABLE 15.—Cyclic variation of pressure difference. Cylindrical condensation chamber.
 $v/V=0.06$. Plug valve (1-inch bore). Goniometer 85 cm. from fog chamber.

δp .	s .	$N \times 10^{-3}$.	δp .	s .	$N \times 10^{-3}$.
Outgoing.			Returning.		
15.2	0.0	0	48.9	4.1	136
18.5	0.0	0	46.3	3.6	77
20.9	(?)	0	43.3	3.7	72
20.1	0.0	0	40.8	2.9	32
20.2	(?)	0	38.4	4.5	110
26.2	*4.0	46	35.7	3.1	31
26.2	2.4	9.6	33.5	5.0	126
26.2	2.5	11	30.8	3.2	29
36.6	3.2	36	28.9	3.4	33
36.6	3.2	36	27.0	1.9	4.9
43.7	4.2	113	24.7	1.8	3.7
43.7	4.3	123	23.1	1.3	2.3
51.4	3.7	112	21.8	? 0.0	0
			20.6	0.0	0
			19.5	0.0	0

* Initial excess.

TABLE 16.—Effect of pressure difference. Cylindrical condensation chamber. Instantaneous valve. Eye at goniometer, 85 cm. from fog chamber. N reduced to normal atmospheric pressure.

δp .	s .	$N \times 10^{-3}$.	δp .	s .	$N \times 10^{-3}$.
20.1	0.0	0	34.7	5.0	132
20.5	0.0	0	34.9	2.7	20
20.7	0.0	0	34.8	5.1	140
23.3	3.0	18	34.8	2.6	18
			34.8	5.1	140
26.1	2.2	7	34.8	2.7	20
26.3	4.0	46	43.6	*5.4	237
26.2	2.6	12	43.5	5.1	202
26.2	4.1	50	43.5	5.8	279
26.2	2.2	7	43.5	3.0	41
26.2	4.3	58			
26.2	2.6	12			

* Valve injured.

In table 16 the occurrence of marked periodicity gives rise to two distinct s -curves, both of which soon approach an asymptote (figs. 22, 23). In the last group of observations the alternations are not regular (leakage of valve), but the extremes are indicated. Differing from this, the results of table 17 in the outgoing series of apertures (δp , increasing) are remarkably free from periodicity and show a tendency to pass through a maximum. In the return series much fresh air was drawn through the filter into the fog chamber and thence into the

vacuum chamber. It is noteworthy that very large coronas are then met with on first exhaustion, a result which may bear on the explanation of periodicity.

In table 17 (figs. 24, 25) the goniometer was moved close to the fog chamber to insure clearer vision. The chart (figs. 20-25) on page 26 shows, n , the number of nuclei per cubic centimeter of the expanded air; in the tables the number, N , reduced to air at normal pressure and temperature is usually given.

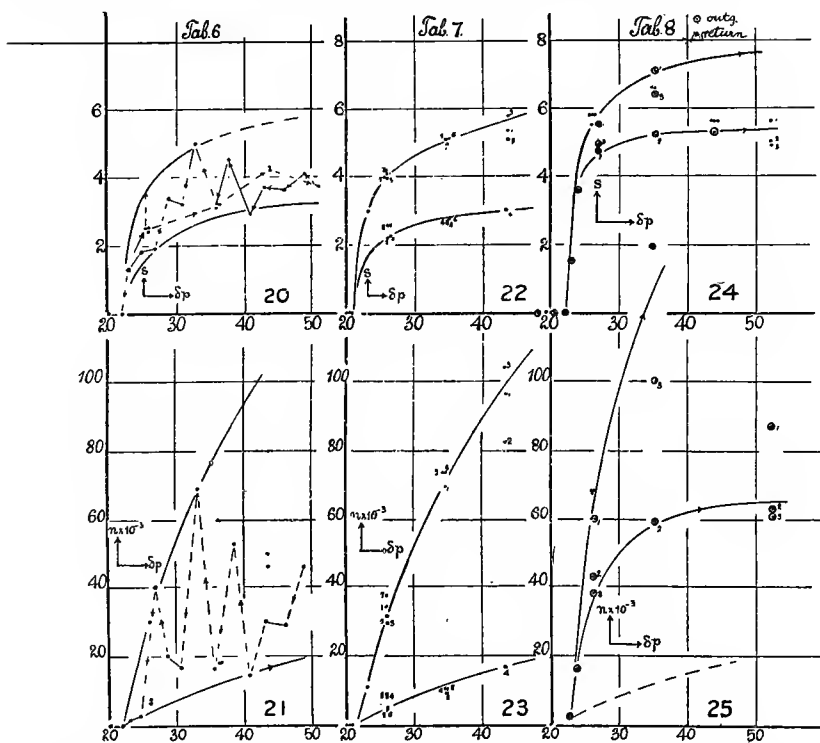
TABLE 17.—Cyclic variation of pressure difference. Cylindrical fog chamber. Plug valve. Eye at goniometer, 50 cm. from axis of cylinder.

δp .	s .	$N \times 10^{-3}$.	δp .	s .	$N \times 10^{-3}$.
Outgoing.			Returning.		
19.5	0.0	0	43.8	5.3	171
26.2	5.8	105			
26.5	5.8	106	35.3	*7.1	267
26.2	5.5	94	35.3	5.2	113
26.2	5.8	105	35.3	6.4	194
35.4	6.6	211	26.5	*5.5	94
35.0	6.6	209	26.3	4.7	59
			26.3	4.9	67
44.2	5.6	207			
43.8	5.6	203	24.0	3.6	24
43.8	5.6	203	22.8	1.5	2.5
			22.2	0.0	0
			20.5	0.0	0
52.3	5.6	297	18.0	0.0	0
52.4	5.0	215			
52.4	4.9	209			

* Nuclei probably enter from large influx of air through filter. Therefore next coronas are small from undersaturation and periodicity. These fine nuclei get gradually out of reach as δp decreases.

21. Remarks on the tables.—It will conduce to clearness to take the last tables showing the increase of apertures, s , with the increase of pressure difference, δp , first in order. All the s -curves, figures 20-25, either pass through a maximum or reach an asymptote. If the exhaustion is insufficient the groups of smaller nuclei will escape precipitation and the coronas be relatively small. This will also occur if relatively large nuclei are accidentally present. After all nuclei, large and small, are caught, higher sudden exhaustion can no longer increase the apertures. More water is instantaneously precipitated per cubic centimeter. Nevertheless this counter-effect, if it is such, will also vanish with increasing pressure differences, because of the accentuated rapidity of thermal radiation. The adiabatic method

ceases to be effective. Finally the necessity of producing sudden cooling simultaneously with extreme dilatation is a complication; for in view of the relative slowness of diffusion, it will eventually be impossible to keep the instantaneously dilated water vapor saturated without arresting the growth of the fog particles. Above $\delta p = 40$ cm. the effect of sudden exhaustion might actually dry the air, seeing that the density of vapor is instantly reduced more than one-half. It is thus conceivable that even slight differences of supersaturation at the outset may show themselves effectively at these high exhaustions. In table 16, however, the nucleation N (reduced to normal pressure) increases almost linearly with the pressure difference even at the highest exhaustions. The evaporation of the smaller fog particles is probably an essential part of the whole phenomenon.



Figs. 20-25.—Change of apertures (s) of coronas and number of efficient nuclei (n) varying with different pressure differences (δp) for the cases of superior and inferior coronas. Dust-free air.

Table 6, referred to in fig. 20, will be found as table 15, p. 24.

Table 7, referred to in fig. 22, will be found as table 16, p. 24.

Table 8, referred to in fig. 24, will be found as table 17, p. 25.

22. Blurred coronas.—The occurrence of an abundance of rain with all the coronas, as well as the blurred appearance of the coronas themselves, shows that gradation of particles is a characteristic feature with all these condensations. The following results for periodicity apparently indicate the presence of a group of markedly large particles in the amount of about one-eighth or more of the total number of nuclei.

23. Time effect.—In the lapse of time exceeding even half an hour the aperture of all coronas usually diminishes in marked degree. Above the fog limit, however, the coronas do not vanish as the result of repeated exhaustion, *i. e.*, the air can not be freed from nuclei by being stored in a closed vessel (fig. 19). What is particularly remarkable is the rapidity with which nuclei precipitated by condensation are again replaced. Whether these come through the filter in quasi-gaseous form (remembering that they must be much smaller than ions), or whether they are spontaneously produced in the imprisoned air, is yet to be decided. In every case something has to be explained away. If the nuclei came through the filter, for instance, they would not come through periodically.

24. Oscillations at variable pressure differences.—With increasing pressure differences, δp , the superior and the inferior apertures each lie on distinct curves, both of which rise rapidly at first, are then rapidly retarded, and tend to reach distinct maxima (figs. 20–25). The limiting ratio of apertures is liable to be nearly one-half. If, however, the pressure difference is carried far enough, both *s*-curves sometimes change character by decreasing and increasing, respectively, eventually to reach a common value. If, then, pressure difference is in turn reduced from these final values, the oscillation of *s* is usually absent and a mean nucleation appears at all subsequent (decreasing) pressure differences.

25. Nucleations at varying pressure differences.—The increase of nucleation, *n*, with the pressure difference, δp , is difficult to interpret, since the inferior and superior values are so much more widely and irregularly distributed (figs. 21, 23, 25). The *n*-curves usually show two limiting rates of increase of *n* with δp , respectively very large and very small. This is particularly well brought out in the data of table 16 and figure 23, where both loci are nearly straight even above $\delta p = 40$ cm. They become more so if the nucleation is reduced to normal pressure, as shown under *N*. Using this suggestion the data of table 13 (wooden fog chamber) are largely referable to inferior coronas. With one exception, this is also the case in table 14 for the

glass cylinder, while in table 15 there is an irregular distribution of observations between both classes of curves. In table 17 inferior coronas are absent, and those observed present an accentuated case of superior corona. The series fails to detect the large coronas after $\delta p = 35$ cm., so well brought out in table 16. One may note the different valves used.

26. Fog limits.—An interesting feature of these results are the fog limits or pressure differences at which condensation in dust-free air just commences. In spite of the different sizes of apparatus and valves used, the fog limits are about the same, viz, in tables 13, 14, 15, 16, and 17.

Table.	$\delta p =$	Apparatus.	Valve.
13	22-23 cm.	Wood, $v/V = .13$	Plug.
14	21.5	Glass, $v/V = .06$	Clapper.
15	22-23	" " "	Plug.
16	21-23	" " "	Clapper.
17	22-23	" " "	Plug.

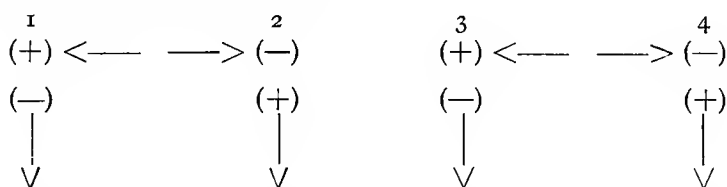
These results are surprising, inasmuch as the effect of the volume ratio of fog and vacuum chambers and the valve effect would naturally be looked to as productive of larger differences. With other apparatus (Chapter I) the data were :

$\delta p =$	Apparatus.	Valve.
22	Wood, $v/V = .7$	Plug.
20	" " .7	Clapper.

Thus the supreme importance of mere rate of exhaustion may well be called in question until more definite results appear ; for with so large a difference of volume ratio, valve obstruction, etc., the essential features should appear more clearly. It is possible that nuclei of extreme fineness (colloidal molecules) may pass through the filter. In such a case these would capture most of the water vapor, reducing the size of coronas by prohibiting condensation on still smaller colloidal molecules. Therefore, if the filter is entirely dispensed with and a closed vessel used, larger coronas may appear at smaller pressure differences.

27. Oscillations at fixed pressure differences.—Effectively the case of oscillation is one in which the large, sparsely distributed fog particles emit more nuclei and the very abundant small fog particles fewer nuclei, *i. e.*, the phenomena may be looked upon as though the nuclei were generated during the growth of the fog particles. This plausible result, however, is not to be maintained; for the emission would have to be as the growth of surface—in other words, as the volume—and the number of particles varies inversely as their volume. A counter supposition may be hazarded to the effect that the fog particles of large coronas absorb more nuclei because of their abundance than the fog particles of small coronas. But the period of suspension of particles is too short a period to be of moment.

If negative ions are more active as condensation nuclei than positive ions, the results observed may be tentatively grouped in accordance with the following scheme :



Let the ions be originally neutral as a whole, and suppose, as in case 1, that the negative ions are first precipitated. In the interval between this and the next exhaustion fresh ions are generated or taken in through the filter, as shown in case 2. If these negative ions partially neutralize the positive ions left over in case 1, the second precipitation takes place on the positive ions. Thereafter, case 3, the first is repeated, etc. But if the coronas are taken as a measure of the number of particles, the number of effective nuclei must be eight times larger in the first case than in the second, whereas the ions should be present in equal numbers. Hence there is serious objection to this hypothesis at the outset, quite apart from the absolute numbers in question, which are enormously too large to be referred to ions.

28. Undersaturation.—Some mechanism of this kind is nevertheless probable, and it will suffice if the undersaturation produced by the precipitation of fog particles is not rapidly made up by diffusion and convection, or, even better, if water nuclei are produced by evaporation of fog particles. Of the above hypotheses that of undersaturation has broad bearings and accounts qualitatively for most of the phenomena, as will presently be pointed out in detail. True, the large coronas

must be supposed to carry down more moisture than the small coronas, but the difference need not be great. The hypothesis encounters a serious obstacle, inasmuch as the coronas obtained from saturated air which has been imprisoned for long intervals of time (section 8) are usually an extremely small type of inferior corona, whereas they should be large superior coronas. Long intervals of waiting between exhaustions bring out not a superior corona but at best one of intermediate size. Another precarious feature is suggested by computing the rate at which saturation should be established in the most unfavorable case of the middle air layer, between the wet top and bottom of the fog chamber, for diffusion alone.

In fact, if diffusion takes place from the wet top and bottom of the rectangular trough of height a into a partially saturated atmosphere of initial vapor pressure p_0 , then at any time t , at the middle plate $x=a/2$

$$p = 1 + \frac{4(p_0 - 1)}{\pi} \left(\sin \frac{\pi}{2} \epsilon - (\pi/a)^2 kt + \frac{1}{3} \sin \frac{3\pi}{2} \epsilon - (3\pi/a)^2 kt + \text{etc.} \right)$$

where $dp/dt = k(d^2p/dx^2)$. Hence if $a = 11$ cm., as in the largest trough (wood), and if $k = 0.23$, the following values obtain :

$t = 30$	$p_0 = 0, p = .28$	$p_0 = 1/3, p = .52$	$p_0 = 2/3, p = .76$
60	.59	.72	.86
120	.87	.91	.96
180	.96	.97	.99

In the above tables a was usually less than 10 cm. (glass fog chamber), making the condition correspondingly favorable.

Hence by diffusion alone there should be saturation after 2 to 3 minutes even at the most distant (middle, $x=a/2$) plane, to within a few per cent, for the central layer is probably always more than half saturated at the outset. In addition to diffusion, however, there is marked convection due to the lightness of water vapor. At the same time there is no evidence that the more numerous but small drops of the superior coronas carry down a sufficient excess of water ; nor are the coronas, though blurred, otherwise distorted, as they would be for a definite diffusion gradient.

29. Undersaturation, continued.—Assuming, however, that undersaturation* does occur and is oscillatory as the result of successive

* It will be shown below, Chapter VI, sections 97, 98, that the probable cause of periodicity is not undersaturation but the production of water nuclei by the evaporation of the small fog particles. The analysis of the phenomena given in section 14 applies, however, with obvious changes, to both cases, and has therefore been retained in the text.

larger and smaller precipitations, the cases may be interpreted in succession as follows :

a. The superior coronas carry down more moisture and should be followed by even larger coronas, and vice versa ; but after the fog particles producing the superior coronas are precipitated, the supersaturation possible for the given pressure applied no longer catches the small nuclei. Hence the inferior coronas appear in succession. Hence, also, apart from what may be time errors in opening the stop-cock, very large pressure differences tend to wipe out the oscillation, as all nuclei are caught.

b. The ratio of 1:2 for coronal apertures and of 1:8 for the volumes of fog particles seems out of keeping with the slight differences of supersaturation instanced in section 28; but this is again a question of catching the group of smaller nuclei.

c. The phenomenon is much too definite an oscillation of aperture between s and $2s$ (nearly) to be referable to an irregular cause like deficient supersaturation; but the two types of nuclei admit of a wide range of saturation, as long as there is a correspondingly wide difference in the sizes of nuclei.

d. A series of minor observation are favorable to the hypothesis of residual undersaturation ; as, for instance, the eventual coalescence of the aperture curves of the superior and the inferior coronas ; the dew effect ; the fog effect and shaking ; the fact that very small inferior coronas are followed (*cet. par.*) by large superior coronas, while the latter are followed by large inferior coronas, etc.

e. Finally, while superior coronas are followed by inferior coronas, and vice versa, mean coronas follow each other.

30. Nucleation.—The values of the nucleation (number of nuclei per cubic centimeter) of the inferior and the superior coronas naturally present a more striking contrast, since the third power of aperture is involved. Otherwise but few new results are to be inferred from them. If the long series of table 10, part II, be taken, which contains the data of twenty successive alternations, the average inferior nucleations are 11,800, and the average superior nucleations 94,000, supposing, of course, that the precipitated water is the same in both cases and that it is all condensed on the available nuclei. In other words, if the two cases are identical, the superior coronas correspond to a number of nuclei 8 times greater (frequently larger than this in the other observations) than the inferior coronas. As this explanation is the more probable, it follows that the nuclei can not be regarded as positive and negative ions. They are rather the groups of large and small nuclei

seen throughout the condensations in connection with the rain and blurred coronas. Apart from this, the numbers obtained throughout are quite out of keeping with any similarly observed ionizations. If, however, free electrons appear only at the destruction or at the origin of nuclei, the association of few ions with many nuclei at any time subsequent to their origin is well accounted for, as already suggested in the earlier paper. It is only while the nuclei are being produced that the ionization and the nucleation must be of the same order; for the latter persists while the former vanishes at once. Finally the following results are implied, at least for the physical structure of air saturated with water vapor:

Air (dust-free) is inseparably intermixed with large and small nuclei, whose number (to be reckoned in millions per cubic centimeter) rapidly increases as the order of molecular size is approached. There seems to be no objection to looking upon these nuclei as a kind of colloidal (air) molecule, particularly as such molecules are frequently producible by the means (Bredig) which produce nuclei. If a large number of free atoms is suddenly introduced into any region (and this is probably what the radiation of the above kind virtually does) the result is not merely a production of typical molecules but of a large concomitant of graded nuclei.

Practically any given nuclear status of air is a counterpart of the intensity of the ionization of the medium in which the nucleation originated, to the effect that the superior limit of size of the nuclei and their number increase with the ionization. But there is no case of ionization free from nucleation, be the exciting cause a mere radiation as above, or ignition, combustion (including the low-temperature cases like phosphorus), or high potential discharge, or violent comminution as in the case of water nuclei.

EXPERIMENTS WITH DUST-FREE AIR ENERGIZED BY RADIUM.

31. Effect of radium in hermetically sealed glass tubes.—A modification was now introduced by inserting a small vial of thin glass (walls 0.04 cm.) containing about 0.01 gram of impure radium (strength 10,000 \times) in the B end of the rectangular apparatus, Chapter I, figure 1. For clearer vision, the eye at the goniometer was placed at about 35 cm. from the nearer glass plate of the fog chamber, and the apertures so obtained, larger than the customary values by about 10 per cent, appropriately corrected. The data of most of the tables are reproduced in the chart containing figures 26–32.

The filtered air was first examined without interference, as in table 18, in the complete absence of radium, and a similar test precedes all the subsequent observations. The results for air are without perio-

dicity here (figs. 27, 28), and show a high fog limit at about $\delta p = 24$ cm., the coronas at $\delta p = 24.7$ being just appreciable. The reason for the raised fog limit (air freer from dust) is not apparent; but the volume ratio of fog and vacuum chambers is here $\delta p = 0.13$.

The immediate effect of introducing radium is seen in the second part of the table, at first without periodicity, and the fog limit is at once reduced to $\delta p = 19$ cm. (figs. 27, 28).

TABLE 18.—Effect of radium immediately after insertion. Long condensation chamber. $v = 11,000$ cm.³; $v/V = 0.13$. Temperature, 26° C. Plug valve. Goniometer close to apparatus.

Filtered air without radium.			Radium tube inserted.					
$\delta p.$	s.	$N \times 10^{-3}$	$\delta p.$	s.	$N \times 10^{-3}$	$\delta p.$	s.	$N \times 10^{-3}$
20.6	0.0	0	29.5	4.8	75	*24.8	6.0	74
21.5	0.0	0	26.9	3.9	33	24.8	3.1	9.6
23.4	0.0	0	24.4	3.6	24	24.8	5.3	70
23.2	0.0	0	22.0	2.5	7	24.8	2.8	6.9
24.7	1.5	2.7	20.1	1.3	2	24.8	5.5	58
24.7	1.3	2.4	18.0	0.0	0	24.8	3.0	8.7
29.5	3.2	20	18.0	0.0	0	24.8	4.8	51
29.6	3.5	27	After 75 min.			24.8	2.3	3.5
29.8	3.4	25				24.8	5.4	55
33.1	3.5	32				24.8	2.8	6.8
33.0	3.4	27	After about 90 min.			After about 90 min.		
						24.8	5.4	55
						24.8	2.4	4.3
						After 18 hours.		
			After 135 min.			24.8	* { 6.2 2.7	† 100 6.8
			24.8	6.0	111			

* Periodicity.

† $N = 150,000$; ratio $1.5 = N/n$.

Nucleation, 75 minutes after the first observations, has much increased (*cæt. par.*); but direct comparison is not possible, because the latter data are now distinctly periodic, and an upper and a lower curve of apertures has appeared, without appreciably displacing the fog limit. After further 135 minutes, the upper limit has probably reached a stationary value (figs. 27, 28).

In the last part of the table the periodicity of aperture, s , for air in the presence of radium, is specially investigated for $\delta p = 24.8$ cm. Exceptionally high superior values of s are again followed by exceptionally high inferior values (fig. 26), while exceptionally low inferior

values are followed by high superior values. The oscillatory curves usually rise from great depth to great height. The s -curves sometimes show a tendency to double inflection after $\delta p = 24$ cm. is exceeded, referable, it would seem, to the normal air ions added to the radium ions.

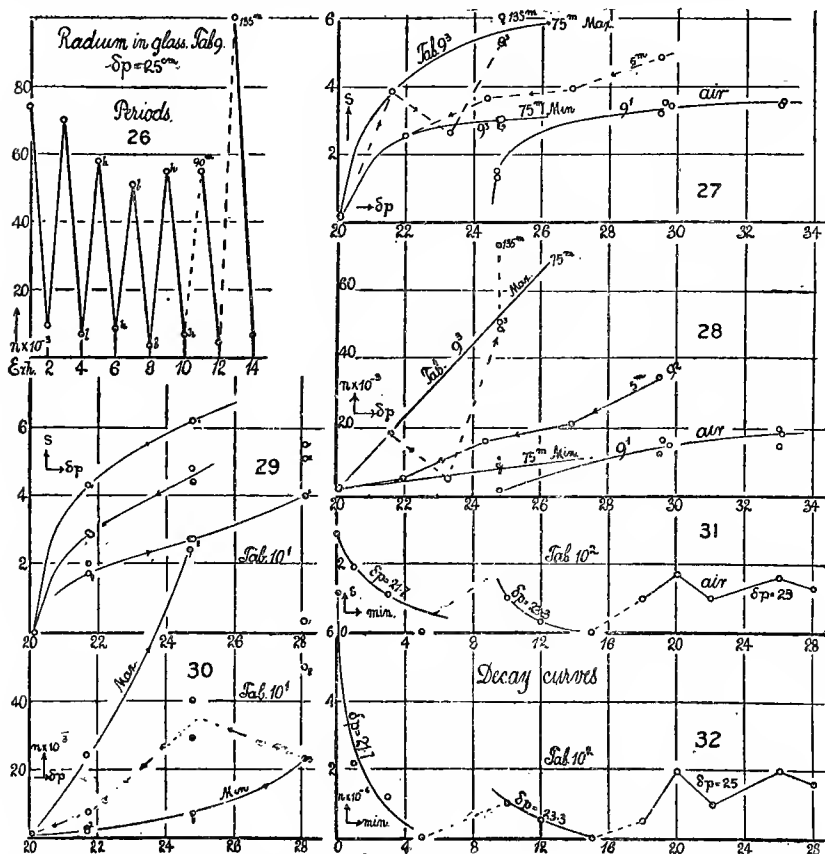


FIG. 26.—Number of efficient nuclei (n) obtained in successive exhaustions of dust-free air energized by radium. Periodicity.

FIGS. 27–30.—Change of apertures (s) of coronas and nucleations (n) varying with the pressure differences (δp) in cases of dust-free air energized or not by radium (in sealed glass). Arrows show the march of the observations. Periodicity is apparent.

FIGS. 31–32.—Decay of nuclei produced by radium after removal of tube from fog chamber. Radium in glass tube.

Table 9, referred to in figs. 26, 27, and 28, will be found as table 18, p. 33.

Table 10, referred to in figs. 29, 30, 31, and 32, will be found as table 19, p. 35.

In table 19 the same effects are studied after the radium was in the apparatus for over 24 hours. The data in the outgoing series (δp increasing) are distinctly periodic, until the highest value $\delta p = 28.1$ cm. is reached, which seems to wipe out the periodicity for the returning series (figs. 29, 30). Curiously enough, the fog limit has apparently risen, being now $\delta p = 20$ cm., instead of 19, as in table 18. If all results be compared at about $\delta p = 25$ for mean values of s , they show for—

Air (no exposure),	$s = 1.4$	$n \times 10^{-3} = 1.7$
Radium, short exposure,	3.6 (no periods)	16
exposure, 2 hours,	4.1 (periods, $s = 30 - 52$)	23
exposure, 24 hours,	4.5 (periods, 27—62)	32
Air (20 minutes after removing radium),	1.4	1.7

Long exposure to radium has increased the amplitude of the variation of aperture, s . The limiting maxima for high values of δp in the case of radium are in excess of the corresponding values for air.

TABLE 19.—Effect of radium left in apparatus 24 hours (23° C.) and thereafter removed.

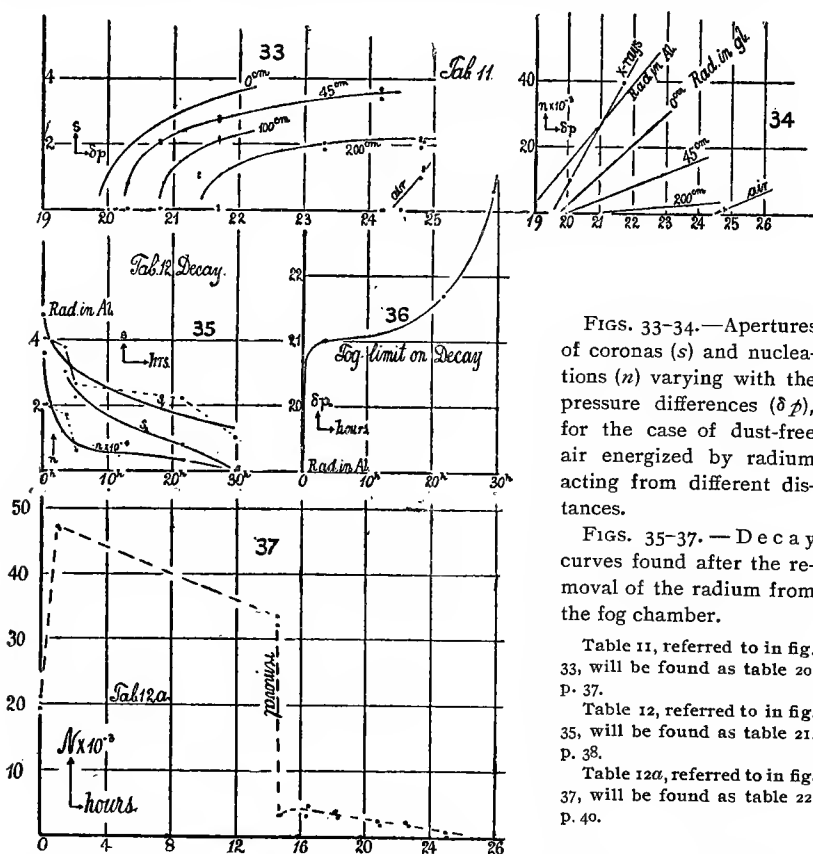
Radium present.			Radium removed.			
δp .	s .	$N \times 10^{-3}$.	Time.	δp .	s .	$N \times 10^{-3}$.
			<i>Min.</i>			
16.0	0.0	0	0	Removed.	...
18.0	0.0	0	1	21.7	1.9	3
20.1	Just seen.	0	3	21.7	1.1	2
*21.7	4.3	34	5	21.7	0.0	0
21.7	1.7	2	10	23.3	1.0	1
24.8	6.2	116	12	23.3	γ'	γ'
24.8	2.7	10	15	25.0	0.0	0
†28.1	5.5	101	17	24.8	* γ'	γ'
28.1	5.1	81	20	24.8	1.7	3
28.1	4.0	37	22	24.8	γ'	γ'
‡24.8	4.4	43	25	24.8	1.6	3
24.8	4.8	60	28	24.8	1.3	2
21.7	2.0	3				
21.7	2.9	10				
21.7	2.9	10				

* Periodicity even in the absence of coronas. † Periodicity ceases. ‡ Returning.

32. Remarks on the tables.—The inference has already been drawn that the number of nuclei as well as their size varies as the ionization per cubic centimeter. The fog limit is reduced by the presence of weak radium in sealed thin glass tubes within the chamber, from $\delta p = 24$ to 19 cm., observations which may be made pretty sharply. This implies (quite apart from number) that the nuclei in the presence of radium are larger, as they are the offspring of a more highly ionized field than exists in nonenergized identically filtered air. But apart from the fog limit, the number of nuclei large enough to fall within the scope of any given δp is correspondingly increased.

The fog limit of filtered air after the radium is withdrawn soon regains its original value; but some definite time (say 15 minutes) is necessary even here. It does not seem to vary appreciably with the time of exposure. (See figs. 31, 32.)

As the radium of low power ($10,000\times$) is inclosed in glass 0.04 cm. thick, it is probable that β and γ rays are chiefly responsible for the nucleation. Hence it appears that nuclei are produced by sufficiently swift moving corpuscles as well as by the X-rays, an important result bearing on an inquiry suggested above. This will be further substantiated in the next chapter in favor of the gamma rays.



FIGS. 33-34.—Apertures of coronas (s) and nucleations (n) varying with the pressure differences (δp), for the case of dust-free air energized by radium acting from different distances.

FIGS. 35-37.—Decay curves found after the removal of the radium from the fog chamber.

Table 11, referred to in fig. 33, will be found as table 20, p. 37.

Table 12, referred to in fig. 35, will be found as table 21, p. 38.

Table 12a, referred to in fig. 37, will be found as table 22, p. 40.

33. Data for nucleation.—The results for nucleation in case of a dust-free atmosphere energized by radium ($10,000\times$) contained in a hermetically sealed glass tube are clearest in the third part of table 18, where nearly straight n -curves for inferior and superior coronas may be made out (fig. 28). Part 2, containing data obtained shortly

after the radium tube was introduced, is not easily interpreted, but the action of radium is obviously weaker. In most cases there is marked periodicity, and part 4 of the table proves that the nucleation is over 9 times greater for the superior than for the inferior coronas. After an exposure of 18 hours, the nucleation of the superior coronas is fully 20 times greater.

In table 19 the nucleations of the superior and the inferior coronas are particularly striking at $\delta p = 25.8$, and the ratio is actually 11 (fig. 30). Thereafter periodicity vanishes with falling nucleations and the return n -curve is along an average path. If periods were due to the gradual growth of nuclei, supposing that the time between *two* successive exhaustions is needed to bring the nuclei within the scope of the given pressure difference, there would be no reason for the relatively unbroken return. Oscillation appears to be wiped out by high pressure differences as well as in a march of decreasing values.

TABLE 20.—Radium at different distances from line of sight. Interval between exhaustions usually 2 minutes.

Distance.	δp .	s.	$N \times 10^{-8}$.	Distance.	δp .	s.	$N \times 10^{-8}$.
∞	24.2	0.0	0	∞	24.5	0.0	0
	24.2	0.0	0		24.8	1.0	2
	24.8	1.2	2				
	24.8	1.3	2				
45	24.2	3.7	27	200	21.7	†2.3	4
	24.2	3.4	19		21.7	1.6	2
	21.7	2.8	9		21.7	0.0	0
	21.7	2.7	9		21.7	0.0	0
	20.1	0.0	0		21.7	2.0	3
	20.3	0.0	0		21.7	1.8	3
45	20.8	2.1	4		21.4	1.1	2
	20.8	2.0	3		21.4	1.0	2
	20.1	0.0	0				
	20.3	0.8	1				
100	21.7	*2.2	4		23.3	1.8	3
	21.7	1.0	2		23.3	2.0	3
	21.7	2.2	4		24.8	1.9	4
	21.7	*(2.5)	7		24.8	2.1	4
	21.7	1.6	2				
	21.7	2.1	4				
	20.8	0.0	0		24.8	†2.2	5
	20.8	0.8	8		24.8	2.1	4

* Periods?.

† After 40 minutes' exposure.

34. Fog limits raised by weaker ionization.—The view taken in this paper that the size of the nucleus increases with the intensity of the ionization may be tested by removing the radium from the apparatus and allowing it to act from increasing distances (figs. 33, 34). This is the case in table 20, where observations to determine the fog limit are

given when the radium is placed at 45 cm., 100 cm., 200 cm., respectively, from the end of the fog chamber, or, better, from the line of sight. Whenever radium is not too far from the apparatus the change of fog limit may be made out sharply as—

Distance,	0	45	100	200	∞	cm.,
$\delta p =$	19	20.2	20.8	21.5	24.5	cm.,

showing that the nuclei increase in size with the intensity of the ionization. These and the following data are mapped out in figure 34 of the chart, n instead of N (reduced to normal pressure) being usually inserted. In case of long distances (200 cm.) the results are apt to be irregular. On removing the radium to a great distance the fog limit of air is soon restored, and it will be seen that all observations are introduced by test experiments with dust-free air.

TABLE 21.—Coronas for a given pressure difference and fog limits after removal of radium (0.01 gram, 10,000 \times , in hermetically sealed aluminum tube) from inside of fog chamber.

Time.	δp .	s_1 .	s_2 .	Fog limit.	n_1 $\times 10^{-3}$	n_2
<i>h.</i>						
0	*21.7	4.8		19	36	
0	*19.0	1.2			2.1	
0.1	†21.7	4.0			20	
0.3	21.7	4.0			20	
0.7	21.7	4.0			20	
3.5	†21.7	3.7	3.0	21	17	8.0
	20.0	0.0			0	
5.0	†21.7	2.6	2.2		5.6	4.0
21.5	†21.7	2.2	0.8	22	3.0	0.8
29.5	21.7	1.0	0.0	23	1.1	0.0
	24.7	1.2			1.4	

* Radium present.

† Radium removed.

‡ Successive exhaustions.

35. Nucleation.—An important interpretation of the preceding results is obtained by mapping out the nucleations, n , in relation to the corresponding pressure differences, δp (fig. 34). The slope of these curves falls off rapidly for radium at 0, 45, 200 cm. from the fog chamber, while the fog limit rises. In other words, the initial slope of the n -curves is steeper as the fog limit is lower. Thus per increment of δp of 1 cm. of mercury, above the fog limit of the ionized medium, and below the fog limit of nonenergized dust-free air, there will be found in succession for radium in—

Sealed aluminum tube within fog chamber,	$\delta n = 12,000$
Sealed glass tube within fog chamber,	6,000
Sealed glass tube, outside, 45 cm. from fog chamber,	3,500
Sealed glass tube, outside, 200 cm. from fog chamber,	1,000
Dust-free air (above fog limit, radium at infinity),	10,000

Hence the gradation is effectively more even, finer, *i. e.*, with fewer gaps, as the fog limit is low and the maximum size of nucleus larger, while for sparse distribution the steps from any nucleus to the next in order of size are relatively large. For a different medium, dust-free air, for instance, as given in the summary, or figure 34, the gradation is characteristically different. Later experiments (Chapter III) make it probable that the curves for dust-free air, not energized, and dust-free air energized by radium and X-rays, make a continuous series.

36. Radium in sealed aluminum tube.—The identical sample of radium (0.01 gram, 10,000 \times) was now removed by cutting the glass tube, put into an aluminum tube (walls about 0.1 mm. thick), and again hermetically sealed. This tube was introduced into the inside of the fog chamber, kept in place 15 minutes or more, and then removed to an infinite distance. The results obtained are different from the preceding case of the same radium in the thin glass tube; for whereas the fog limit of dust-free air was regained 15 minutes after the removal of the glass tube (figs. 31 and 32), it took at least 30 hours to restore the same fog limit after the removal of the aluminum tube. Table 21 shows the results, where s_1 and s_2 are apertures obtained in successive exhaustions about 2 minutes apart, dust-free air being added to the fog chamber in the interval (fig. 35).

The successive fog limits for radium sealed in the thin aluminum tube are, therefore, in centimeters of mercury (fig. 36),

Radium in place,	$\delta p = 19$
Radium tube removed:	
Fog limit $3\frac{1}{2}$ hours later	21
“ 21 “	22
“ 30 “	23

provided time is allowed for the excited activity within the chamber to saturate the air with nuclei (cases s_1). When such time is not allowed as in the succeeding exhaustions (cases s_2), the fog limit of dust-free air is practically regained in 30 hours. Something like an emanation seems here to escape from the aluminum tube rapidly and from the glass tube slowly, in spite of their thickness, relatively speaking, and induces radio-activity at the inner walls of the fog chamber; or possibly this induced activity is a kind of phosphorescence produced by the impinging β and γ rays. It seems probable that the life of the excited activity may be prolonged at pleasure within limits, by gradually decreasing the walls of the aluminum tube hermetically sealing the radium excitor.

The loss of the activity shown by the rise of the fog limits in the lapse of time is naturally of an exponential character (fig. 36). It rises quickly after the removal of the radium from $\delta p = 19$ to about

$\delta p = 21$, after which the true exponential march due to the excited activity begins. It would be better to state these data in terms of the number of nuclei produced after indefinite exposure (nuclear saturation), the number to be found by a given sufficiently high pressure difference below the fog limit of dust-free air. But the observations of table 21 are scarcely advanced enough for this purpose. In fact, the irregularity of size of the coronas s_1 obtained at the given pressure-difference, $\delta p = 21.7$, is worthy of remark. The curves obtained in the second exhaustion (s_2), whereas but a few minutes of exposure of the air to the excited activity are in question, are much smoother. The n -curves do not suggest any further comment.

The above experiments on radio-activity, induced by radium contained in a closed aluminum tube placed within the fog chamber, having been made soon after the tube was filled and sealed, it was thought necessary to repeat the work two months later with the same tube. As a safeguard this was additionally sealed at the ground joint (screw plug) with resinous cement. Data so obtained with the wood fog chamber were curiously irregular, showing periodicity occurring in triads. Large coronas appeared after long waiting (15 hours), and it is therefore probable that there was some slight leak whereby air nuclei entered the fog chamber and captured much of the precipitated water. In contrast with these suspicious results, the data for decay curves were consistent, showing an increase of nucleation within about 20 to 30 minutes subsequent to removal, after which a gradual decay occurred to about one-half in 6 hours. But the data as a whole were discarded.

The experiments were now repeated in the glass fog chamber, which had been specially tested for freedom from leaks. The exhaustions made below the fog limit for dust-free air are shown in table 22 and figure 37.

TABLE 22.—Radium in fog chamber. Sealed aluminum tube. $\delta p = 25$ cm. Successive exhaustions, 1^m-2^m apart.

Exh. No.	s.	$N \times 10^{-3}$	Exh. No.	s.	$N \times 10^{-3}$	Exh. No.	s.	$N \times 10^{-3}$
1	4.5	48.0	9	4.4	44.0	16	2.3	5.4
2	2.6	9.2	10	2.2	5.0	17	2.5	8.0
3	1.0	1.8	11	.0	.0	18	2.7	10.4
4	*5.0	67.0	12	3.4	20.4	19	4.0	32.4
5	2.7	10.4	13	3.3	18.6	20	†5.2	74.4
6	1.0	1.8	14	*3.8	30.0	21	3.7	28.6
7	4.4	44.0	15	*2.0	3.8	22	3.7	27.6
8	2.2	5.0						

* Renewed after waiting 5 minutes or more.

† Next day.

The new data are, in fact, quite different from the old. After introducing the sealed radium tube the nucleation rises rapidly to a maximum, falling off, however, to a mean value in 14 hours. On removing the radium tube from the chamber, the nucleation falls off at once to about 10 per cent of its original value. This appreciably increases a little at first, but vanishes practically in the ensuing 12 hours. One may note that the second and subsequent exhaustion usually show smaller nucleations than the first, as though it were possible to reduce the nucleation faster than it is restored. It is probable therefore that in the first experiments something like an emanation escaped from the ground joint or that the outside of the aluminum tube had become radio-active during filling. Nevertheless, a residual effect is in evidence in the last experiments made, which can not be explained away. Something has escaped through the aluminum tube which produced the lingering radio-activity of the chamber (fig. 37).

EXPERIMENTS WITH DUST-FREE AIR ENERGIZED BY THE X-RAYS.

37. Persistence of nuclei produced by X-rays in the lapse of time.—The nuclei produced by the X-rays of sufficient intensity (*i. e.*, when the bulb is near the fog chamber), if left without interference, are indefinitely persistent as compared with the initial ionization. Table 23 shows some incidental results. It is not possible to determine the law of decay (probably exponential) by this method, as the nuclei are lost or otherwise destroyed by the condensation which determines their number. The initial nucleation must therefore be inferred. Again, the first coronas (if the X-ray bulb is at one end of the fog chamber as was here the case) are apt to be distorted, so that the corona obtained on first exhaustion is not available for definite measurement. To some extent the datum is supplied by the corona of the second exhaustion (s_2), observed after the fog particles of the first corona (s_1) have subsided, filtered air slowly replacing the exhausted air. m refers to the precipitation of water per cubic centimeter, at the pressure differences shown by the subscripts.

Within an hour or more after the exposure the coronas are invariably strong. Within 16 minutes, 36 minutes, even 85 minutes, they show diminutions of aperture comparable with that usually observed in the case of other nuclei. In half an hour the nucleation has not fallen below $\frac{1}{2}$, in an hour not below $\frac{1}{4}$, etc. After 4 hours, however, all nuclei within the scope of the exhaustion have vanished.

TABLE 23.—Decay of X-ray nucleation in lapse of time. Exposure, 3 minutes;

6 cells. $\left\{ \begin{array}{l} m_{18}/m_{17} = .82. \\ m_{16}/m_{17} = 1.00. \end{array} \right\}$ Goniometer close up.

Time.		$\delta p.$	$s'_1.$	$s'_2.$	n'_1	$10^{-3} \times n'_2$	n_1	$10^{-3} \times n_2$
<i>h.</i>	<i>m.</i>							
4	16	13.5	6.9	3.0	80	6.6	66	5.4
	0	13.5	0.0	0	.0
	0	13.5	6.0-7.0	3.5	68	11	56	9
	36	16.7	4.7	1.5	28	1.4	28	1.4
	0	16.7	*Spindle	5.6	4.6	46
	1	16.7	3.8	1.2	15	1.1	15	1.1

* Narrow spindle throughout A side.

TABLE 24.—Fog limits obtained with X-ray nuclei. X-ray bulb at different distances. Exposure for different times. Line of sight 15 cm. from end of fog chamber. Goniometer close up.

Remarks.	Time of exposure.	Distance from chamber.	$\delta p.$	<i>s.</i>	$n \times 10^{-3}.$	Remarks.	Time of exposure.	Distance from chamber.	$\delta p.$	<i>s.</i>	$n \times 10^{-3}.$
	<i>Min.</i>	<i>cm.</i>					<i>Min.</i>	<i>cm.</i>			
Current on...	2	35	18	0.0	0	Current on..	2	2	†18.5	4.5	26
off.....	22	.8	1.0	on.....	16.5	4.1	17
off.....	23	.8	1.0	on.....	14.9	0.0	0
off.....	*25	1.4	1.7	Fog limit	15.5
off.....	25	1.4	1.7						
on...	2	35	24.8	7.0	110	Current on..	4	2	14.9	5.3	36
on...	2	35	21.7	5.0	39	on..	4	2	11.9	5.2	28
on...	2	35	20.1	2.9	9.4	on..	4	2	8.9	0.0	0
on...	2	35	18.0	0.0	0	Fog limit	10
off.....	20.1	0.0	0						
off.....	21.7	0.0	0	Current on..	8	10	18.5	3.1	8
off.....	23.3	0.0	0	Fog limit	†17
Fog limit	19						
Current on...	2	10	20.1	2.9						
on.....	18.5	1.4						
Fog limit	18						

* Spontaneous condensation in dust-free air.

† Distorted coronas.

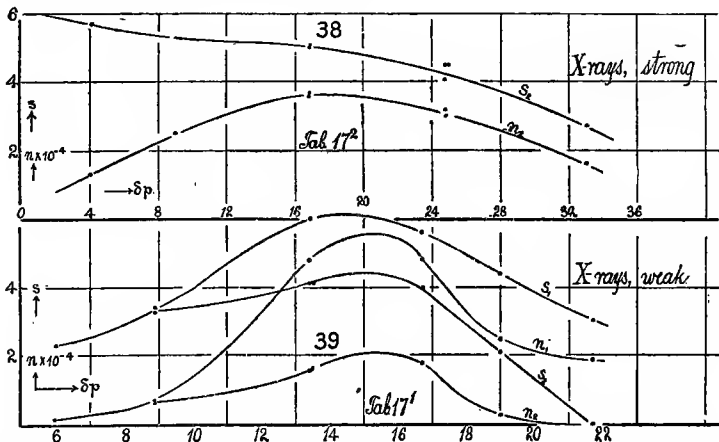
‡ About.

38. Fog limits of nuclei produced by X-rays.—To obtain lower fog limits than were producible with the weak radium above employed, the following experiments with the X-rays (table 24) were undertaken. Even here the radiation is not strong (coil with 4-inch spark gap and energized by 4 storage cells).

The following fog limits were made out with the aid of the same fog chamber of waxed wood, used above :

X-ray bulb from chamber.	Exposure.	Fog limit.
35 cm.	2 min.	$\delta p = 19$
10	2	18
10	4	17
2	2	15.5
2	4	10
2	10	Vanishing.

A few other cases will be added below, giving for stronger radiation at a distance of 2 cm. and for only 2-minute exposure fog limits at 5 and 4 cm. In each case the air was rigorously freed from dust by filtration before the exposure began. Hence the nuclei are due to the X-rays alone, and their size increases indefinitely with the intensity of the ionized field. Indeed as to size they eventually in no wise differ from phosphorus or other efficient nuclei, and require almost no supersaturation to induce condensation.



FIGS. 38-39.—Apertures (s) and nucleations (n) varying with the pressure differences (δp) for the case of persistent nuclei produced in dust-free air by the X-rays.

Table 17, referred to in figs. 38 and 39, will be found as table 27, p. 45.

39. Sudden exhaustion in the absence of condensation.—In many of the experiments the nuclei seemed to be destroyed by sudden exhaustion even when no condensation took place, the pressure differences lying below the fog limit. As this is an important question bearing on the flying to pieces of the nucleus, special investigations were made as detailed in the following tables. The point at issue may be stated

definitely as follows: Let δp be the fog limit of the given gas saturated with moisture. Let $\delta p' > \delta p$ be a pressure difference producing strong coronas. Let $\delta p'' < \delta p$ produce no condensation at all in the dust-free gas (below the fog limit). Then if the fog chamber is exposed to radiation in a definite way, in a definite time, and thereafter left without interference, $\delta p'$ will produce coronas for hours after the radiation ceases. If, however, immediately after the exposure $\delta p''$ is applied, producing no condensation, and if (dust-free air being introduced at once), without loss of time, $\delta p'$ is now applied, will coronas appear or will they not appear in spite of the excessive exhaustion? In other words, has the nucleus returned to dust-free air?

Thus, in table 25, experiment 1 shows that mere lapse of time has no relatively important effect. In experiments 2 and 3, the first exhaustion at $\delta p = 18$ has all but destroyed the corona, for $\delta p = 25$ subsequently applied, which should, by experiment 3, have been $s = 7.0$ cm. Similar remarks apply to experiment 4. Experiments 5 and 7 instance the usual case, that if a corona is produced in the first exhaustion, there will always be a smaller one in the second exhaustion. These are the favorable experiments; but experiment 6 and others which might be added show that the effect of the lower exhaustion does not disrupt the nucleus for the higher exhaustion. Thus there is no trustworthy evidence for the flying to pieces of the nucleus, and, in fact, the next section (table 27) shows that X-ray nuclei sustain high sudden exhaustions without being dissipated or failing to produce condensation. The difficulties encountered are without doubt referable to the variability in action of the X-ray bulb.

TABLE 25.—Possible rupture of the nucleus.

First exhaustion.		Time elapsed.	Second exhaustion.	
δp .	s .		δp .	s .
.....	<i>Min.</i>		
18	0.0	3	20.1	3.7
.....	25	*1.3
.....	25	7.0
6	(†)	2-3	13.4	2.6
13.4	6.0	2-3	13.4	4.1
6	(†)	2-3	13.4	4.5
13.4	5.8	2-3	13.4	3.4

*Spontaneous condensation.

†Thin drifting fog.

Experiments were also made under satisfactory conditions with the bulb at 80 cm. (table 26). But the nuclei so obtained are essentially fleeting and would vanish without the first exhaustion.

TABLE 26.—Attempted breaking to pieces of nuclei. Bulb axial at 80 cm. from end. Exposure, 3 min. Fog-limit air, $s = 1.0 \dots \dots 1.5$ at $\delta p = 24.7$; with X-rays originally: $\delta p = 24.8$, $s = 3.8$. Filter with wet-spunge tube.

δp_1 .	s_1 .	δp_2 .	s_2 .	$N_1 \times 10^{-3}$.	$N_2 \times 10^{-3}$.
24.8	3.9	24.8	1.5	30.0	2.7
22.1	3.0	22.1	.0	11.3	.0
19.7	.8	24.8	1.8	1.1	3.1
19.2	.0	24.8	2.1	.0	4.3
24.8	3.6	24.8	.8	24.7	1.4
19.2	.0	24.8	1.0	.0	1.8
19.1	.0	24.8	1.5	.0	2.7
24.8	*3.3	24.8	†1.5	18.5	2.7

* Exposure, 7 min: $\delta p = 24.8$, $s = 3.6$.

† Accidental influx rapid and large: $\delta p = 24.8$, $s_3 = 2.8$, $s_4 = 2.4$, $s_5 = 0.8$.

40. X-ray nuclei at different high-pressure differences.—The following experiments originated in a somewhat similar purpose to the preceding section. In table 27, s_1 and s_2 show the apertures of the coronas on first and second exhaustion, filtered air being added in the meantime, after an exposure to relatively weak radiation. The apertures are a maximum at $\delta p = 15-17$ cm., after which they decrease faster than the increased precipitation on the nuclei warrants (fig. 39). The n -curves and the s -curves with increasing δp are both similar. As the final fall of curve depends on the difference of the opposed effects of larger precipitation and greater number of particles within the range of condensation, the very small nuclei must here be in absence.

TABLE 27.—X-ray nuclei at different pressure differences. Distance of bulb from apparatus, 3 cm.

Interval of exposure, 5 min.					Exposure, 3 min.				
δp .	s'_1 .	s'_2 .	$N_1 \times 10^{-3}$	$N_2 \times 10^{-3}$	δp .	s'_1 .	s'_2 .	$N_1 \times 10^{-3}$	$N_2 \times 10^{-3}$
21.7	3.0	0.0	12.5	.0	24.7	8.0	4.4	180	45
19.0	4.4	2.1	33.7	3.4	24.7	8.0	4.1	180	37
16.7	5.6	4.0	61.9	23.2	33.1	5.0	2.7	102	15
13.4	6.0	4.1	58.6	19.5	24.7	8.0	4.4	175	46
8.9	3.3	3.3	7.4	7.4	16.7	(†)	5.0	47
6.0	(*)	2.3	(*)	1.3	8.9	(†)	5.3	28
13.4	5.5	4.1	46.4	19.5	4.0	(‡)	5.7	14
					16.7	(†)	5.0	46

* Thin drifting fog.

† Long spindle.

‡ Floating veil.

Corresponding experiments given in the second part of the table were therefore made with more powerful radiation (fig. 38). Here there is a regular decrease of aperture from the beginning where pressure differences are vanishing to the end where they are very high. The nucleations nevertheless pass through a determined maximum at about $\delta p = 16$ to 20 cm. The endeavor was made to guard against variation of efficiency of the X-ray bulb and other causes by repeated redetermination of the fiducial pressures. The fog limit of dust-free air is $\delta p = 24.7$ here. Hence it is noteworthy that the computed nucleation decreases at the highest pressure differences in spite of the accession of air nuclei to augment the number of X-ray nuclei present. The figures (38, 39) show the changes of n ; but the reduction to N (nuclei per cubic centimeter at normal pressure) adds nothing new to the results.

To determine the nucleations for the high exhaustions is precarious, because the efficiency of the apparatus in producing truly adiabatic conditions will rapidly grow less, and because the data needed for the vapor pressure of water 20° or more below freezing are not forthcoming. A method of quadratic extrapolation had to be used in the present table. Indeed, with the possibility of temperatures below freezing even after the condensation of the water vapor, the whole phenomenon becomes very complicated. Hence the values of N in table 27 are mere estimates for values of δp exceeding 20 cm.

It may be observed, in conclusion, that in all the above cases the X-radiation was cut off some minutes before the exhaustion, so that persistent nuclei are alone in question, to the exclusion of the fleeting nuclei discussed in the next chapter.

CHAPTER III.

CRITICAL CONDITIONS IN THE FORMATION OF IONS AND OF NUCLEI.

The present chapter is a close continuation of the last, and is separated from it for convenience in treatment. Dust-free air, energized or not by radiation, is always in question. The subject considered in the earlier paragraphs is a comparison of fleeting and of continuous nuclei and the passage of one form into the other either by increasing the strength or quality of the radiation, or by solution. The effect of both methods in changing the fleeting into the persistent form is possibly the same. Afterwards the inquiry is reversed and the radiation itself examined in terms of the nucleation produced. It is noteworthy that penetrating radiation is a powerful nucleator.

41. Apparatus—X-ray bulbs.—A number of medium-sized bulbs of German pattern, about 10 cm. in diameter with an anticathode 2 cm. in diameter, were used. The differences between these were no greater than the differences between the same bulb after varying periods of action. The table summarizes a few data. There seems to be a voltage at which the nucleation (N) produced is a maximum.

TABLE 28.—Comparison of different bulbs. Pressure difference $\delta p = 25$ cm. X-ray bulb 200 cm. from fog chamber. Exposure, 3 sec. Exhaustion during exposure. Bulbs 10 cm. diameter. Anticathode 2 cm. diameter, except No. 2, which was smaller.

Bulb.	Bulb vacuum.	Coronal aperture. s_1 .	Nucleation. $N \times 10^{-3}$.
No. 0 (used above).....	Low.	5.0-6.0	60-110
1.....	High.	5.5	87.6
2 (small)	"	5.5	87.6
3.....	"	5.8	101.0
4.....	"	5.8	101.0
4 with lead plate; 0.14 cm..	"	3.8	30.0

The radium referred to was a weak sample (10,000 \times), 0.01 gram of which inclosed in a hermetically sealed tube of thin aluminum (walls 0.1 mm. thick) sufficed for the experiments.

42. Fog chambers—Filters with saturator.—The long rectangular fog chamber (Chapter II, section 16) of capacity $v=13,000$ cc., having the volume ratio $v/V=0.13$ to the volume V of the vacuum chamber, was largely used. It is often difficult, however, to keep plate-glass windows perfectly tight. Hence the cylindrical fog chamber (length 45 cm., diameter 12 cm.) was substituted for it, in which case $v/V=0.06$. Both the former and the latter were often incased in sheet lead, 0.14 cm. thick, leaving merely an open strip in the broad-sides for observation of the coronas.

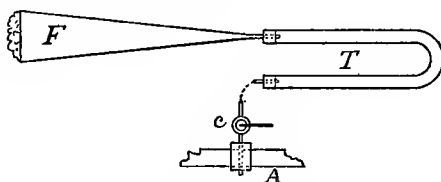


FIG. 40.—Filter with wet-sponge tube (saturator).

In view of the difficulties encountered in the preceding chapter, the attempt was finally made to counteract the effect of periodicity by saturating the filtered air with water vapor before introducing it into the fog chamber. To do this the U tube, figure 40, filled with pieces of wet sponge was added to the filter F , the filtered air from B entering the fog chamber very slowly by way of the stopcock C . This innovation seemed at first to be remarkably successful, as the results of table 29 on page 50 will show. Later, however, there was a very definite recurrence of periodicity, the true cause of which I ultimately traced to the inevitable formation of water nuclei. In addition to the filter mentioned, an ordinary dry-cotton filter and a Pasteur filter were often used; but the latter was soon discarded, as it gave no additional freedom from dust and prolonged the time of filtration inordinately.

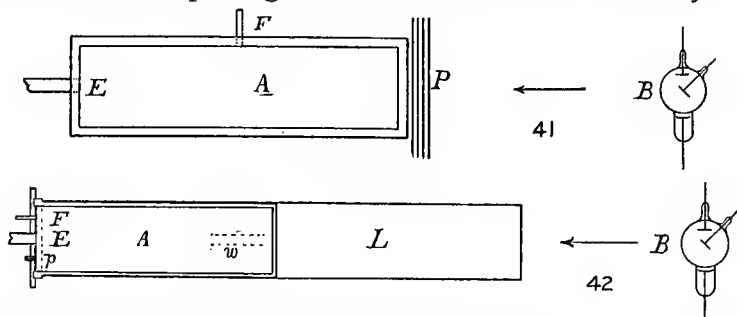


FIG. 41.—Rectangular wood fog chamber A , with screening lead plates P and X-ray bulb B , exhaust pipe E , and filter pipe F .

FIG. 42.—Cylindrical glass fog chamber A , with lead case L and bulb B . E is the exhaust pipe, F the filter pipe, p the plug for cleaning, and w the window.

43. Notation.—As above, the angular diameters, ϕ , of coronas will be given in terms of s , where $30 \times \sin \phi/2 = s/2$, as the arms of the goniometer are 30 cm. long; usually $\phi = s/30$, nearly. To secure clearer vision, the goniometer was moved up to the plate-glass window, placing the eye somewhat over 30 cm. off. The source of light, however, was left at 250 cm. from the trough, as above, and a correction applied for the distances.

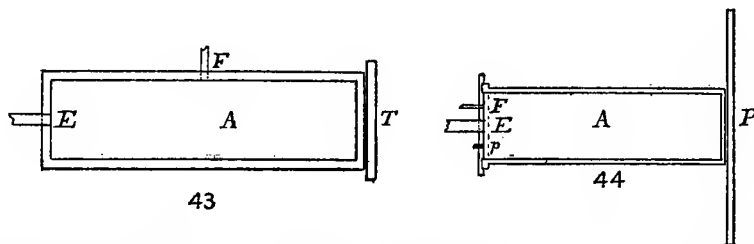


FIG. 43.—Rectangular fog chamber A , with lead tube T , filter pipe F , and exhaust pipe E .

FIG. 44.—Cylindrical fog chamber A , with lead tube P , exhaust pipe E , filter pipe F , and plug p .

In the tables, n usually denotes the number of nuclei per cubic centimeter of the exhausted air, N the number per cubic centimeter of the air at normal pressure and temperature. In successive exhaustions, without fresh nucleation, the apertures will be written $s_1 s_2 s_3 \dots$ and the nucleations corresponding $N_1 N_2 N_3 \dots$. If, however, fresh nuclei are added, or if the exposure to the radiation is continuous, $s_1' s_1'' s_1'''$ and $N_1' N_1'' N_1'''$ are usually used. The difference of pressure in centimeters of mercury between the inside and the outside of the fog chamber (taken at 76 cm.) is denoted by δp . Hence if p' is the vapor pressure of water vapor, the corresponding volume expansion is $(76 - p') / (76 - p' - \delta p)$. D denotes the distance of the source of radiations (X-ray bulb, etc.) from the end of the fog chamber nearest it. δp_0 usually refers to the fog limit, *i. e.*, the pressure difference, below which there is no condensation in saturated dust-free air, within the scope of measurements made by aid of coronas. L shows the time elapsed between the end of the exposure to radiation and the condensation.

EFFECT OF LARGE PRESSURE DIFFERENCES.

44. Nuclei in dust-free air not energized.—In table 29 periodicity has been all but wiped out, and the incoming and outgoing series lie as nearly on a curve as may be expected.

TABLE 29.—Fog limit and effect of pressure difference for combined filter and wet-sponge tube. Dust-free air, not energized.

δp .	s .	$N \times 10^{-3}$	δp .	s .	$N \times 10^{-3}$	δp .	s .	$N \times 10^{-3}$
24.8	2.3	5.2	2.2	5.3	24.7	1.3	2.4
.....	1.7	3.0	28.0	3.0	15.1	23.3	7	.0
.....	2.1	4.4	29.7	3.1	18.0	Pasteur filter dry.		
.....	2.1	4.4	3.0	16.4			
.....	2.1	4.5	33.0	3.0	18.4			
22.6	.0	.0	38.0	3.1	24.9	25.0	1.5	2.7
24.2	1.0	1.8	38.0	3.1	24.9	Cotton filter dry.		
25.5	1.4	2.5	33.8	3.2	24.1			
26.4	2.7	11.1	30.5	3.2	21.2			
.....	2.2	5.3	27.3	2.7	11.1	25.0	.8	1.4

The data for aperture, s , reach a limit as δp continually increases; but beyond the highest pressure difference applied, s will probably again decrease. N therefore must continually increase within the limits observed, but beyond them it will also eventually decrease (curves 45 and 46).

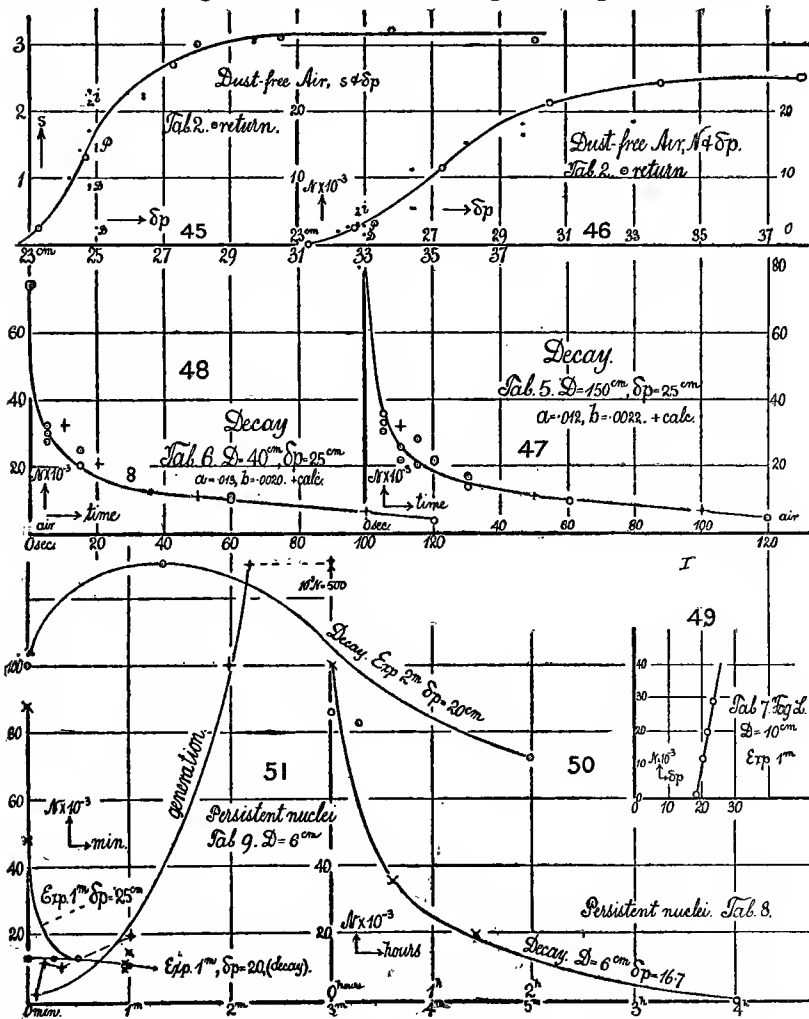
Incidental observations show the relative effect of a cotton filter without the sponge tube (D , figs. 45 and 46) and of the Pasteur filter, P . The former is apparently more efficient in its filtrations than the Pasteur filter, which has the additional disadvantage of being too slow for purposes of the present kind (period of influx prolonged over 10 minutes).

Curiously the fog limit of dust-free air is reduced by the sponge tube, lying in the given apparatus below $\delta p = 23$ cm. for rain and below $\delta p = 24$ for cloud. Such precipitations therefore cease when the volume increase on expansion in the two cases is respectively below 1.45 or just below 1.48, data which are naturally larger than C. T. R. Wilson's (Phil. Trans. Royal Soc. 1897, vol. 189, p. 265), in view of the differences of the apparatus employed. The reduced fog limit with the wet-sponge tube may be referable to increased supersaturation, but there is probably some specific cause yet to be investigated.* The highest nucleations observed lie within $N = 25,000$, which is very far below the conditions at which axial colors occur.

The following chart (figs. 45-51) illustrates tables 29, 32, 33, 34, 35, 36. "*Exp.*" refers to time of exposure to radiation; " δp ," to lapse of time after radiation ceases. D is the distance of the ionizer (X-ray bulb or radium tube) from the nearer end of the fog chamber.

* It will be shown elsewhere that the (*very slow*) rate of filtration is here essentially in question.

δp is the pressure difference observed after exhaustion. The ordinates are often merely distributive or show the number of an observation in a series. The fog chambers are wood or glass as specified,



In the above chart the terms tables 2, 5, 6, 7, 8, 9 refer to the tables in text now numbered 29, 32, 33, 34, 35, 36.

45. Dust-free air energized by the X-rays from a distance.—In table 30 data are given for the case of dust-free air feebly energized by the X-rays, the filter having the same sponge-tube attachment. I was not at the time aware of the rapid decay of the nuclei or ions produced by these means, and about one-half minute was allowed to elapse after

the exposure to the radiation before the observation was taken. The resulting apertures are thus reduced, about two-thirds of the nucleation having vanished; but they are otherwise comparable and much smoother than in the absence of a lapse of time, L , between the end of the exposure and the condensation. Two successive exhaustions are often made for the same exposure, for which N_1 and N_2 are the nucleations reduced to air at normal pressure.

TABLE 30.—Fog limit and effect of pressure difference for combined filter and wet-sponge tube. Dust-free air energized by X-rays. Observation after lapse of about 30 seconds.

Part I.—Bulb 80 cm. from end of fog chamber; exposure, 3 min.					Part II.—Bulb 150 cm. from end of fog chamber; lapse, 30 sec.				
δp .	s_1 .	s_2 .	$N_1 \times 10^{-3}$	$N_2 \times 10^{-3}$	δp .	s_1 .	s_2 .	$N_1 \times 10^{-3}$	$N_2 \times 10^{-3}$
20.9	2.1	3.6	20.9	r 1.7	$\dagger r$ 1.5	2.5	2.3
24.8	4.0	*2	32.0	3.8	24.8	3.9	1.3	29.6	2.3
28.9	4.0	3.1	38.7	17.4	28.9	3.7	33.0
33.0	(†)	3.2	23.2	33.0	4.0	2.9	47.2	16.6
37.1	4.0	53.3	37.1	3.7	3.0	45.4	21.7
41.2	3.7	53.8	41.2	3.1	3.2	\S 30.4	32.4
37.1	3.7	45.4	41.2	3.3	37.4
33.1	4.1	49.3	41.9	3.2	45.2
28.9	3.8	35.8	48.0	2.8	23.1
24.8	3.8	30.0	37.1	3.3	30.6
20.9	1.8	2.6	33.0	3.5	33.5
19.2	.00	28.9	3.8	2.7	35.8	11.7
19.7	.8	1.1	24.8	3.3	r 1.0	18.3	1.8
22.1	3.0	.0	11.3	.0	24.8	** 1.3	2.4
					24.8	$\dagger\dagger$ 5.4	83.4
					24.8	$\dagger\dagger$ 3.8	30.0

* Air nuclei. † Nonenergized air. ** Lapse, 3 min. †† Lapse, 30 sec.
 ‡ Accidental delay. § Same as air not energized. †† Lapse, 0 min.

In the first part of the table (curves 52, 53), while the values of s_1 and s_2 reach a limit, the nucleations N_1 and N_2 continually increase and are about $N=25,000$ apart throughout the whole range $\delta p=25$ to 41 cm. N_1 shows the number of nuclei left in dust-free air about half a minute after exposure to the X-rays; N_2 presents the case of dust-free air.

The second part of the table is irregular. The mean curves, however, preserve the same relations at first, the nucleations of the energized air being 25,000 in excess. Toward the end of the curves both the energized and nonenergized air show apparently decreased nucleation, while the former falls to the low values due to the normal air nuclei alone. The X-ray excess has been quite wiped out at $\delta p=41$ cm.

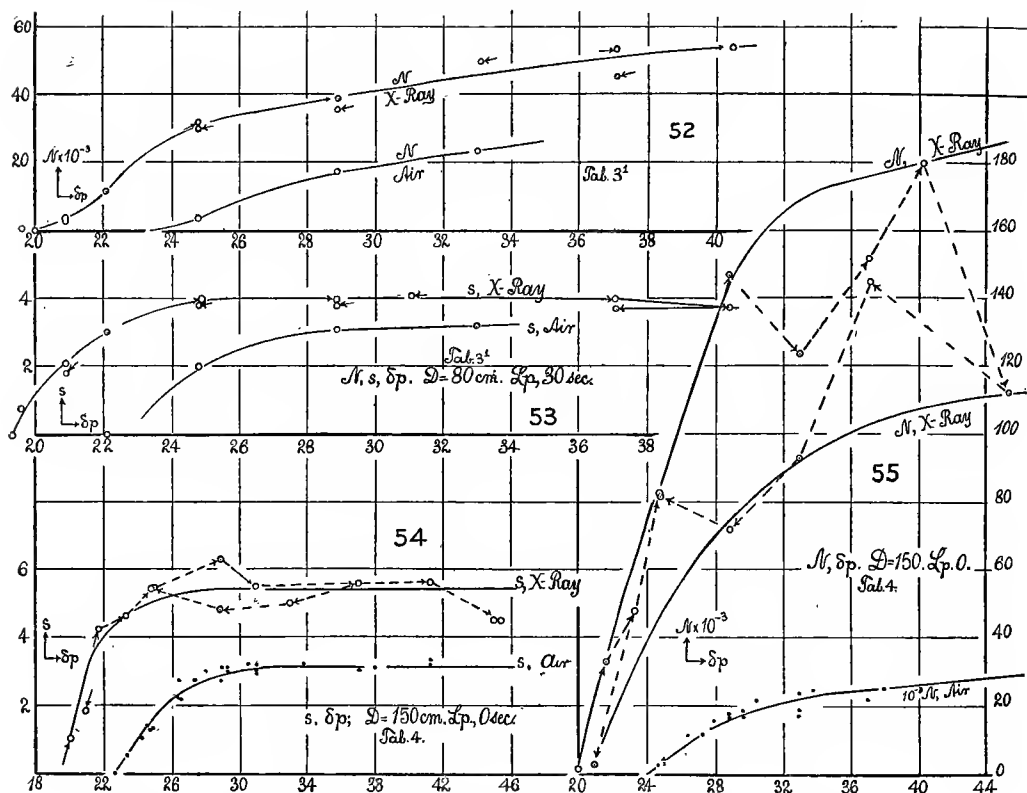
At the end of the table the preponderating effect of lapse of time after exposure is indicated. All excess of nuclei is gone after 3 minutes, while the original excess of 83,000 is reduced almost two-thirds in half a minute.

46. Continued—Rays not cut off during condensation.—Table 31 (curves 54, 55) contains data for the coronal apertures obtained without cutting off the radiation until after condensation has been produced. The two minutes' interval of exposure is excessive (as the following paragraphs show) when weak radiation (distance of X-ray bulb from end of fog chamber, $D=150$ cm.) is in question. The results in table 31 are distributed cyclically, and the return series shows less nucleation in general than the outgoing series. This is attributable to the gradual temporary loss of efficiency of the X-ray bulb. Similarly the fog limit is slightly below 20 cm. in the outgoing series and slightly below 21 cm. in the return series, the rise being toward the nonenergized dust-free air ($\delta p_0 = 24$ cm.).

TABLE 31.—Fog limit and effect of pressure difference for combined filter and wet-sponge tube. Dust-free air energized by X-rays. Bulb 150 cm. from end of fog chamber. Exposure, 2 min. Observation taken *during* exposure, or lapse, 0 sec.

$\delta p.$	$s_1.$	$s_2.$	$N_1 \times 10^{-3}$	$N_2 \times 10^{-3}$	$\delta p.$	$s_1.$	$s_2.$	$N_1 \times 10^{-3}$	$N_2 \times 10^{-3}$
20.0	1.0	1.3	45.4	4.5	112
21.7	4.2	32.5	47.2	3.3	36.3
23.3	4.6	47.5	37.1	5.5	144.1
24.8	5.4	82.2	33.0	5.0	92.7
28.9	6.3	147.0	28.9	4.8	71.7
33.0	5.5	123.1	24.8	5.4	82.3
37.1	5.6	151.3	20.9	1.8	2.6
41.2	5.6	179.4					

In addition to this, the outgoing and the return series show a curious case of periodicity which may or may not be real; but it is probable that there is decreased nucleation after δp exceeds 40 cm. The initial increase of N with δp is nearly straight and exceedingly rapid ($\delta N/\delta p = 15,000$, nearly). This is somewhat greater than the above values for radium (about 12,000), but of the same order as the datum for weak X-ray radiation. The corresponding data for dust-free nonenergized air, given in the same chart, show that initially $\delta N/\delta p = 5,000$, nearly, in correspondence with the earlier data so far as can be made out. The nucleations N are throughout small as compared with energized air, the excess in the latter case, if mean values be taken, being of the order of 100,000 nuclei per cubic centimeter.



FIGS. 52-55.—Illustrating tables 30, 31.

Tab. 3, in the above chart, is replaced by the present table 30 in the text; Tab. 4, by the present table 31.

GENERATION AND DECAY OF NUCLEI.

47. Fleeting nuclei.—This brings the work to the main purposes of the present paper, viz, to compare the generation and decay of the nuclei produced by the X-rays when the density of ionization or of electrification has different values. It was shown conclusively above that with strong radiation the nuclei persist for hours, and it follows from the foregoing paragraphs that for weak ionization they are fleeting. Hence there must be transitional conditions, and these are to be investigated, both for the production and for the decay of nuclei.

With such an end in view a strong X-ray tube may be placed at different distances from the end of the fog chamber and the results referred to the nucleation within, or the same bulb in the efficient and the partially fatigued condition may be placed at a fixed distance near the apparatus. The second method is usually inseparable from the first.

Data are given in table 32 *et seq.*, the pressure difference being chosen at the fog limit of dust-free air, which under these conditions contributes but a few per cent of the nuclei. The first part of table 32 shows that the origin of nuclei is practically instantaneous. Within 5 seconds after the radiation from the X-ray bulb (placed at $D=150$ cm.) begins, the air within the fog chamber is saturated with nuclei (curve 47).

Decay is not quite instantaneous, but enormously rapid as compared with the case for intense radiation of the preceding chapter. The number of nuclei per cubic centimeter is reduced one-half in about 2 seconds and reduced one-fifth in 20 seconds. After 120 seconds the nucleation of dust-free air is practically regained. The decay is not apparently exponential in character. If $N=N_0 e^{-at}$, the data of tables 32 and 33 are badly reproduced. With $N=N_0/(1+b't)$ or $1/N=a+b't$, the agreement is as good as the observations. Hence $-dn/dt=bn^2$, or the decay is as the square of the number, showing that the destruction is mutual between the nuclei as if they were positive and negative ions.

TABLE 32.—Generation and decay of the nuclei. X-radiation, bulb at $D=150$ cm. $\delta p=25$ cm. Filter and wet-sponge tube.

I. Generation.			II. Decay.		
Time of exposure.	s.	$N \times 10^{-3}$	Time after exposure.	s.	$N \times 10^{-3}$
<i>Sec.</i>			<i>Sec.</i>		
* 0	1.5	3.0	10	3.6	25.0
30	5.3	79.0	15	3.7	27.6
15	5.5	87.6	15	3.6	25.0
† 5	5.4	83.4	20	3.4	21.2
* 0	1.0	1.8	20	3.4	21.2
II. Decay.			0	5.6	92.0
Time after exposure.	s.	$N \times 10^{-3}$	30	† 2.0	3.8
			30	3.0	13.2
Time after exposure.	s.	$N \times 10^{-3}$	30	3.2	16.6
			30	3.2	16.6
Time after exposure.	s.	$N \times 10^{-3}$	60	2.6	9.2
			60	2.6	9.2
Time after exposure.	s.	$N \times 10^{-3}$	120	2.2	5.0
			120	2.1	4.4
Time after exposure.	s.	$N \times 10^{-3}$	0	5.4	83.4
			0	† 4.8	60.0
Time after exposure.	s.	$N \times 10^{-3}$	0	4.8	60.0
			5	† 3.2	16.6
Time after exposure.	s.	$N \times 10^{-3}$	5	4.0	32.4
			5	4.0	32.4

* Dust-free air not energized.

† Nucleation produced instantly.

‡ Note the low apertures after full corona.

TABLE 33.—Continuation of the preceding. Bulb at 40 cm. $\delta p = 25$ cm.

I. Generation.			III. Decay.		
Time of exposure.	s.	$N \times 10^{-8}$	Time after exposure.	s.	$N \times 10^{-8}$
<i>Sec.</i>			<i>Sec.</i>		
0	0.8	1.4	5	3.8	30.0
60	5.2	74.4	5	4.0	32.4
15	5.2	74.4	5	3.7	27.6
* 5	5.2	74.4	15	3.4	20.4
0	8.8	1.6	3.6	25.0
II. Fog limit at 20 cm.			60	2.7	10.0
			2.8	11.0
			120	2.0	3.8
			30	3.3	18.6
δp	3.2	16.6
			0	5.6	92.0
21.6	3.0	11.1			
20.1	1.5	2.2			
18.4	0.0	.0			

* Nucleation produced instantly.

TABLE 34.—Continuation of the preceding. Bulb at 10 cm.

Time of exposure.	s.	$N \times 10^{-8}$	Time after exposure.	s.	$N \times 10^{-8}$	Time of exposure	s.	$N \times 10^{-8}$
I. Generation. $\delta p = 20.1$. (Rays on.)			II. Decay. Exposure 60 sec. $\delta p = 20.1$.			IV. Generation. $\delta p =$ 24.8. (Rays on.)		
<i>Sec.</i>			<i>Sec.</i>			<i>Sec.</i>		
15	2.1	3.4	15	1.7	2.5	5	4.0	34.4
60	3.1	11.4	10	1.9	3.0	5	4.5	48.0
120	3.4	15.9	5	2.3	4.2	60	4.5	48.0
5	1.9	2.8	0	3.1	11.4	5	4.5	48.0
5	2.0	3.0				60	4.7	56.0
15	3.2	? 12.9						
5	1.2	1.7	δp .	s.	$N \times 10^{-8}$	V. Generation. $\delta p =$ 20.1.		
5	.0	.0						
5	.0	.0						
30	2.8	8.6						
30	2.3	4.2	III. Fog limit. 1 min. exposure. (Rays on.) Fog limit, 18 cm.			<i>Sec.</i>		
60	3.0	10.3				15	2.1	3.4
120	3.4	15.9				60	3.1	11.4
			20.1	3.1	11.4	120	3.4	15.9
			18.4	.8	.8			
			21.6	3.5	19.2			
			23.3	3.9	28.5			
			24.8	4.9	63.0			

If N be expressed in thousands per cubic centimeter, the following is a summary of the results obtained:

	0 sec.	20 sec.	60 sec.
First series, $a = 0.0128$, $b = 0.0020$...	observed..... 78	19	8
	calculated..... 78	19	7
Second series, $a = 0.0120$, $b = 0.00218$	observed..... 83	18	7
	calculated..... 83	18	7

The effect of periodicity is still in evidence, seeing that the large coronas are apt to be followed by relatively small coronas. Some special results are given in the table. The coronas at these distances are round, but blurred, showing the occurrence of nuclei of all sizes.

At $D = 40$ cm. (table 33 and curve 48), the results are not essentially different. The X-ray bulb is weak at first, but seems to recuperate in the course of the work. In other respects the two curves are essentially the same, as the above data show. In spite of the variability of the X-ray bulb, the insignificant differences of nucleation in these two cases are astonishing, for the distances vary from 40 to 150 cm. The law of inverse squares would predicate a fourteen-fold decrease. In fact, the same anomalous result seems to hold quite up to the fog chamber, as suggested in the data of table 34.

The bulb in table 34 is unfortunately weaker, showing only about half the nucleation of the preceding case ($N=48,000$ at $\delta p=24.8$ cm., for instance) in spite of greater nearness ($D=10$ cm.). The earlier data may have been larger, $N=63,000$ being among these. The fog limit has been definitely reduced from 20 cm. to 18 cm.

Generation is now no longer instantaneous; certainly not at $\delta p = 20.1$, though the data at the larger pressure difference $\delta p = 25$ are not decisive. It takes at least 2 minutes for the given radiation to saturate the air with nuclei corresponding to $\delta p = 20.1$. (See curve 51.)

In conformity with the slow generation of nuclei the period of decay is now definitely prolonged. In 3 to 4 minutes the nucleation is reduced one-half.

48. Persistent nuclei.—The data for stronger radiation, showing remarkably persistent nuclei by comparison, have already been given in Chapter II, section 37 *et seq.*, and are repeated in the annexed curve (50). Roughly, the reduction is one-half in about 10 minutes and four-fifths in 80 minutes, contrasting sharply with the reductions in 2 seconds and 20 seconds, respectively, in the case of weak ionization.

TABLE 35. —Data for persistent nuclei. $D = 6$ cm.

Time of exposure.	Time after exposure.	δp .	s_1 .	s_2 .	$N_1 \times 10^{-3}$.	$N_2 \times 10^{-3}$.
<i>Min.</i>	<i>h. m.</i>					
3	0	13.5	* 7.0	3.5	86.0	12.7
	0 16	13.5	6.9	3.0	82.9	6.8
	4 0	13.5	.0	.0	.0	
3	0	16.7	*Spindle.	5.6	(100)	60.0
	36	16.7	4.7	1.5	36.4	1.8
	1 25	16.7	3.8	1.2	19.5	1.5

* Distorted.

Assuming the above equation $1/N = a + bt$, or $-dN/dt = bN^2$, for which, however, there is no immediate justification here and which does not fit well, values of the order of $a = 0.01$ and $b = 0.00001$ follow. The decay is thus shown to be several hundred times slower than above, under like assumptions.

In table 36 and curve 51 specific results for the generation and decay of nuclei have been added, obtained with a bulb strong at first, but eventually losing intensity below the necessary limit. The first part of the table shows a law of generation increasing with the time of exposure at an accelerated rate, consistently throughout the 180 seconds of observation. The remaining conditions have already been investigated in Chapter I. Measurement is difficult because of the distorted coronas, which soon become densely stratified fogs. The pressure difference used ($\delta p = 20$ cm.) is below the fog limit for air.

The curve (51) for nucleation (N) shows an enormously rapid increase after 1 minute of exposure, as though the nuclei themselves became radio-active, temporarily. This increase is sustained even if the radiation is cut off. (Section 56.)

The results for decay, in case of the persistent nuclei here obtained, are complicated and must be given in curves. In the second part of the table the minute exposures show but slight, if any, decay, in the absence of radiation, after the lapse of 1 minute. The 2-minute exposures actually seem to show increased nucleation in the minute succeeding exposure (secondary radiation, section 16); but in the ensuing 5 minutes after radiation, decay is manifest (curve 51). The behavior of the fatigued X-ray bulb may be contrasted with this, in the same position (part IV). The nuclei vanish as in the third part of the table, in spite of the 2-minute exposures as compared with the

1-minute exposures of the former case; and these inferences are corroborated by the last observation (part V) at the original low $\delta p = 20$ cm.

TABLE 36.—Continuation of the preceding. Bulb at 6 cm.

Time of exposure. (Rays on.)	Time after exposure. (Rays off.)	δp .	s_1 .	s_2 .	$N_1 \times 10^{-3}$.	$N_2 \times 10^{-3}$.
I. Generation.						
5 sec.	0 sec.	20.1	1.8	2.5
10	0	3.1	11.4
20	0	3.0	10.3
60	0	3.6	19.5
180	0	Strata (9.4)	5.5	(500)	68.3
60	0	3.6	19.5
120	0	Strata (5.4)	3.2	(100)	12.9
II. Decay.						
60	0	20.1	3.2	12.9
60	15	3.2	12.9
60	30	3.2	12.9
60	60	*2.8	(4.4)
60	120	*3.0	10.3
120	120	Strata (6.0)	3.5	(130)	17.6
120	300	†5.6	3.0	71.8	10.3
III. Decay. Larger δp .						
60	0	24.8	5.5	87.6
60	60	3.1	14.6
60	0	4.5	48.0
60	0	4.5	48.0
60	60	2.6	9.2
60	60	2.8	11.0
IV. Decay.						
120	60	24.8	2.9	11.8
120	0	‡5.0	66.0
<hr/>						
Bulb tested } 120	0	20.1	‡2.4	5.1

* Coronas distorted with much rain. Heavy fogs near bottom. Coronas more blurred and foggy as the time after exposure increases.

† Corona after 5 minutes' waiting, round; not stratified, but blurred.

‡ Bulb too weak for strata. Ionization density below entrance valve.

A comparison of the 1-minute exposures in parts II and III is noteworthy (curve 51). The high-pressure difference in part III ($\delta p = 25$) catches over four times as many nuclei as the low-pressure difference ($\delta p = 20$), *cætl. par.*, but the excess vanishes at once to the value of those within the reach of $\delta p = 20$ cm. Hence evanescent and persistent nuclei are always present together.

49. Persistence of fleeting nuclei after solution.—A result occurring throughout the observations is the following: Whether the nuclei are fleeting in character or not, there is invariably a second strong corona. This is obtainable on the succeeding exhaustion without fresh nucleation, even if the fog particles of the first corona are allowed to completely subside, before the addition of the dust-free air prior to the second exhaustion. If there were no first exhaustion during the exposure of the fog chamber to the radiation, no nucleation would have been found after the lapse of time needed preparatory to the second exhaustion. The reevaporation of fog particles from the first exhaustion, in every case changes about one-eighth of the fleeting nuclei into the stable nuclei observed in the second corona. This is obviously an important observation, bearing on the whole phenomenon of nuclei, condensation and rain.

To investigate this case the data of table 37 were collected, in which, as soon as possible after first condensation, dust-free air is admitted into the fog chamber to dispel the fogs by evaporation. When this is done the coronas on second exhaustion are invariably larger and denser (curves 56, 57), showing that more nuclei have been preserved, *i. e.*, converted from the fleeting into the stable form. The only effect producible by the premature influx is to diminish the number of fog particles lost by subsidence. It follows, then, that all nuclei upon which condensation has once taken place become stable nuclei.

It is somewhat difficult to measure the first corona and at the same time to provide for a quick influx of air so that but little subsidence of fog particles may take place. The data of table 37, therefore, quite apart from periodicity and other difficulties, can not be expected to be very uniform. It was not thought necessary to prolong the interval of persistence (time from influx of air to second exhaustion) beyond a few minutes, for these suffice to indicate persistence. The table shows that from 25 to 50 per cent of the nuclei may be preserved indefinitely by reevaporating them from fog particles. The mean datum of all results apart from the time interval entering the test is actually 39 per cent.

TABLE 37.—Showing that fleeting nuclei become stable on solution. Rectangular wooden fog chamber in lead casket. $\delta p = 25$ cm. Exposure to X-rays, 3 sec. Distance of X-ray bulb, 200 cm. Mere rain denoted by r .

Time elapsed after exposure to first exhaustion.	Time elapsed from first ex- haustion to influx.	Time elapsed from influx to second ex- haustion.	s_1 .	s_2 .	s_3 .	$N_1 \times 10^{-3}$.	$N_2 \times 10^{-3}$.
---	--	---	---------	---------	---------	------------------------	------------------------

Part I.

Sec.	Sec.	Sec.					
o	o	60	4.7	3.3	*1.7	56.0	18.6
o	o	60	3.3	1.7	(49)	18.6
o	o	60	(4.3)	3.1	r	41.0	14.6
o	o	60	3.8	2.9	r	30.0	11.8
60	60	1.9	r	3.6
60	60	1.7	r	3.0
o	o	60	4.4	3.4	r	44.0	20.4
o	o	120	3.8	2.8	r	30.0	10.4
o	o	300	4.7	3.1	r	56.0	14.6

Part II.

o	o	60	4.3	3.2	r	41.0	16.6
o	o	60	3.9	2.9	r	31.2	11.8
o	o	60	3.4	2.6	r	20.4	9.8

Part III.

o	o	60	4.5	3.2	r	48.0	16.6
o	o	120	3.7	2.9	27.6	11.8
o	o	60	3.0	2.5	o	13.2	8.0
o	o	120	4.7	3.0	r	56.0	13.2

Part IV. Cylindrical glass fog chamber. $\delta p = 22$. $D = 10$ cm.

o	o	120	5.0	2.9	r	66.0	11.8
o	o	60	5.7	3.4	r	96.4	20.4
o	o	180	5.2	3.0	r	74.4	13.2
60	60	2.0	r	3.8	1.8
120	60	1.0	r	1.8	1.8
o	o	300	†6.7	3.7	r	146.6	27.6

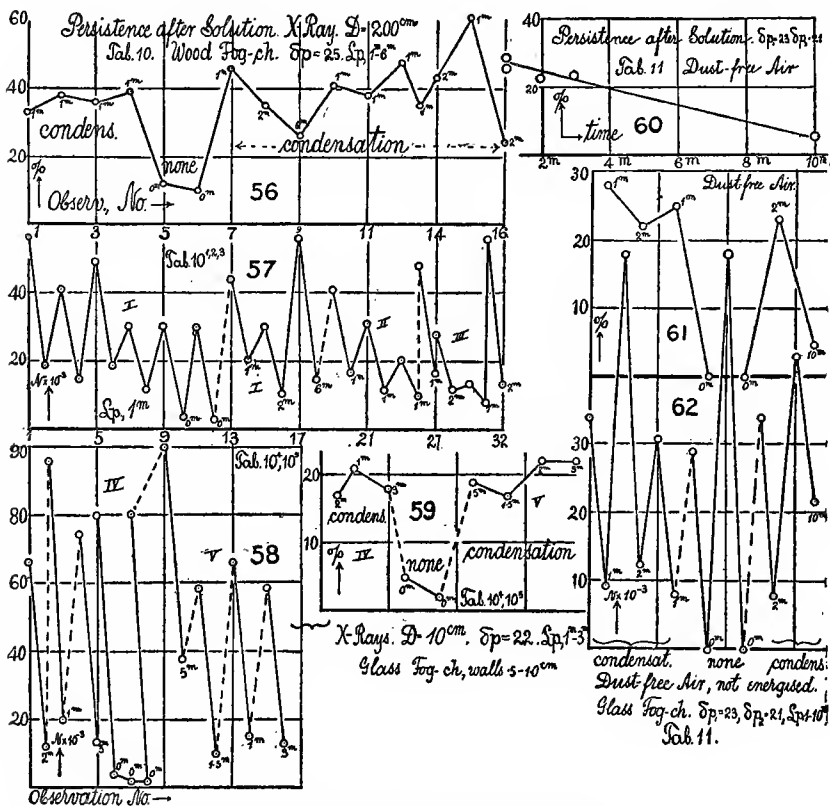
Part V.

o	o	90	5.0	2.8	58.4	9.7
o	o	60	5.2	3.2	65.8	14.7
o	o	180	5.0	3.1	58.4	12.9

* Representing about 3,000 nuclei due to nonenergized, dust-free air.

† Persistence tested but not found (2-minute exposure, 1-minute lapse, $s = 1.0$).

The data of table 37 were at first obtained in the wooden fog chamber. It was thought advisable to repeat them with the cylindrical glass fog chamber, as this could be kept rigorously free from leakage (curves 58, 59). The mean results show that about 20 per cent of the particles persist indefinitely. This datum, which in any case is an inferior limit, is smaller here, because the amount of subsidence is relatively greater in a more shallow vessel. Without condensation, *i. e.*, in the absence of solution, only 2 to 5 per cent of the nuclei persist after 1 minute. With solution, the decay is not appreciably different in 1 to 3 minutes, showing that long periods of persistence are in question.



FIGS. 56-62.—Illustrating tables 37, 38.

Tab. 10 in the above chart is replaced by the present table 37; Tab. 11, by the present table 38.

50. Enlargement of nuclei in dust-free nonenergized air.—An exceedingly interesting correlative result is obtained by converting the nuclei of dust-free nonenergized air into solutional nuclei. Here the first exhaustion must necessarily be made at a pressure difference (say

$\delta p = 23$ cm. in the cylindrical apparatus) decidedly above the fog limit, so that a corona of appreciable size may appear. If this is dispelled on admission of filtered air by evaporation, the second corona may be obtained at a pressure difference ($\delta p = 21$ cm. in the table) below the fog limit, showing that large nuclei have been produced by evaporation. In the data of table 38, or in curves 61, 62, different intervals of waiting are tested, these intervals referring to the time elapsed (1 to 10 minutes) between the evaporation of the first corona and the condensation of the second. After 3 minutes about 25 per cent of the nuclei persist and require smaller exhaustions to induce condensation than the original nuclei. After 10 minutes about 5 per cent are left (curve 60), though a greater number of observations are here desirable. It should be noticed that without the preliminary condensation no condensation whatever would take place at the lower pressure difference.

TABLE 38.—Persistence in solution. Air nuclei. Fog chamber glass cylinder.
 $\delta p_2 = 23.2$; $\delta p_1 = 21.4$.

Time from first exhaustion at $\delta p = 23.2$, to influx.	Time from influx to second exhaustion at $\delta p = 21.4$.	s_1 .	$*s_2$.	$N_1 \times 10^{-3}$.	$N_2 \times 10^{-3}$.	Ratio.
<i>Sec.</i>	<i>Sec.</i>					
0	60	4.2	2.8	34	9.4	.28
0	120	4.9	3.1	58	12.4	.22
0	60	4.1	2.6	31	7.8	.25
† 60	30	4.0	0	29	.0	0
60	30	4.9	0	58	.0	0
0	180	4.2	2.6	34	7.8	.23
0	600	4.5	1.3	43	2.2	.05

* $s_3 = 0$ always tested.

† Sufficient for complete subsidence.

51. Occurrence of water nuclei.—An explanation of the phenomena of the preceding paragraphs is not far to seek. Clearly the ions or fleeting nuclei go into solution, and the result on reevaporation of the fog particles is a solutional or water nucleus. Such a nucleus is obviously larger than the original nucleus or ion which furnishes the solute. Hence the condensation in the succeeding exhaustion must first take place on these residual nuclei, and they are therefore apt to capture all the available water. What makes the water nucleus stable is either the solute, by which the vapor pressure is reduced on continued evaporation to a degree equal to the excess of vapor pressure due to curvature, or possibly electrical potential may have a corresponding effect.

It is particularly interesting that if the nuclei or dust-free nonenergized air become the solute of water nuclei, that the new nuclei require pressure differences much below the fog limit of the original air for condensation, and the solutional nuclei are stable.

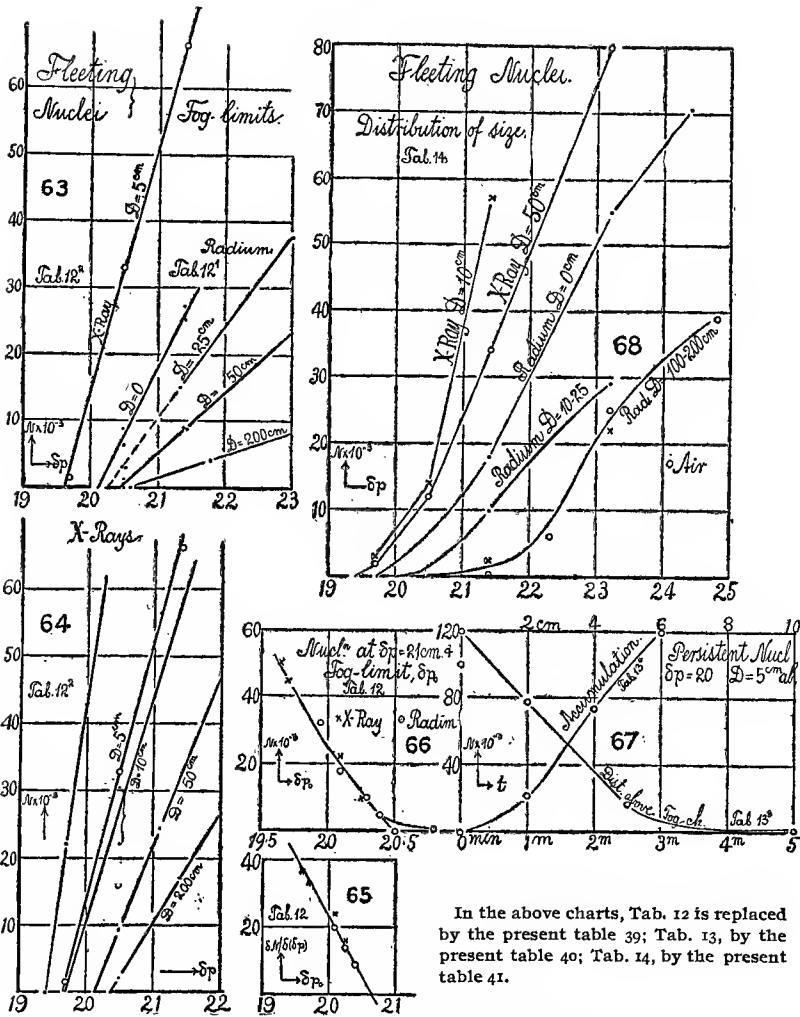
52. Cause of periodicity.—Very many of the occurrences which accompany condensation may be explained by the result just announced. In particular the alternations of large and small coronas (*cf.* Chapter II, sections 24, 27) so frequent throughout the present work are fully accounted for. The small fog particles, *i. e.*, those condensed on the smaller nuclei and caught near the end of the exhaustion, evaporate into the larger particles and become the water nuclei available in the next exhaustion.* Hence if the other condensation nuclei are all small, like those due to weak radiation or those normally present in air, the next condensation will take place on the water nuclei only. Thus a small inferior corona follows the large superior corona of the primary exhaustion. In the next exhaustion water nuclei will be absent, relatively speaking, and the condensation now occurs on all the small nuclei available for producing a large superior corona; and so on in succession. In general there are thus three groups of nuclei, x, y, z , concerned in any given condensation—a group, x , of water nuclei from the preceding exhaustion; a group, y , of nuclei belonging to the condensation in question and corresponding to the observed superior coronas; a group, z , of nuclei belonging to the same condensation, but which will evaporate their water and make the water nuclei for the next condensation. In case of periodicity the successive exhaustions would run,

1.	y_1	z_1	Superior corona on y_1 .
2.	$x_2 = z_1$	$z_2 = 0$	Inferior corona on x_2 .
3.	$x_3 = z_2 = 0$; $y_2 + y_3$	z_3	Superior corona on $y_2 + y_3$.
4.	$x_4 = z_3$	$z_4 = 0$	Inferior corona on x_4 .
5.	$x_5 = z_4 = 0$; $y_4 + y_5$	z_5	Superior corona on $y_4 + y_5$.

etc. If the nuclei are fleeting the superior corona of the n -th exhaustion is condensed on y_n only, and under these circumstances, $y_n + z_n$, the total nucleation may often be replaced by $x_n + y_n$, or the total nucleation is the sum of the values belonging to the superior and inferior coronas. In this way the analysis of Chapter II, sections 28, 29, admits of easy interpretation.

53. Rain.—In any exhaustion the group $z_n = x_{n+1}$ are accountable for the rain which almost always accompanies coronal display. In such cases the water nuclei are comparable in smallness with the other nuclei, and the former are not able to capture all the available water.

* Incidentally the medium is kept saturated while temperature rises after exhaustion.



FIGS. 63-68.—Illustrating tables 39, 40, 41.

54. Persistent nuclei in general.—It is not improbable that persistency may generally be due to some cause favorable to the production of water nuclei.* Those heavy rains, for instance, which accompany the X-ray corona when the bulb is close to the fog chamber may be due to the fact that condensation occurs spontaneously *without* the need of supersaturation, if an exposure to very intense X-light is in question. The nuclei in the X-field behave like hygroscopic bodies.

* For more detailed statements see my investigation on the "Structure of the Nucleus," Smithsonian Contributions, No. 1373, 1903.

TABLE 39.—Fog limits of fleeting nuclei. Cylindrical fog chamber, without casket.
 $s_2 = 0$, but tested.

Exposure to—	Distance.	δp .	s_1 .	s'_1 .	$N_1 \times 10^{-3}$.	$N'_1 \times 10^{-3}$.
I. Radium in aluminum . .	<i>cm.</i>					
	50	21.4	2.7	2.7	8.7	8.7
	20.5	.0	1.0	.0	1.4
	25	20.5	2.0	2.0	3.0	3.0
	19.7	.00
	0	20.5	2.8	2.5	8.8	6.4
	19.7	.0	.0	.0	.0
	21.4	3.9	4.0	25.2	27.2
	200	21.4	3.4	17.1
	20.5	1.4	2.1
II. X-rays.....	50	20.5	3.4	2.9	16.3	9.4
	19.7	.0	.0	.0	.0
	10	20.5	4.2	3.7	30.4	22.1
	19.7	.0	.0	.0	.0
	5	20.5	4.3	32.8
	19.7	<i>r</i>	.0	1.4
	20.5	3.0	10.6
	21.4	5.3	66.3

TABLE 40.—Fog limits of persistent nuclei. Bulb above.

Exposure to—	Height of bulb.	δp .	s_1 .	s_2 .	N_1 .	N_2 .	Remarks.
III. X-rays, 3^m ..	<i>cm.</i>						
	.5	18.0	(*)	3.1	(83)	10.2	Radiation through earthed aluminum plate. Do. Do. Do. Do.
	.5	18.0	†(8.6)	3.5	(118)	15.8	
	2.0	18.0	†(6.1)	3.2	(78)	11.6	
	5.0	18.0	* 3.6	2.2	17.5	3.5	
	10.0	18.0	<i>r</i>	.0	1.4	
IV. X-rays.....	3.0	18.0	† 2.4	4.6	
	.5	18.0	00	.0	Exposure, 1 min.
	.5	19.7	3.8	<i>r</i>	22.2	1.5	Do.
	.5	19.7	* 5.8	2.0	17.2	2.9	Exposure, 2 min.

* Oblong corona.

† After this, bulb (?) ceases to be efficient.

† Spindle or gourd-shaped corona.

Radium,	<i>cm.</i>	<i>cm.</i>	$\delta N/\delta(\delta p) = 9 \times 10^{-3}$.	$N(\text{at } \delta p = 21) = 5 \times 10^{-3}$.
	$D = 50$	Fog limit = 20.4		
	25	(20.3)		
	0	20.1		
X-rays,	200	20.3	(14)	10
	50	(20.1)		
	10	(19.7)		
	5	19.6		

55. Gradation of size of fleeting nuclei—Fog limits.—The preceding observations, as well as the work of Chapter II, section 34, figure 34, make it probable that the fog limit varies slowly but definitely with the density of the ionization, while the rate, $\delta N/\delta(\delta p)$, or slope of the

curves, *i. e.*, the increment of nucleation per centimeter of pressure difference, increases very rapidly. It makes little difference how the ionization is produced, whether by instantaneous exposure to the X-rays or to other radiation. In fact, the curves become nearly vertical in relative steepness. Additional experiments are nevertheless needed, and table 39 contains such results. In the first part radium (10,000 \times) in the thin aluminum tube is the energizer; in the second part, the X-rays perform a similar function more strongly. The results may be summarized in curves 63, 64, 65, 66, and as follows:

Both series are in general agreement and indicate the extremely slow depression of the fog limit (indicating the nuclei of maximum size) with the increase of number, $\delta N/\delta(\delta p)$ (fig. 65). In fact, the method for measuring δp is rather too crude to bring out the fog limits properly. They may be found from two consecutive measurements of N for two values of δp close together and near the fog limit. Figures 65 and 66 contain a comparison between the fog limits, δp_0 , and $\delta N/\delta(\delta p)$, as well as N for $\delta p = 21$ cm., below the fog limit of dust-free air. They show the accentuated variation of the nucleations; but they announce also the decided variation of the fog limits for the case of fleeting nuclei, *i. e.*, that the maximum size of nucleus is a variable quantity among the gradations.

The last part of the table shows data for the persistent nuclei (curves 67). These were produced here by placing the bulb above one end of the cylindrical fog chamber, for the glass at the bottom was too thick to admit a sufficiently intense radiation. The inevitable difficulty in the investigation of these results is the weakening of the X-ray bulb in continued use. In a measure, this is a proof that electrical resonance or any more direct induction is not operative, for these effects would not vary with the past history of the bulb. Nevertheless, to avoid the possibility of such disturbances an earthed sheet of aluminum was adjusted to cover the top of the fog chamber. Experiments showed that all these precautions are unessential.

The curves (67) show the rapid decrease of the number of persistent nuclei with the height of the bulb (measured from the outside) above the cylindrical glass chamber (walls 0.3 cm. thick). They also show the extremely rapid increase of the nucleation with the time of exposure, suggesting radio-activity on the part of the nuclei as stated in section 56.

In table 41 the endeavor was made to determine the fog limit from two observations of N lying slightly above it. The work was very carefully done, but the data nevertheless fail to mark out definite loci. Beginning with the coronas for nonenergized air* (radium at infinity),

*The curve for air in case of high pressure differences is very difficult to determine, and will again be treated elsewhere.

which are always blurred and rainy, the probability of a curve doubly inflected near the fog limit is apparent, particularly if mean values be taken (curves 68).

Radium at $D=200$ and at $D=100$ cm. show data lying very nearly in this curve, but the last observations of the series prove that the fog limit is nevertheless definitely lower, or that the largest groups of nuclei are appreciably larger than the largest nuclei in dust-free non-energized air.

TABLE 41.—Fog limits of fleeting nuclei. Cylindrical fog chamber. $s_2=0$, tested.

Exposure to—	Distance.	$\delta \phi$.	s_1 .	s'_1 .	$N_1 \times 10^{-3}$	$N'_1 \times 10^{-3}$
	<i>cm.</i>					
I. Air	24.8	4.2	4.3	37.4	40.4
	23.2	3.7	3.6	25.3	22.9
	22.3	2.3	2.5	4.7	7.0
	21.4	.0	.5	.0	.8
II. Radium in aluminum tube	200	23.2	3.5	3.7	20.6	25.3
	22.3	2.2	4.4
	100	22.3	2.6	2.5	8.1	7.5
	23.2	3.4	3.5	18.7	22.5
	50	23.2	3.4	3.6	18.7	22.9
	21.4	2.7	2.7	8.7	8.4
	25	21.4	2.9	2.8	9.9	9.4
	23.2	4.0	3.9	29.7	28.3
	10	23.2	4.0	4.0	29.6	29.6
	21.4	2.8	3.1	9.2	13.1
	* 0	21.4	3.1	3.4	13.1	17.1
	23.2	5.1	4.5	63.7	43.9
	† (Top)	23.2	4.8	4.9	54.9	56.7
	21.4	3.6	† 3.6	21.0	21.0
	200	21.4	1.8	1.8	2.7	2.7
	21.4	.0	.5	.0	.8
III. X-rays.....	50	19.7	1.2	1.7
	20.5	3.1	11.7
	21.4	4.2	4.8	31.9	50.4
	4.0	4.0	27.2	27.2
	23.2	5.5	5.7	80.1	88.2
IV.....	10	19.7	2.1	1.7	3.4	2.4
	20.5	3.0	3.5	10.5	18.1
	21.4	5.3	4.7	66.4	47.0

* Radium 15 cm. from line of sight.

† Radium 5 cm. from line of sight.

‡ Growth from $s=3.3$ to $s=3.8$; radium 5 cm. from line of sight.

Radium at $D=10$ and at $D=25$ cm. form a similar group with an obviously much lower fog limit, and the case is accentuated for radium at $D=0$ cm. from the end, or 15 cm. and 5 cm. (on top) from the line of sight. At this point the data for the X-rays with the anticathode at

distances $D = 10$ to 26 cm. form a prolongation of the series, showing further reduced fog limits and the probability of a doubly inflected curve of the same type throughout.

As a whole these observations corroborate what has already been inferred, that nuclei of all sizes are present simultaneously; that by far the greater number have a size depending on the density of the ionized field by which they are produced. These nuclei correspond to the steeper ascent of the curves. With this given, the exceptionally large nuclei at the lower end of the curve and the exceptionally small nuclei at the upper end bring about the double inflection, since the numbers of each gradually vanish. The more intense the ionization, the more nearly are the nuclei of the same size, while for weak ionization the gradation shown by the flat curves is accentuated.

56. Secondary generation.—In table 42 the endeavor was made to compare the effects of the X-ray bulb acting to produce persistent nuclei from different distances from the end of the fog chamber. Unfortunately dense stratified fogs occur in the first exhaustion, which makes it necessary to use the second exhaustion for the same nucleation as a means of measurement. The pressure difference $\delta p = 20$ cm. is below the fog limit, when air is not energized.

The first two parts of the table show the rapid decrease of N with increasing D ; but it is particularly remarkable that after the lapse of 2 minutes subsequently to the exposure, the nucleation (*cet. par.*) has apparently increased (curves 74, 76), precisely as if there were induced radio-activity in the nuclei, or in the apparatus, after the X-radiation has been cut off. The incessant danger from undersaturation is probably ineffective in view of the low-pressure difference. It follows, then, that the decaying nucleus is radio-active (for which reason probably the fleeting nuclei, though instantly generated, do not decay at the same enormous rates), or that the larger nuclei break up into smaller nuclei (increasing their number about threefold on the average), or that small nuclei beyond the range of the exhaustion gradually grow to a larger size.

Special experiments to bring out this feature of secondary generation were made in table 42 and in the third, fourth, and fifth parts of table 43. The phenomenon is put in evidence strongly on all cases, but with an additional result, showing a tendency in the alternations to disappear after several repetitions (curves 72, 73). The fifth part of table 43 shows the occurrence of secondary generation even for distances of 20 cm. between the anticathode and the fog chamber. The last datum is an indication of the growth of fog particles in the lapse of time (curve 75). In the fourth part of table 43 (curve 72) the alter-

nations are a maximum, while the time elapsed after the exposure (4 minutes) is longest. The amplitude of the alternations is in all cases initially about 2.5 : 1, but it must be remembered that the coronas are observed after the second exhaustions. The nuclei caught in the first exhaustions may be estimated at 50,000 to 100,000.

TABLE 42.—Secondary generation.

Part.	$\delta p.$	D.	Time of exposure. (Rays on.)	Time after exposure. (Rays off.)	$s_1.$	$s_2.$	$N_1 \times 10^{-3}.$	$N_2 \times 10^{-3}.$
I.	20	6	Min. 2	Min. 0 2 0 * 2 2 0 0 2	Strata. " " " " " " "	2.4 3.4 2.5 2.5 3.1 2.1 2.2 3.0	5.1 15.8 6.2 6.2 11.3 3.4 3.9 10.5
II.	25	6	2	0 1 1 0	4.0 4.8 4.9 3.7	2.8 2.5 2.3 2.4	32.4 60.0 64.0 27.6
III.	25	6	1	1 0	3.9 4.3	2.1	32.0 41.0

* Fails.

TABLE 43.—Continuation of the preceding. Secondary generation. D , distance of X-ray plate (anticathode) of bulb from end of fog chamber.

D.	Time of exposure. (Rays on.)	Time after exposure. (Rays off.)	$\delta p.$	$s_1.$	$s_2.$	$N_1 \times 10^{-3}.$	$N_2 \times 10^{-3}.$
----	---------------------------------	-------------------------------------	-------------	--------	--------	-----------------------	-----------------------

Part I. Effect of distance.

cm.							
5	120	0	20.1	Strata.	3.7	21.5
10	120	0	"	1.9	2.8
20	120	0	Fog.	.56

Part II. Secondary generation.

5	120	120	20.1	Dense strata.	5.2	58.0
10	120	120	Strata.	2.8	8.5
20	120	120	1.0	(1.0)

TABLE 43, continued.—Continuation of the preceding.

D.	Time of exposure. (Rays on.)	Time after exposure. (Rays off.)	δp .	s_1 .	s_2 .	$N_1 \times 10^{-3}$.	$N_2 \times 10^{-3}$.
Part III. Secondary generation.							
5	120	120	20.1	Strata.	4.2	30.0
5	0	"	3.2	12.9
5	120	"	4.4	34.3
5	0	"	4.2	30.0
Part IV.							
5	120	0	20.1	Strata.	3.6	19.5
....	240	"	5.0	51.5
....	0	"	3.6	19.5
....	240	"	4.3	32.0
....	0	"	4.0	25.0
Part V.							
20	120	0	20.1	Veil.	Veil .0
....	120	2.9	9.2
....	240	0	3.5	17.6

In the first part of table 42 the alternations are promiscuous, but they fail but once in 8 observations (curve 71; failure at*). In the second part, where the coronas are nearly measurable, there is no failure (curve 70). The third part shows that exposures of 1 minute are not sufficient to bring out the phenomenon.

NUCLEATION DUE TO RAYS PENETRATING FROM A DISTANCE OR THROUGH DENSE MEDIA.

57. Effect of distance of the X-ray bulb from the free wooden fog chamber.—The probability of a residual effect in case where the X-ray bulb is moved to a considerable distance from the fog chamber is suggested by many of the above results. It is worked out in detail in table 44, where the condensations described were all made at the pressure difference corresponding to the fog limit of dust-free nonenergized air, and without cutting off the radiations. There is thus no decay. Nevertheless, the results are, as usual, disappointingly irregular, the first datum of each pair of results being low, the second high. Periodicity therefore occurs in spite of the wet-sponge tube added to the filter. The observed variation of results is moreover impossible in relation to distance, even though the data for inferior and superior coronas are apparently consistent in both outgoing curves. Again, in

the return series inferior, superior, and mean coronas occur together. It would be difficult to conjecture any reason for the apparent minimum at $D=50$ cm. and the apparent maximum at $D=200$ cm., and they will presently be shown to be referable to the bulb. In any case, however, the mean decrement of nucleation within 6 meters is certainly less than one-fourth, evidencing an astonishingly small distance effect.

TABLE 44.—Nucleating effect of X-radiation from different distances; $\delta p = 25$ cm.
Time of exposure, τ min., prolonged through condensation.

Part.	D.	s_1 .	s_2 .	$N_1 \times 10^{-3}$.	$N_2 \times 10^{-3}$.	Part.	D.	s_1 .	s_2 .	$N_1 \times 10^{-3}$.	$N_2 \times 10^{-3}$.
I.	5	*5.1	2.5	69.6	8.0	II.	600	5.4	τ	83.4
	50	2.0	1.3	3.8	2.4		200	5.4	τ	83.4
	50	4.2	2.0	38.0	3.8		6	5.5	τ	87.6
	100	3.4	2.0	20.4	3.8		†6	2.7	10.0
	100	4.1	2.0	35.0	3.8	III.	600	5.3	(†)	79.0
	200	4.3	1.9	41.0	3.6		200	5.3	79.0
	200	4.9	2.0	64.8	3.8		6	5.3	79.0
	400	3.3	1.8	18.6	3.2	IV.	600	5.5	(†)	87.6
	400	4.4	2.1	60.0	4.4		200	5.6	92.0
	600	4.0	1.6	32.4	3.0		6	5.6	92.0
	600	3.9	1.5	31.0	2.8	V.	6	6.3	3.1	123.0	14.6
	400	4.3	2.0	41.0	3.8		50	4.9	(†)	64.0
	200	4.9	2.0	64.8	3.8		50	4.9	64.0
	100	4.5	2.0	48.0	3.8		6	5.2	74.4
	50	3.7	1.3	27.6	2.4		6	5.2	74.4
	5	4.0	1.7	32.4	3.1		50	6.0	112.4
	200	4.3	2.0	41.0	3.8		50	5.4	83.4

* 7 cells in remaining experiments.

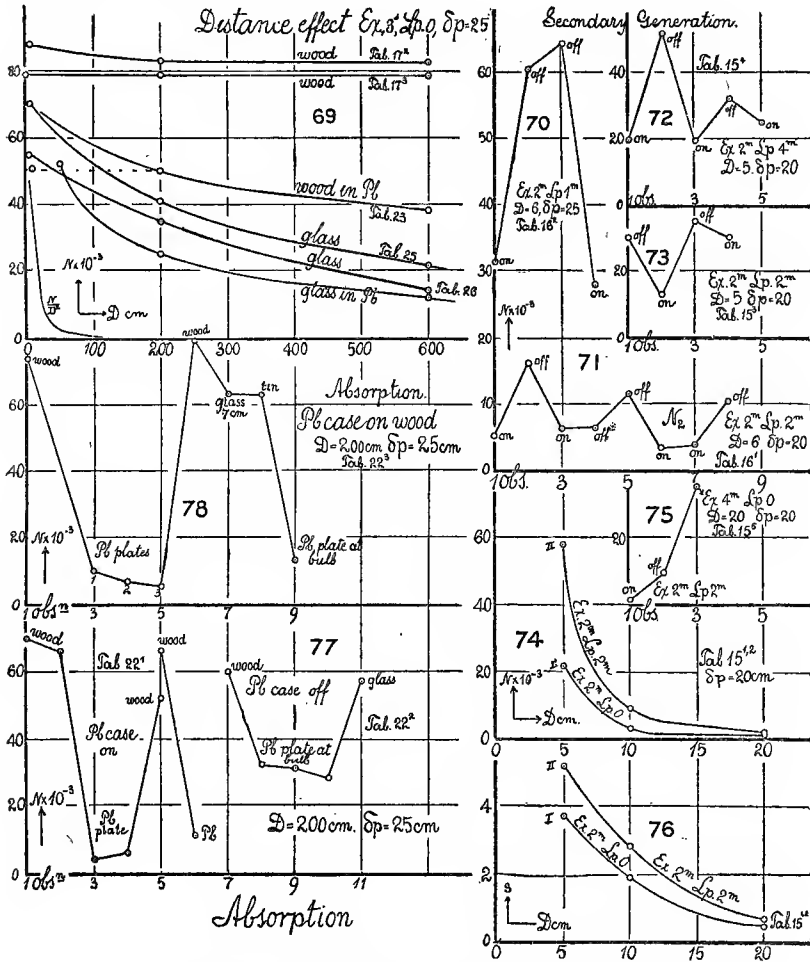
† Taken but not recorded.

† 1 minute after exposure.

To guard against variations of the tube, the abbreviated series were made as given in the second, third, and fourth parts of the table (upper curves 69); and these show what was to be expected from the preliminary results, that within the 6 meters of observation about the same nucleation is produced in the fog chamber (*cet. par.*) irrespective of distance. Finally, part V of the table proves that the apparent minimum at $D=50$ cm. is an error.

The absence of a distance effect in the case of the nonincased wooden fog chamber is astonishing and implies that the space within the 6 meters of observation is everywhere equally full of the nucleus-producing radiation. This behavior, moreover, is different from the fluorescent, photographic, or even the electrical effect of the X-rays. Thus the phosphorescent screen is intensely illuminated at $D=5$ cm., while at 2 meters it is very dim and at 6 meters quite dark. It is natural to infer that the constancy of radiation is due to atomic disintegration of the platinum anticathode, when bombarded by the cathode

torrent, and that the issuing rays are akin to the gamma rays of radium and quite distinct from the undulatory phenomenon of X-radiation. In fact, each part of the medium within the radius of 6 meters behaves as if it were the source of such rays.



FIGS. 69-78.—Illustrating tables 43, 44, 45, 49, 50, 53, 54.

58. Generation and decay for radiation from $D=200$ cm.—Before proceeding with the investigation it will be advisable to examine the generation and decay of nuclei when the radiation comes from long distances. The data of table 45 are of the kind to be anticipated from the results of section 17. The experiments were made at the fog limit of dust-free air. The first part of the table shows that exposures

of 1 and 2 minutes produce about the same nucleation, which vanishes with the lapse of 1 or 2 minutes after exposure to negligible residues. In the second part of the table the radiation is stronger and maximum nucleation appears after 3 seconds of exposure, so that the nucleation is produced instantaneously. Initial nucleations obtained (*cet. par.*) in air which has been long stagnant are apt to be very low. The mean nucleation after less than 3 seconds' exposure is about 90,000 per cubic centimeter.

The effect of longer exposures is again investigated in the third part of the table, but the possibility of a slight increase of the nucleation in the lapse of time is negatived by the last observation. The fourth part also shows that fog limit to be at $\delta p = 20$ cm., and that there is no accumulation of nuclei as time goes on. There is no appreciable persistence.

TABLE 45.—Generation and decay of nuclei. $D=200$. $\delta p=25$ cm. Wood fog chamber.

Part.	δp .	D.	Time of exposure. (Rays on.)	Time after exposure. (Rays off.)	s_1 .	s_2 .	$N_1 \times 10^{-3}$.	$N_2 \times 10^{-3}$.
			<i>Min.</i>	<i>Min.</i>				
I.	25	200	1	0	4.2	1.7	38.0	3.0
			1	1	2.6	r	9.2	r
	25	200	2	0	3.7	1.7	27.6	3.0
			2	2	1.8	1.0	3.2	2.0
II.	25	200	<i>Sec.</i>					
			60	0	* 3.6	1.7	25.0	3.0
			5	0	6.1	2.4	115.0	6.6
			3	0	5.3	79.0
			3	0	† 4.3	41.0
			3	0	5.9	2.2	108.0	5.0
			3	0	5.7	2.0	96.4	3.8
			3	0	* 3.6	25.0
			3	0	5.6	2.8	92.0	10.4
			3	0	5.7	2.7	96.4	10.4
III.	25	200	10	0	4.9	63.0
			10	0	4.2	38.0
			30	0	5.2	74.4
			30	0	5.2	74.4
			60	0	5.3	79.0
			60	0	5.4	2.6	83.4	9.2
			3	0	5.1	69.6
IV.	20	200	3	0	r	r	r	r
			30	0	1.7	2.6
			60	0	1.7	2.6
			120	0	1.7	r	2.6	r

* After long waiting. Stagnant air.

† Follows preceding high nucleation.

As a whole the observations for $D=200$ are irregular, for the usual reasons instanced above.

59. Electrical effect for different distances.—To roughly estimate the state of the room in relation to the ionizing effects of the X-rays, the time of collapse of the gold leaves was taken, when the galvanoscope standing on an earthed brass plate was covered with a glass bell jar. Table 46 needs no explanation. In the second part of the table the time of collapse decreases about as the square of the distance and is thus quite different from the fog-chamber effect. At short distances the galvanoscope registers a sudden throw when the circuit through the X-ray tube is first made. The effect of this throw is the same as if negative electricity entered the metal frame of the electroscope, and it is therefore probably electrostatic induction on the brass foot plate coming from the cathodal conductor.

TABLE 46.—Electrical effects of X-rays. Galvanoscope in glass bell jar, walls 0.5 cm. thick.

D.	Remarks.	Time of collapse.
<i>cm.</i>		<i>Sec.</i>
200	Without screen *	< 5
	With lead plate 0.14 cm. thick.....	10-15
	With semicylindrical lead screen and semicircular lid	30-40
	With glass bell jar on brass plate.....	> 120
	With wide (7 mm. thick) glass plate.....	30
		Observed.
15	+ charge: impulsively increased divergence; then collapse, computed	Instantaneous.
	- charge: impulsively decreased divergence; then collapse, computed	
		< 1
50	+ charge * }	3-4
	- charge }	
100	+ charge }	8-10
	- charge }	
200	+ charge }	25-30
	- charge }	
600	+ charge }	Say 300
	- charge }	

* Positive and negative charges behave alike.

60. Apparent penetration of the X-rays coming from 600 cm.—The astonishingly small distance effect observed made it seem probable that the effective rays are of a penetrating kind. Table 47 (to be interpreted later) apparently bears this out, though in reality it merely separates the axial and lateral radiations. Advantage is taken of the sufficiency of short exposures whereby the tube is kept more constant. The apparatus is shown in figure 41, where *A* is the fog chamber and *P* the plates.

To take first the experiments in table 47, when the distance between the lead screen at the fog chamber and the X-ray bulb is $D = 600$ cm., which are smoothest (curve 79), it appears that a single lead plate 0.14

cm. in thickness is more than sufficient to reduce the nucleation one-half. Thereafter the remaining thicknesses up to 1 cm. or more does not reduce it further. A close comparison is given at the end of the work, in which $N=76,000$ falls off to $N=32,000$ for 6 plates, or a thickness of about 0.84 cm. (curve 81).

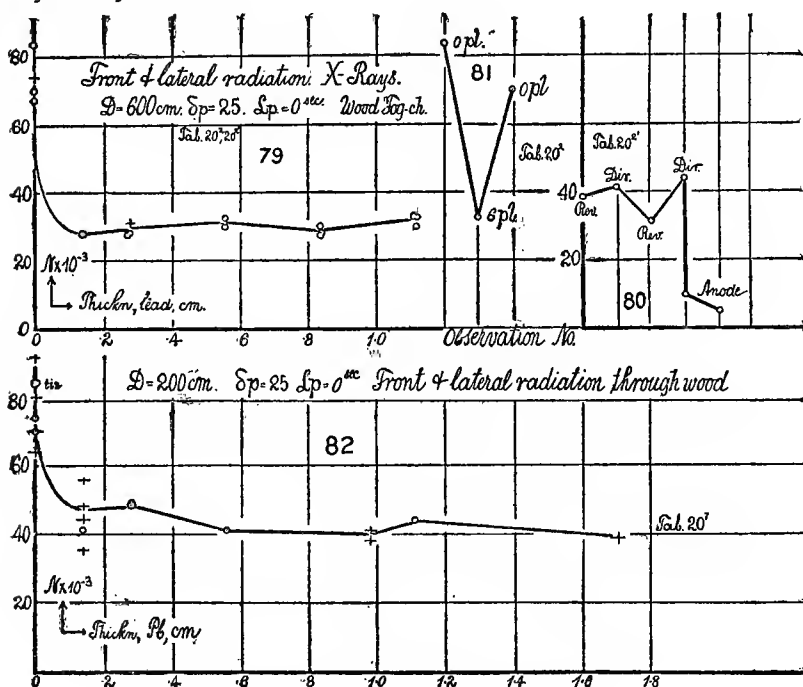
An interesting comparison is given for the efficiency of the X-ray tube radiating from this distance either from the front face of the anticathode or from the rear face of the anticathode, the tube in the latter case being completely reversed (curve 80). The mean results are respectively $N=42,500$ and $N=34,600$, showing the anticathode to behave as if it were transparent or at least radiating from both faces in all directions. Indeed, even if the anode and the cathode are exchanged (reversed current), considerable radiation is sent out; as, for instance,

Concave mirror the cathode, $N=47,000$,

Concave mirror the anode, $N=7,000$,

or about 16 per cent of the nucleation has been retained (curve 80).

The coronas obtained when lead screens are used in front of the fog chamber are clear and often multi-annular, showing the nuclei to be very nearly of a size.



FIGS. 79-82.—Illustrating table 47.

In the above chart Tab. 20 = present table 47.

TABLE 47.—Penetration of rays and reversal of tube; $\delta p = 25$ cm. Exposure about 3 sec. prior to condensation without cutting off the radiation; air, $s = 1.2$; wood fog chamber not cased (fig. 41).

Part.	D.	s_1 .	s_2 .	$N_1 \times 10^{-8}$.	$N_2 \times 10^{-8}$.	Remarks on penetration.
I.	200	5.4	3.2	83.4	16.6	Screens removed.
		5.4	83.4	Tin plate, 0.50 mm. thick.
		4.3	(*)	41.0	Lead plate, 1.4 mm. thick.
		4.5	48.0	Lead plate, 2.8 mm. thick.
		4.5	48.0	Lead plate, 2.8 mm. thick.
		5.4	83.4	Screen removed.
II ¹ .	600	5.2	74.4	Do.
		3.9	<i>r</i>	31.0	Lead plate, 2.8 mm. thick.
	600	4.2	<i>r</i>	38.0	Screen removed. Tube reversed.
		4.3	<i>r</i>	41.0	Screen removed. Tube directed.
		3.9	<i>r</i>	31.2	Screen removed. Tube reversed.
		4.4	<i>r</i>	44.0	Screen removed. Tube directed.
	600	2.6	9.2	Anodal rays.
		2.2	5.0	Do.
		II.	600	4.2	<i>r</i>	† 38.0
5.0			67.0	Do.
† 3.7			27.6	1 do., thickness, 1.4 mm.
3.7			27.6	Do.
§ 3.7			28.0	2 do., total thickness, 2.8 mm.
3.7			27.6	Do.
4.0			32.4	4 do., total thickness, 5.6 mm.
3.8			30.0	Do.
3.8			30.0	6 do., total thickness, 8.4 mm.
3.7			27.6	Do.
3.7			28.0	Do.
4.0			32.4	8 do., total thickness, 11.2 mm.
3.8			30.0	Do.
5.4	1.0			83.4	1.8	0 do.
4.0			32.0	6 do.
5.1	1.5			69.6	2.8	0 do.
III.	6	5.4	¶ <i>r</i>	87.6	0 plate.
		5.3	79.0	1 plate.
		5.3	(2)	79.0	0 plate.
		5.3	(2)	79.0	1 plate.
IV.	600	5.3	(2)	79.0	1 plate.
	600	** 4.0	(2)	79.0	0 plate.
V.	200	5.3	(2)	79.0	0 plate.
	200	5.3	(2)	32.4	1 plate.
	200	4.5	(2)	48.0	2 plates.
		4.3	(2)	41.0	4 plates.
		4.4	(2)	44.0	8 plates.
		5.1	(2)	69.6	0 plate.
	5.2	(2)	74.4	0 plate; 1 min. exposure; no growth.	

* Second exhaustion made, but not recorded.

† Initial low datum.

‡ Galvanoscope discharged at 6 meters and through lead plate, but much more slowly than the instant collapse at 6 cm.

§ First plate filters out the axial rays. The remainder have no observable effect, and are virtually transparent. Coronas clear and multi-annular apart from rain.

¶ Second exhaustion necessary to avoid periodicity.

** Note the reduction of N at 600 for 1 plate, which does not occur at $D = 6$ cm. and $D = 200$ cm.

TABLE 47, continued.—Penetration of rays and reversal of tube, etc.

Part.	D.	s_1 .	s_2 .	$N_1 \times 10^{-3}$.	$N_2 \times 10^{-3}$.	Remarks on penetration.
VI.	7	6.4	2	129.0	0 plate.
		5.4	2	83.4	1 plate.
		5.3	2	81.2	2 plates.
		5.9	108.4	0 plate.
		5.7	96.4	4 plates.
		4.9	64.8	7 plates.
		5.6	92.0	4 plates.
		4.9	64.8	0 plate.
VII.	200	4.7	(*)	56.0	0 plate, thickness, 0.0 cm.
		4.9	64.0	0 plate, thickness, 0.0 cm.
		4.4	44.0	1 plate, thickness, 0.14 cm.
		4.1	35.0	1 plate, thickness, 0.14 cm.
		5.6	92.0	0 plate, thickness, 0.0 cm.
		5.1	69.6	0 plate, thickness, 0.0 cm.
		4.5	48.0	1 plate, thickness, 0.14 cm.
		4.7	56.0	1 plate, thickness, 0.14 cm.
		5.3	81.2	0 plate, thickness, 0.0 cm.
		4.2	38.0	7 plates, thickness, 0.98 cm.
		4.3	41.0	7 plates, thickness, 0.98 cm.
		4.2	38.0	12 plates, thickness, 1.68 cm.
		5.6	92.0	0 plate, thickness, 0.0 cm.
		5.5	87.6	0 plate, thickness, 0.0 cm.
	600					

* Taken, but not recorded. In the first two data the bulb is gaining strength.

61. Apparent penetration of the X-rays coming from 200 cm. and from 6 to 7 cm.—The results for $D=200$ cm. are similar to the preceding. It again takes less than one lead plate (thickness 0.14 cm.) to stop the absorbable rays (curve 82). There is no extra thickness of lead as an equivalent of the layer of 400 cm. of air removed. Again, about one-half of the radiation is stopped by the first plate and greater thicknesses produce no further effect. At the end of the table a wall of lead 1.7 cm. thick shows no additional absorption. Moreover, tinned iron plate $\frac{1}{2}$ mm. thick has no appreciable effect on the radiation whatever (curve 82).

The first experiments for $D=6$ cm. show apparent previousness of the single lead plate (0.14 cm. thick); but this seems to be referable to the intensity of the initial radiation without the lead screen, for in the experiments at $D=7$ cm., a single plate shows marked reduction of the very large coronas observed. On the other hand, a plate even 1 cm. thick absorbs very little of the radiation, for, roughly, about 80 per cent passes, in spite of the indefinite thickness of lead, between the bulb and the fog chamber, completely screening off the latter. The results throughout are curiously irregular and difficult to interpret, as seems not unexpected, since all secondary radiators must now be close at hand (curve 83).

TABLE 48.—Penetration ; miscellaneous experiments on case of lead plates ; 0.14 cm. thick ; $\delta p = 25$ cm. Wood fog chamber.

Part.	D.	Rays on.	Rays off.	Number of plates.	s_1 .	s_2 .	$N_1 \times 10^{-3}$.	$N_2 \times 10^{-3}$.
I.	7	<i>Sec.</i>	<i>Sec.</i>					
		3	60	0	2.7	10.4
		60	60	0	3.2	16.6
		120	60	0	Strata (5.7)	3.2	96.0	16.6
		120	0	0	Fog (5.0)	(2)	68.0
		120	60	1	Veil 2.7	1.4	10.4	2.6
II.	7	120	60	1	Veil 3.0	12.2
		120	60	0	Strata (4.8)	3.4	60.0	20.4
Case of tinned iron plate, 0.5 mm thick.								
III.	6	3	0	0	5.6	92.0
		180	0	0	Strata (6.8)	3.1	153.0
		180	120	0	Strata (7.1)	3.1	170.0
		180	0	1	5.8	2.3	101.0
		180	120	1	2.0	<i>r</i>	3.8
		3	0	0	5.8	(3)	101.0
		3	60	0	2.7	<i>r</i>	10.4
IV.	* 6	120	60	1	2.9	<i>r</i>	11.8	<i>r</i>
		120	0	0	4.0	2.8	32.4	10.4

* Another bulb.

62. Generation through lead plate and through iron.—The data of table 48 show the usual accelerated increase of the nucleation, N , with the time of exposure, when nuclei of the persistent type are produced (curve 84). When, however, the lead screen (thickness 0.14 cm.) intervenes, there is no accelerated increase and no accumulation above a relatively small value, $N = 13,000$. These nuclei may be a transitional type, but it is difficult to interpret the case of very small coronas. Another similar test was made with a screen of tinned sheet iron $\frac{1}{2}$ mm. thick. The results are in the main the same; in other words, marked persistent nucleation is not produced through the iron plate in spite of its slight thickness and lower density. Parallel observations for 3 seconds' exposure show that about as many nuclei are thus generated as are obtained after a 3-minute exposure through the plate.

On the other hand, for 3 minutes' exposure there is growth of nucleation, if observation is made 2 minutes after exposure; in the presence of the plate the nucleation falls off to a negligible datum in the same lapse of 2 minutes after exposure. The decrement in this case is of the same order as is observed for the short exposure (3 seconds) tested a minute after exposure ceases. The use of another bulb with the plate does not change the results.

FOG CHAMBERS INCLOSED IN METAL CASKETS.

63. Wood fog chamber in lead casket—Penetration.—In table 49 data of a crucial kind are given for the purpose of separating the radiation which actually passes the lead screens from that derived from secondary or lateral sources. The first part of the table is at once decisive (curves 77). Less than 7 per cent of the radiation which passes the wood and glass walls of the chamber will pass through the front face (toward the bulb), if this face is closed by a lead plate 0.14 cm. thick. When the chamber is freed from the casket and the plate placed at the bulb, more than half of the radiation gets into the fog chamber secondarily, as shown in the second part of the table and curve 77.

TABLE 49.—Wood fog chamber in a lead casket, open in front, toward the bulb.
 $D=200$ cm; $\delta p=25$ cm. Thickness of lead plate, 0.14 cm; of glass plate, 0.7 cm.
 Exposure, 3 sec.; lapse, 0 sec.

Part.	Front of casket, etc.	s_1 .	s_2 .	$N_1 \times 10^{-3}$.	$N_2 \times 10^{-3}$.
I.	Open, bulb 4.....	5.1	1.7	69.6	3.0
	Open.....	5.0	1.5	66.0	2.8
	Closed by lead plate.....	2.0	3.8	5.0
 do.....	2.2	5.0	5.0
	Open.....	4.6	51.6	...
II.	Open, bulb 0.....	5.0	1.7	66.0	3.0
	Closed by lead plate.....	2.8	11.0	5.4
	Casket removed.....	4.8	2.0	60.0	3.8
	Lead plate at bulb.....	4.0	1.7	32.4	3.0
 do.....	3.9	1.7	31.2	3.0
 do.....	3.7	1.7	27.6	3.0
	Glass plate.....	4.7	1.9	56.0	3.6
III.	Open.....	6.3	2.4	123.0	6.6
 do.....	5.2	1.7	74.4	3.0
	Closed by lead plate.....	2.7	2.7	10.0	10.0
	Closed by 2 lead plates.....	2.4	2.0	6.6	3.8
	Closed by 4 lead plates.....	2.3	2.6	5.4	9.2
	Closed by 6 lead plates.....	5.3	2.0	79.0	3.8
	Closed by glass plate.....	4.9	1.7	63.0	3.0
	Closed by tin plate.....	4.9	r	63.0	r
	Lead plate at bulb.....	3.0	2.4	13.2	6.6

With an improved and more fully lead-incased chamber, the data given in the third part of the table were investigated, in which successive thicknesses of 0.14, 0.28, 0.42 cm. of lead plate allow 14, 9, and 7 per cent of the radiation to pass (curve 78). The differences from the above datum are due to the greater intensity of the radiation here applied and to other incidental conditions. Furthermore, a glass plate 0.7 cm. thick, and a tinned iron plate 0.05 cm. thick, each allow nearly all the radiation to pass, *i. e.*, about 90 per cent, while a lead plate placed near the bulb at $D=200$ cm. cuts off about 17 per cent of the radiation (curve 78).

Hence it follows in the above experiments with the lead envelope removed, since one-half of the radiation was cut off by a single frontal lead plate 0.14 cm. thick, that about half of the radiation enters the wooden fog chamber, not from primary, but from secondary sources (using this term in its broadest sense), through the lateral walls of the apparatus. When the chamber is inclosed in the lead case open in front, the inside walls of the lead become a source of radiation, so that the corona need not decrease in size, as the data show. In general, the behavior is such as if the whole medium between the bulb and chamber were equally "polarized" (to use this word with a special meaning). At the lower pressure difference ($\delta p = 20$ cm.) the lead plate proves to be quite impervious, but the tin plate certainly admits an accumulation of 3,000 nuclei.

64. Continued—Radiation from a distance.—Experiments made to find the effect if the distance, D , of the bulb from the lead-incased fog chamber, open toward the bulb only, are given in table 50.

TABLE 50.—Wood fog chamber in lead casket. Effect of distance, D . $\delta p = 25$ cm. Exposure, 3 sec; lapse, 0 sec.

D.	s_1 .	$N_1 \times 10^{-3}$.	Mean.
<i>cm.</i>			
600	* 4.0	32.4	38
....	3.7	27.6
200	4.9	62.0	50
6	4.3	41.0	50
6	4.8	60.0
200	4.2	38.0
600	4.4	44.0

* s_2 always taken, but not recorded. Usually $s_2 = 1.5$ cm.

The bulb is as usual variable, but the nucleation produced is about the same for all distances up to 200 cm., after which there is a possible decrease of about one-fifth as far as 600 cm., the limit of observation (curves 69). This relatively insignificant effect of distance is again remarkable, inasmuch as all remote secondary radiation is excluded. Whatever produces the nucleation, if secondary, must come from the inside of the casket, or it must be primary. At all events it is again manifest that the whole medium within the room is almost equally energized throughout.

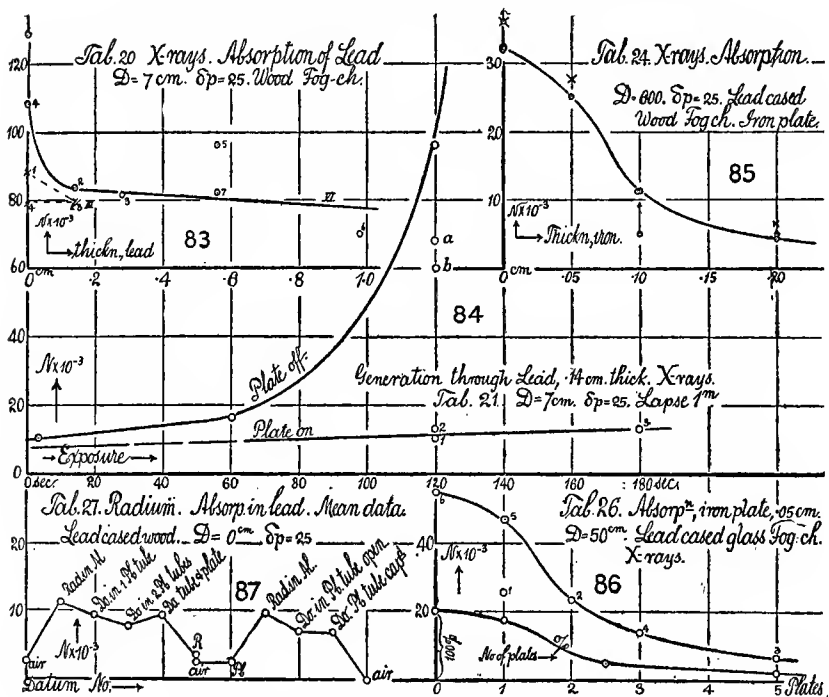
Table 51 and curve 85 show the penetration of tinned iron plates, each 0.5 mm. in thickness, when the X-ray bulb is 600 cm. from the lead-cased fog chamber. Several millimeters of iron plate are still

appreciably penetrable even from this remote distance. So far as the data go the absorption is relatively marked between 0.5 and 1 mm. of thickness, the rates being much larger here than for greater or smaller thicknesses.

TABLE 51.—Penetration of tinned iron plates, 0.05 cm. thick. $D=600$ cm.
 $\delta p=25$ cm. Wood fog chamber in lead casket.

Number of plates.	Total thickness.	s_1 .	$N_1 \times 10^{-3}$.	Mean.
	cm.			
0	0.00	* 4.0	32.4	32
1	05	3.6	25.0	25
2	10	2.2	5.0	8
2	10	2.8	11.2
4	20	2.2	5.0	5
4	20	2.1	4.4
0	00	3.9	32.0	36
1	05	3.7	27.6	28
2	10	2.8	11.2	11
4	20	2.4	6.6	7
0	00	4.3	41.0

* Second exhaustion made, but not recorded. Usually $s_2=1.0$.



FIGS. 83-87.—Illustrating tables 47, 51, 53, 54.

TABLE 52.—Distance effect of X-rays. Glass fog chamber. $\delta p = 22$ cm. (fog limit of air). No lead casket. Walls, 0.3 cm. Bottom 1 cm. thick.

Distance.	s_1 .	s_2 .	$N_1 \times 10^{-3}$.	$N_2 \times 10^{-3}$.
<i>cm.</i>				
200	4.6	* 1.6	51.6	3.0
	4.3	1.7	41.0	3.2
10	5.0	1.5	67.0	2.6
	5.0	1.5	67.0
600	3.4	1.5	20.4
	3.5	1.5	22.6
200	3.7	<i>r</i>	27.6
	4.4	<i>r</i>	44.0
10	5.3	<i>r</i>	79.0
	5.0	<i>r</i>	67.0

* Faint and small, due to dust-free air.

TABLE 53.—Distance effect of X-rays. $\delta p = 22$ cm. Lead plate 0.14 cm. thick. $s_2 = 0$, but always tested.

Distance.	Lead plates.	s_1 .	$N_1 \times 10^{-3}$.	Distance.	Lead plates.	s_1 .	$N_1 \times 10^{-3}$.
-----------	--------------	---------	------------------------	-----------	--------------	---------	------------------------

Part I. Cylindrical fog chamber, without casket.

200	I	3.2	13.9	200	0	4.3	34.4
	0	4.8	50.4	10	0	5.0	55.4
	* 0	3.7	23.2	600	0	3.3	15.6
	I	3.8	25.2		0	3.1	12.2

Part II. Cylindrical fog chamber, lead-cased, with tubular end of lead 50 cm. long. (Fig. 42.)

50	0	4.7	47.0	400	0	3.5	19.0
	I	1.8	2.7		0	3.6	21.0
	I	2.0	3.2	200	0	3.8	25.2
	2	1.8	2.7		0	4.1	29.4
	0	4.8	50.0	50	0	5.0	55.4
200	0	3.6	21.0		0	5.0	56.3
	0	3.7	23.2	50	I	1.5	2.3
600	0	3.0	11.1		I	1.5	2.3
	0	3.1	12.3				

Part III. Lead-cased fog chamber as before. Penetration through tinned iron plates 0.05 cm. thick.

Distance.	Tin plates.	s_1 .	$N_1 \times 10^{-3}$.	Per cent transmitted.
50	I	3.8	25.2	46
	2	3.7	23.2	42
	5	2.5	6.7	12
	3	3.2	13.9	25
	I	{ 4.7	47.0	{ 86
		{ 4.7	47.0	
	0	5.0	55.0	100

* Double glass envelope.

65. Glass fog chamber—Radiation from a distance.—The experiments on the nucleation produced by X-rays coming from a distance were now continued by aid of the cylindrical fog chamber (glass walls 0.3 mm. thick and 1 cm. thick at the bottom), the lead casket being here removed (curve 69). The data are given in table 52, and may be restated from the mean results,

$D = 0 + 30$ cm.	$N = 70,000,$
200 + 30	41,000,
620 + 30	22,000,

where N is measured from the line of sight, 30 cm. from the end of the fog chamber nearest the bulb. Very much of the lateral radiation is thus cut off by the thick glass walls and bottom of the fog chamber; but the decrements are far from suggesting the law of inverse squares even in a remote degree. As the distance from the line of sight increases over 20 times, N decreases only 3 times.

The repetition of these experiments with a less active bulb gave about the same results (table 53). For distances from the line of sight, $D = 20, 210, 610$, the average nucleation was $N = 55,000, 34,000, 14,000$. About one-half the total radiation is absorbed by a frontal lead plate, or a double glass envelope, as usual (curves 69).

66. Radiation from a distance—Glass fog chamber in lead case.—The endeavor was finally made to stop off all secondary radiation by providing a close-fitting lead tube (L , fig. 42), which not only incased the fog chamber A , but extended about 50 cm. beyond the end nearest the bulb. If distances are measured from the line of sight, the mean results may be estimated as $D = 60, 210, 610$ cm., corresponding to $N \times 10^{-3} = 52, 25, 12$. The nucleation falls off a little more rapidly than before (a part of which may be referable to imperfect alignment of the distant bulb), but after 200 cm. the decrease is slow (curves 69).

In the present case a single lead plate (thickness, 0.14 cm.) cuts off nearly all the radiation, *i. e.*, all but 4 to 6 per cent. Hence very little secondary radiation has entered, while the small penetration of the lead is probably referable to the distance of the plate from the end of the chamber (*cf.* distance effect for gamma rays, next paragraph). Compared with lead, the absorption of tinned iron is small (curves 86), the plates (eventually 0.25 cm. thick) allowing 26 per cent of the radiation to pass for the same thickness of plate which was used in the case of lead. This result is quite out of proportion with the relative densities,

NUCLEATION DUE TO GAMMA RAYS.

67. Lead-cased wooden fog chamber—Penetration.—In order to interpret the above data for X-rays, it will first be necessary to determine the facility with which nuclei are produced by very penetrating radiation. The radiation of radium filtered through lead walls about 1 cm. thick was therefore tested. Table 54 gives a series of results in which the radium ($10,000\times$) was first tested when hermetically sealed in a thin aluminum tube and placed 6 to 10 cm. from the line of sight (curve 87). In this case the radiator nearly touched the free end of the lead-cased fog chamber *A* (fig. 43). The aluminum tube was then successively enveloped in one or more lead tubes, *T*, with wall 0.5 cm. in thickness. The length of the tubes exceeded the width of the fog chamber, and they were placed with their axes parallel to the plane of the end, so that any radiation entering would have to pass through the lead; or, passing out of the lead tube, enter the fog chamber laterally under very unfavorable conditions. Leaving the latter case (which is here negligible) for further experiment, table 54 gives the coronal apertures s_1, s_2, s_3 , etc., and nucleations N_1, N_2, N_3 , etc., found in successive exhaustions under the conditions stated. The figures show that periodicity is a frequent and unavoidable occurrence. Many exhaustions were therefore made in each case and the means taken in triads. These are given in detail in the summary at the end of the table, and in the curve (87). Sometimes the particular adjustment of the tube (as, for instance, the position of the radium in the tube) seems to be of importance, for the results in any given position are fairly uniform. An additional lead plate is ineffective. The summary shows that of the radiation which escapes from the aluminum tube, 85 per cent passes through 0.5 cm. of lead and 70 per cent through 1 cm. of lead, assuming that there is no secondary radiation. In one case (tube capped by a lead plate) nothing at all seems to enter the fog chamber. This suggested the following group of experiments, which show that zero nucleation may occur periodically under any conditions.

68. Continuation.—The new results (table 54, part IV) show a curious irregularity, which is borne out by the behavior of radium when placed in the fog chamber (Chapter II, section 31). In the present case the tube was 60 cm. long (similar to *P*, fig. 44), parallel to the plane of the end (about 20 cm. across) of the fog chamber and placed close to it. The data for the open and closed tube are about the same. In both cases the values of N at times descend to the low nucleations of nonenergized air, though as a whole they lie pro-

nouncedly above it. The lead tube without radium is inactive. Moreover, in the final part of the work all data are decidedly lower than at first, as if the energizing quality were fatigued. This occurs not only within the radium in lead tubes, sealed or not, but in the case where the radium is in the sealed aluminum tube only. The air values give evidence of an almost entire absence of nuclei. Reasons for this unsatisfactory behavior can not even be conjectured. The mean values given in thousands per cubic centimeter are: For air, $N^* = 2.6$; radium in open lead tube, $N = 22-12$; radium in capped lead tube, $N = 21-18$; air, $N = 2.2$; lead tube without radium, $N = 2.4$; radium in aluminum tube only, $N = 10$; radium in open lead tube, $N = 7$; radium in capped lead tube, $N = 7$; air, $N = 0$, remembering that the radium is in all cases surrounded by the sealed thin aluminum tube.

Apart from the fatigue it is clear that the open and capped tube behave alike, proving that the rays actually penetrate the walls and that secondary radiation is ineffective. This also follows from the next paragraph, as the distance effect of radium is marked. The amount of radiation passing 5 mm. of lead is here about 73 per cent, but the present result is not as good as the above.

TABLE 54.—Penetration of γ -rays of radium. $\delta p = 25$ cm. Lead-cased fog chamber. Radium in thin (0.1 mm.) aluminum tube, hermetically sealed. Walls of each lead tube 0.5 cm. thick. Plate, 0.14 cm. thick. $D = 6-10$ cm. Lead tubes parallel to walls of chamber, 20 cm. long.

Part.	Remarks.	s_1	s_2	s_3	s_4	$N_1 \times 10^{-3}$	$N_2 \times 10^{-3}$	$N_3 \times 10^{-3}$	$N_4 \times 10^{-3}$
I.	Radium in Al only.....	2.9	3.2	3.0	2.8	11.8	16.6	13.2	11.2 (11.8)
	Radium in lead tube...	3.3	1.9	3.0	1.9	18.6	3.6	13.2	3.6
	Radium with 1 plate and tube.....	2.7	2.6	2.7	2.5	10.4	9.2	10.4	8.0 (10.4)
	Radium in lead tube...	2.9	2.9	3.2	2.7	11.8	11.8	16.6	10.4
	Radium with reflector...	1.0	2.1	2.0	1.8	4.4	3.8
	Radium in lead tube...	2.6	2.6	1.5	2.3	9.2	9.2	2.8	5.4
	Radium removed.....	1.5	1.5	1.0	2.0	2.8	2.8	1.8	3.8
II.	Radium removed.....	1.4	2.2	1.7	1.0	2.6	5.0	3.0	1.8
	Radium in Al tube...	2.7	2.8	2.0	3.2	10.0	10.6	3.8	16.6
	Radium in lead tube...	1.8	2.7	3.0	1.5	3.2	10.0	13.2	2.8 (18.6)
	Radium in double lead tube.....	2.8	1.9	2.9	1.0	10.6	3.6	11.8	1.8 (5.4)
	Radium in double lead tube.....	1.0	3.0	2.2	3.3	1.8	13.2	5.0	18.6
	Radium removed.....	1.6	1.0	1.7	1.0	3.0	1.8	3.0	1.8

* Given in thousands per cubic centimeter.

TABLE 54, continued.—Summary.

Part.	Radium at ∞ .	Radium in Al tube.	Radium in 1 lead plate; wall 0.5 cm.	Radium in 2 lead tubes; wall 1 cm.	Miscellaneous.	
					Tube and plate.	Tube and reflector.
III.	$N \times 10^{-3} = \begin{Bmatrix} 2.5 \\ 2.5 \\ 3.9 \\ 2.7 \\ 2.4 \\ 2.4 \end{Bmatrix}$	$\begin{Bmatrix} 14.5 \\ 11.9 \\ 8.8 \\ 8.7 \end{Bmatrix}$	$\begin{Bmatrix} 9.8 \\ 8.4 \\ 13.0 \\ 13.9 \\ 7.6 \\ 5.0 \\ 9.1 \\ 9.3 \end{Bmatrix}$	$\begin{Bmatrix} 7.4 \\ 5.2 \\ 8.3 \\ 10.5 \end{Bmatrix}$	$\begin{Bmatrix} 9.8 \\ 9.2 \end{Bmatrix}$	$\begin{Bmatrix} 3.6 \end{Bmatrix}$
	Means.. 2.7	11.3	9.5	7.9	9.5	3.6

TABLE 54, continued.—Tubes of lead 60 cm. long often capped. Wall, 0.5 cm. thick.

Part.	Remarks.	s_1 .	s_2 .	s_3 .	s_4 .	$N_1 \times 10^{-3}$	$N_2 \times 10^{-3}$	$N_3 \times 10^{-3}$	$N_4 \times 10^{-3}$
IV.	Air.....	0	1.7	2.0	2.0	0.0	3.0	3.8	3.8
	Radium in Al in lead tube with ends open..	3.8	3.2	3.3	2.6	29.0	16.6	18.6	9.2
	Do.....	1.6	3.5	3.2	22.6
	Radium in lead tube capped.....	3.4	3.2	3.7	3.3	20.4	16.6	27.6	18.6
	Do.....	3.4	0	2.0	3.2	20.4	0	3.8	16.6
	Air.....	1	1.6	1	1.8	3.0	1.8
	Lead tube without radium.....	* 1	1.9	1	1.8	3.6	1.8
	Radium in Al tube.....	2.9	2.0	3.0	11.8	3.8	13.2
	Radium in lead tube open.....	2.2	3.1	1	5.0	14.6	1.8
	Radium in lead tube capped.....	2.7	2.3	2.2	10.4	5.4	5.0
	Air.....	0	0	0	0

* No induced radio-activity.

69. Continued—Effect of distance.—Radiations from radium are in curious contrast with the corresponding results for the X-rays, inasmuch as the corresponding nucleating power falls off rapidly with the distance of the sealed aluminum tube from the fog chamber. At 200 cm. the effect is but just appreciable above the nucleation of nonenergized dust-free air, as shown in table 55.

Marked excess of nucleation is observed within 100 cm., apparently increasing as the distance from the fog chamber decreases; but it is difficult to make definite statements here, because all the effects are small and successive exhaustions show marked periodicity. The mean values are estimates. Though 5 minutes of exposure was at first allowed, the effect is probably instantaneous and the succeeding sections show that the effect is very penetrating.

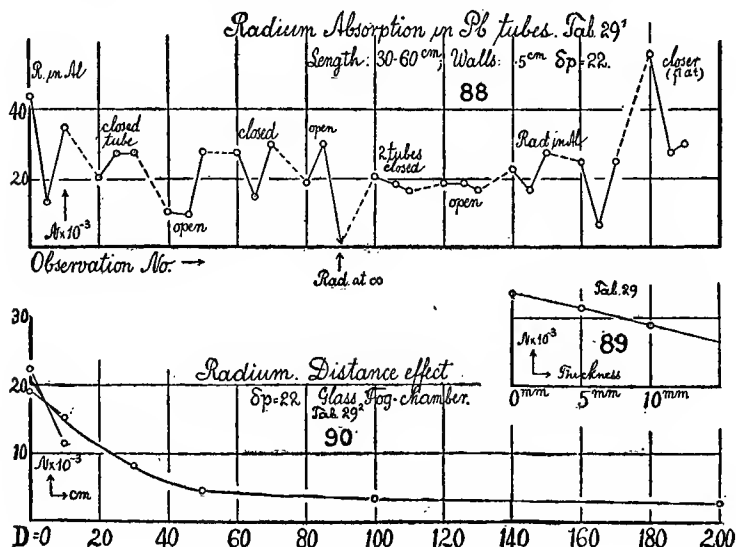
TABLE 55.—Radium effect from different distances outside of fog chamber. $\delta p = 25$ cm. Wood fog chamber in lead casket. First exposure 5 min. Radium in sealed aluminum tube.

D.	s_1 .	s_2 .	s_3 .	$N_1 \times 10^{-3}$.	$N_2 \times 10^{-3}$.	$N_3 \times 10^{-3}$.	Mean $N \times 10^{-3}$.
cm.							
600	0.0	0.0	0
400	1.9	<i>r</i>	3.6	<i>r</i>	2
200	2.0	<i>r</i>	3.8	<i>r</i>	2
100	2.6	2.2	<i>r</i>	9.2	5.0	<i>r</i>	7
50	3.1	1.7	14.6	3.0	9
25	3.2	1.9	* 3.1	16.6	3.5	14.6	10
10	3.0	<i>r</i>	* 3.1	13.2	<i>r</i>	14.6	8
0	3.4	2.0	* 3.3	20.4	3.8	18.3	12
∞	1.2	1.8	† <i>r</i>	2.2	3.2	<i>r</i>	2

* Five or six periods observed in succession, same amplitude.

† Radium effect lost at once; apparent air periods.

70. Glass fog chamber—Penetration.—It seemed necessary to repeat the work on the penetration of radium radiations as well as the experiments on their effect from a distance with the aid of the cylindrical fog chamber of glass; for a vessel of this type may be made rigorously tight, whereas entire freedom from leakage is often difficult to maintain in the plate-glass apparatus. From what has been stated, leaks of any kind, even if small, are favorable to the occurrence of water nuclei and therefore to periodicity. The data are given in table 56 and curves 88.



FIGS. 88-90.—Illustrating table 56.

TABLE 56.—Penetration of radium radiation. Cylindrical glass fog chamber without casket. $\delta p = 22$ cm. Lead tube, 30 cm. or 60 cm. long. Walls, 0.5 cm. thick.

Part.	Remarks.	Distance.	s_1 .	s_2 .	s_3 .	$N_1 \times 10^{-3}$	$N_2 \times 10^{-3}$	$N_3 \times 10^{-3}$
I.	Radium in Al tube.....	0	4.4	3.0	4.1	44.0	13.2	35.0
	Radium in 1 Pb tube, capped..	0	3.4	3.7	3.7	20.4	27.6	27.6
	Radium in 1 Pb tube, cap off..	0	2.7	2.7	3.7	10.4	9.8	27.6
	Radium in 1 Pb tube, cap on..	0	3.7	3.1	3.9	27.6	14.6	30.0
	Radium in 1 Pb tube, cap off..	0	3.3	3.9	18.6	30.0
	Radium at ∞^*	∞	0	0	0	0
	Radium in 2 Pb tubes, cap off..	0	3.4	3.3	3.2	20.4	18.6	16.6
	Radium in 2 Pb tubes, cap on..	0	3.3	3.3	3.2	18.6	18.6	16.6
II.	Radium in Al tube.....	0	3.5	3.2	3.7	22.6	16.6	27.6
		10	2.9	2.8	2.9	11.8	11.0	11.8
		0	3.6	2.4	3.6	25.0	6.6	25.0
		10	3.1	3.1	3.2	14.6	14.6	16.6
		30	2.3	2.4	3.0	5.4	6.6	13.2
		100	1.9	1.9	1.9	3.6	3.6	3.6
		200	1.5	1.5	1.5	2.8	2.8	2.8
		50	2.1	2.2	2.2	4.4	5.0	5.0
		\dagger 0	4.7	2.7	3.9	56.0	27.6	30.0
	Radium at ∞	0	0	0	0	0	0

* Air effect frequently tested.

 \dagger Flat against chamber.

In the first part of table 56 the radiation passes through thick lead tubes, P , placed parallel to and contiguous with the end of fog chamber A , as shown in fig. 88. There is no observable effect due to the cap, nor to the length of the lead tubes, whence it follows that the rays producing the nuclei actually pass through the heavy walls of lead. If mean values be taken for the periodic data, the results are (curve 89):

Radium in thin sealed aluminum tube, $N = 27,000$ Radium in lead tube, walls 0.5 cm., $N = 23,000$ walls 1.0 cm., $N = 18,000$

or 85 per cent and 67 per cent pass, respectively, through the walls of lead 0.5 cm. and 1 cm. thick. The important result follows here, as above, that the extremely penetrating rays are responsible for the observed nucleation.

71. Radiation from a distance.—It is surprising to compare with the penetrating effect of the radiation the relatively marked diminution of its intensity with distance. Indeed, if distances be reckoned from the line of sight (supposing this to be justified) about 10 cm. from the end of the chamber, the mean data are (curve 90):

$D =$	10	20	40	60	110	210 cm.
$N \times 10^{-3} =$	30	13	8	5	3	2
$ND \times 10^{-4} =$	30	26	32	30	33	42

where the decrease is about inversely as the distance, except at long distances, when the data become uncertain. All this is in strong contrast with the X-ray effect, where the removal of the bulb to a distance is so much less significant than the presence of a dense screen in the path of the rays.

72. Distribution of nucleation along the axis within the fog chamber.—This makes a final anomalous feature of the results. Whereas the nucleating effect falls off nearly 25 per cent when the radium is placed axially at a distance of 40 cm. from the end of the fog chamber, outside of it the size of the coronas is about the same from end to end of the inner length of about 40 cm., no matter what may be the position of the radium outside.* It will be remembered that the decay and generation of the nucleus is so nearly instantaneous, that convection or like discrepancy is quite out of the question. These observations are difficult because of the short length of the chamber and the rapid subsidence; but so far as they have gone, there seems to be an entire contrast between the behavior of the radiation outside of the chamber and the behavior inside of it, the aluminum tube being in every case outside of the chamber and axial in position.

SUMMARY AND CONCLUSIONS.

73. General remarks.—The results of this chapter relate to fleeting nuclei (ions), to persistent nuclei, to fog limits, to persistence of fleeting nuclei or ions on solution, to the alternations of large and small numbers of efficient nuclei in successive identical exhaustions, to the secondary generation of nuclei after intense X-radiation, to the distribution of radiation in the space surrounding the X-ray tube in contrast with the corresponding case of the sealed tube with weak radium, to the nucleation produced by the gamma rays and its distribution within the fog chamber, etc. They are thus of considerable importance in their bearing on the present research, and will therefore be advantageously summarized at the end of this memoir, in Chapter VI, section 91 *et seq.*, in connection with other relevant matter.

* The statement in the text needs correction. My recent experiments have shown that there is an axial gradation of the number of fleeting nuclei within the fog chamber. This gradation becomes very marked when the fog chamber consists of parts which are unequally strong secondary radiators. Discussion will be made elsewhere.

PLATE I.



Station of U. S. Weather Bureau at Block Island, illustrating barren nature of Island.

CHAPTER IV.

THE NUCLEATION OF THE ATMOSPHERE AT BLOCK ISLAND.

BY ROBINSON PIERCE, JR.

74. Introductory.—The present series of experiments, during the winter of 1904-5, was undertaken with a view to comparing the nucleation in pure country air with the results obtained at the same time in Providence.* After a consideration of several places, Block Island, R. I., was chosen as a station, on account of its location, in the ocean (see fig. 94) 10 miles south of Point Judith, and the freedom from smoke and other refuse commonly found in the air of cities. At the same time, the two stations are, in other respects, meteorologically nearly identical. Through the courtesy of Prof. Willis L. Moore, chief of the United States Weather Bureau, the office of the Bureau on the island was placed at our disposal, and the apparatus was duly installed there during the latter part of November. The chief occupations on Block Island are fishing and farming, and the only smoke is that from dwellings, which are to a great extent scattered. As the high readings usually occurred with north to west winds, the situation of the Weather Bureau building northwest of the village gave complete freedom from all such local influences.

I have here to express my thanks to Mr. W. L. Day, the local observer, for his assistance in many ways during my stay at the island. Mr. Day took the observations at various times, and the results from March 10-14 and April 19-25 are his.

75. Apparatus.—The apparatus used was similar to that employed by Professor Barus,† and the two were operated side by side for some time previous to leaving Providence, with results well in accord. A brass cylindrical trough was substituted for the wooden one late in December and a few minor changes were made from time to time, all of which were tested to make sure that they did not affect the readings of the instrument.

* C. Barus : Smithsonian Contributions, Vol. xxxiv, 1905, Chap. IX ; also Chap. V of the present memoir.

† Barus : Loc. cit.

In the following table the weather is given in terms of F fair, Fc partly cloudy, C cloudy, R rain, Sn snow, S sun; the wind directions, in points of the compass. The coronal angular diameter, ϕ , is such that $30 \times 2 \sin \phi/2 = s$, or nearly $\phi = s/30$, when the eye at the goniometer and the source of light were at distances 85 cm. and 250 cm., respectively, from the fog chamber between them. N is not corrected for the temperature ($^{\circ}\text{C}.$) of the apparatus, this being added in the next table. The reduction from s to N is made as in Barus's memoir (Smithsonian Contributions, 1905, Vol. xxxiv), and the measurement of s made to the outer edge of the red ring, coinciding with the inner edge of the blue or green rings. Exhaustions were made to a pressure difference of $\delta p = 17$ cm.

TABLE 57.—Successive observations of the nucleation (N in thousands per cubic centimeter) of the atmosphere at Block Island.

Date.	Time.	Weather.	Wind.	Temperature of apparatus, $^{\circ}\text{C}.$	Temperature of atmosphere, $^{\circ}\text{F}.$	Aperture s .	Corona col-ors.	Number, $n \times 10^{-3}$.	Remarks.
1904.									
Nov. 26	3.5	F	NW	18.0	38	—	—	Leaky trough.
	3.8	F	NW	18.0	38	—	—	Do.
	4.4	F	NW	15.0	38	3.1	10.2	New trough,
	4.6	F	NW	14.5	37	2.8	7.3	
27	9.8	C	No wind	17.8	34	2.2	cor	3.3	
	9.9	C	No wind	18.0	34	2.7	cor	6.6	
	12.7	C Sn	SW	17.6	31	3.0	cor	9.3	
	12.8	C Sn	SW	17.7	31	3.0	cor	9.3	
	2.5	C	NW	18.0	32	2.2	cor	3.3	
	4.2	C	NW	17.6	32	4.3	w b p	28.0	Possibly some warm air
28	5.0	C	NW	18.3	32	2.3	cor	4.0	
	9.5	F	NW	15.0	25	2.6	cor	5.9	
	10.4	F	NW	14.8	24	2.6	cor	5.9	
	11.8	F	NW	15.0	23	3.1	cor	10.2	
	2.5	F	NW	14.8	26	3.3	w b cor	12.5	
	3.7	F	NW	15.0	26	3.2	cor	11.3	
29	5.0	C	NW	15.0	25	3.1	cor	10.2	
	9.5	C	SW	15.2	37	2.2	cor	3.3	
	12.0	C	S	16.2	—	3.4	w b cor	13.8	
	1.5	C	S	16.4	—	3.6	w b cor	16.2	
	3.1	C	S	16.7	—	2.6	cor	5.9	
	4.2	C	S	17.0	—	2.3	cor	4.0	
	5.5	C	S	17.0	50	2.3	cor	4.0	
30	9.3	C	SW	16.6	47	1.4	cor	1.4	Repeated same.
	10.9	C	SW	16.9	49	1.3	cor	1.3	Rain at night.
	12.0	C	SW	17.8	50	2.0	cor	2.5	Thick, almost foggy.
	1.5	C	SW	17.6	49	1.8	cor	1.9	
	3.1	C	—	17.3	48	1.7	cor	1.8	
	4.1	C	SW	17.0	48	2.0	cor	2.5	
Dec. 1	5.3	C	SW	16.8	47	1.8	cor	1.9	
	8.4	C	W	18.3	34	2.2	cor	1.3	
	10.8	C	W	18.5	36	1.7	cor	1.8	
	11.2	C	W	18.5	36	1.9	cor	2.2	
	12.1	C	W	18.5	36	2.1	cor	2.7	
	2.0	C	W	18.2	37	2.2	cor	3.3	
	3.5	C	W	18.2	37	2.2	cor	3.3	
	5.6	C	W	18.3	36	2.0	cor	2.5	
2	8.7	C	NW	16.3	33	1.4	cor	1.4	Very faint; influx tube shortened from 34 to 14 feet.
	9.1	C	NW	16.3	33	1.4	cor	1.4	
	10.8	C	NW	16.6	32	1.9	cor	2.2	
	12.2	C	NW	16.8	32	1.9	cor	2.2	

TABLE 57.—Successive observations of the nucleation, etc.—Continued.

Date.	Time.	Weather.	Wind.	Temperature of apparatus.	Temperature of atmosphere.	Aperture s.	Corona col- ors.	Number. $n \times 10^{-3}$.	Remarks.
1904. Dec.				°C	°F				
2	1.8	C	NW	17.0	32	2.8	cor	7.3	
	3.8	C	NW	16.9	32	2.2	cor	3.3	
	5.3	C	NW	16.9	31	2.4	cor	4.6	
3	8.6	C	NE	15.5	27	1.8	cor	1.9	
	10.3	C	NE	15.6	28	2.0	cor	2.5	
	12.4	C	NE	16.1	28	1.6	cor	1.6	
	2.9	C	NE	16.1	29	2.2	cor	3.3	
	4.4	C	NE	15.8	30	2.9	cor	6.6	
	5.4	C	NW	15.8	25	1.7	cor	1.8	
4	9.1	C	NW	15.6	27	2.9	cor	8.3	
	12.4	C	W	16.1	30	3.1	cor	10.2	
	2.7	C	W	16.2	30	2.3	cor	4.0	
	6.7	C	NE	15.0	27	1.5	cor	1.5	
5	8.4	C	E	15.8	31	1.6		1.6	
	10.5	C	SE	16.3	33	1.6		1.6	
	12.3	C	SE	16.5	34	1.1		1.1	
	2.1	Su	S	16.8	33	2.1		2.7	
	3.7	Su	S	16.4	33	2.0		2.5	
6	5.2	Su	NW	14.5	30	1.6		1.6	Snow fell, 3.5 inches.
	8.9	F	NW	14.9	32	2.9		8.3	
	10.7	F	NW	15.3	33	2.6		5.9	
	12.3	F	NW	15.8	32	3.0	w b p	9.3	
	1.9	F	NW	16.1	32	2.9		8.3	
	3.4	F	NW	16.5	31	2.7		6.6	
7	5.6	C	SW	16.5	36	1.5	cor	1.5	
	9.2	C	SW	16.0	36	2.3		4.0	
	10.5	C	SW	16.1	36	2.5		5.2	
	12.5	C	SW	16.1	37	2.7		6.6	
	2.7	C	W	16.5	37	3.0		9.3	
	4.0	C	W	16.8	38	2.6		5.9	
8	5.2	C	SW	16.6	31	2.5		5.2	
	9.0	Su	SW	17.0	33	2.5		5.2	
	10.5	Su	W	17.4	35	2.6		5.9	
	12.3	Su	W	17.5	35	2.9		8.3	
	1.9	Su	W	17.6	37	2.0		2.5	
	3.5	Su	W	17.5	35	2.1		2.7	
9	5.3	F	NW	14.1	23	2.1		2.7	
	8.6	F	NW	14.0	24	2.4		4.6	
	9.9	F	NW	13.9	24	2.5		5.2	
	11.3	F	NW	14.0	26	3.0		9.3	
	12.7	F	NW	13.3	25	3.7		17.5	
	2.6	F	NW	14.0	24	3.7		17.5	
	4.3	F	NW	14.4	24	3.0		9.3	
10	5.4	C	NE	13.4	18	—		—	Too small to measure.
	8.7	C	N	13.4	17	1.9		2.2	
	12.2	C	N	12.2	18	2.8		7.3	Hand pump.
	1.8	Su	N	11.0	18	2.0		2.5	
11	5.3	F	NW	10.0	15	—		—	Oil lamp.
	10.0	F	NW	10.6	16	4.7		37.2	Hand pump.
	11.6	F	NW	11.0	17	3.9		20.5	Do.
	12.8	F	NW	10.8	20	3.6		16.2	Do.
	3.1	F	NW	11.0	22	2.8		7.3	Do.
12	6.8	C	SE	13.6	31	—		—	Too small to measure.
	9.1	C	SE	14.6	32	—		—	Do.
	10.5	C	SE	14.9	33	1.3		1.3	
	12.0	C	NE	14.6	31	—		—	
	3.4	Su	NE	14.8	31	1.9		2.2	Do.
13	4.8	Su	N	11.6	24	3.0		9.3	
	9.2	Su	N	11.8	24	2.7		6.6	
	9.4	Su	N	11.9	24	2.6		5.9	
	10.7	Su	N	12.0	24	2.9		8.3	
	12.1	C	N	12.0	26	2.9		8.3	
14	2.7	C	NW	11.9	28	3.5	w p cor	15.0	
	4.8	F	NW	12.0	15	3.7	w p cor	17.5	
	9.0	F	NW	12.0	16	4.7	w b p	37.2	
	10.8	F	NW	12.3	17	4.7	w p cor	37.2	
	12.3	F	NW	12.1	17	4.9	w b p	41.7	
	2.5	F	NW	12.7	17	3.8	w p cor	18.0	
	4.6	F	NW	12.5	19	3.7	w p cor	17.5	

TABLE 57.—Successive observations of the nucleation, etc.—Continued.

Date.	Time.	Weather.	Wind.	Temperature of appara- tus.	Temperature of atmos- phere.	Aperture s.	Corona col- ors.	Number. $n \times 10^{-8}$.	Remarks.
1904.				°C	°F				
Dec. 14	9.3	F	NW	12.5	18	3.2	w P cor	11.3	
	11.3	F	NW	12.2	20	2.6	cor	5.9	
15	8.9	C	NE	12.0	22	3.0	cor	9.3	
	11.0	C	NE	13.0	22	2.9	8.3	
	12.2	C	NE	12.9	30	2.5	5.2	
	1.9	C	NE	13.4	31	2.9	8.3	
	5.5	C	NE	13.5	30	4.3	w p g	28.0	Snow at night.
16	9.6	C	N	14.6	29	0.00	
	12.3	C	N	14.4	31	2.3	4.0	
	3.2	F	NW	15.3	32	2.7	6.6	
	4.5	F	NW	15.5	32	2.8	7.3	
	5.4	F	NW	15.4	31	3.2	11.3	
	7.1	F	NW	15.9	31	2.7	6.6	
	9.2	F	NW	15.9	30	2.4	4.6	
17	10.6	F	NW	16.3	29	2.9	8.3	
	9.0	F	NW	13.9	25	2.4	4.6	
	10.8	F	NW	13.8	29	3.0	9.3	
	12.1	F	NW	15.5	29	3.3	12.5	
	3.3	C	NW	16.6	29	3.4	13.8	
	4.2	C	N	16.9	29	2.5	5.2	
	5.3	C	N	16.8	29	2.7	6.6	
18	10.7	C	NW	14.0	29	2.7	6.6	Blizzard at night.
	12.3	C	NW	14.0	29	3.7	w br g	17.5	
	1.1	C	NW	14.4	30	3.4	w p g	13.8	
19	9.3	C	S	13.6	35	2.7	6.6	
	12.6	C	S	14.0	41	3.1	10.2	
	3.4	C	SW	15.6	41	2.1	2.7	
	6.0	C	W	16.2	36	2.7	6.6	
20	8.7	F	NW	16.3	31	3.0	9.3	
	10.7	F	NW	16.6	32	3.1	10.2	
	12.0	F	NW	17.0	32	3.7	17.5	
	2.1	F	NW	17.6	32	2.9	8.3	
	3.6	F	NW	17.8	32	3.7	17.5	
	6.0	C	W	18.0	32	3.0	9.3	
21	9.1	C	W	15.0	31	2.3	4.0	
	10.5	C	NW	15.3	31	3.2	11.3	
	12.2	C	NW	15.6	31	2.8	7.3	
	1.6	F	NW	15.1	30	2.5	5.2	
	4.6	F	NW	15.3	26	3.7	17.5	
	5.6	F	NW	15.2	25	3.4	13.8	
22	8.9	F	SW	13.7	27	2.4	4.6	
30	3.5	F	SW	18.0	30	3.1	10.2	Snow in morning.
	5.7	F	SW	18.0	30	2.8	7.3	Brass trough.
31	9.4	F	SW	17.8	32	1.9	2.2	
	10.8	F	SW	18.8	39	2.4	4.6	
	12.1	F	SW	18.8	41	2.3	4.0	
	3.3	F	SW	19.4	41	2.2	3.3	
	5.8	F	SW	19.8	40	2.4	4.6	
1905.									
Jan. 1	10.5	F	W	18.6	40	1.7	1.8	
	12.5	F	W	19.3	43	2.7	6.6	
	2.6	F	W	19.8	45	2.2	3.3	
	6.7	F	W	20.0	40	1.9	8.3	
2	9.4	C	SW	18.4	44	0.0	0.0	
	10.6	C	SW	20.8	43	2.3	4.0	
	12.2	C	SW	20.4	44	2.1	2.7	
	2.4	C	SW	20.0	43	1.8	1.9	
	4.1	C	SW	19.0	42	1.8	1.9	
	5.4	C	SW	18.9	42	1.8	1.9	
3	8.6	R	NE	17.4	38	0.0	0.0	
	10.0	R	NE	17.8	38	0.0	0.0	
	12.2	R	NE	17.8	37	0.0	0.0	
	2.8	R	NE	17.3	35	0.0	0.0	
	5.0	R	N	17.5	32	0.0	0.0	
4	9.7	Sn	N	11.7	17	2.9	8.3	Blizzard, 60 miles.
	11.3	C	NW	12.0	17	1.9	2.2	
	12.3	C	NW	12.4	18	2.8	7.3	
	2.8	C	NW	12.8	19	2.1	2.7	
	5.2	F	NW	13.6	17	2.9	8.3	
5	9.0	F	SW	12.2	18	2.3	4.0	

TABLE 57.—Successive observations of the nucleation, etc.—Continued.

Date.	Time.	Weather.	Wind.	Temperature of apparatus.	Temperature of atmosphere.	Aperture s.	Corona col-ors.	Number. $n \times 10^{-3}$.	Remarks.
1905. Jan. 5	10.7	F	W	13.0	21	2.8	7.3	
	12.3	F	W	13.2	25	2.8	7.3	
	2.1	F	NW	13.5	25	2.8	7.3	
	3.6	F	NW	13.8	25	4.3	28.0	
	4.9	F	NW	13.9	23	2.9	8.3	
	5.8	F	NW	13.9	22	2.0	2.5	
	8.8	Sn	E	13.9	30	0.0	0.0	
6	10.1	Sn	E	14.2	32	0.88	
	12.3	Sn	E	14.7	34	1.0	1.0	
	3.3	R	E	15.4	36	9.09	
	5.9	C	E	15.8	37	1.0	1.0	Rain at night.
7	9.7	C	SE	18.5	49	0.88	
	11.0	C	SE	19.0	50	1.3	1.3	
	12.5	F	SW	19.5	48	1.5	1.5	
	3.5	F	SW	20.0	44	1.7	1.8	
	5.9	F	SW	19.7	42	1.8	1.9	
8	8.0	F	W	14.4	31	1.6	1.6	
	1.5	F	W	17.6	33	2.9	8.3	
	3.4	F	W	16.9	33	2.3	4.0	
	7.6	F	W	16.9	31	2.0	2.5	
9	8.8	F	NW	15.5	28	1.8	1.9	
	10.7	F	NW	15.7	29	2.7	6.6	
	12.2	F	NW	16.0	30	2.6	5.9	
	1.9	F	NW	16.5	31	2.2	3.3	
	3.8	F	NW	16.1	31	2.2	3.3	
	5.6	C	NW	16.1	31	1.8	1.9	
10	8.7	C	SW	17.2	36	1.5	1.5	
	10.6	C	W	17.4	36	2.0	2.5	
	12.3	C	W	17.4	37	2.4	4.6	
	2.6	C	W	17.4	36	2.5	5.2	
	4.4	C	W	17.4	34	2.7	6.6	
	5.8	C	W	17.5	32	3.4	13.8	
11	9.0	C	NW	13.0	25	1.4	1.4	
	10.5	F	NW	15.5	26	2.3	4.0	
	12.4	C	N	16.0	27	2.1	2.7	
	3.1	C	NE	16.5	29	2.3	4.0	
	4.9	C	NE	17.1	29	2.7	6.6	
	5.9	C	NE	17.0	29	3.3	8.3	
12	8.8	R Fog	SE	13.6	41	2.0	2.5	Do.
	10.7	Fog	SW	15.7	46	2.3	4.0	
	12.5	Fog R	SW	16.7	47	1.5	1.5	
	2.4	R Fog	SW	17.8	46	1.8	1.9	
	3.4	R	SW	18.2	44	1.8	1.9	
	5.6	R Fog	SW	18.8	40	1.8	1.9	
13	9.0	F	NW	16.9	29	1.8	1.9	
	11.6	C	NW	16.2	28	2.6	5.9	Hazy.
	3.5	C	N	16.4	29	2.8	7.3	
	5.7	C	N	16.4	28	2.8	7.3	
14	9.5	F	N	12.7	19	1.7	1.8	
	12.7	F	NW	17.0	22	3.0	9.3	No cloth in trough from here on.
	3.6	F	NW	14.6	22	2.8	7.3	
	5.3	F	NW	14.0	21	2.8	7.3	
15	8.4	F	NW	11.5	16	2.2	3.3	
	11.0	C	W	12.1	20	2.5	5.2	
	12.8	C	SW	13.0	21	2.9	8.3	
	3.3	C	W	13.0	23	2.7	6.6	
	8.0	F	W	14.0	26	3.3	12.5	
16	9.3	F	W	13.7	25	3.6	16.2	Cleaned trough.
	3.5	F	W	15.0	28	3.2	11.3	
	4.9	F	W	15.0	28	4.5	32.4	
	6.0	F	W	15.0	28	3.7	17.5	
	8.1	F	W	15.0	27	3.3	12.5	
	9.6	F	W	15.0	27	2.9	8.3	
17	9.0	F	W	14.7	30	2.5	5.2	
	10.6	F	W	15.7	32	3.3	12.5	
	12.5	F	W	16.6	34	3.4	13.8	
	3.2	F	W	16.4	34	2.8	7.3	
	6.0	F	W	14.1	33	2.6	5.9	
18	9.0	F	NW	16.3	32	2.2	3.3	

TABLE 57.—Successive observations of the nucleation, etc.—Continued.

Date.	Time.	Weather.	Wind.	Temperature of appara- tus.	Temperature of atmos- phere.	Aperture s.	Corona col- ors.	Number. $n \times 10^{-3}$.	Remarks.
1905.				°C	°F				
Jan. 18	10.5	F	NW	16.4	34	2.7	6.6	
	12.0	F	NW	16.5	35	2.9	8.3	
	3.0	F	NW	17.2	36	2.5	5.2	
	4.6	F	NW	17.5	34	2.7	6.6	
	5.8	F	NW	17.4	33	2.6	5.9	
19	8.8	F	SW	16.5	40	1.9	2.2	
	11.0	F	SW	16.9	42	2.5	5.2	
	12.4	F	SW	17.0	42	3.1	10.2	
	2.4	F	SW	17.6	39	2.7	6.6	
	3.7	F	SW	17.6	39	2.3	4.0	
	6.0	F	SW	17.5	39	2.2	3.3	
20	9.1	C	NW	17.7	37	1.3	1.3	
	11.0	C	NW	17.8	37	2.5	5.2	
	12.5	C	NW	18.0	40	2.7	6.6	
	3.2	F	NW	18.4	39	3.1	10.2	
	5.9	F	NW	18.7	36	3.0	9.3	
21	9.0	F	NE	14.7	31	1.9	2.2	
	12.2	C	NE	17.7	34	4.2	25.8	
	2.5	E	E	16.9	35	3.5	15.0	
	5.1	SE	SE	16.9	36	3.1	10.2	
22	9.0	C	S	18.9	40	1.9	2.2	Mist, almost rain. Light rain, almost sun- shine.
	12.0	C	NW	19.0	38	2.5	5.2	
	1.5	C	NW	19.3	37	2.5	5.2	
	4.0	C	NW	19.0	37	2.1	2.7	
23	7.5	C	NW	18.7	36	1.8	1.9	
	9.0	F	NW	12.4	19	2.8	7.3	Cleaned trough.
	12.2	F	NW	14.7	21	4.2	25.8	
	3.3	F	NW	14.6	23	3.4	13.8	
24	6.1	F	NW	14.3	23	3.1	10.2	
	8.8	F	NE	8.5	20	1.8	1.9	
	12.2	C	NE	11.0	23	2.4	4.6	
	2.8	C	NE	11.9	27	1.9	2.2	
	5.7	C	E	12.8	29	1.4	1.4	
25	8.9	Sn	NE	12.0	20	1.9	2.2	Blizzard.
	11.8	Sn	NE	10.8	21	2.8	7.3	Do.
	1.9	Sn	NE	10.5	22	2.6	5.9	Do.
	5.1	Sn	N	10.5	12	2.5	5.2	Do.
26	9.0	F	NW	8.6	10	2.4	4.6	
	10.8	F	NW	8.6	12	3.0	9.3	
	12.6	F	NW	8.5	14	3.2	11.3	
	3.2	F	NW	8.5	14	3.1	10.2	
	5.6	F	NW	8.5	22	3.0	9.3	
27	8.8	F	W	10.0	18	2.9	8.3	
	12.3	F	W	11.7	22	4.0	22.0	
	3.3	F	SW	12.8	24	3.9	20.5	
	5.5	F	SW	13.0	26	3.3	12.5	
28	9.3	Sn	SW	14.6	29	2.8	7.3	
	12.0	C	SW	15.4	34	2.9	8.3	
	3.1	C	W	15.6	33	2.1	2.7	
	5.7	C	W	15.6	30	4.1	24.0	
29	9.3	F	NW	13.6	19	1.9	2.2	
	12.0	F	NW	14.6	21	2.1	2.7	
	1.7	F	NW	14.7	24	2.6	5.9	
	3.1	F	SW	15.0	24	3.2	11.3	
30	9.2	Sn	N	15.0	20	1.9	2.2	
	12.3	Sn	NE	14.7	22	2.9	8.3	
	3.3	Sn	NE	14.8	24	3.1	10.2	
	5.4	C	NE	13.9	23	3.6	16.2	
31	8.9	C	NE	12.7	17	1.4	1.4	
	12.3	C	NE	13.5	22	2.6	5.9	
	2.8	C	NE	13.7	23	3.2	11.3	
	5.6	C	NE	13.6	22	3.4	13.8	
Feb. 1	9.0	F	NW	14.0	19	2.6	5.9	
	12.4	C	NW	15.6	24	4.3	28.0	
	3.0	W	W	15.3	26	3.6	16.2	
	5.7	C	SW	15.1	26	3.4	13.8	
2	9.0	C	NW	12.2	22	3.1	10.2	
	12.3	C	NW	14.0	22	4.1	24.0	
	2.3	C	NW	13.9	21	4.6	34.8	Snow at night.

TABLE 57.—Successive observations of the nucleation, etc.—Continued.

Date.	Time.	Weather.	Wind.	Temperature of apparatus.	Temperature of atmosphere.	Aperture <i>s</i> .	Corona col-ors.	Number. $n \times 10^{-3}$.	Remarks.
1905.				°C	°F				
Feb.									
2	5.4	Q	NW	15.0	19	4.6	34.8	
	9.0	Q	NW	10.0	9	3.7	17.5	
3	10.5	Q	NW	10.0	11	4.8	39.5	
	12.2	Q	NW	10.0	15	5.1	46.0	
	3.0	Q	NW	11.6	19	4.7	37.2	
	6.2	Q	NW	12.9	17	3.7	17.5	
4	9.5	Q	NW	10.0	10	4.0	22.0	
	10.7	Q	NW	10.0	12	4.2	25.8	
	12.2	Q	NW	10.0	14	4.7	37.2	
	3.0	Q	NW	11.9	16	4.5	32.4	
	6.3	Q	NW	11.6	16	3.7	17.5	
5	8.4	N	N	12.0	14	2.5	5.2	
	10.0	Q	NE	12.0	18	3.9	20.5	
	1.3	Q	NE	13.6	24	3.6	16.2	
	3.3	Q	E	15.3	24	3.0	9.3	
	6.3	Q	E	15.4	24	3.7	17.5	Snow at night.
6	9.4	R	E	13.8	32	0.0	0.0	Cleaning apparatus.
	6.0	Fog	NW	17.4	33	2.1	2.7	
7	9.3	Q	NW	14.7	22	4.2	25.8	Mending apparatus.
	3.7	Q	NW	14.1	23	4.7	37.2	
	6.2	Q	NW	13.6	21	3.6	16.2	
8	9.2	Q	NW	11.4	16	3.9	20.5	
	12.5	Q	NW	12.6	26	4.0	22.0	
	2.6	Q	NE	13.6	30	3.6	16.2	
	5.7	Q	W	14.0	27	4.1	24.0	
9	9.3	Sn	E	14.6	30	1.3	1.3	Snow at night.
	12.5	Q	E	15.5	33	2.0	2.5	
	3.3	Q	E	13.7	33	0.0	0.0	
	5.6	Q	E	15.5	33	0.8	0.8	
10	9.2	Q	W	17.0	32	3.6	16.2	
	12.4	Q	SW	18.0	34	4.4	30.0	
	3.1	Q	W	17.5	34	3.2	11.3	
	5.8	Q	W	17.5	32	2.7	6.6	
11	9.4	Q	NW	13.6	21	3.0	9.3	
	12.2	Q	NW	13.7	23	4.9	41.7	
	3.5	Q	W	14.1	24	4.3	28.0	
	5.8	Q	W	14.2	23	3.9	20.5	
12	8.5	Q	SE	14.3	25	2.7	6.6	
	11.5	Q	SE	14.8	29	2.9	8.3	
	1.0	Q	SE	15.7	31	2.5	5.2	
	3.0	Q	SE	16.0	34	2.7	6.6	
	6.4	Q	SE	16.4	37	2.7	6.6	
13	9.1	Q	SW	17.0	35	2.9	8.3	Rain at night.
	10.8	Q	SW	17.0	36	2.6	5.9	
	12.5	Q	W	16.4	35	2.7	6.6	
	3.2	Sn	NW	16.4	28	2.7	6.6	
	5.8	Q	NW	15.8	25	2.9	8.3	
14	9.4	Q	W	12.1	13	4.3	28.0	
	12.3	Q	W	11.0	15	3.7	17.5	
	2.5	Q	SW	11.0	16	3.8	19.0	
	6.0	Q	SW	12.7	17	3.8	19.0	
15	9.3	Q	E	11.4	24	1.8	1.8	
	11.3	Q	E	12.7	24	2.2	3.3	
	11.8	Q	E	12.7	24	2.0	2.5	
	3.5	Sn	NW	13.5	24	3.3	12.5	
	5.7	Q	NW	14.3	23	3.1	10.2	
16	9.4	Q	NW	10.0	10	5.9	68.0	
	12.2	Q	NW	10.0	14	5.1	46.0	
	3.3	Q	NW	11.5	17	4.8	33.5	
	5.9	Q	NW	12.6	17	3.9	20.5	
17	9.4	Q	SW	12.8	32	2.7	6.6	
	12.0	Q	SW	13.7	36	2.6	5.9	
	2.9	Q	SW	15.0	32	2.7	6.6	
	5.5	Q	SW	15.8	31	2.8	7.3	
18	9.2	Q	W	13.9	21	3.6	16.2	
	12.3	Q	W	13.9	22	4.4	30.0	
	3.0	Q	W	14.1	22	3.8	19.0	
	6.0	Q	NW	14.0	20	3.6	16.2	
19	8.6	Q	NW	11.7	15	2.9	8.3	
	12.3	Q	W	12.9	18	3.7	20.5	

TABLE 57.—Successive observations of the nucleation, etc.—Continued.

Date.	Time.	Weather.	Wind.	Temperature of apparatus.	Temperature of atmosphere.	Aperture s.	Corona col- ors.	Number. $n \times 10^{-3}$.	Remarks.
1905.				°C	°F				
Feb. 19	3.8	F'	W	13.9	21	4.2	25.8	Aspirator hereafter.
	6.5	F'	W	13.8	21	3.6	16.2	
	9.1	F'	W	14.9	33	2.4	4.6	
20	12.3	Sn	SW	15.4	31	3.1	10.2	Rain at night.
	3.0	Sn	SW	15.6	32	3.0	9.3	
	5.4	C	SW	17.0	32	3.3	12.5	
21	9.2	F	NW	18.3	35	2.9	8.3	
	12.0	F	NE	18.3	38	3.2	11.3	
	4.3	F	E	18.8	36	1.7	1.8	
	6.0	F	E	18.9	35	1.5	1.5	
22	9.1	C	NE	17.3	31	1.0	1.0	
	11.0	C	NE	17.0	31	1.2	1.2	
	12.3	C	NE	16.9	30	1.4	1.4	
	3.0	C	NE	16.6	30	0.8	0.8	
	6.0	C	NE	16.4	30	0.0	0.0	
23	9.3	C	N	11.7	23	2.6	5.9	
	12.0	C	N	12.6	25	4.5	32.4	
	2.2	C	NE	13.4	29	4.6	34.8	
	4.6	F	NE	14.5	32	4.0	22.0	
	5.8	F	NE	14.8	31	3.6	16.2	
24	8.8	F	N	14.9	28	2.3	4.0	
	12.2	F	N	15.0	35	3.9	20.5	
	3.0	F	NW	15.8	36	4.6	34.8	
	6.0	F	NW	15.8	35	3.4	13.8	
25	8.9	F	NW	17.0	27	2.6	5.9	
	12.3	F	W	17.5	32	4.2	25.8	
	2.9	F	W	18.0	35	3.4	13.8	
	5.8	F	W	18.3	31	3.1	10.2	
26	8.7	C	NE	18.2	33	2.4	4.6	
	12.1	C	N	17.5	32	2.6	5.9	
	3.1	C	NW	18.2	34	3.0	9.3	
	6.3	F	W	18.4	35	3.4	13.8	
27	9.1	F	W	14.0	22	3.8	19.0	
	12.1	F	W	14.5	25	4.2	25.8	
	3.2	F	W	15.0	25	4.2	25.8	
	5.8	F	W	15.5	26	3.7	17.5	
28	9.0	F	W	15.2	31	3.9	20.5	
	12.2	F	SW	15.4	35	3.0	9.3	
	3.3	F	SW	15.7	34	3.0	9.3	
	6.0	F	W	17.0	32	4.0	22.0	
Mar. 1	9.2	F	NW	15.7	25	5.1	w b p	46.0	
	12.0	F	W	16.3	28	4.1	24.0	
	3.1	F	W	17.0	29	4.4	30.0	
	6.0	F	W	17.7	28	3.6	16.2	
2	9.2	F	W	14.4	20	4.4	30.0	
	12.0	F	W	13.0	24	4.0	22.0	
	3.1	F	W	12.4	27	4.7	37.2	
	6.0	F	W	13.4	28	3.7	17.5	
3	9.0	F	NW	15.2	24	4.0	22.0	
	12.2	F	NW	15.8	29	4.2	25.8	
	3.4	F	W	16.4	31	3.5	15.0	
	6.0	F	W	17.0	30	3.8	19.0	
4	9.2	C	S	13.2	34	4.0	22.0	
	12.2	C	S	15.0	34	3.1	10.2	
	3.0	C	{ E N }	16.9	37	2.3	4.0	
	5.8	C	N	17.4	35	2.2	3.3	
5	8.8	F	NW	13.9	19	2.1	2.7	
	12.2	F	S	15.0	24	3.5	15.0	
	3.5	C	SW	15.8	25	3.2	11.3	
	6.2	F	SW	16.0	26	2.9	8.3	
6	9.0	F	N	15.5	37	2.3	4.0	
	12.3	F	N	16.0	31	3.1	10.2	
	3.2	F	W	16.6	33	3.9	20.5	
	5.6	F	W	17.1	31	3.7	17.5	
7	8.9	C	S	17.4	34	3.5	15.0	
	12.3	C	S	17.6	34	3.1	10.2	
	2.8	C	S	18.3	35	2.6	5.9	
	6.0	Sn	SE	18.4	33	2.6	5.9	
8	9.0	Fog	SW	18.0	35	2.4	4.6	Rain at night.

TABLE 57.—Successive observations of the nucleation, etc.—Continued.

Date.	Time.	Weather.	Wind.	Temperature of apparatus.	Temperature of atmosphere.	Aperture s.	Corona col- ors.	Number, $n \times 10^{-3}$.	Remarks.
1905. Mar. 8	11.9	Fog	SW	°C	°F	2.5	5.2	
	3.6	Fog	SW	18.1	35	3.0	9.3	
	5.7	Fog	SW	18.1	34	2.6	5.9	
	9.0	F	W	18.3	34	3.0	9.3	Rain at night.
	12.5	F	SW	19.0	35	2.5	5.2	
	3.3	CC	SE	18.6	38	2.6	5.9	
	5.9	CC	N	17.6	37	2.5	5.2	
	9.0	CC	N	17.3	34	2.7	6.6	Do.
	12.1	CC	NW	18.8	36	2.8	7.3	
	3.2	F	W	19.3	37	2.4	4.6	Clearing.
	6.0	F	W	19.7	37	3.3	12.5	
	9.0	FF	NW	20.0	34	3.5	w r g	15.0	
	12.0	FF	NW	15.0	28	4.3	w r g	28.0	
	3.1	FF	W	15.6	30	4.6	w r p	34.8	
	6.0	FF	W	16.4	31	3.9	w r g	20.5	
	9.0	FF	SW	17.0	30	3.4	13.8	
	12.1	CC	SW	17.0	35	3.1	10.2	
	3.0	CC	SW	17.4	37	3.1	10.2	
	8.2	CC	SW	18.0	36	3.1	10.2	
	9.1	FF	N	18.3	33	2.5	5.2	
	12.1	FF	N	14.7	27	3.1	10.2	
	3.2	FF	NE	15.8	30	3.6	16.2	
	6.1	FF	SW	16.6	32	3.6	16.2	
	9.0	FF	N	17.0	29	2.9	8.3	
	12.1	CC	N	17.4	31	2.9	8.3	
	3.2	FF	NE	17.5	34	3.4	w r g	13.8	
	5.9	FF	SW	18.2	36	3.5	w r g	15.0	
	9.3	FF	NW	18.5	32	3.1	10.2	
	12.4	FF	NE	15.5	28	3.4	w r b p	13.8	
	2.9	FF	SW	16.8	34	2.9	8.3	
	6.0	FF	SW	16.8	34	3.3	w b p	12.5	
	9.3	FF	W	19.0	30	3.7	w r o g	17.5	
	12.3	FF	SW	17.9	33	3.6	w b r b	16.2	Haze.
	2.6	FF	SW	18.3	39	2.4	w b p	9.3	
	5.7	CC	SW	18.3	36	2.1	cor	4.6	
	8.8	CC	NE	18.7	36	2.1	cor	2.7	
	12.1	FF	NE	18.5	33	2.9	cor	8.3	
	2.6	FF	H	18.6	37	3.1	w b p	10.2	
	6.0	FF	SE	19.4	39	2.6	cor	5.9	
	9.0	FF	S	19.0	33	2.8	cor	7.3	
	12.1	CC	SW	17.5	42	3.1	cor	10.2	
	3.0	CC	SW	17.5	47	2.5	cor	5.2	
	6.0	FF	SW	18.3	45	2.4	4.6	
	8.8	FF	SW	18.0	44	2.4	4.6	
	12.1	RR	SW	14.8	42	2.2	3.3	
	3.6	RR	SW	16.2	42	2.6	5.9	
	6.3	RR	W	18.9	42	3.1	w b p	10.2	
	8.8	Fog	W	18.5	40	2.4	cor	4.6	
	12.0	R Fog	NE	14.7	34	1.0	cor	1.0	
	3.4	C	NE	15.2	35	1.4	1.4	
	6.2	Fog	NE	16.2	34	1.6	1.6	
	9.3	C	NE	16.4	33	1.9	2.2	
	12.1	RR	NE	16.1	34	1.0	1.0	
	2.8	RR	NE	15.8	34	1.3	1.3	
	5.7	RR	NE	15.6	33	1.1	1.1	
	9.0	RR	NE	15.4	33	1.0	1.0	
	12.5	CC	NE	12.0	33	2.9	cor	8.3	
	3.0	CC	NE	13.7	35	2.9	w b r	8.3	
	6.0	FF	NE	14.0	36	2.5	cor	5.2	
	9.0	FF	E	15.4	35	2.1	2.7	
	12.0	FF	NE	15.0	35	2.6	5.9	
	3.0	FF	E	16.5	36	1.9	2.2	
	5.8	FF	SE	17.5	37	1.6	1.6	
	9.0	FF	SE	16.7	36	2.0	cor	2.5	
	12.2	Fog	E	17.0	36	1.4	cor	1.4	
	3.0	C	S	18.0	33	1.7	cor	1.8	
	5.9	C	E	18.0	40	1.9	cor	2.2	
	9.0	C	E	18.0	39	1.5	cor	1.5	
	12.3	Fog	S	20.0	43	1.9	cor	2.2	
	3.0	Fog	SW	20.0	42	2.4	cor	4.6	
		Fog	SW	20.0	42	2.7	cor	6.6	

100 NUCLEATION OF THE UNCONTAMINATED ATMOSPHERE.

TABLE 57.—Successive observations of the nucleation, etc.—Continued.

Date.	Time.	Weather.	Wind.	Temperature of appara- tus.	Temperature of atmos- phere.	Aperture s.	Corona col- ors.	Number. $n \times 10^{-3}$.	Remarks.
1905.				°C	°F				
Mar. 25	5.8	R	NW	20.0	40	2.1	cor	2.7	
26	8.9	F	W	20.0	43	3.3	w b p	12.5	Rain at night.
	12.0	F	W	20.0	50	3.2	w b p	11.3	
	3.1	F	SW	21.0	48	2.6	cor	5.9	
	6.3	F	S	21.0	40	2.7	cor	6.6	
27	9.0	F	SW	19.0	43	1.8	cor	1.9	
	12.3	F'	SW	18.0	48	2.2	cor	3.3	
	3.0	F'	W	19.0	49	2.4	cor	4.6	
	6.1	F	SW	18.0	45	2.5	cor	5.2	
28	9.3	F	W	19.0	47	2.6	cor	5.9	
	12.0	F'	SW	19.0	52	2.6	cor	5.9	
	3.0	F'	SW	19.0	55	2.3	cor	4.0	
	6.0	F	SW	19.0	49	2.0	cor	2.5	
29	9.3	F	E	21.0	43	1.3	cor	1.3	
	12.2	F	E	22.0	44	1.3	cor	1.3	
	3.0	F	E	22.0	43	1.1	cor	1.1	
	6.0	F	E	20.0	40	1.2	cor	1.2	
30	9.0	F Fog	E	19.0	41	1.0	cor	1.0	Fog at night.
	12.0	F'	S	20.0	47	1.2	cor	1.2	
	2.5	F' Fog	SW	20.0	45	1.2	cor	1.2	
	6.0	F'	SW	19.0	46	1.0	cor	1.0	
31	8.7	F	W	16.0	45	2.3	cor	4.0	Rain at night.
	12.0	F	W	19.0	52	3.1	w b p	10.2	
	3.0	F	W	20.0	52	2.5	cor	5.2	
Apr. 1	9.0	F	SW	21.0	49	2.6	cor	5.9	
	12.0	F	NW	18.0	45	2.3	cor	4.0	
	3.0	F	NW	17.0	48	3.6	w br bg	16.2	
	5.8	F	NW	18.0	47	2.8	cor	7.3	
	9.2	F	NW	19.0	45	3.0	w b p	9.3	
2	12.0	F	NW	16.0	35	1.9	cor	2.2	
	2.5	F	NW	16.0	40	2.0	cor	2.5	
	6.1	F	N	17.0	43	2.1	cor	2.7	
3	9.0	F	NW	18.0	41	2.5	cor	5.2	
	12.0	F	NW	18.0	38	3.4	w b p	13.8	
	3.0	C'	W	19.0	46	3.6	w ro bg	16.2	
	6.0	C'	W	19.0	51	3.0	w b p	9.3	
	9.0	C' Fog	SE	18.0	48	3.0	w b p	9.3	
4	12.1	C	SE	20.0	41	2.5	cor	5.2	
	3.0	C	SE	20.0	43	2.0	cor	2.5	
	6.0	C	SE	20.0	42	2.3	cor	4.0	
5	9.0	C Fog	NE	20.0	41	1.8	cor	1.9	
	12.1	Fog	N	20.0	41	2.1	cor	2.7	Rain and thaw at night.
	3.0	Fog	E	20.0	43	1.9	cor	2.2	
	5.9	Fog	E	19.0	42	2.2	cor	3.3	
	9.0	C Fog	NE	18.0	41	2.2	cor	3.3	
6	12.1	Fog	S	20.0	47	1.6	cor	1.6	Do.
	3.0	C	SW	20.0	44	1.9	cor	2.2	
	6.0	F	W	19.0	42	3.3	w b p	12.5	
	9.0	F	W	18.0	42	1.8	cor	1.9	
7	12.0	F'	W	14.0	39	2.3	cor	4.0	Cleaned flue in morning.
	12.2	F'	W	13.0	42	4.9	w b p	41.7	
	12.2	F'	W	13.0	42	5.7	w cr g	61.5	{ Test in afternoon showed that this did not produce maximum. No steamers in harbor.
	3.0	F'	W	17.0	44	2.9	w b p	8.3	
	6.0	F'	W	18.0	40	3.0	w b p	9.3	
8	8.6	F'	W	19.0	38	2.7	cor	6.6	
	12.3	F'	W	19.0	43	3.1	w b p	10.2	
	3.1	F'	W	20.0	43	2.9	cor	8.3	
	6.0	F'	W	20.0	40	2.2	cor	3.3	
9	9.3	F	W	18.0	41	2.8	cor	7.3	
	12.0	C'	W	19.0	45	3.0	cor	9.3	
	3.0	C'	SW	19.0	45	2.9	cor	8.3	
	6.3	C'	SW	17.0	41	1.9	cor	2.2	
10	8.5	C'	SW	13.0	46	2.2	cor	3.3	
	12.1	C'	SW	16.0	49	2.1	cor	2.7	
	3.0	C'	SW	19.0	51	2.1	cor	2.7	
	6.0	C	SW	20.0	48	1.3	cor	1.3	
11	9.3	R Fog	SW	18.0	—	2.2	cor	3.3	
	12.6	Fog	NE	17.0	—	1.5	cor	1.5	
	4.0	Fog	NE	17.0	—	1.4	cor	1.4	
	6.2	R Fog	NE	16.0	—	1.6	cor	1.6	

76. Observations.—In the data as given in table 57, the first column contains the date and daily average ; the second and third, the time in twentieths of a day and hours ; the fourth shows the condition of wind and weather, R denoting rain, Sn snow, H haze, S sun, F fair, Fc or F' or C' partly cloudy, C cloudy. The fifth column shows the temperature of the instrument in degrees Centigrade, and the sixth, the temperature of the outside air in Fahrenheit degrees. Column 8 shows the aperture of the corona on the given goniometer ; 9, the principal colors from the center outward ; 10 (from March 29), the relative humidity and vapor pressure ; finally, the last column gives the nucleation in thousands of nuclei per cubic centimeter.


It will be noticed that the temperature of the air in the trough varies considerably at times from 20° C., the temperature for which reductions were made. Each reading was later corrected and the results thus obtained plotted, where the correction amounted to more than a thousand. The corrections as a rule were not large, however, and the original curve shows the relative values equally well. The chief effect is a slight reduction of the maxima on cold days.

In the plates of the next chapter (figs. 95-101) the individual observations are plotted with the weather and mean temperature, the nucleation being given in thousands of nuclei per cubic centimeter. The lower curve belongs to Block Island, the upper curve to Providence, as will there be specified.

77. Remarks on the tables (wood fog chamber).—With the beginning of observations at the island, there is a marked drop from the high readings taken in Providence, showing that a large part of the nucleation observed in the latter place is due to local effects. The same variations with meteorological changes are, however, observed, perhaps even more strikingly. Thus one may note the sudden rise in the afternoon of November 27, when the sky cleared and the wind changed to northwest. On the 30th the rain of the preceding night is followed by a minimum, which, owing to cloudy weather, lasts several days. Snow from the east and south on December 5 cuts down the nucleation, which rises again with the clear sky and northwest wind of the 6th (note the midday minimum) and holds during the two cloudy but dry days following. The clear weather and northwest winds of the 9th, 11th, and 14th bring decided maxima, while minima accompany the northeast wind and cloudiness of the 10th, and the snow from the same quarter on the 12th and 13th. Midday minima occur again on the 15th and 16th ; the high reading late in the afternoon of the 15th is unusual. The 16th shows the increase of nuclea-

tion with clear northwest wind, while the following day (17th) well illustrates the effect of clouds and northeast wind. It is interesting to note that the blizzard and snow produced no further diminution. On the 20th another midday minimum occurs, with a clear west wind all day. The 21st shows the rise due to clearing sky.

78. Remarks on the tables (brass fog chamber).—The observations were interrupted from the 22d to the 29th on account of some needed repairs, and after that date the brass trough replaced the wooden one previously used. With the low nucleations frequently found, a fog chamber rigorously free from leaks is essential.

During January, maxima, usually accompanying clear weather and west to north wind, occur on the 5th, 10th, 16th, 23d, and 27th to 28th; minima due to rain or snow, with wind from the opposite quarter, appear on the 3d, 6th, 12th, 22d, and 24th to 25th. On the 4th, the notched minimum is uncommon, for the weather at the several times of observations is . The 5th shows a high reading, as the wind passes through the northwest, and the 11th a sun and cloud effect. One may notice a curious gradual decrease on the 16th, 17th, and 18th, with continual clear weather and westerly wind. Clouds on the morning of the 20th bring the maximum later in the day, and the next day (21st) shows an unusual maximum, with cloudy sky and northeast wind.

During January and February there is a noticeable tendency to a uniform type of day curve, rising rather steeply from 9 o'clock until noon or later, and falling more gradually during the afternoon and evening. This is what one would expect on sunny days, in view of the fact that nuclei seem to persist for some time in the atmosphere. This curve is quite well shown on the 17th, 18th, and 19th.

In February the maxima are higher, and occur on the 1st to 5th, 7th to 8th, 10th to 11th, 14th, 18th to 19th, 23d to 25th, and 27th to 28th. On the 6th, 9th, 12th to 13th, and 20th we have rain minima, and low readings due to clouds on the 15th, 17th, and 26th. The 8th shows an interesting minimum during a temporary shift of the wind to northeast, and the 13th a depression during the rain in the middle of the day. Clearing weather on the afternoon of the 15th brings a rise of nucleation, which attains an unusual value next day. A quick drop occurs on the 21st when the wind changes to east, and the opposite effect appears on the 26th. Another curious midday minimum may be noticed on the 28th. Throughout the month the minima are very quickly established by clear weather and northwest wind.

In March the maxima are less pronounced; they occur on the 1st to 3d, 11th, 13th to 16th, and 26th. Minima of longer duration than heretofore accompany the rains of 7th to 10th, 19th to 21st, 23d to 25th, and 29th to 31st. One may note the midday minima on the 1st, 2d, and 3d. The 4th shows a reversal of the usual agreement between the wind and nucleation. On the 7th the readings fall during the day as rain sets in. The wind on the 13th, 14th, and 15th changes suddenly, near noon, from northeast to southwest, but no definite corresponding change appears in the nucleation. A fine cloud effect is shown on the 16th when the sky becomes overcast in the afternoon. On the 23d one may note a minimum, as the wind passes through the east to south.

The variations in the nucleation in April are even less marked; low maxima occur on the 1st, 3d, 7th, and 14th to 16th, while minima accompany rain and fog on the 4th to 6th, and 10th to 14th. An unusually low value is obtained on the 2d, with clear northwest wind, and on the 7th is an unaccountable high reading which seems to have no connection with local influences. From the 16th the weather is warm, with considerable fog, and the nucleation runs low, with little variation to the end of the month.

79. Summary and comparisons.—In figures 91 and 92 are shown together the current nucleations (continuous heavy black line), sunshine (continuous light black line), vapor pressure (heavy broken line), temperature (light broken line), and general weather conditions for each day. The nucleation and temperature given is the *average* of the observations taken during the day, as is the vapor pressure after March 28th; before that date the vapor pressure is the mean of the regular morning and evening observations at the station. Both the temperature and vapor pressure are laid off positively downward. The sunshine is the total for the day as recorded by the office sunshine recorder.

The graph as a whole shows a rather marked similarity in the nature of the several curves. In many cases of discrepancies the nucleation appears to show the effect of conflicting causes. On November 29, with no sun, the nucleation persists from the fairly high reading of the day before, although the other curves drop. Warm rain and further increase of vapor pressure on the 30th cut it down, and it ascends very slowly during the cloudy days following. A decrease accompanies the rise in temperature and vapor pressure of December 5, which is quickly reversed by the sunshine and northwest wind of the 6th. The nucleation curve remains nearly level, as does that of the water vapor, during the two cloudy days succeeding. The sun-

shine of the 9th and 11th gives maxima which themselves rise with the moisture and temperature curves, while all drop on the 12th. The rise on December 13 seems to accompany the sudden fall in tempera-

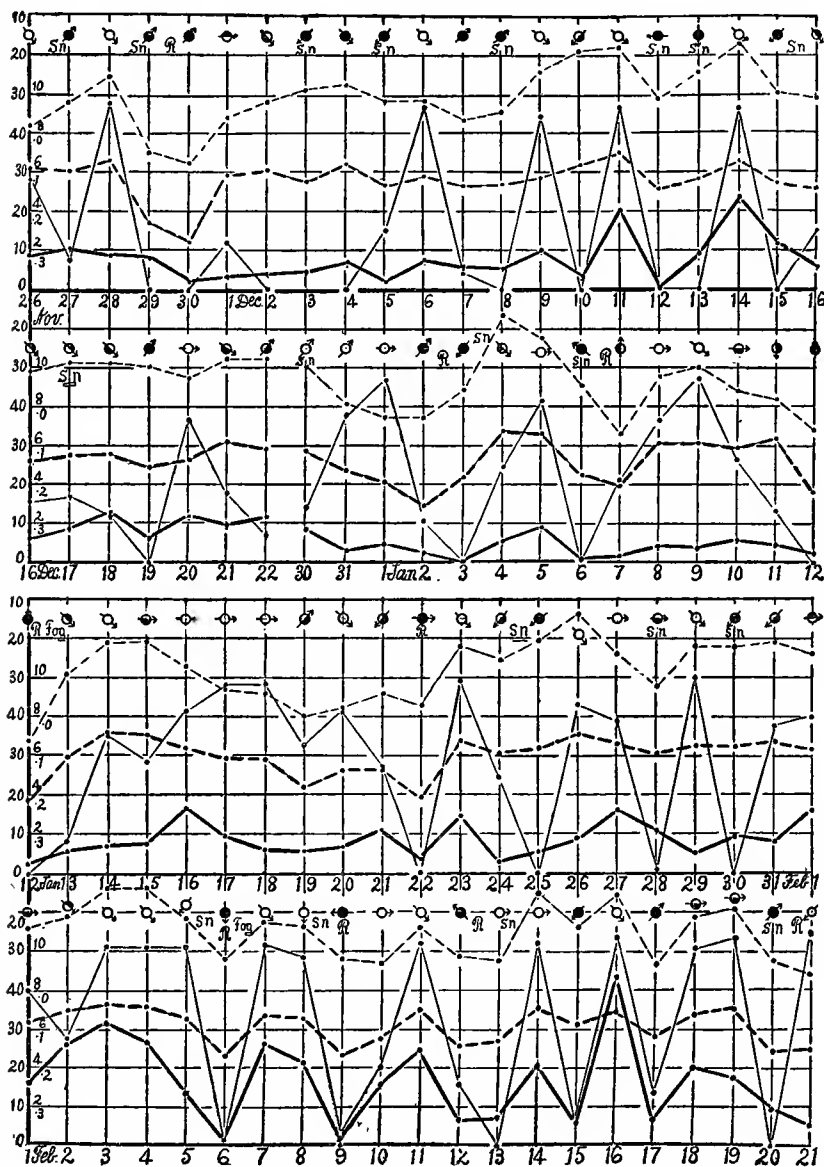


FIG. 91.—Graphs showing current nucleations, etc., November 26 to February 21.

ture and change of wind to north. The maxima of the 18th lags behind the rest, but the readings fall into step next day.

☐ Increase of sunshine on January 1 shows its effect on the nucleation,

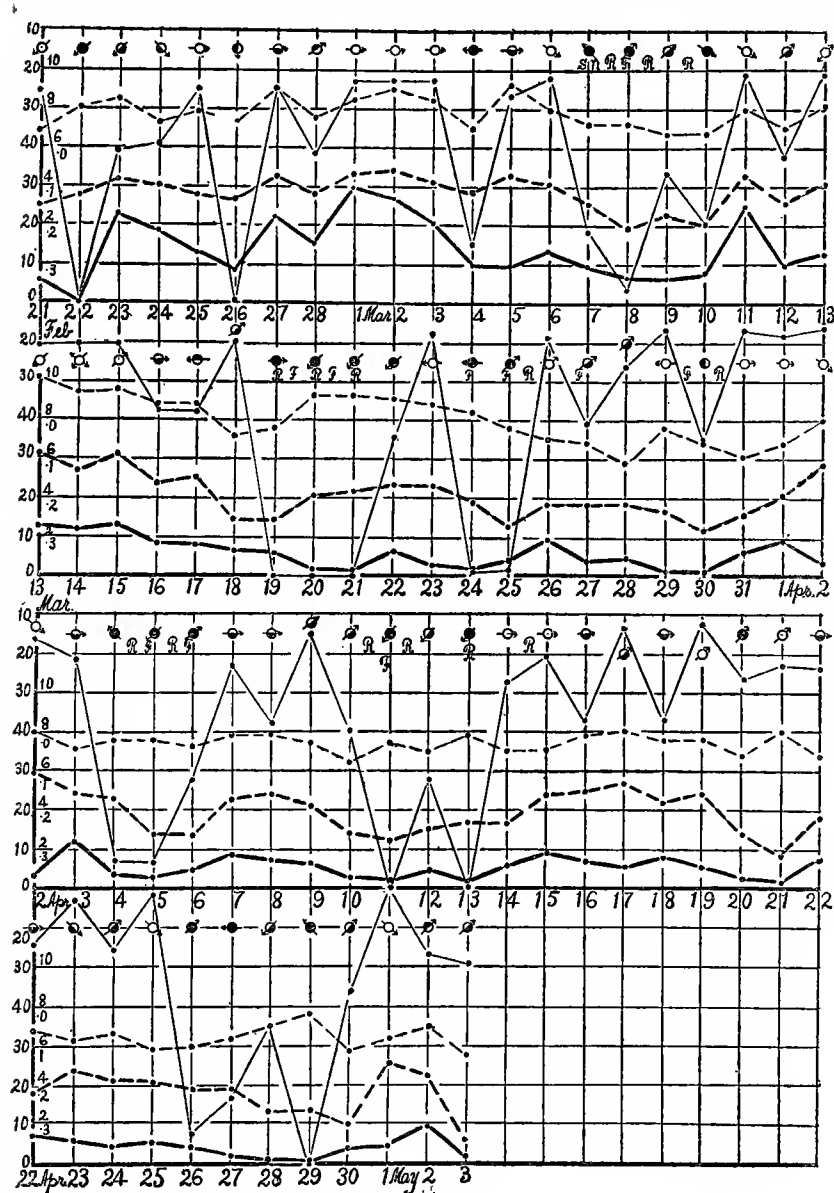


FIG. 92.—Graphs showing current nucleations, etc., February 21 to May 3.

as also on the 5th and 16th. On the 3d the nuclei seem to have been completely wiped out by rain, and we get no more till the sun shines next day. From the 12th to the 16th the nucleation lags behind the other curves in recuperating, and again on the 21st and 27th. As is often the case for low values, the nucleation does not follow the other curves on January 19. During the last days of the month the behavior of the nuclei is quite unusual, although the snow on those days is light and dry.

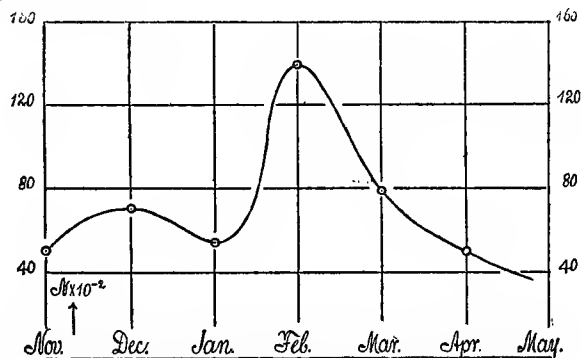


FIG. 93.—Chart showing the average daily nucleations at Block Island, in hundreds per cubic centimeter, from December to May, 1904-5.

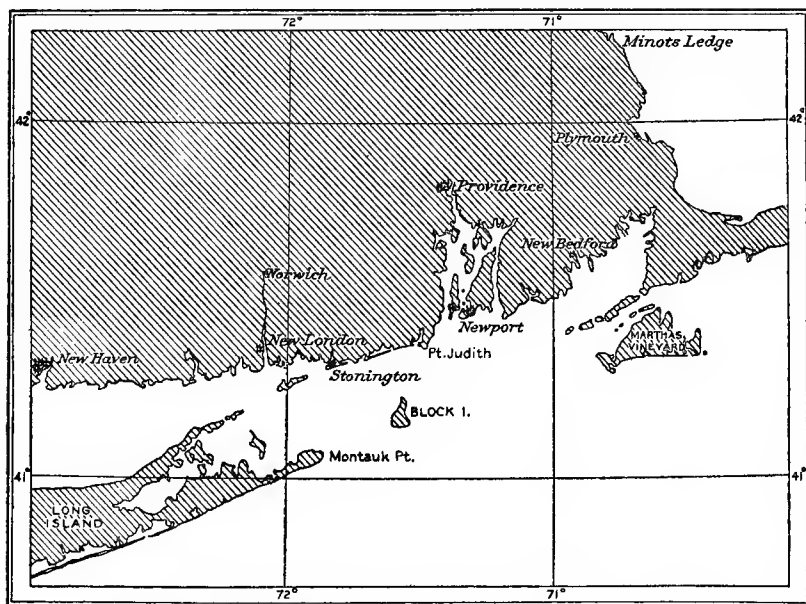


FIG. 94.—Location of the stations at Providence and at Block Island.

The dry, cold weather of February gives a striking series of maxima and minima, with the highest readings of the winter. It is interesting to note the fall in nucleation on the 5th, accompanying rise in temperature and vapor pressure, and east wind, although the sunshine remains the same. Again, on the 13th, following rain in the night, the vapor pressure and nucleation are at their previous value, although there is no sun during that day. On the 20th the nuclei persist through cloud and snow, while on the 22d they disappear entirely with cloudy weather.

The 1st, 2d, and 3d of March, with steady sunshine and wind constantly from the west, show well the agreement between the nucleation and vapor pressure. On the 6th, one notes again the lag of the nucleation in building up, and that the light rain and fog of the succeeding days does not cut down the nucleation entirely. During the rest of March and April there is a considerable amount of water vapor and the temperature runs higher; the nucleation, while it follows the changes in the other curves, remains low, although there is at this period plenty of sunshine. The rains of this time never wash out the nuclei entirely, and readings of several thousand are often obtained in thick fog.

80. Tentative inferences.—Perhaps the most striking result shown by these observations is the variation of the nucleation with change in wind direction. It is very probable that nuclei are brought by the land breeze from towns over which it passes. Our winds from the northeast to southwest, through the east, are pure sea breezes; there is no land in those directions for a great distance, and the readings when such winds occur are usually low. High readings, on the other hand, commonly accompany wind from the other quadrants. Such winds (as seen in fig. 94) pass over towns and cities comparatively near; Newport, R. I., is a little east of north 30 miles distant; the towns on the Connecticut shore lie between northwest and west at distances from 20 miles up; New York, from which one would expect a vast number of nuclei, is a little south of west, distant about 100 miles. When the wind is from this quarter, however, the nucleation is as a rule considerably less than for northwest winds, possibly because the nuclei may not survive so long a journey.

This wind effect, however, must not be overestimated. During the winter months here, clear, cold weather, with small amount of water vapor, occurs quite regularly with northwest winds, and all these conditions usually accompany high nucleation. It is difficult to determine the active factors or their relative influence from a limited series

of observations at one station, particularly as the prevailing winds are land winds. Data from places where the northwest wind blows over no cities, and where the northwest wind is warm and the south-east wind dry, would be interesting.

Again, the daily averages of the nucleation appear to vary inversely with those of the temperature and vapor pressure, while in most cases they all vary directly during the day, rising to a maximum near noon. This would seem to suggest an overbalancing effect of the sun in producing nuclei. As regards the relative influence of temperature and vapor pressure, one might look for an increase of nucleation after a sudden fall of temperature, but would hardly expect nuclei to be produced because of continued cold. It seems quite possible, however, that, with a high vapor pressure, there is continual condensation of moisture on the nuclei present, with a persistent tendency to drag them to the earth. The inverse agreement between the nucleation and the relative humidity is even more general, for the latter more often descends to a minimum during the day. The percentage of saturation, moreover, ought to be some index of the condensation taking place, remembering that condensation may be in progress at higher levels when the air at the surface is not saturated, and that, at those planes, small variations of temperature may be producing saturation. The absorption of the sun's rays, if they produce nuclei, would also have some effect, but probably to a less degree.

In the case of sunshine and cloud, likewise, the effect is obscured for sudden changes by variation at the same time in the vapor pressure. The cloud effect is partly the opposite of that attributable to the sun, which has been assumed to produce nuclei throughout the day in the upper atmosphere. Clouds catch these if they come within range, and prevent the formation of others near the surface. Clouds, however, are at the same time apt to be an index of a region denucleated by rain.

The persistence of nuclei is shown in two ways. Readings, usually less than 10,000, are often obtained through several days of cloud, snow, fog, and even light rain. These have either penetrated through the clouds or they have been brought from cities, in which case the land effect here must be small. Persistence, and therefore the supposed cumulative action of the sun, is shown in the day curve, in which the 3 o'clock reading is nearly as high as that at noon, although the sun is then as low as at 9 o'clock. Similarly, the lag of the nucleation in building up after rain, or after a persistent cloud effect, would seem to indicate the cumulative action of the sun.

Taken as a whole, therefore, it seems to me probable that something more than the displacement of a land effect, produced artificially and locally elsewhere, chiefly by combustion, has been observed. In other words, it would be premature to attribute the phenomena as a whole to atmospheric convection.

TABLE 58.—Average daily nucleations of the atmosphere at Block Island, 1904-5.

Date.	$N \times 10^{-3}$.	Date.	$N \times 10^{-3}$.	Date.	$N \times 10^{-3}$.	Date.	$N \times 10^{-3}$.
1904.		1905.		1905.		1905.	
Nov. 21	Jan. 5	8.1	Feb. 14	17.4	Mar. 26	9.1
22	6	.7	15	5.3	27	3.7
23	7	1.5	16	35.5	28	4.5
24	8	3.9	17	5.9	29	1.3
25	9	3.5	18	17.9	30	1.1
26	7.9	10	5.4	19	15.4	31	6.2
27	9.5	11	4.2	20	8.4	Apr. 1	8.8
28	8.6	12	2.1	21	5.5	2	3.0
29	7.3	13	5.2	22	1.8	3	11.8
30	1.8	14	5.8	23	19.4	4	3.4
Dec. 1	2.6	15	6.2	24	16.7	5	2.8
2	3.3	16	15.0	25	13.3	6	4.4
3	3.7	17	8.3	26	7.8	7	16.2
4	5.6	18	5.6	27	19.7	8	7.0
5	1.7	19	5.0	28	14.0	9	6.6
6	6.1	20	6.3	Mar. 1	27.0	10	2.3
7	5.1	21	12.6	2	22.9	11	1.8
8	4.7	22	3.4	3	18.9	12	4.4
9	8.3	23	12.7	4	8.7	13	1.4
10	2.5	24	2.1	5	8.5	14	5.7
11	16.7	25	4.2	6	12.2	15	7.8
12	0.6	26	6.9	7	8.8	16	5.9
13	7.5	27	13.4	8	6.0	17	5.1
14	19.7	28	9.7	9	6.2	18	8.0
15	10.1	29	5.0	10	7.7	19	5.4
16	5.5	30	8.2	11	22.7	20	2.2
17	8.0	31	7.1	12	9.4	21	1.4
18	11.1	Feb. 1	14.5	13	11.8	22	6.3
19	5.8	2	22.9	14	11.4	23	6.1
20	11.5	3	21.9	15	12.3	24	4.5
21	8.9	4	22.0	16	7.9	25	5.6
22	10.1	5	12.0	17	7.8	26	4.3
30	8.4	6	1.2	18	5.9	27	2.2
31	3.7	7	23.4	19	5.7	28	1.4
		8	17.8	20	1.4	29	1.3
1905.		9	1.0	21	1.0	30	4.2
Jan. 1	5.0	10	15.3	22	5.3	May 1	8.6
2	2.6	11	21.9	23	2.8	2	2.1
3	0	12	6.1	24	1.6	3	4.5
4	4.9	13	6.6	25	4.0		

81. Average daily nucleations at Block Island.—The mean variations of the nucleation at Block Island from day to day are given in table 58, and they have been already charted in figures 91 and 92. The

data are constructed for rapid inspection in figure 102, of Chapter V (lower curve). The initial (high) observations marked with a circle were made with the same apparatus in Providence. The curve as a whole shows two well-defined undulations, one extending from December into the beginning of January and the other from this epoch to the beginning of April. After this the data are scattering. Further discussion will be appropriately given in connection with the corresponding data found at Providence and detailed in the next chapter.

82. Average monthly nucleations at Block Island.—Table 59, below, contains the monthly average of the number of nuclei in the atmosphere of Block Island in thousands per cubic centimeter. The data are reproduced in figure 93. The curve contains definite indications of a maximum in December practically coinciding with those found in the two preceding years in Providence, as suggested by the dotted line. After January, however, the enormous increment of nucleation which characterizes the February observations appears. This is the feature of the present results, and the effects continue with general moderations during March and April; for the nucleation of March actually exceeds that of December, while April is not much below January, showing, therefore, that very unusual conditions prevail in the atmosphere.

To interpret this curve, *i. e.*, to discriminate between terrestrial and cosmical interferences with the atmosphere, it will be necessary to compare it with the corresponding monthly distribution of the meteorological constants of the atmosphere. This will be appropriately done in Chapter V, section 5, in connection with the other data there given.

TABLE 59.—Average monthly nucleations at Block Island, 1904-5.

	$N \times 10^{-3}$.
* November, 1904.....	< 7.0
December, 1904.....	7.1
January, 1905.....	5.4
February, 1905.....	13.9
March, 1905.....	7.9
April, 1905.....	5.0
† May, 1905.....	< 5.0

* November 21-30, only. Average datum therefore too high.

† May 1-3, only. Average datum therefore much too high.

CHAPTER V.

THE COTEMPORANEOUS NUCLEATIONS OF THE ATMOSPHERE AT PROVIDENCE AND AT BLOCK ISLAND.

83. Introductory.—In the preceding chapter, Mr. R. Pierce, jr., has given an account of his observations of the nucleation of the atmosphere at Block Island. I purpose in this place to give the corresponding data for Providence. The two stations lie nearly enough together to have about the same general meteorological elements, while the conditions as to nucleation may be totally different. Block Island is surrounded by a body of water the least radius of which, measured from the center of the island, is nearly 20 kilometers. It lies about 70 kilometers from Providence in a direction about 10° west of south. Fully one-half of Block Island fronts the ocean, as is seen in figure 94, Chapter IV. The atmosphere at the former place should be relatively free from pollutions due to the habitation of man, while the reverse is naturally true of the latter. It is unfortunate that in both cases the prevailing winds are land winds, at least from a distance, and in discussing observations it must be borne in mind that the wind bearing is not indiscriminately in all directions. I shall at the same time avail myself of the series of observations, extending over two years, contained in my report* to the Smithsonian Institution, which, with the present series, complete a three years' period.

84. Observations.—These are taken with less frequency than in the former paper (*loc. cit.*), but are otherwise on the same plan. The entries of the table are at once intelligible. The time of day is in hours and tenths of an hour. Weather variations are noted from cloudy (C), partly cloudy (FC) to fair (F). The temperature of the apparatus is given in degrees Centigrade; those of the atmosphere in degrees Fahrenheit. The coronal diameter, is shown under *s*, which is the chord of a radius of 30 cm., when the eye at the goniometer and the source of light are 85 cm. and 250 cm., respectively, from the fog chamber. The number of nuclei per cubic centimeter, given under *n*, has not been corrected for temperature, as the difference for the present purposes is unessential.

*Smithsonian Report, vol. xxxiv, 1905.

112 NUCLEATION OF THE UNCONTAMINATED ATMOSPHERE.

TABLE 60.—Number of nuclei (n) per cubic centimeter in the atmosphere of Providence, R. I., from November 1, 1904, to May 1, 1905.

[Weather: C cloudy, CF partly cloudy, F fair. Coronal colors (r red, b blue, p purple, w white, o orange, y yellow, g green, hr brown) are given from the center outward. An accent denotes an approach to the color (y' yellowish); a perpendicular line, a thin ring of indeterminate color. If ϕ is the angular diameter of the corona measured to the outside of the first red ring, $2 \sin \phi/2 = s/30$.]

Date.	Time.	Weather.	Wind.	Temp. of apparatus.	Temp. of atmosphere.	s.	Corona colors.	n. Number.	Remarks.
1904.	Hour.			°C	°F	cm.			
Nov. 1	9.6	F	W	16.1	50	3.2	w b p	42,000	
	1.0	C	NW	17.1	54	3.1	w h p	38,000	
	4.0	C	N	—	53	3.1	w h p	38,000	
2	9.8	F	N	17.1	43	3.1	w o g	38,000	
	4.2	F	S	19.1	48	3.1	w b p	38,000	
	5.8	F	—	19.1	45	6.4	w r g	86,000	
3	9.4	C	S	18.1	50	6.1	y' c g	75,000	
	11.9	C	S	19.1	53	5.1	w b p	46,000	
	3.1	C	SW	19.1	56	4.8	cor	39,000	
4	10.4	F	N	19.1	55	4.6	w r g	35,000	
	10.8	F	—	20.1	—	5.1	w h p	46,000	
	11.3	F	N	20.1	57	4.7	w o g	37,000	
	12.3	F	—	20.1	57	3.9	cor	21,000	
	4.4	C	NW	20.1	51	3.5	—	15,000	
	6.0	C	—	20.1	47	3.8	—	19,000	
5	10.1	C	N	18.1	44	3.5	cor	15,000	
	1.0	C	N	19.1	45	4.6	w r g	34,800	
	3.2	C	NE	19.1	42	3.8	w r g	19,000	
	6.1	C	—	21.1	38	4.9	w h p	41,700	
6	9.6	C	N	18.1	37	4.3	cor	28,000	
	11.8	F	NW	17.1	43	5.4	wp cor	54,200	
	12.2	F	—	—	44	5.3	w b p	50,500	
	6.0	F	—	17.1	42	4.7	w r g	37,200	
7	9.5	C	W	15.1	36	4.8	g b p	39,500	
	12.0	F	—	16.1	—	4.9	g b p	41,700	
	4.9	F	—	17.1	39	4.8	w r g	39,500	
8	10.5	F	NW	16.1	42	6.6	w o b g	90,000	
	11.6	F	—	17.1	44	5.8	w c g'	64,500	
9	9.5	C	NW	17.1	37	4.9	w h p	41,700	
	11.9	Sn!	—	17.1	36	6.3	y' r g	80,500	
	4.4	C Wet	—	18.1	37	5.5	wp cor	56,200	
	6.0	C	—	18.1	36	5.8	w r g	64,500	
10	9.3	F	NW	17.1	37	6.6	y' o r g	90,000	
	11.7	F	N	18.1	43	4.8	w r g	39,500	
	—	F	S	19.1	43	5.5	wp cor	56,200	
11	10.4	C	—	18.1	38	4.8	g' b p	39,500	
	5.5	F	N	20.1	34	6.2	w r g	76,500	
12	9.9	F	W	18.1	42	6.0	w r p g	70,500	
	9.9	F	W	18.1	47	6.0	w r p g	70,500	
	5.3	F	—	20.1	46	6.0	w r p g	70,500	
13	10.0	R	W	18.1	46	4.8	w b p	39,500	
	12.6	R	NE	18.1	44	3.8	cor	19,000	
	5.8	R!	—	18.1	42	2.8	cor	7,300	Gale!
14	9.4	C	NW	17.1	40	5.0	w b p	43,800	
	12.3	C	NW	16.1	43	5.5	wp cor	56,200	
	4.2	C' S	—	17.1	42	7.0	g' b' p'	120,000	Vapor.
	4.8	—	—	—	—	6.1	w r g	73,300	
15	9.3	F	N	17.1	41	4.8	g' b p	39,500	
	12.7	F	NW	19.1	49	5.3	wp cor	50,500	
	1.2	F	—	20.1	50	6.2	w r g	76,500	
16	3.0	F	NW	19.1	51	4.8	w o b g	39,500	
	6.0	F	—	20.1	44	4.9	g b p	41,700	
17	9.4	F	N	18.1	28	6.3	w r g	30,500	
	1.2	F	N	19.1	32	6.1	w r g	73,300	
	5.0	F	—	19.1	29	4.8	g h p	39,500	
18	9.4	F	N	17.1	25	5.7	w r p g	61,500	
	12.4	F	—	17.1	32	6.0	w r g	70,500	
	6.0	F	—	20.1	32	6.3	w r o g	80,500	
19	9.3	F	NW	—	30	5.8	w r p g	64,500	
	12.5	F	—	19.1	—	5.8	—	—	
						6.0	w r p g	64,500	

TABLE 60.—Number of nuclei (n) per cubic centimeter, etc.—Continued.

Date.	Time.	Weather.	Wind.	Temp. of apparatus.	Temp. of atmosphere.	s .	Corona colors.	n . Number.	Remarks.
1904.	Hour.			°C	°F	cm.			
Nov. 19	3.3	F	NW	20.1	52	5.7	w rp g	61,500	
	5.2	F	21.1	47	5.0	wbr cor	58,700	
	9.8	F	No wind	18.1	46	5.6	w p g	41,700	
	1.3	F	W	18.1	58	4.9	g' b p	34,800	
	5.6	F	18.1	52	4.6	w r g	46,000	
	12.3	F	18.1	52	5.1	w b p	32,400	Haze.
21	9.4	F	W	18.1	52	4.5	w r g	—	About the same.
	12.3	F	NW	19.1	51	—	—	—	
22	9.7	F H	19.1	42	5.7	wp cor	61,500	
	1.1	F	S	20.1	46	5.0	w b p	43,800	
	6.0	F	20.1	42	6.2	w r g	76,500	
23	9.0	F	NW	19.1	45	4.8	g' b p	39,500	
	12.1	F	19.1	52	4.8	w o cor	39,500	
	5.8	F	19.1	44	4.8	g' b p	39,500	
24	9.6	F	N	18.1	42	4.8	g' b p	39,500	Fog.
	12.0	C	N	18.1	43	5.3	wp cor	50,500	
	7.0	F	17.1	41	4.9	w br p	41,700	
	9.6	F	19.1	36	4.6	w o g	34,800	
25	9.8	F	16.1	40	6.7	w o bg	92,500	
	1.6	C	NW	17.1	42	5.8	wp cor	64,500	
	4.7	C	17.1	48	4.6	w r g	34,800	
26	9.6	F	NW	17.1	33	5.6	w rp g'	58,700	
	12.2	F	18.1	37	5.6	w rp g'	58,700	
	5.6	F	19.1	34	5.7	w rp g'	61,500	
27	9.0	F	N	15.1	25	5.6	w rp g'	58,700	
	12.0	C	14.1	32	4.3	w r g	28,000	
28	9.7	F	NW	14.1	24	6.3	w o g	80,500	
	12.0	F	14.1	27	6.4	w y g	85,500	
	5.0	C	15.1	26	5.3	wp cor	50,500	
29	11.3	F	14.1	34	7.0	w o bg	120,000	Vapor.
	11.9	F	SW	14.1	38	5.9	w rp g	68,000	
	12.3	C	14.1	—	5.9	w rp g	68,000	
	3.7	C	16.1	44	5.8	w rp g	64,500	
	5.8	C	16.1	48	6.2	w r o g	76,500	
30	9.3	C	W	18.1	—	6.2	w r o g	76,500	Rain at night.
	12.3	C	SW	19.1	53	4.8	g b p	39,500	
	6.0	C	20.1	46	5.4	wp cor	54,200	
Dec. 1	9.4	C	W	19.1	35	6.4	w o g	83,500	
	3.5	C	19.1	37	5.8	w rp g'	64,500	
2	10.0	C	NW	19.1	34	5.8	w rp g'	64,500	
	1.5	C	NW	19.1	36	5.8	w rp g	64,500	
	3.5	C	N	19.1	33	5.8	w r g	64,500	
	6.0	C	19.1	28	5.8	w r g	64,500	
3	9.3	C	N	18.1	23	5.8	w r g	64,500	
	1.0	C	19.1	27	6.0	w o g	70,500	Snow'.
	3.2	C	N	19.1	27	6.0	w o g	70,500	
	6.3	C	19.1	26	5.3	wp cor	50,500	
4	9.5	F	NW	17.1	25	5.3	wp cor	50,500	Repeated same.
	12.8	C	W	18.1	30	5.6	w p g'	58,700	
	4.3	C	W	19.1	29	5.6	w p g'	58,700	
	6.0	F	19.1	28	4.8	g' b p	39,500	
5	9.2	F	N	18.1	26	6.8	w o g	95,000	
	10.6	F	S	18.1	—	6.4	w o g	83,500	
	12.4	C	18.1	33	4.9	g b p	41,700	
	3.3	C	SW	18.1	32	5.6	w r g	58,700	
	5.0	C	18.1	30	4.8	w' b p	39,500	
6	9.3	F	NW	18.1	30	5.8	w rp g	64,500	Snow at night.
	1.0	F	18.1	35	6.0	w r g	70,500	
7	9.1	F	SW	18.1	23	6.5	w o g	86,500	
	1.6	F	18.1	39	5.0	w b p	43,800	
	4.6	F	W	19.1	37	6.0	w r g	70,500	
	6.0	F	19.1	36	6.3	w o g	80,500	
8	9.5	F	S	18.1	29	4.9	g' b p	41,700	Snow'.
	12.0	C	NE	18.1	31	4.8	w r g	39,500	Do.
	4.1	C	N	19.1	31	4.9	w o g'	41,700	
9	9.6	F	W	17.1	23	6.8	w o bg	95,000	
	12.0	F	W	18.1	25	6.9	w go bg	100,000	
	3.7	F	W	17.1	24	6.8	w r o g	95,000	
	6.0	F	18.1	20	6.8	w r o g	95,000	
10	9.5	C	N	18.1	15	5.8	w rp g	64,500	
	9.8	C	—	—	6.6	w y o g	90,000	
	12.0	C	N	18.1	17	6.8	w' y bg	95,000	

114 NUCLEATION OF THE UNCONTAMINATED ATMOSPHERE.

TABLE 60.—Number of nuclei (n) per cubic centimeter, etc.—Continued.

Date.	Time.	Weather.	Wind.	Temp. of appa- ratus.	Temp. of atmos- phere.	s.	Corona colors.	n . Num- ber.	Remarks.
1904.	<i>Hour.</i>			°C	°F	<i>cm.</i>			
Dec. 10	4.0	C	N	18.1	16	6.8	$g' y' bg$	95,000	Snow'.
11	9.0	N	N	19.1	11	6.8	$g' y' bg$	95,000	
	12.7	NW	NW	21.1	19	6.0	$y' rg$	70,500	
	6.0	22.1	20	6.1	$w rg$	73,300	12
	9.5	C	N	21.1	19	7.1	$w yg$	120,000	
	12.0	C'	NE	—	26	4.8	$w rg$	39,500	
	3.7	Sn!	E	20.1	26	4.9	$w b p$	41,700	13
	9.0	Sn!	N	22.1	21	6.1	$w rg$	73,300	
	12.0	C	NE	22.1	25	5.9	$w cg$	68,000	
	4.0	C	21.1	28	5.1	$w br cor$	46,000	14
	9.2	F	NW	22.1	13	7.1	$gy o bg$	90,000	
	12.5	F	21.1	21	7.0	$gy o bg$	90,000	
	3.5	F	20.1	23	5.8	$w cg$	64,500	15
	5.6	F	21.1	20	6.4	$w og$	83,500	
	9.0	F	N	21.1	14	6.7	$g b p$	92,500	
	12.4	F	20.1	26	7.0	$w oy bg$	100,000	Repeated same.
	3.0	C	—	28	6.7	$w og$	92,500	
	5.4	C	21.1	28	6.1	$w rg$	73,300	
	9.0	C	N	22.1	30	6.7	$g b p$	92,500	16
	5.6	F	22.1	29	6.0	$w cg$	70,500	
	8.7	F	NW	18.1	20	6.9	$w p cor!$	100,000	
	12.1	F	20.1	30	6.2	$w rg$	76,500	17
	3.4	C	S	21.1	30	5.6	$wp cor$	58,700	
	6.4	C	21.1	30	6.3	$w rg$	80,500	
	10.3	C	NW	23.1	31	4.8	$g' b p$	39,500	18
	12.3	F	W	23.1	32	5.0	$w b r$	43,800	
	5.5	C'	23.1	29	5.5	$wp cor$	56,200	
	9.7	C	S	23.1	27	6.3	$w rg$	80,500	19
	12.3	C	23.1	34	5.7	$wp cor$	61,500	
	5.1	C	23.1	40	6.4	$w rg$	83,500	
	9.2	F	NW	22.1	30	6.7	$w yo g'$	92,500	20
	12.7	F	W	23.1	35	6.0	$w cg$	70,500	
	3.7	C	W	23.1	34	6.6	$w og$	90,000	
	8.8	C	W	23.1	31	6.0	$w c g'$	70,500	21
	12.7	F	N	23.1	31	7.0	$w y' g'$	120,000	
	4.0	C'	NW	23.1	28	5.8	$g b p$	64,500	
	5.8	F	23.1	22	5.2	$w cg$	48,200	22
	10.0	C	W	22.1	25	6.6	$g b p$	90,000	
	12.7	C	SW	22.1	32	7.0	$gy o g'$	90,000	
	4.7	C	22.1	31	6.2	$w rg$	76,500	23
	6.0	C	—	31	6.4	$w og$	83,500	
	10.1	C	SW	23.1	40	5.4	$wp g'$	54,200	
	1.0	C	SW	23.1	47	5.5	$wp cor$	56,200	24
	4.7	C	23.1	46	5.5	$wp cor$	56,200	
	6.0	C	23.1	46	5.5	$w dg$	56,200	
	10.0	C	N	25.1	34	4.9	$w o cor$	41,700	25
	12.7	C	24.1	29	4.0	$w br cor$	22,000	
	4.7	C	24.1	25	4.5	$w r cor$	32,400	
	6.0	C	—	—	4.5	$w ro g$	32,400	26
	10.4	F	N	23.1	15	6.3	$w' rg$	80,500	
	12.5	F	23.1	22	5.8	$w cg$	64,500	
	5.2	F	23.1	21	5.5	$wp cor$	56,200	27
	9.6	F	N	22.1	21	6.2	$w rg$	76,500	
	12.0	C	N	22.1	25	5.8	$w cg'$	64,500	
	3.3	C	22.1	28	5.6	$wp g'$	58,700	28
	6.3	C	22.1	29	5.3	$w P cor$	50,500	
	9.7	R	SE	23.1	38	4.8	$w oy cor$	39,500	
	12.6	R	S	22.1	41	4.9	$w B p$	41,700	Foggy. Do. Rain! at night. Fog.
	4.0	R'	N	22.1	42	6.1	$w rg$	73,300	
	6.7	Fog	22.1	39	4.8	$g b p$	39,500	
	10.0	F	E	23.1	39	6.7	$w o bg$	92,500	31
	12.3	F'	W	23.1	47	5.3	$w P cor$	50,500	
	3.5	F'	23.1	42	6.6	$w ro bg$	90,000	
	6.0	F	23.1	34	5.8	$w P g$	64,500	Do.
	11.3	F	S	23.1	43	6.0	$w rg$	70,500	
	12.5	C'	SW	23.1	46	6.1	$w rg$	73,300	
	5.9	F	23.1	44	5.8	$w P g$	64,500	1905. Jan. 1
	9.3	F	NW	25.1	46	5.0	$w o cor$	43,800	
	12.7	F	W	26.1	57	4.6	$w r cor$	34,800	

TABLE 60. Number of nuclei (n) per cubic centimeter, etc.—Continued.

Date.	Time.	Weather.	Wind.	Temp. of apparatus.	Temp. of atmosphere.	s.	Corona colors.	n. Number.	Remarks.
1905.	Hour.			°C	°F	cm.			
Jan. 1	5.6	F	25.1	44	3.9	cor	20,500	
2	9.5	C'	S	26.1	41	5.1	w br b r	46,000	
	12.0	C C'	S	26.1	44	5.8	w c g	64,500	
	5.7	C R'	25.1	44	6.8	w o g	95,000	
3	9.4	C R'	NE	23.1	37	3.5	cor	15,000	
	12.6	C	E	23.1	34	4.0	cor	22,000	
	3.5	C Sn!	22.1	30	3.7	cor	17,500	
	5.8	C Sn!	22.1	26	4.7	w b p	37,200	
4	9.8	C Sn!	N	22.1	17	7.0	y o b g	120,000	
	12.7	F	N	21.1	18	6.9	y o g	100,000	
	3.3	F	21.1	17	6.8	y o r g	95,000	
	6.0	F	21.1	12	6.0	w c g	70,500	
5	10.0	F	W	20.1	14	6.2	w c g	76,500	
	12.8	F	W	20.1	22	6.6	y o g	90,000	
	6.0	F	20.1	18	6.0	w c g	70,500	
6	9.5	C Sn	20.1	14	6.8	y o g	95,000	
	12.7	C	20.1	20	6.0	w c g	70,500	
	5.8	C	20.1	30	6.0	w c g	70,500	
7	9.5	C R!	22.1	49	4.7	w o g	37,200	
	12.6	C	S	22.1	48	5.6	w P cor	58,700	
8	9.7	F	W	18.1	32	5.7	w P cor	61,500	
	1.0	F	W	17.1	34	6.0	w c g	70,500	
	6.0	F	16.1	31	5.3	w P cor	50,500	
9	9.0	F	W	17.1	25	6.2	w c g	76,500	
	11.8	F	NW	17.1	31	5.0	w P cor	43,800	
	4.3	F	SW	17.1	32	6.3	w c g	80,500	
10	10.0	F	W	20.1	37	5.7	w P cor	61,500	
	12.7	F	W	20.1	39	4.3	g' B p	28,000	
	6.0	F	20.1	29	4.9	w B p	41,700	
11	9.1	C	21.1	24	4.7	g' B p	37,200	
	4.3	C	20.1	31	4.7	w' B p	37,200	
	6.0	C	21.1	32	4.6	w' B p	34,800	
12	9.5	C R'	S	22.1	35	5.1	w P cor	46,000	
	12.0	C	22.1	39	6.6	w o g	90,000	
	3.5	C R	N	22.1	40	5.3	w Br cor	50,500	
13	9.0	F	NW	23.1	28	5.3	w Br cor	50,500	
	4.0	F	N	21.1	28	6.8	w o g	95,000	
	6.0	F	21.1	26	5.8	w c g	64,500	
14	10.1	F	N	21.1	19	6.4	w c g	83,500	
	1.3	F	NW	19.1	24	6.7	w o g	92,500	
	4.3	F	W	19.1	20	5.4	w Br cor	54,200	
	6.1	F	20.1	18	5.5	w P g	56,200	
15	10.7	F	W	20.1	18	6.8	w o g	95,000	
	12.7	F	W	20.1	21	6.6	w o g	90,000	
	6.0	F	20.1	22	5.8	w P g	64,500	
16	9.4	F	W	20.1	22	6.4	w o g	83,500	
	5.0	F	19.1	28	6.9	g y o b g	100,000	
17	9.7	F	W	20.1	28	6.0	w c g	70,500	
	1.0	C	19.1	35	6.0	w c g	70,500	
	6.0	C	21.1	36	6.2	w r g	76,500	
18	9.4	C'	W	22.1	33	6.0	w c g	70,500	
	4.2	C	N	21.1	34	4.4	cor	30,000	
	6.0	C	21.1	34	4.4	w r g	30,000	
19	9.3	F	SW	22.1	39	5.3	w Br cor	30,500	
	12.3	F	W	21.1	46	5.7	w P cor	61,500	
	5.0	F	W	21.1	45	6.0	w c g	70,500	
20	9.7	F	W	22.1	41	4.7	g b p	37,200	
	11.2	F	22.1	41	4.8	g b p	39,500	
	6.3	F	22.1	36	5.5	w P cor	56,200	
21	9.7	F	NW	—	31	5.1	w Br cor	46,000	
	1.0	C	21.1	37	5.1	w Br cor	46,000	
	6.1	C Sn	22.1	34	5.4	w Br cor	54,200	
22	9.7	C R'	S	22.1	49	5.7	w C	61,500	
	1.0	C	W	—	40	3.8	cor	19,000	
	6.2	C	23.1	38	4.7	w o g	37,200	
23	9.3	F	N	22.1	18	6.9	g b p	100,000	
	12.3	F	NW	20.1	22	5.7	w c g	61,500	
	5.0	F	20.1	21	5.7	w c g	61,500	
24	9.4	F	N	21.1	14	5.7	w c g	61,500	
	1.2	F	NW	20.1	25	4.8	w o r g	39,500	
	5.7	F	20.1	26	4.7	g' B p	37,200	
25	10.3	Sn	20.1	15	5.9	w c g	68,000	

Rain! at night.
Gale.

Fog.

Gale and drift.

116 NUCLEATION OF THE UNCONTAMINATED ATMOSPHERE.

TABLE 60.—Number of nuclei (*n*) per cubic centimeter, etc.—Continued.

Date.	Time.	Weather.	Wind.	Temp. of apparatus.	Temp. of atmosphere.	<i>s</i> .	Corona colors.	<i>n</i> . Number.	Remarks.
1905.	<i>Hour.</i>			°C	°F	<i>cm.</i>			
Jan. 25	12.4	Sn	20.1	15	6.3	w r g	80,500	Blizzard.
	5.7	Sn	19.1	11	7.0	gy o b g	90,000	
26	9.5	F	NW	19.1	10	7.0	g (v) B p	90,000	
	12.7	F	N	18.1	16	6.6	g' B p	100,000	
	6.0	F	20.1	16	5.9	w c g	68,000	
27	9.1	F	NW	20.1	17	7.1	g' o b g	90,000	
	12.2	F	W	20.1	27	6.9	g' o b g	90,000	
	6.4	F	21.1	27	6.5	w r g	86,500	
28	9.7	Sn'	SW	22.1	27	6.6	w c g	90,000	
	11.6	C	22.1	32	6.5	w r g	86,500	
	5.6	C	23.1	24	5.1	w B p	46,000	<i>s</i> = 5.5 close up.
29	9.6	F	NW	22.1	19	6.9	w o r g	100,000	<i>s</i> = 7.7 close up.
	12.7	F	W	22.1	26	4.8	g' B p	39,500	
	6.0	F	—	25	6.1	w c g	73,300	<i>s</i> = 7.3 close up.
30	9.3	C	22.1	21	5.8	w P g'	64,500	<i>s</i> = 6.8 close up.
	3.5	C	21.1	24	6.9	w y b g	100,000	<i>s</i> = 7.7 close up.
	5.0	C	21.1	23	6.4	w r g	83,500	<i>s</i> = 7.3 close up.
31	9.5	F	N	21.1	17	7.1	gy o b g	120,000	<i>s</i> = 7.9 close up.
	12.6	F	21.1	23	7.0	w o g	120,000	<i>s</i> = 7.8 close up.
	3.2	F	20.1	23	5.7	w P cor	61,500	<i>s</i> = 6.6 close up.
Feb. 1	6.1	F	21.1	22	6.9	w y o g'	100,000	<i>s</i> = 7.9 close up.
	9.5	F	NW	20.1	17	6.1	w c g	73,300	<i>s</i> = 7.4 close up.
	12.4	F	—	26	7.2	w y g	120,000	
	6.0	F	20.1	27	6.2	w c g	76,500	<i>s</i> = 7.4 close up.
2	9.4	F	W	21.1	23	4.9	g' B p	41,700	<i>s</i> = 5.8 close up.
	3.5	F	20.1	22	5.8	w P g'	64,500	<i>s</i> = 6.6 close up.
3	9.4	F	W	20.1	10	6.7	y' o b g	92,500	
	12.3	F	20.1	17	6.8	y' o b g	95,000	
	5.7	F	21.1	16	6.8	w o b g	95,000	
4	9.8	F	NW	20.1	10	7.0	g B P	120,000	
	12.9	F	W	19.1	16	7.6	gy o b g	120,000	
	4.0	F	NW	—	18	5.8	w P cor	64,500	
	6.0	F	20.1	17	6.6	g B P	90,000	
5	9.8	F	N	19.1	15	6.7	g B P	92,500	
	10.8	F	—	—	6.9	g B P	100,000	
	12.9	F	W	20.1	25	6.7	w r g	92,500	
	4.8	F	S	20.1	25	5.0	w B P	43,800	
6	9.3	Sn!	NE	21.1	28	4.8	g' B P	39,500	
	12.0	R	E	21.1	32	4.8	g' B P	39,500	
	5.0	R	N	21.1	35	6.6	G B P	90,000	
	6.0	R'	—	—	—	gy o b g	(90,000)	
7	9.2	F	W	22.1	22	6.8	w o g	95,000	
	12.5	F	NW	21.1	23	6.0	w C g	70,500	
	4.3	F	N	21.1	25	6.9	y o b g	100,000	
	6.0	F	21.1	22	5.9	w c g	68,000	
8	9.6	F	N	20.1	21	6.4	v B R O	83,500	
	12.4	F	20.1	30	6.7	g B P	92,500	
	4.9	F	N	21.1	31	6.0	w c g	70,500	
	6.0	F	—	31	6.8	gy o b g	95,000	
9	9.5	Sn!	N	22.1	26	5.5	w P cor	56,200	
	12.5	C	E	21.1	35	3.8	cor	19,000	Small corona for east wind.
	3.7	R	E	20.1	35	4.3	w R g	28,000	
	5.0	R'	NE	20.1	34	4.3	w R g	28,000	
10	9.8	F	W	23.1	37	5.1	w P cor	46,000	
	12.1	F	NW	23.1	41	5.0	g' B P	43,800	
	4.5	F	NW	21.1	34	4.4	w R gr	30,000	
	6.0	F	21.1	31	5.2	w B p	48,200	
11	9.3	F	W	22.1	21	6.4	w r g	85,500	
	12.1	F	W	21.1	25	6.5	w r g	86,500	
	5.1	F	—	24	6.1	w c g	73,300	
12	9.5	C	W	20.1	20	6.7	w r g	92,500	
	12.5	C	W	20.1	23	6.8	w o g	95,000	
	5.0	C Sn	W	21.1	29	5.6	w P cor	58,700	
13	9.4	R'	W	22.1	41	5.6	w P cor	58,700	
	3.8	R'	20.1	29	4.8	w o g	39,500	
	5.0	—	—	25	4.8	w o g	39,500	
14	9.3	F	W	20.1	10	6.8	y o b g	95,000	
	12.4	F	W	20.1	14	6.5	w o g	86,500	
	5.8	F	W	—	17	6.8	y o b g	95,000	
15	9.5	F	W	20.1	20	6.1	w c g	73,300	Haze.

NUCLEATION AT PROVIDENCE.

117

TABLE 60.—Number of nuclei (*n*) per cubic centimeter, etc.—Continued.

Date.	Time.	Weather.	Wind.	Temp. of appa- ratus.	Temp. of atmos- phere.	s.	Corona colors.	n. Num- ber.	Remarks.
1905.	Hour.			°C	°F	cm.			
Feb. 15	5.6	F	NW	20.1	25	5.2	w B P	48,200	
16	11.8	F	NW	19.1	16	6.9	g' B P	100,000	
	3.5	F	NW	20.1	21	6.0	w C g	70,500	
	6.0	F	20.1	19	6.7	w o r g	92,500	
17	9.0	C	SW	20.1	23	6.9	w o g	100,000	
	12.3	C	SW	20.1	36	6.4	w r g	83,500	
	4.3	C	SW	20.1	35	6.4	w r g	83,500	
	6.5	C	20.1	34	5.6	w P cor	58,700	
18	8.9	F	W	22.1	21	6.6	w o g	90,000	
	12.5	F	NW	22.1	23	6.4	w o g	83,500	
	5.9	F	NW	21.1	18	6.0	w r g	70,500	
19	10.3	F	21.1	17	6.7	w o g	92,500	
	12.7	F	W	21.1	21	7.0	w o b g	120,000	
	4.8	F	21.1	24	5.0	g' B P	43,800	
	6.4	F	21.1	23	6.2	w R g	76,500	
20	7.9	C	21.1	34	6.2	w C g	76,500	
	12.3	Sn!	20.1	33	5.6	w P cor	58,700	
	6.0	R'	21.1	36	5.7	—	61,500	
21	9.7	F	N	23.1	41	6.2	w r g	76,500	
	12.2	F	N	23.1	45	6.0	w c g	70,500	
22	9.5	C	NE	23.1	32	4.3	w P cor	28,000	
	12.3	C	NE	23.1	33	4.8	cor	39,500	
	5.8	C	23.1	31	4.3	cor	28,000	
23	9.4	F	NE	22.1	21	7.1	g' o b g	90,000	
	12.0	F	22.1	26	6.9	y o g	100,000	
	5.1	C	NE	23.1	32	5.2	w Br cor	42,200	
24	9.7	C	N	22.1	33	6.8	g B P	95,000	
	12.3	—	—	38	—	—	—	
	4.0	F	NW	23.1	41	5.7	w P g	61,500	
26	9.7	C	23.1	36	6.7	w o g	92,500	
	12.4	C	S	23.1	40	5.0	w br cor	43,800	
	5.5	C	W	23.1	40	4.4	w r cor	30,000	
27	9.4	F	W	23.1	24	6.8	w o g	95,000	
	4.3	F	W	20.1	30	5.8	w P cor	64,500	
28	9.3	F	W	23.1	30	4.9	g' B P	41,700	
	12.7	C	W	21.1	38	6.4	w o g	83,500	
	3.9	F	W	21.1	39	4.8	g' B p	39,500	
	6.1	F	22.1	38	4.7	g' B p	37,200	
Mar. 1	10.1	F	W	21.1	29	6.0	w C g	70,500	
	12.4	F	W	20.1	32	6.0	w c g	70,500	
	9.3	F	21.1	30	5.4	cor	54,200	
2	3.5	F	NW	20.1	22	6.5	w o g	86,500	
	5.0	F	W	20.1	32	5.1	w Br cor	46,000	
	9.7	F	20.1	31	5.4	w P cor	54,200	
3	12.2	F	W	21.1	30	6.8	w o g	95,000	
	6.3	F	W	20.1	35	6.3	w r g	80,500	
4	9.2	C	22.1	36	5.6	w P cor	58,700	
	12.0	C	S	23.1	37	5.9	w r g	68,000	
	5.8	F	W	22.1	43	4.7	w r g	37,200	
	9.7	F	N	22.1	35	5.3	cor	50,500	
5	1.1	F	N	21.1	23	6.2	w o g	76,500	
	7.0	F	S	21.1	29	5.5	w P cor	56,200	
	9.2	F	21.1	28	5.0	w Br cor	43,800	
6	4.3	F	NW	22.1	29	6.8	w o g	95,000	
	6.7	F	N	20.1	35	4.8	cor	39,500	
	9.7	F	20.1	33	5.9	w r g	68,000	
7	1.0	C	S	21.1	31	5.2	w br cor	48,200	
	6.1	C	S	21.1	38	4.7	w B P	37,200	
	9.5	C	21.1	35	4.7	w B P	37,200	
8	3.2	C	N	21.1	39	5.7	w r g	61,500	Fog.
	5.3	C	W	21.1	42	6.4	w r g	83,500	Fog.
	9.5	C	SW	21.1	40	4.7	w B P	37,200	
9	1.4	C	NW	23.1	40	4.7	w B P	37,200	
	5.0	C	23.1	45	4.6	w r g	34,800	
	9.2	C	S	—	40	4.6	w o g	34,800	Rain! at night.
10	5.1	C	N	23.1	40	4.9	w o g	41,700	
	9.3	C	S	23.1	47	4.9	w o g	41,700	
11	1.0	F	W	23.1	31	7.0	w o b g	90,000	
	6.0	F	23.1	35	6.1	w r g	73,300	
	9.8	F	W	23.1	32	4.8	w B P	39,500	
12	4.6	C	23.1	36	5.6	w P cor	58,700	
					41	5.0	g' B P	43,800	

TABLE 60.—Number of nuclei (n) per cubic centimeter, etc.—Continued.

Date.	Time.	Weather.	Wind.	Temp. of appa- ratus.	Temp. of atmos- phere.	s.	Corona colors.	n. Num- ber.	Remarks.
1905.	Hour.			°C	°F	cm.			
Mar. 13	9.5	F	N	22.1	29	5.5	w P cor	56,200	
	12.3	F	W	22.1	34	5.9	w r g	68,000	
	6.3	F	S	22.1	31	6.2	w c g	76,500	
14	9.3	F	N	20.1	31	5.3	cor	50,500	
	12.5	F	N	21.1	38	4.9	wo cor	41,700	
	6.3	F	21.1	32	4.8	wo cor	39,500	
15	9.7	F	NE	22.1	31	6.0	w c g	70,500	
	12.0	F	N	22.1	37	5.6	w P cor	58,700	
	5.8	F	S	22.1	35	5.0	—	43,800	
16	9.7	F	NW	22.1	43	5.7	w P cor	61,500	
	1.0	F	22.1	49	4.8	g' B P	39,500	
	6.0	F	23.1	44	4.6	cor	34,800	
17	9.5	F	NE	23.1	39	5.0	w B P	43,800	
	2.6	F	S	23.1	46	4.7	g' B P	37,200	
	6.2	F	23.1	39	4.5	w r g	32,400	
18	9.6	F	S	23.1	46	4.8	g B P	39,500	
	1.5	F	S	23.1	63	4.8	g B P	39,500	
	6.5	F	23.1	52	4.6	w r g	34,800	
19	9.6	R'	W	22.1	53	4.5	w o g	32,400	
20	9.7	R'	NE	20.1	36	3.8	cor	19,000	
	6.0	C	20.1	34	4.8	w B P	39,500	
21	9.4	C R'	NE	20.1	36	3.5	cor	15,000	
	3.3	R Sn	20.1	34	3.6	cor	16,200	
	6.0	R'	20.1	32	3.7	cor	17,500	
22	9.5	C	N	21.1	35	5.2	w P cor	48,200	
	12.6	C'	N	21.1	41	4.8	w y g	39,500	
	6.0	F	NE	22.1	37	4.8	w y g	39,500	
23	9.4	F	SE	19.1	39	4.8	g B P	39,500	
	1.0	F	S	—	44	4.8	g B P	39,500	
	6.2	F	21.1	38	5.5	w c g	56,200	
24	9.3	C	S	22.1	40	5.4	w P cor	54,200	
	1.3	C	22.1	43	4.8	w r g	39,500	
25	9.5	C	S	23.1	48	4.7	w r g	37,200	
	1.3	C	23.1	53	4.8	w o g	39,500	
26	10.0	F	W	24.1	52	4.8	w B P	39,500	
	1.5	F	W	24.1	60	5.3	w P cor	50,500	
	6.8	F	S	24.1	48	4.6	w r g	34,800	
27	9.5	C	SW	25.1	54	4.9	w o g	41,700	
	3.0	C	W	24.1	58	4.9	w o g	41,700	
	5.5	C	W	24.1	55	4.7	w B P	37,200	
28	9.1	F	W	24.1	56	4.7	g B p	37,200	
	6.4	F	W	24.1	62	5.6	w c g	58,700	
29	8.7	F	NE	23.1	57	4.6	w r g	34,800	
	6.4	F	S	22.1	53	4.6	w r g	34,800	
30	10.3	C'	S	21.1	52	4.0	cor	22,000	
	12.7	F	S	21.1	54	3.7	cor	17,500	
	6.2	F	21.1	—	4.6	—	34,800	
31	9.2	F	W	19.1	57	5.6	w P cor	58,700	
	12.3	F	NW	19.1	64	5.2	w B P	48,200	
Apr. 1	9.5	F	NW	19.1	50	6.2	w o g	76,500	
	4.2	F	W	19.1	50	4.9	w B P	41,700	
	6.4	F	N	19.1	45	4.8	w P cor	39,500	
2	9.5	F	NW	17.1	37	5.3	w P cor	50,500	
	1.5	F	NW	17.1	45	6.5	w o g	86,500	
	6.7	F	17.1	41	5.8	w C r g	64,500	
3	9.3	F	W	16.1	44	6.6	g B P	90,000	
	3.4	F	NW	17.1	57	6.1	w c g	73,300	
	6.0	F	W	17.1	54	4.8	w B —	39,500	
4	9.4	R'	NE	17.1	45	4.7	g B P	37,200	
	2.7	C	S	18.1	49	4.9	w o g	41,700	
	6.3	C	S	19.1	47	4.6	—	34,800	
5	9.1	C	N	20.1	46	6.0	w c g	70,500	
	3.3	R	20.1	47	3.8	cor	19,000	
	5.5	R	NE	21.1	46	3.8	cor	19,000	
6	9.0	C	S	22.1	49	4.6	w o g	34,800	
	12.8	R	SW	22.1	52	4.6	w o g	34,800	
	6.4	F	—	47	4.7	g B P	37,200	
7	9.3	F	N	20.1	44	4.8	g B P	39,500	
	3.0	F	NW	19.1	51	4.7	w B P	37,200	
	6.1	F	—	47	4.8	w r g	39,500	
8	9.0	F	W	18.1	41	5.0	w B P	43,800	
	1.5	F	18.1	50	5.0	cor	43,800	

Fog.

TABLE 60.—Number of nuclei (n) per cubic centimeter, etc.—Continued.

Date.	Time.	Weather.	Wind.	Temp. of appa- ratus.	Temp. of atmos. phere.	s.	Corona colors.	n. Num- ber.	Remarks.
1905.	Hour.			°C	°F	cm.			
Apr. 8	6.0	F	NW	18.1	43	4.4	cor	30,000	
9	9.7	F	W	20.1	48	6.2	w o g	76,500	
	12.1	F	W	21.1	56	4.7	w r g	37,200	
	5.6	F	W	21.1	56	4.6	w r g	34,800	
10	9.0	F	SW	20.1	56	5.5	w P cor	56,200	
	12.5	F	—	65	4.9	cor	41,700	
	6.5	F	—	—	4.7	cor	37,200	
11	9.3	R!	NE	23.1	49	3.5	cor	15,000	
	12.3	R	N	22.1	49	3.6	cor	16,200	
	5.7	R'	NE	23.1	45	3.4	cor	13,800	
12	9.6	C	N	19.1	49	4.8	cor	39,500	
	3.4	F	N	22.1	58	4.9	w B P	41,700	
	6.2	F	S	22.1	52	4.8	w r g	39,500	
13	9.4	C	NE	21.1	51	4.1	cor	24,000	
	12.7	C	21.1	55	4.3	cor	28,000	
	6.5	C	—	—	3.6	cor	16,200	
14	9.4	F	W	20.1	50	6.1	w c g	73,300	
	12.4	F	20.1	58	5.8	wp cor	64,500	
	6.3	F	S	20.1	52	4.6	wrg	34,800	
15	9.5	F	N	18.1	48	6.4	w r g	83,500	
	1.5	F	NW	19.1	54	4.8	w r g	39,500	
	6.2	F	NW	20.1	51	4.7	w r g	37,200	
16	10.3	C'	NW	19.1	49	4.8	w B P	39,500	
	1.1	C	W	19.1	52	3.8	cor	19,000	
	6.5	C	20.1	42	3.8	cor	19,000	
17	9.7	C	W	17.1	41	5.6	wp cor	58,700	
	12.4	C	—	48	6.2	wp cor	76,500	
	6.3	F	17.1	42	5.1	w B P	46,000	
18	10.4	C'	19.1	48	5.0	w B P	43,800	
	1.0	C	20.1	49	4.9	G B P	41,700	
	6.0	C'	20.1	43	4.7	w r g	37,200	
24	3.8	F	S	20.1	58	5.9	w c g	68,000	
	6.3	F	SW	19.1	53	4.9	g B P	41,700	
25	9.7	F	NW	18.1	52	4.9	w o cor	41,700	
	12.8	F	19.1	60	4.9	w o cor	41,700	
	6.0	F	W	19.1	62	4.8	cor	39,500	
26	9.0	C'	SW	20.1	62	5.4	w P cor	54,200	
	4.5	R'	21.1	69	4.8	g B P	39,500	
27	9.6	C	NE	21.1	57	3.5	cor	15,000	
	6.1	C'	20.1	58	3.5	cor	15,000	
28	9.5	C	NE	20.1	51	3.2	cor	11,300	
	12.4	C'	20.1	57	3.0	cor	9,300	
	6.2	F	E	20.1	59	3.5	cor	15,000	
29	9.5	C	E	18.1	50	3.3	cor	12,500	
	12.5	C'	S	19.1	60	5.2	w B cor	48,200	
	3.7	—	20.1	—	4.0	—	22,000	
30	10.0	F	W	19.1	65	4.4	cor	30,000	
	12.7	F	S	19.1	67	4.4	cor	30,000	
	6.6	C'	NW	20.1	64	3.7	cor	17,500	
May 1	9.4	F	NW	18.1	52	4.8	wocor	39,500	
	6.5	F	18.1	—	4.0	cor	22,000	
2	9.7	F	NW	18.1	51	5.5	w c g	56,200	
	4.0	F	W	19.1	62	5.6	wp cor	58,700	
3	9.5	C'	W	19.1	66	5.6	w P cor	58,700	
	3.8	F	21.1	74	5.5	w P cor	56,200	
	6.0	F	SW	21.1	70	4.9	w B P	41,700	

All data are given in the upper curves of figures 95 to 101, the abscissas showing the current times, the ordinates the nucleations, in thousands per cubic centimeter. The usual symbols of wind and weather are inserted, R denoting rain, R' rainish, Sn snow, etc. The lower curves have already been referred to and are the cotemporaneous data found by Mr. Pierce at Block Island.

85. Comparison of the data for Providence and for Block Island.—A discussion of the details of the type of results obtained for Providence has already been given in the Smithsonian report (*loc. cit.*), and the new data add no essential novelty. It will suffice, therefore, to compare the two classes of curves throughout their extent.

Figures 95 to 101 show the daily record of the nucleations of Providence (upper curve) and of Block Island (lower curve) in thousands

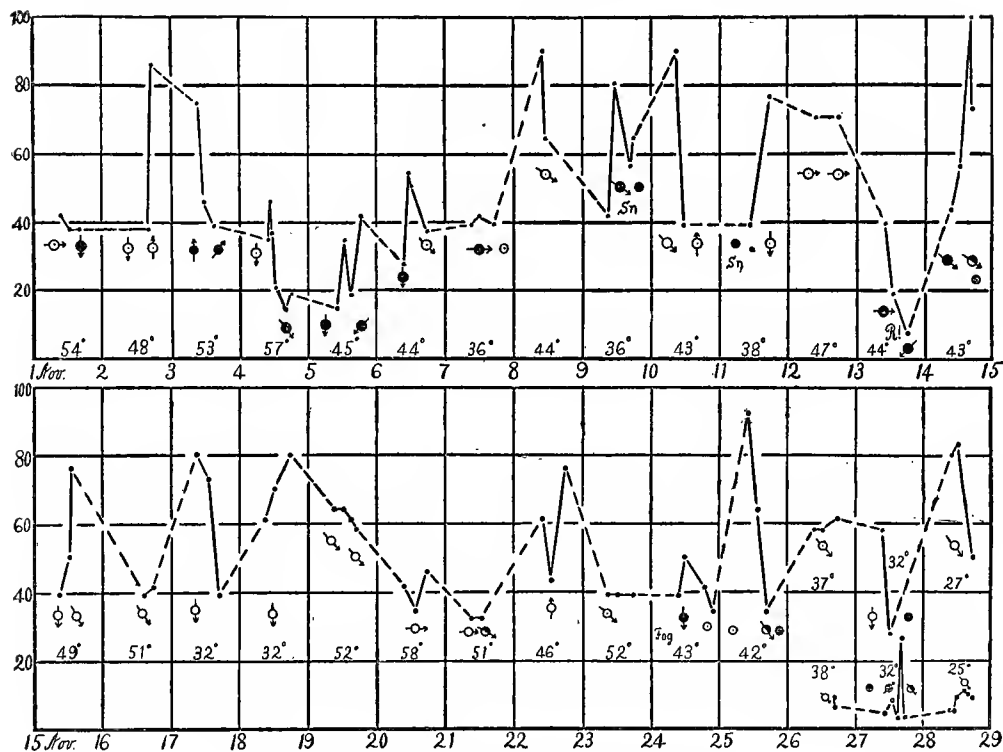


FIG. 95.—Showing daily record for November 1 to 29.

of nuclei per cubic centimeter for the dates given by the abscissas, *i. e.*, from November, 1904, to May, 1905. The prevailing winds and weather and the temperatures of both places are roughly given on the curves.

In the earlier results, from November, 1904, to January, 1905, there is as yet no striking opportunity for comparison, except that both cases show a general rise of nucleation to the high maximum following December 14 and December 20. It is clear that similarity in the

two cases must be marred by the snow effect, which is necessarily of unequal value in the two cases, the depression being as a rule larger and more striking as the antecedent nucleation is higher. On December 12 the two curves behave similarly, but not so December 3, 8, 13, 18, 21. The remarkable depression of the upper curve on December

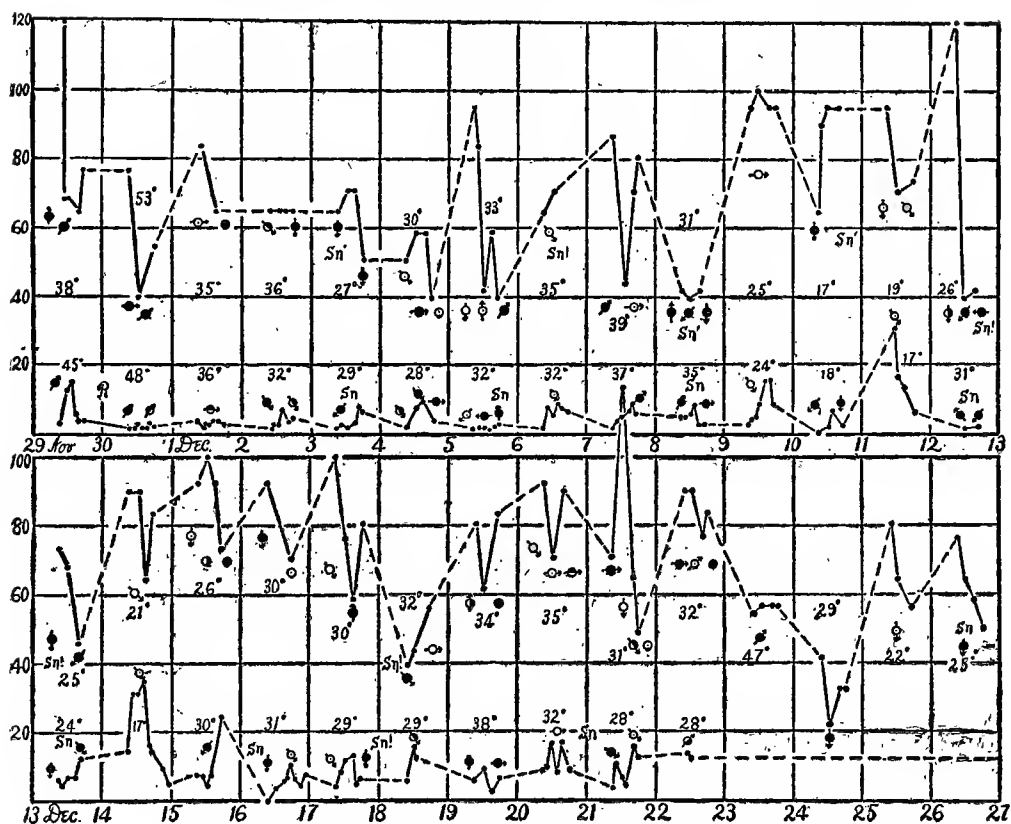


FIG. 96.—Showing daily record for November 29 to December 27.

24 is noteworthy. Some instances of detailed similarity (December 4, 9, 20, etc.) might be pointed out, but in general the curves in their details are dissimilar.

Differences in winds and temperatures, here as elsewhere, are in the main influenced by the times at which observations were severally made. The two sets of results show, as a whole (beginning with November 27), the state of high contamination of the atmosphere of Providence as compared with that of Block Island. Rarely do the

former curves dip down to meet the latter, while the nucleation may be 50 or more times greater. The difference must be due (since it is exaggerated in the winter months) to the originally ionized products of combustion. The two curves give evidence of a rapid self-purification (probably due to dilution) of the atmosphere, from which it follows that the nuclei observed in Providence are to a large extent generated

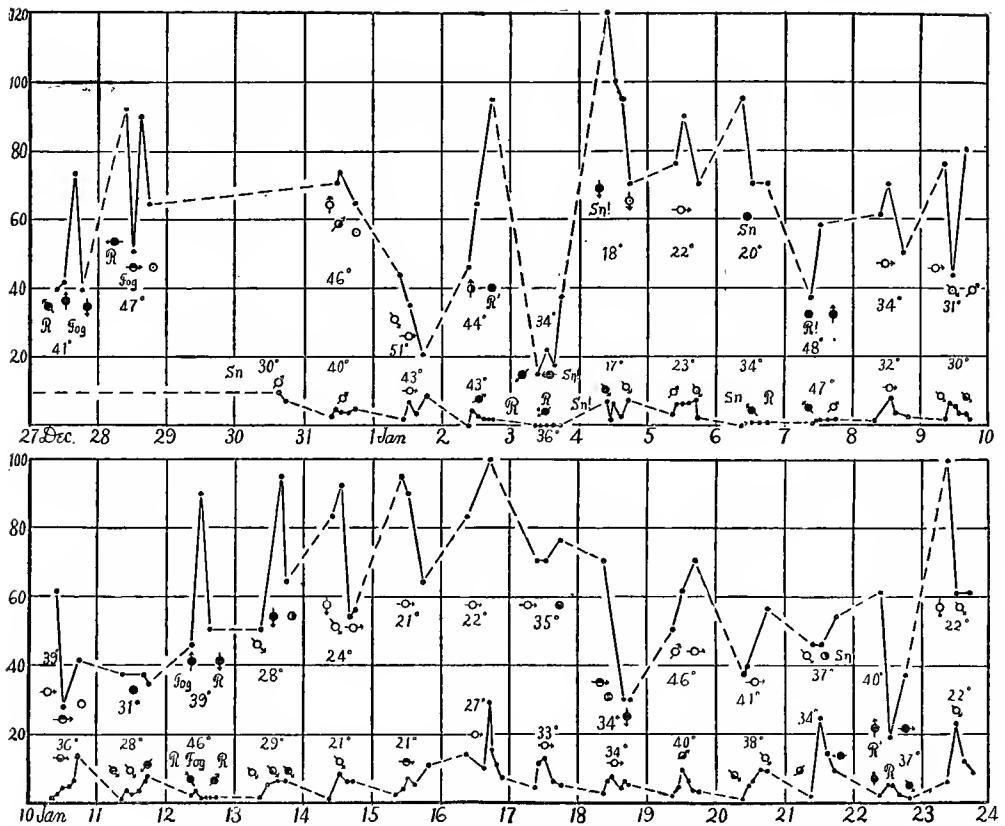


FIG. 97.—Showing daily record for December 27 to January 24.

there. It would be hazardous to assume, however, that all the nuclei are artificially generated, and Mr. Pierce is of the opinion that there is an outstanding nucleation in the Block Island results which can not in this manner be explained away.

The early part of January is subject to rains, and the sustained maximum at Providence following January 4 is but obscurely represented at Block Island. On the other hand, the maximum following

January 13 is fairly well reproduced at Block Island and coincident high values on January 16 are probably not due to chance. The same may be said of January 23.

Toward the end of February the pronounced maximum in the Block Island results (February 23-26) is in keeping with the Providence data. The sustained high wave of nucleation at Block Island from

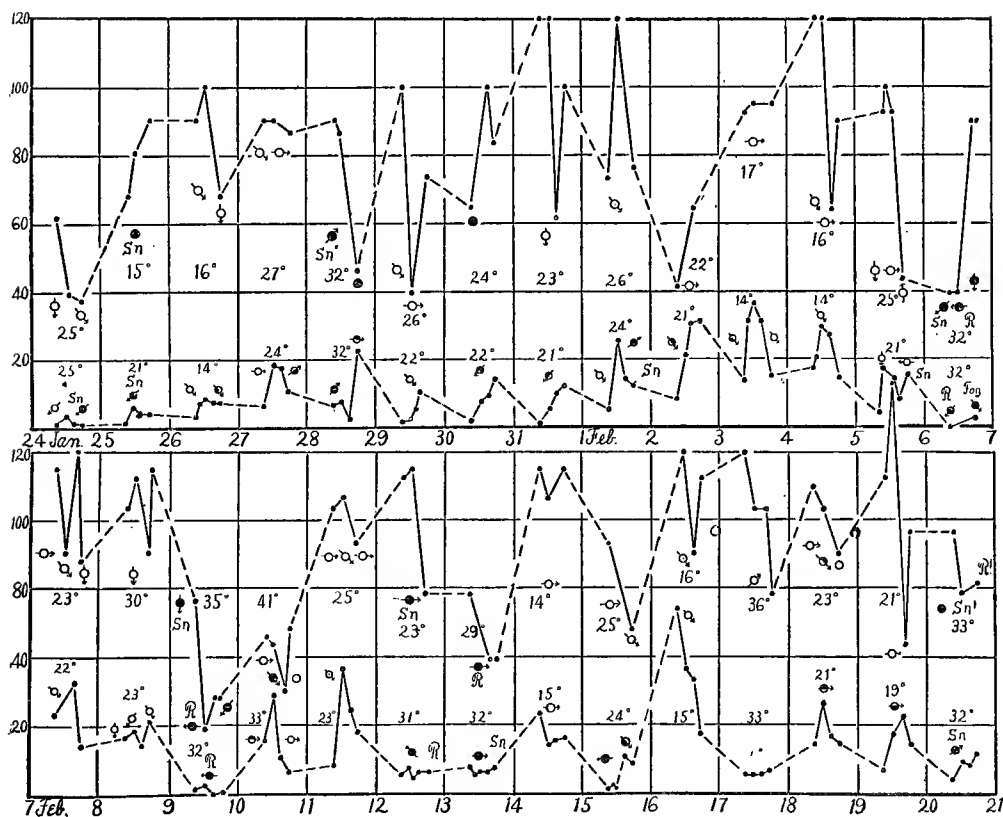


FIG. 98.—Showing daily record for January 24 to February 21.

February 26 to March 4 does not correspond to an equally sustained case at Providence, though the nucleation is at times high. In this region there are instances (not cotemporaneous, however) in which the Block Island nucleation exceeds that of Providence.

Following January 25 the extremely high nucleations which hold general sway up to February 6 are well reproduced by both curves. There are here some striking coincidences, as on February 1, 8, etc.,

with divergences on February 2, 3, etc. The exceptionally high results for Block Island on February 11, 14, 16, 18, penetrate, as it were, into corresponding elevations in the upper curve. In fact, between February 10 and 20 the wave of both places is of the same general type, with the Providence data somewhat behind the other in phase. This is one of the most interesting parts of the results. It may be seen more or less clearly on February 3, 4, 7, 11, 14, 16, 18.

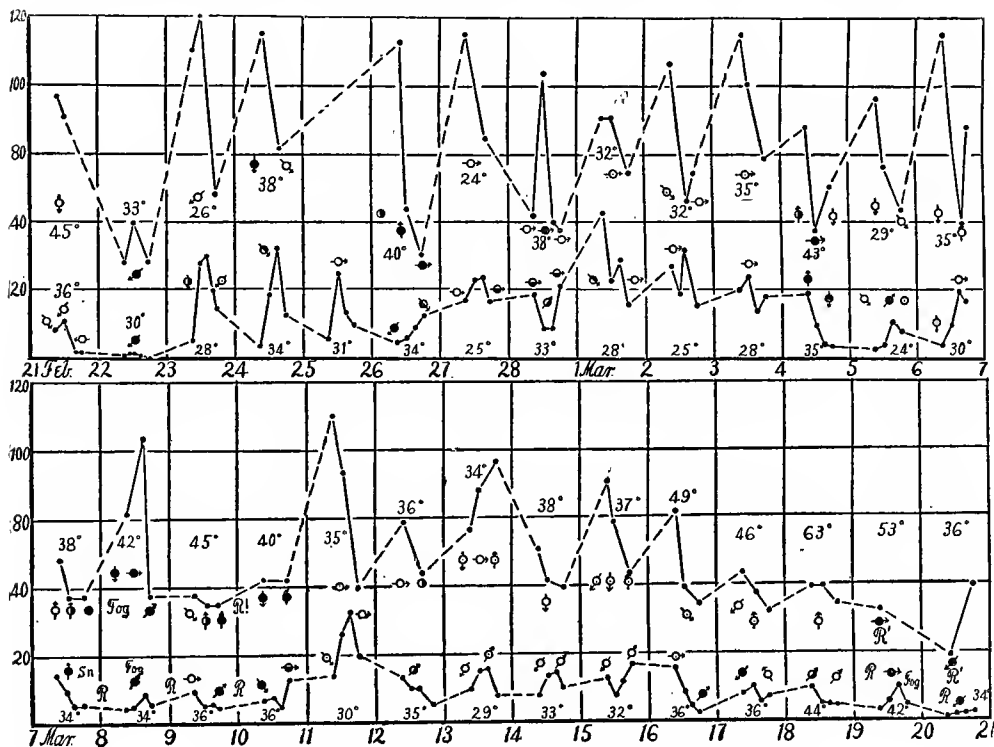


FIG. 99.—Showing daily record for February 21 to March 21.

Late in March (8–20) there is a final attempt at a sustained maximum at Block Island, while the Providence data gradually decrease to the rain on March 20. From March 20 to March 31 both curves are relatively low. March 31 to April 4, April 6 to April 11, April 14 to April 18, show a distinct tendency of both curves to pass through moderate maxima. The remaining data to March 4 are too low for further comparison. As a whole, therefore, little more than a general correspondence can be made out, in which the correspondence of exceptionally high winter nucleation correspond in the data of both stations.

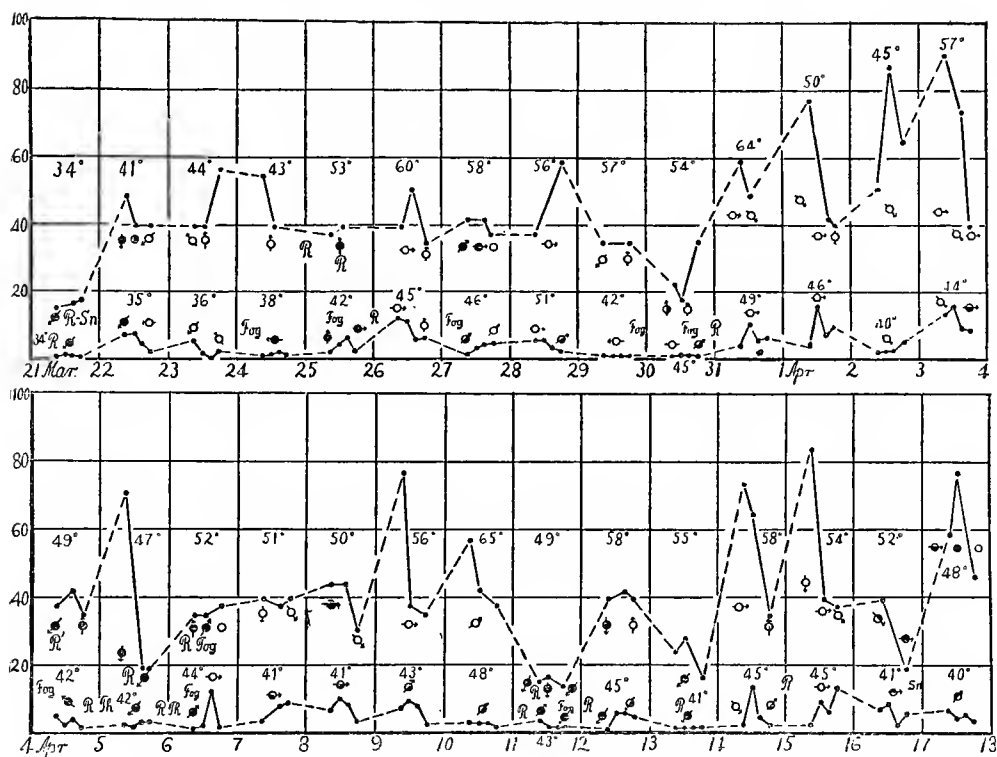


FIG. 100.—Showing daily record for March 21 to April 18.

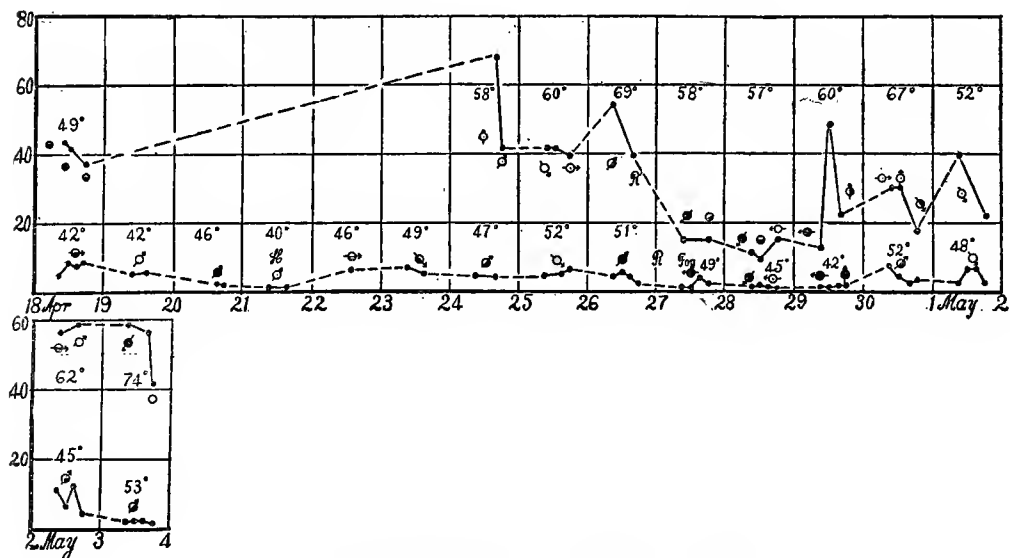


FIG. 101.—Showing daily record for April 18 to May 4.

126 NUCLEATION OF THE UNCONTAMINATED ATMOSPHERE.

TABLE 61.—Average daily nucleations of the atmosphere at Providence, 1904-5.

Date.	Weather.	$N \times 10^{-3}$.	Date.	Weather.	$N \times 10^{-3}$.	Date.	Weather.	$N \times 10^{-3}$.
1904.			1905.			1905.		
Nov. 1	FC	39	Jan. 1	F	33	Mar. 2	F	62
2	F	54	2	CR'	68	3	F	78
3	C	53	3	CR Sn	23	4	CF	52
4	F	29	4	C Sn F	96	5	F	59
5	C	27	5	F	79	6	F	67
6	CF	42	6	C Sn	79	7	FC	41
7	CF	40	7	R	48	8	C	61
8	F	77	8	F	61	9	FC	36
9	Sn	61	9	F	67	10	C	42
10	F	62	10	F	43	11	F	61
11	CF	58	11	C	36	12	FC	51
12	F	71	12	CR	62	13	F	67
13	R	22	13	FC	70	14	F	44
14	CF	73	14	F	95	15	F	58
15	F	55	15	F	83	16	F	44
16	F	41	16	F	92	17	F	38
17	F	64	17	FC	72	18	F	38
18	F	71	18	C	43	19	R'	32
19	F	62	19	F	61	20	R/C	29
20	F	41	20	F	44	21	R Sn	16
21	F	32	21	FC Sn	49	22	C	42
22	F	60	22	C	39	23	F	45
23	F	39	23	F	78	24	C	47
24	CF	42	24	F	46	25	RC	38
25	FC	62	25	Sn	80	26	F	41
26	F	59	26	F	86	27	CF	40
27	FC	43	27	F	89	28	F	48
28	F	71	28	Sn' C	74	29	F	35
29	C	80	29	F	71	30	F	25
30	C	57	30	C	83	31	F	53
Dec. 1	FC	74	31	F	100	Apr. 1	F	52
2	C	64	Feb. 1	F	90	2	F	67
3	C	64	2	F	53	3	F	67
4	FC	52	3	F	93	4	R/C	38
5	FC	63	4	F	98	5	R	36
6	F	67	5	F	82	6	RF	36
7	CF	70	6	Sn' R	65	7	F	39
8	C	41	7	F	84	8	CF	39
9	F	96	8	F	85	9	F	49
10	C	86	9	Sn R	33	10	F	45
11	F	80	10	FC	42	11	R	15
12	Sn	67	11	F	81	12	CF	40
13	Sn	62	12	C Sn	82	13	C	23
14	F	82	13	R	44	14	F	57
15	FC	90	14	F	92	15	F	53
16	CF	81	15	F	61	16	C	26
17	FC Sn	79	16	F	88	17	CF	60
18	CF	43	17	C	81	18	C	41
19	C	75	18	F	81
20	F	84	19	F	83	24	F	55
21	CF	76	20	Sn R	65	25	F	41
22	C	85	21	F	73	26	CR'	47
23	C	56	22	C	32	27	C	15
24	C	32	23	F	79	28	CF	12
25	F	67	24	CF	78	29	C	28
26	C	62	25	30	FC	26
27	R	48	26	C	55	May 1	F	31
28	RF	74	27	F	80	2	F	57
...	28	F	51	3	F	52
31	F	69	Mar. 1	F	65			

86. Average daily nucleations.—These are given in table 61, together with the date and the weather. They are further shown in the chart, figure 102, where the abscissas denote the successive days and the ordinates are the corresponding nucleations in thousands per cubic centimeter. The different points are distinguished by the usual Weather Bureau symbols, ● ○ , r, Sn, etc., so that the weather conditions are included in the curves.

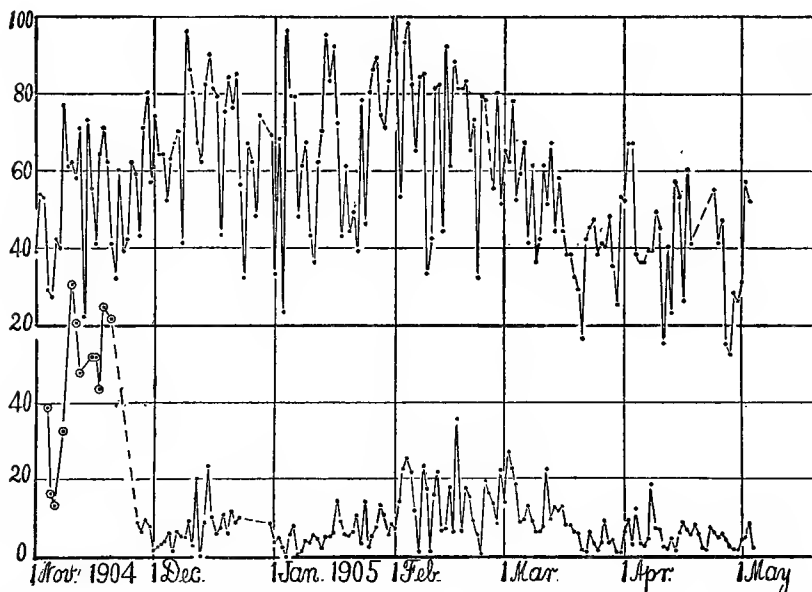


FIG. 102.—Average daily nucleations in thousands per cubic centimeter at Providence (upper curve) and at Block Island (lower curve, excepting the data marked with a circle, which were taken at Providence) for November, 1904, to May, 1905.

This curve is quite distinct from the types obtained in 1902-3 and 1903-4 and shown in my earlier report,* inasmuch as the new curve has an incidental strongly marked maximum in February. Other features, however, appear as in the earlier figures. Thus, there is a definite tendency to reach a maximum in December.

* Smithsonian Contributions, Vol. XXXIV, 1905.

TABLE 62.—Average monthly nucleations.

Month.	Providence.	Block Island.	Ratio.
	$n \times 10^{-3}$.	$n' \times 10^{-3}$.	n/n' .
November.	53.0	<(7.0)
December.	68.6	7.1	9.7
January...	66.1	5.4	12.3
*February..	71.5	13.9	5.1
March....	47.0	7.9	5.9
April.....	40.3	5.0	8.1
May.....	<(5.1)

*The February effect, which is merely superimposed at Providence, becomes fundamental at Block Island. The ratios show that it outlasts March and even April.

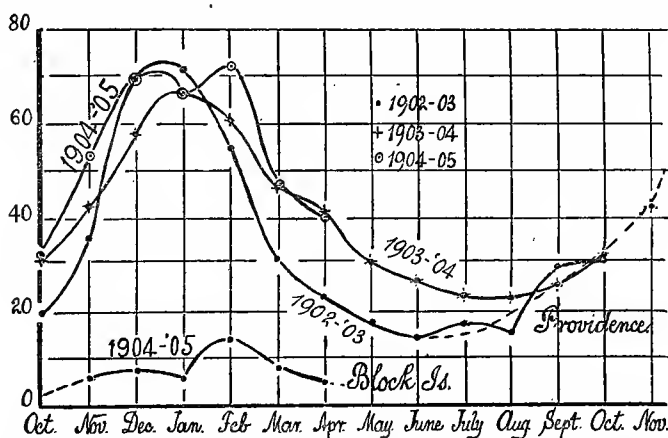


FIG. 103.—Average monthly nucleations at Providence in thousands per cubic centimeter from October, 1902, to May, 1905. The lower curve shows corresponding results taken at Block Island.

87. Average monthly nucleations.—The properties of the new curve just referred to appear more obviously if the monthly averages are drawn in their dependence on time, as is done in table 62 and in figure 103. In the latter the data for 1902-3 and 1903-4 are included, the points of the different curves being suitably distinguished. The tendency to reach a maximum in December appears in all these curves, but the curve for 1904-5 departs from them in its pronounced march toward the duplicate maximum in February, after which, however, there is clear agreement between the 1903-4 and 1904-5 curves, neither of which falls to the low nucleations for March, April, etc., in 1902-3.

The chart, moreover, contains the average monthly nucleations observed by Mr. Pierce at Block Island. It is interesting to note that the general march here is the same as at Providence, a definite tendency toward a maximum in December and then a relatively enormous maximum in February, from which there is slow descent to the summer nucleation which would be nearly vanishing. To accentuate these relations, figure 104 has been drawn, in which the nucleations at Providence and at Block Island are given in ten thousands and in thousands of nuclei per cubic centimeter, respectively. The same February disturbance is thus superimposed on the high local nucleations due to combustion, etc., at Providence, which exists in comparative freedom from local discrepancy at Block Island. It is hard to resist the conclusion that so marked an interference with the usual distribution of nucleation can result from local or terrestrial causes. Thus, the average March nucleation at Block Island exceeds the December nucleation, while the April nucleation is nearly as high as the January nucleation.

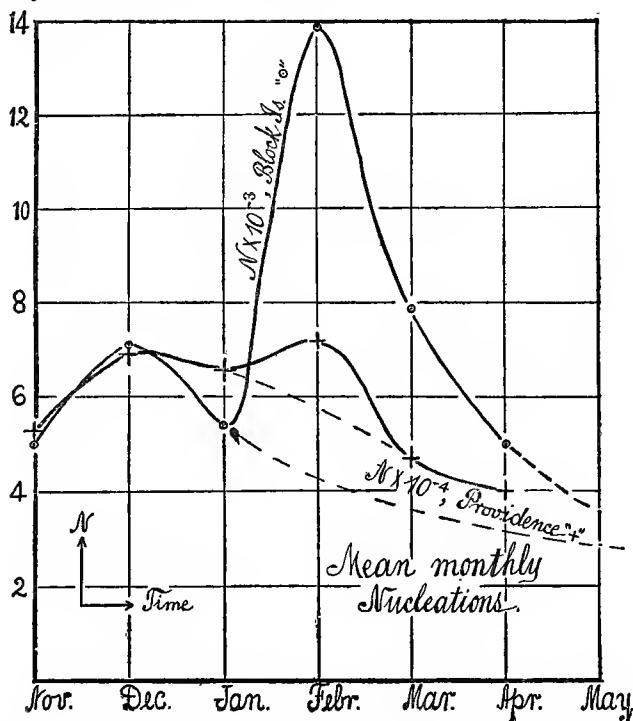


FIG. 104.—Average monthly nucleations from November, 1904, to May, 1905, at Providence in ten thousands per cubic centimeter, and at Block Island in thousands per cubic centimeter, showing the probable run of the curves in the absence of the February maximum and the coincidence of the maxima and the minima.

Mr. Pierce has compiled the following summary of monthly averages of vapor pressure, temperature, barometer, sunshine, rainfall, etc. Of these the data for temperature and precipitation are most important. The latter was, in fact, a minimum (0.05) in February, but differing in value but slightly from November (0.06) and March (0.07). It is not probable that any effect was thus produced. Similarly the temperature is a minimum in February (25°), differing, however, by but 3° from January (28°), while the nucleation is more than doubled (14/5.4). Moreover, the December maximum of nucleation does not exist for temperature. It seems, therefore, equally improbable that for so small a difference of temperature, so enormous differences in general combustion (if this were the cause) could be evoked, and more likely that both the temperature minimum and the nucleation are different effects of some other common cause.

TABLE 63.—Meteorological Data.

Average values of—	1904.		1905.		
	Nov. 26-30.	Dec. 1-22, 30, 31.	January.	February.	March.
Vapor pressure.....	159	128	116	96	166
Temperature.....	38	30	28	25	32
Relative humidity.....	68	76	73	70	81
Sunshine.....	3.3	2.7	6.4	6.8	7.8
Precipitation.....	.06	.09	.08	.05	.07
Range of temperature variation..	13.0	11.4	11.7	12.1	10.8
Wind velocity (hours).....	22.3	22.9	24.2	22.2	15.5
NE. to S.....	.00	.23	.19	.18	.37
SW. to N.....	1.0	.78	.81	.82	.63
Cloudiness.....	.46	.70	.44	.40	.47

There does not, therefore, seem to be in the weather conditions in February any reason for so marked a change in the nucleation. Neither is the temperature low enough nor the rains sufficiently infrequent to account for the accumulation of nucleation observed.

These facts also appear in the ratios in table 62, showing that whereas the Providence nucleation was 10 to 12 times larger in December and January than the Block Island nucleations, the ratios fall off to but 5 in February, from which low datum they slowly recuperate.

88. Conclusion.—While the Block Island observations have therefore proved that much the greater part of the nucleations observed at Providence is of local origin, it has not proved that all of it is of this character. In fact, there remains a residue of 5 to 10 per cent of the

observed nucleation in question, which is still present and undergoing phenomenal variations in places remote from the habitations of man.

Moreover, the arithmetical character of the fluctuation of nucleation in the lapse of time is the same at the two stations, however widely the geometrical character may differ. It is thus probable that in both cases there is superimposed on a local nucleation (large at Providence and vanishing at Block Island), fairly constant for long periods during the winter months, a specific effect, due to causes which are certainly not local. In fact, the same character of variations was observed at the two stations in spite of the fact that the air under examination is necessarily quite different.

The outstanding February maximum may be a distant land effect, due to artificial causes, chiefly combustion, and nearly uniformly distributed over the whole inhabited territory; but from the suddenness of its appearance, its pronounced character, and the extended occurrence as instanced at both stations, one is tempted to regard it as an actual invasion of the atmosphere on the part of some external radiation or nuclei-producing agency.

It would have been better if the pressure difference at the station, where the air is relatively pure had been more nearly equal to the fog limit of dust-free air ($\delta p = 22$), *i. e.*, decidedly above the fog limit for ionized air ($\delta p = 19$); but at the outset it was thought wise to avoid this complication. In such a case the coronas reached by the present method ($\delta p = 17$) would all have been obtained; but in the comparative absence of ordinary nuclei, a response from ionized material might be anticipated. The treatment of filtered air, however, for purposes like the present or the interpretation of the results obtained is an extremely precarious matter, as I shall point out in a subsequent paper. Meanwhile we may note that the curve of average monthly nucleations is apt to show a maximum and minimum, respectively, at about the time of the winter and summer solstices, and that any definite fluctuation from this curve is due to causes which are at least nonlocal in character.

CHAPTER VI.

SUMMARY AND CONCLUSIONS.

89. **Introductory.**—Researches have been made both with respect to the ordinary relatively large or dust-like nuclei contained, *i. e.*, such as will not pass through the cotton filter, and with respect to the nuclei much smaller in size and probably belonging to the molecular system of air, as they are inseparable from it by filtration. Nuclei of the former class are usually (though not necessarily) foreign in character. Those of the latter class may also be so; but as they are demonstrably small, even when compared with the ions, and are speedily reestablished if withdrawn from the air, their true nature may be that of colloidal air molecules. Being present in thousands and millions per cubic centimeter, in proportion as the order of molecular size is approached, they are not to be identified with the ions for this reason alone, as the number of the latter is insignificant in comparison. From what has been stated, colloidal air molecules (nuclei) can not be regarded as stable chemical bodies, since, if precipitated by condensation, they are immediately reproduced in the medium of moist air out of which the precipitation took place. They can not be brought to vanish in long periods of decay. In fact, the coronas of filtered air attain their maximum size after long waiting; for in this way all other larger nuclei which may incidentally be present are brought to vanish.

Hence one must conclude that the nuclei which pass the filter are present in a definite ratio dependent on the conditions of chemical equilibrium of the most general kind.* As a rule, for each such nucleus which decays, another is generated in the nonenergized dust-free air in question, leaving the nuclear status constant.

If we, furthermore, suppose that the formation of a nucleus is accompanied by the expulsion or the absorption of a corpuscle representing the ionization, it is clear that a very high degree of nucleation may be compatible with a very low order of ionization, such as is the case with ordinary dust-free air; for the concomitant ionization represents the degree to which a decaying nucleus is not at once replaced by a newly generated nucleus of the same type, and *vice versa*. In other words, the ionization present represents the oscillation of the system

*Including the effect of internal and possibly external radiations.

around its state of chemical equilibrium, the sense of the departure being in the long run as frequently positive as negative.

These are the chief features of the hypothesis by which I have been guided in my work. It will now be desirable to present an outline of such facts bearing on the whole question as occur in my own researches. To obtain sufficiently varied conditions it will manifestly be necessary to produce nuclei in the condensation chamber (briefly called the fog chamber) itself, without introducing foreign material. This may be done by aid of the X-rays or the beta and gamma rays of radium, preferably to the exclusion of the emanation and even of the alpha rays. Changes of nucleation so obtained may be regarded as arising out of the dust-free contents of the fog chamber.

90. Notation.—The nucleations, N , referred to in these paragraphs, are computed from the angular radius, ϕ , of the corona seen in the fog chamber and the quantity of water precipitated in the given exhaustion, in the way detailed in my report to the Smithsonian Institution (1905). In the figures, which for brevity are referred to in place of the tables, D denotes the distance of the X-ray bulb or the radium tube (of thin aluminum, hermetically sealed) from the near end of the fog chamber. *Exp.* is the time of exposure in minutes to the radiation stated; Lp , the lapse of time after exposure to the radiation ceases, or the time during which the nuclei under observation are left without interference. The abscissas (unless otherwise specified) frequently indicate the number of an observation; *i. e.*, they are merely distributive and represent the character of successive phenomena to the eye. The fog chambers used were sometimes rectangular boxes of wood impregnated with wax and provided with plate-glass windows; at other times clear glass cylinders, 15 cm. long and 15 cm. or more in diameter. The latter case insures greater freedom from traces of leakage, but coronal aperture, 2ϕ , must be measured parallel to the axis of the cylinder. Usually the chord, s , for a radius of 30 cm. will be given, so that $2 \sin \phi = s/30$.

Exhaustions are preferably made at a pressure difference (δp) between the outside and inside of the fog chamber, just below the point (to be called *fog limit* δp_0) at which dust-free nonenergized saturated air condenses without foreign nuclei. δp_0 depends on the particular apparatus used.

91. Fleeting nuclei—Ions.—Let the X-radiation to which the dust-free air is exposed be relatively weak, so that the density of ionization may remain below a certain critical value. The nuclei observed on condensation are then very small, and they require a high order

of exhaustion, approaching but always below the fog limit of non-energized air. They are usually instantaneously generated (within a second) by the radiation, so that their number is definite independent of the time of exposure. They decay in a few seconds after the radiation ceases, *i. e.*, roughly, to one-half their number in 2 seconds to one-fifth in 20 seconds, in the usual way. (*Cf.* Chapter III, figs. 42, 43.) I fancy that these nuclei are what most physicists would call ions; but nevertheless the particles are not of a size, the dimensions depending on the intensity of the penetrating radiation to which they are usually due, and they pass continuously into the persistent nuclei, as shown in the next paragraph, where decay of ionization and of nucleation are very different things. They are abundantly produced by the γ -rays, which, though weak ionizers, become from this point of view strong nucleators (section 16). Finally (section 6) they are stable on solution. The case seems rather to be one in which the rate of decay exceeds the rate of production. The following is an example of data bearing on this case, N being the number of nuclei caught per cubic centimeter of the dust-free air at normal pressure. The anticathode is at a distance from the fog chamber and the exhaustion carried to the verge of the fog limit of dust-free air.

Time of exposure (rays on),.....	0	5	15	30	60	120 secs.
$N \times 10^{-3}$,.....*	1.6	74	74	—	74	—
Time after exposure (rays off),...	0	5	15	30	60	120 secs.
$N \times 10^{-3}$,.....	.92	30	23	18	10	4

The two series refer respectively to generation and to decay.†

If N is expressed in thousands of nuclei per cubic centimeter, and time, t , reckoned in seconds, and if $1/N = a + bt$, so the $dN/dt = -bN^2$, the datum $b = 0.002$ reproduces the results satisfactorily, while a simple exponential law will not do so. The decay is of the kind characterizing mutual action between ions. In figures 42, 44, Chapter III, computed data are distinguished by crosses.

92. Fog limits of fleeting nuclei.—The mean increment of nucleation, δN , per centimeter of increment of pressure difference, δp , varies very rapidly as compared with the fog limit, δp , so long as the reference is to the interval of large variation. It makes no difference by what radiation the nucleation is produced (X-rays or other radiation), $\delta N/\delta(\delta p)$ is rapidly larger as the intensity of ionization is greater, while δp_0 become slowly smaller within the interval in question (Chapter III, figs. 49, 63 to 68). Below the fog limit of air and

* Fog limit of dust-free air just exceeded.

† Including loss by diffusion or other time loss.

slightly above the fog limit of the ionized medium the following data are typical. N_{21} shows the number of nuclei caught when $\delta p = 21$ cm., which lies within the pressure interval stated.

Radium (10,000 ×)	$D = 200$	$\delta p_0 = (20.5)$	$10^{-3} N_{21} = 1$	$10^{-3} \delta N / \delta(\delta p) = 4$
	50	20.4	5	9
	25	20.3	10	(14)
	0	20.1	18	20
X-rays	200	20.3	10	16
	50	(20.1)	22	(24)
	10	(19.7)	45	(33)
	5	19.6	50	36

The full N curves are best given graphically. Data for the radium at $D = 100$ –200 cm. are scarcely distinguishable from air (fig. 68, Chapter III) except near the fog limit; for radium at $D = 10$ –25 cm. they lie close together, above the former and below the data for $D = 0$. With these, the X-ray effects at $D = 10$ –50 are in sequence. Thus there is general continuity between the air curves, the radium curves, and the X-ray curves. As a whole, the curves for D and δp are doubly inflected; relatively large (efficient) nuclei are rapidly fewer in number as δp decreases; relatively small nuclei are also rapidly fewer in number as δp increases. Nevertheless the efficient nuclei of intermediate dimensions are of all sizes, while this size tends to become more uniform as the ionization is greater, *i. e.*, the slopes of the curves become steeper. Gradation is accentuated for the case of weak ionization. The case of nonionized air is shown in figs. 45, 46, Chapter III.

The efficiency here referred to depends not merely on the apparatus (suddenness of exhaustion), but in particular on the degree to which larger nuclei are present, remembering that all the nuclei in question are produced in dust-free air. As the nuclei are essentially graded in size, the larger soon capture all the available moisture to the exclusion of the smaller, and the coronal diameter ceases to increase with δp . The question will be specifically treated elsewhere.

93. Persistent nuclei.—If the X-ray bulb is approached nearer the fog chamber, or if a more efficient bulb is used, so that the density of the ionization within the fog chamber is sufficiently increased, the rate of production of nuclei will eventually exceed the rate of decay. (See figs. 50, 51, 67, 84, Chapter III.) Under these conditions there is not merely an increase of number in the lapse of the time of exposure to the radiation, but essentially an increase of size, *i. e.*, the nuclei grow indefinitely. They are now persistent for hours after the radiation ceases. The number, N , per cubic centimeter increases, therefore, in marked degree and at an accelerated rate with the time of exposure, certainly for 10 minutes or more, barring the invariable loss of efficiency

of the X-ray bulb. These nuclei are large, requiring very little supersaturation for condensation, and are much like any ordinary nuclei. They are pronouncedly of all sizes, and the initial coronas are apt to be distorted and stratified beyond recognition. Whirling rains (section 94) and fog accompany the first condensation. While small nuclei occur throughout the chamber, the end near the bulb is at first the seat of growth, which gradually extends to the other end, as I have shown elsewhere.* The following two series of data, showing the generation and decay of nuclei in question, may be cited as illustrations. The pressure difference, $\delta p = 20$ cm., is much below the fog limit for dust-free air, in the given apparatus.

Time of exposure	0	5	10	20	60	120	180 sec.
$N \times 10^{-3}$	0	2	11	10	80	†(100)	†(500)
Time after exposure..		0	36	85	240 minutes.		
$N \times 10^{-3}$		(100)	36	20	Vanishing.		

Hence there is a decay of one-half in 10 minutes and of one-fifth in 80 minutes, or the degree of persistence is 200 to 300 times larger than in the first paragraph. The data indicate, moreover, that both of these extreme types of nuclei and all intermediate types now occur together, as may be tested by changing the pressure difference, δp , on exhaustion. (Cf. fig. 51, Chapter III, for $\delta p = 25$.) Intermediate rates of generation and decay may be obtained by moving the bulb nearer to or farther from the end of the fog chamber. Finally, the rates at which the nuclei and the ionization severally decay, between which it would be difficult to distinguish in the case of the very fleeting nuclei, stand in sharp contrast with the persistence of the nuclei of the present paragraph.

If N be expressed in thousands of nuclei per cubic centimeter, and time of decay, t , in seconds, the equation $1/N = a + bt$ (for which there is here but little justification) shows that $b = 0.000013$, over 200 times smaller than in section 91. (Cf. fig. 50, Chapter III.)

First exhaustion data of the generation of persistent nuclei are difficult to obtain, because the coronas soon become heavy fogs, distorted beyond recognition, and the fog limits variable over wide limits, often approaching vanishing smallness. The number of persistent nuclei generated varies with the time of exposure at an accelerated rate, as if the nuclei themselves assisted in the generation. (Cf. section 100; also fig. 84, Chapter III.) For instance, at $\delta p = 19.7$ cm., after the times of exposure, 1, 2, 3 minutes, the nucleations were $N = 10^{-3} 22, 77, (120)$, respectively.

* American Journ. Sci., XIX, 175.

† Computed from second exhaustion, after subsidence of the dense fogs of first.

94. Fleeting nuclei become persistent on solution—Origin of rain.—

Let the fog chamber be exposed to radiation for a few seconds and thereafter exhausted ($\delta p = 25$) as usual. Closing the exhaustion cock and allowing only time enough to measure the first corona, let the influx cock be opened and the fog chamber be refilled with dust-free air. The (primary) corona observed is thus dispelled before much subsidence of fog particles can take place, though the rain will naturally drop out. If the fog chamber is now left without interference (the radiation having been cut off immediately after the first exhaustion) for one or more minutes or longer, a second exhaustion to the stated limits will show a large (secondary) corona relatively to the primary corona. In other words, relatively many of the fleeting nuclei or ions caught in the first fog have persisted, whereas without condensation they would have vanished at once after the radiation was cut off. (Cf. figs. 56–59, Chapter III.) The following is an example of data bearing on this point, t denoting the time elapsed from the evaporation of the first corona to the precipitation of the second, N_1 the number of nuclei in the first, and N_2 the number in the second corona:

	Secs.	Secs.	Secs.
$t = \dots\dots\dots$	60	120	300
$N_1 \times 10^{-3} = \dots\dots\dots$	53	27	53
$N_2 \times 10^{-3} = \dots\dots\dots$	16	7	15

The experiments are complicated by the variable X-ray bulb; but it is obvious that while all the nuclei would have vanished in a few seconds without condensation, about one-fourth (in other experiments more) persist indefinitely, if reëvaporated after condensation from fog particles.

This result has an important bearing on the whole phenomenon of condensation and nuclei. Clearly the latter, after the evaporation specified, becomes solutional or water nuclei, in which the original fleeting nucleus or ion behaves as a solute. The decreased vapor pressure due to solution eventually compensates the increased vapor pressure due to curvature, after which, at a definite radius, evaporation ceases and a water nucleus results. Such a nucleus, however small, must be large in comparison with the dissolved ion. Hence, on condensation, the water nuclei will capture the moisture soonest and grow largest. Now, in any exhaustion about one-eighth of the fog particles, *i. e.*, those which are smallest and whose nuclei have been caught at the end of the exhaustion, regularly evaporate into the larger particles to a residue of water nuclei. These are, then, the first to be caught in a succeeding exhaustion. This is the explanation of the *rain* which not only accompanies all coronas in dust-free air, but is

often dense. It is also an explanation of those indefinite alternations of large and small coronas (periodicity).

Further experiments in the wooden fog chamber showed that 25 to 50 per cent of the fleeting nuclei could be caught and made stable on solution. The mean datum of all results, irrespective of the time interval (the effect of which within a few minutes is probably inappreciable), is a preservation of 39 per cent on reëvaporation of the originally fleeting nuclei from the fog particles condensed on them. In the absence of subsidence of fog (which can not here be allowed for), the result would be larger. In the glass fog chamber, which could be made rigorously free from leakage, but in which the subsidence loss was greater, 20 per cent persisted, while all but 2 to 5 per cent were lost in one minute in the absence of solution. Persistence in the 1 to 3 minutes following evaporation was not appreciably different, indicating long periods of decay. (*Cf.* fig. 60, Chapter III.)

95. Solutional enlargement of the nuclei of dust-free air.—The most interesting case observed is the marked decrement of the fog limit of dust-free air producible by solution of the nuclei. (*Cf.* figs. 61, 62, Chapter III.) Let the first exhaustion be made decidedly above the fog limit, $\delta p = 22$ cm. (say here at $\delta p = 23$ cm.), to obtain a corona of appreciable size. On evaporating the fog particle, let the second exhaustion be made decidedly below the fog limit (say at $\delta p = 21$ cm.). A large corona, which would otherwise be quite absent, will be observed. Within 3 minutes about 25 per cent of the nuclei are found to persist. After 10 minutes not more than 50 per cent were left. Whether, without solution, air nuclei are possibly evanescent, and therefore maintained by some penetrating radiation, remains to be seen. It should be recalled that the nuclei in question are small, even as compared with ions.

96. Water nuclei—Solutional nuclei in general.—Apart from the functions suggested in sections 94 and 98, it is clear that the water nucleus must play an important part throughout all phenomena in nucleation. It seems probable that immediately after exhaustion precipitation takes place on all nuclei, large and small, within the scope of the pressure difference applied. The smaller fog particles then at once begin to evaporate until the decrement of vapor pressure, due to increasing concentration of the solution, is equivalent to the increment of vapor pressure due to decreasing size, whereupon evaporation ceases. This is the condition of persistence of a water nucleus, the ultimate size of which depends on the original strength of the solu-

tion partially evaporated. Clearly the water nucleus is always larger than the original nucleus which it holds in solution.

Phenomena of the present kind may be examined by identically agitating solutions of different bodies in different solvents and of different strengths, beginning with the pure solvent. This may be water or any other volatile liquid. The number of nuclei obtained, *cæt. par.*, varies both with the solvent and the solute. Thus on shaking 1 per cent solutions identically and computing the number of nuclei, N , from the coronas observed in each case the following data were found: Pure water, $N=130$; organic bodies dissolved in water (sucrose, glucose, glycerin, urea, etc.), $N=600$; mineral salts dissolved in water (nitrates, chlorides, sulphates, etc.), $N=1,300$; naphthalene dissolved in benzol, $N=3,500$; paraffin in benzol, $N=5,000$. A definite demarcation of groups is thus apparent, but it is difficult to even conjecture an explanation.

If the solvent is pure, the nuclei produced by shaking are excessively fleeting, a result attributable to their relatively small size. As the concentration increases for a given solvent, persistence increases with the number of nuclei produced.

If the absorption per second takes place at the walls of the vessel as the first power of the number of nuclei present, the following constants (k) show the character of the phenomena:

Pure water.....	1	per cent.....	$k=5-10$
Inorganic saline solutions.....	0.01	per cent.....	$k=0.05$
	0.0001	per cent.....	$k=0.08$
		per cent.....	$k=2$
Neutral organic solutes in water,.....	1	per cent.....	$k=0.2$
	0.01	per cent.....	$k=0.6$
Neutral liquid organic solutes in water.....	1	per cent.....	$k=1.2$
	0.01	per cent.....	$k=2.4$
Solid hydrocarbons in liquid hydrocarbons, 1.....		per cent.....	$k=0.02$ to 0.04

When the solvent is a hydrocarbon, etc., the fog particles are relatively large as compared with the water particles (*cæt. par.*). Hence the coronas remain normal (white-centered and showing the usual diffraction pattern) even when the nuclei are present in millions per cubic centimeter. These coronas, moreover, are intensely brilliant, and but for the difficulty in keeping the heavy vapors saturated, they would offer exceptionally good conditions for the measurement of nucleations. Again, the exhaustion method is available for investigating the diffusion of the heavy vapors into nucleated air. Finally, sulphuric-acid nuclei, sulphur and sulphide nuclei (oxidizable to sulphates) are probably a special class of water nuclei which are stable because they contain an intensely hygroscopic solute.

97. Alternations of large and small coronas—Periodic distributions of efficient nuclei in dust-free air.—The coronas in question may be distinguished as superior and inferior coronas. They are obtained in successive exhaustions of dust-free air, under conditions of experiment which are quite identical, filtered air being introduced in the periods between the exhaustions, after all the fog particles have subsided. The efficient nuclei are therefore present in large and small number, alternately, usually in the ratio of about 8 to 1. Figures 14 and 15, Chapter II, give an example of the changes of angular coronal diameter, s , in the successive observations with dust-free air enumerated by the abscissas. The pressure difference is $\delta p = 31$ cm. and the time between the exhaustions 2 minutes. Twenty exhaustions are recorded, but the experiment might have been prolonged indefinitely. In figure 17, Chapter II, there are 3-minute periods between the exhaustions. In figure 18 the periods are 5 minutes in length, but the phenomenon here vanishes. All the graphs show that relatively high inferior coronas (h) are followed by relatively low (l) superior coronas, and low inferior coronas are followed by relatively high superior coronas; furthermore, that coronas of mean aperture are followed by coronas of the same kind, so that the periodicity ceases, as seen in figures 16 and 18 of Chapter II. In figure 16 alternations and steady aperture were obtained under otherwise like conditions. In figure 26 the same phenomenon is exhibited in case of dust-free air energized by weak radium. The ordinates here show the number of nuclei per cubic centimeter, so that the sweep of the alternations is more striking.

An explanation of these phenomena may be given (sections 96, 98) in terms of the occurrence of water nuclei produced by the evaporation of the small fog particles to a size at which solutational decrement of vapor pressure balances the increment due to increased curvature. In figures 14 and 15, Chapter II, the average inferior nucleations of dust-free air are about 12,000, the average superior nucleations over 90,000, so that explanations in terms of negative and positive ions are out of the question.

To precipitate nuclei which, as is usual, are more or less graded in size, in a single exhaustion, must be generally impossible for similar reasons. While temperature after exhaustion approaches its original isothermal value, the small particles caught at the end of the exhaustion to the amount of about 10 per cent of the total number evaporate to the water nuclei stage, to be precipitated in the next exhaustion. This evaporation probably accounts for the permanence of coronas throughout the period of subsidence of fog particles, during the early stages of which temperature rapidly increases.

98. Cause of periodicity.—In cases of large and small coronas, whether the persistence be attributed to electrical potential or to solution, a water nucleus is always in question. Small fog particles are caught on small nuclei near the limit of exhaustion and these evaporate and become the water nuclei available for the next exhaustion. In general, there are three groups of nuclei (x, y, z) concerned in any exhaustion: A group, x , of water nuclei form the preceding exhaustion; a group, z , which will evaporate to make the water nuclei of the succeeding exhaustion; finally, the group y , comprising nuclei adapted to become the efficient nuclei of the exhaustion in question.

In case of periodicity the successive exhaustions follow the scheme—

Exhaustion 1	—	y_1	z_1	Superior corona on y_1
2	$x_2 = z_1$	—	$z_2 = 0$	Inferior corona on z_1
3	$x_3 = z_2 = 0$	$y_2 + y_3$	z_3	Superior corona on $y_2 + y_3$
4	$x_4 = z_3$	—	$z_4 = 0$	Inferior corona on z_3
5	$x_5 = z_4 = 0$	$y_4 + y_5$	z_5	Superior corona on $y_4 + y_5$

All the details observed with alternations are thus explained. In view of the rapidity of decay, the corona will be formed on the saturation value of $y_n + y_{n+1}$.

99. Persistence in general.—This may reasonably be ascribed to the formation of water nuclei, a point of view carried out in my memoir on the structure of the nucleus (Smithsonian Contributions, No. 1373, vol. 29, 1903), but much enhanced by the data of the present investigation. The heavy rains accompanying condensation in case of the persistent X-ray nuclei are attributable to spontaneous condensation without supersaturation, the nucleus acting under intense X-radiation like a hygroscopic solute. The same result may follow the action of ultraviolet light, as it certainly must result from the presence of phosphorus and of sulphuric-acid nuclei.

100. Secondary generation.—This is a curious phenomenon, showing that the decaying persistent nucleus produced by the X-rays is apparently radio-active, or that the walls of the fog chamber are so, or else that the large nuclei, if left without interference, break into a number (on the average about three) of smaller nuclei, whereby the nucleation is actually increased in the lapse of time after exposure. In other words, if the nucleation is observed without cutting off the radiation in one case, and if in the second case the nucleation identically produced is observed at a stated time after the radiation has ceased, the number in the latter case (anomalously enough) is in excess. (Cf. fig. 70-76, Chapter III.) The following examples make this clear, the X-ray bulb being 5 cm. from the fog chamber, and the

exhaustion carried to $\delta p = 20$ cm. These data are computed from the second exhaustions, as the first show the densely stratified fogs unavailable for measurement.

Rays on.....	2	2	2	2	2	2	2	2	2 minutes.
Rays off.....	0	4	0	4	0	2	0	20	0 minutes.
$N \times 10^{-3}$	20	52	20	32	25	30	13	34	30

With the bulb at different distances from the fog chamber, the following data admit of the same interpretation (figs. 74, 76):

Distance, $D =$	5	10	15	5	10	15 cm.
Rays on	2	2	2	2	2	2 minutes.
Rays off	0	0	0	2	2	2 minutes.
$N \times 10^{-3}$	22	3	1	58	9	1

The phenomenon vanishes when the radiation is too weak to produce persistent nuclei, therefore, either when the bulb loses efficiency or when it is too far from the fog chamber.

101. Space surrounding the X-ray tube a plenum of radiations.—While the phosphorescent, photographic, and electric effects of X-radiation decrease rapidly with the distance, D , from the tube, the nucleating effect (N , nuclei generated per cubic centimeter, instantly) is nearly constant over relatively enormous distances.* (Cf. fig. 69, Chapter III.) Thus to give two examples among many ($\delta p = 25$ cm.):

$D =$	6	200	600	6	200	600 cm.
$N \times 10^{-3}$	88	83	83	79	79	79

The laws of inverse squares would predicate a reduction of 10,000 to 1 between these limits; and, in fact, at 6 cm. the phosphorescent screen is intensely luminous, at 200 cm. very dim, at 600 cm. quite dark, as in the case of any ordinary illumination. The leaves of an electroscope within a glass bell jar collapse in a time which is directly as the square of the distance from the energized X-ray bulb. The result obtained with nuclei is astonishing; the nuclei-producing radiation would, at first sight, seem to be of an extremely penetrating kind, akin to the gamma rays of radium, and distinct from the ordinary phosphorescence-producing X-rays. This impression is accentuated by the fact that the radiation can not be stopped by lead screens many centimeters in thickness, placed between bulb and fog chamber. (Cf. figs. 79, 81, 82, 83, Chapter III.) The following are typical examples, in which the distance between the lead plates screening the fog chamber and the X-ray tube is $D = 600$ and 200 cm., respectively. N

* Supposing that the fog chamber is not inclosed in impervious metal. In the latter case, with the lead covering open toward the X-ray bulb only, there is constancy of N within 20 per cent over 61 meters.

shows the number of nuclei instantly generated behind the lead plates in the two cases.

Thickness of lead screen.....	0	0.14	0.28	0.56	0.84	1.12	0 cm.
$D=600$ cm. $N \times 10^{-8}$	67	28	28	31	29	31	76
$D=200$ cm. $N \times 10^{-8}$	79	44	48	41	—	44	70

Again, the X-ray bulb apparently emits this radiation forward as well as rearward, as if the thin anticathode were quite pervious. I found, for instance, for the radiation of the anticathode at 6 meters from the fog chamber—

From the front face (tube directed), $N \times 10^{-8} = 42$
 From the rear face (tube reversed), $N \times 10^{-8} = 35$

or 81 per cent of the former apparently issues from the rear face (fig. 80, Chapter III). Even the reversal of the current does not stop the radiation, for about 16 per cent of the normal intensity is still radiated when the concave mirror is made the anode (fig. 80, Chapter III).

The total efficient radiation may be reduced to a limit by lead screens a few millimeters in thickness, or less; thereafter it can not be further reduced by lead screens many centimeters in thickness. For instance, when the radiation comes from 600 cm., a single lead plate (thickness 0.14 cm.) is more than sufficient to reduce the effective radiation to a minimum, which amounts to (somewhat less than) one-half of the total intensity, at least when estimated in terms, of the number of nuclei produced. (Figs. 81, 83, Chapter III.) If the nucelation comes from 200 cm., one plate has the same effect, even though a thickness of 400 cm. of air has been removed. The thickness, 0.14 cm., is more than enough to reduce the radiation to the limit in question. This again amounts to a little more than one-half the total intensity. (Fig. 82, Chapter III.) At a distance of 5 cm. no more plates may be needed; but the conditions are now too complicated to be described here, chiefly because persistent nuclei are producible. Moreover, 80 per cent of the total intensity may ultimately escape absorption. Thus the rays from different distances behave alike for the more pervious media and in relation to very dense screens. (Fig. 83, Chapter III.)

102. Lead-cased fog chamber.—To interpret these surprising results it will be necessary to surround the fog chamber with a casket of lead, having a lid on the side fronting the X-ray bulb; for even though the lead plates above may efficiently cut off the primary rays, they would leave the secondary radiation free to enter laterally through the broad-sides of the fog chamber. When this was done the results reduced the penetrability of lead to a more reasonable figure, as may be seen

from the following example of results when the distance between bulb and fog chamber was 2 meters :

Thickness of lead penetrated=	0	0.14	0.28	0.42 cm.
$N \times 10^{-8}$	77	10	7	5

i. e., 14, 9, and 7 per cent of the total intensity passes one, two, and three plates, respectively. (Figs. 77, 78, Chapter III.) A glass plate, 7 mm. thick, and an iron plate, 0.5 mm. thick, allowed about 90 per cent to pass ; when the casket was left open, and the lead plate placed near the bulb, 17 per cent of the total radiation was effective, the excess being of secondary origin. The passage through a plate of tinned iron (*cf.* figs. 85, 86, Chapter III) may be observed for a bulb 6 meters distant, as follows :

Thickness of plate....	0	0.05	0.10	0.20 cm.
$N \times 10^{-8}$	36	28	11	7

It follows, then, that in the above examples (101) nearly one-half of the total radiation was derived from secondary sources, since the primary radiation was certainly stopped off to within 10 per cent by the lead plates. To the eye of the fog chamber, therefore, the walls of the room are aglow with radiation, and no matter in what position the bulb may be placed (observationally from 6 cm. to 6 m. between bulb and chamber), the X-illumination, as derived from primary and secondary sources, is constant everywhere. It is to be understood that the X-illumination here referred to may be corpuscular. In fact, so far as I see, the primary and secondary radiation here in question may be identical ; for the corpuscles may come from the circumambient air molecules shattered by the shock of gamma rays.

The fog chamber, if open at the end toward the bulb, shows the same total intensity ; but in such a case the inner walls of the casket, etc., become the source of secondary rays.

The behavior of the wooden fog chamber in relation to rays coming from different distances being such as if the circumambient medium were equally energized with something recalling the character of galvanic polarization throughout, the following mean data are designed to throw further light upon this behavior (fig. 69, Chapter III).

Fog chamber	$D = 6$	50	200	600 cm.
Wood, lead-cased.....	$10^{-8} N = 50$		50	38
Glass, walls 0.3 cm., bottom 1 cm. thick....	{	70	41	22
		55	34	14
Glass, cased in close-fitting lead tube, prolonged 50 cm. toward bulb.....	—	* 52	25	12

Media pervious with difficulty eliminate the secondary radiation entering the broadsides of the fog chamber, and to close the end toward

the bulb is to eliminate nearly all the rays (figs. 77, 78, Chapter III); but if this is open, the number of nuclei instantly generated decreases much more slowly than the first power of distance. The fact that to the very pervious wooden fog chamber the medium within a sphere of at least 6 meters in radius remains almost equally energized throughout remains a result of importance.

103. Possibility of two kinds of radiation from the X-ray tube.—It has been shown that for very short exposures (sections 101 and 102) the nucleation is the same, whether the bulb is placed at 6 cm. or 6 m. from the fog chamber. But only in the former case ($D=6$ cm.) is the effect cumulative; only for very short distances will persistent or very large nuclei appear if the exposure is prolonged several minutes. I have, therefore, suspected that the radiation from the X-ray bulb is twofold in character; that the instantaneous effect (fleeting nuclei) is due to a gamma-like ray, quick moving enough to penetrate several millimeters of iron plate appreciably even for $D=6$ meters; furthermore, that the cumulative effect (persistent nuclei) is due to X-light, properly so called, which produces the usual effects subject to the laws of inverse squares; but it is noteworthy that while the penetration of X-rays is relatively small, and the distance effect negligible (section 101), they are both large for the radiation from radium (section 104).

104. Nucleation due to gamma rays.—To what extent nucleation is producible by gamma rays may be tested by radium inclosed in a thick chamber of lead. The results are strikingly confirmatory. (Figs. 87 to 89, Chapter III). For instance, in case of 10 mg. of radium ($10,000\times$) inclosed in a hermetically sealed aluminum tube and placed outside but close to the end of the fog chamber (bottom nearly 1 cm. thick, walls 0.3 cm. thick), the data were (fig. 89, Chapter III):

Radium in sealed aluminum tube.	$10^{-8}N=27$	Transmission 100
Radium in lead tube 0.5 cm. thick	23	85
Radium in lead tube 1 cm. thick	18	69

The nuclei are thus very largely due to this extremely penetrating radiation. By using lead tubes, capped and not capped, 30 cm. and 60 cm. long, and placed parallel to the fog chamber and in contact with its sides, no evidence of secondary radiation was discernible, the effective radiation passing through the lead walls as specified.

In comparison with the abundant nucleation after the penetration specified, the decrease of nucleation observed when the tube is at different distances, D , from the fog chamber is remarkably large. For example (fig. 90, Chapter III),

$D =$	0	10	30	50	100	200 cm.
$N \times 10^{-8} =$	30	13	8	5	3	2

* Through 0.14 cm. of lead $10^{-8}N=3$; through 0.05 cm. of iron $10^{-8}N=44$.

If measurement be made from the line of sight (10 cm. from the ends of the fog chamber), the nucleation decreases less rapidly than the first power of distance. Hence, whereas the distance effect in case of X-rays is small, it is very large in case of radium. On the other hand, rays from radium show remarkable nucleating power after penetrating many centimeters of lead, whereas the nucleating power of the X-rays after such penetration is relatively negligible. (Figs. 69 and 78, 89 and 90, Chapter III.)

105. Distribution of nucleation within the fog chamber—Radium.— Finally, when the rays have once entered the fog chamber, the nucleation along the axis seems nearly uniform. Measurements are difficult; but while the nucleation decreases nearly to one-fourth when the radium is placed on the outside of the fog chamber, 40 cm. axially from the end, the coronas along 40 cm. within the fog chamber are nearly of the same aperture for any given position of the radium tube.

106. Distribution of nucleation within the fog chamber—X-rays.— Obviously when the X-ray bulb is at a distance from the fog chamber and the nuclei fleeting, they will be uniformly distributed within the chamber, being everywhere at saturation density for the given intensity of radiation.

The conditions are far different, however, when the bulb, as in figure 1, Chapter I, is near the chamber and the nuclei persistent. In such a case, if we distinguish between the A and the B sides of the fog chamber (where A is nearer the bulb), and if we use a pressure difference, δp , decidedly below the fog limit, δp_0 , of dust-free air, the nuclei within the given range of condensation are for short times of exposure found on the A side only. The coronas are relatively small in size, roundish, decreasing in aperture to a vanishing angular radius from the bulb end of the chamber toward the middle. Beyond this, on the right, nuclei are too small to respond to the given pressure difference, δp , and the B side remains clear on exhaustion. As the time of exposure to the X-radiation is increased from 1 to 10 minutes, the nucleation of the A side becomes denser, coarser, and nonuniform in distribution, vertically as well as horizontally, while the efficient nuclei are found in continually increasing numbers, and at greater distances on the B side, until they eventually occur throughout the chamber. The growth of the coronas seen on the first exhaustion after successively increasing times of exposure show a characteristic sequence of types (figs. 2-6, Chapter I), as they pass (when seen through plate-glass apparatus) from roundish to oval, spindle-shaped, gourd-shaped with a long serpentine neck,

and finally wedge-shaped forms, showing, therefore, continued symmetry about the middle horizontal plane or plane of vision, in spite of the whirling rains and densely stratified fogs which accompany the advanced condensations. The design lasts but an instant, for although the nuclei may be suspended in accordance with the given distribution, this is not possible for the heavy fog particles after condensation.

These phenomena bear fundamentally on the origin of persistent nuclei, and these are obviously graded in size, decreasing from the A to the B sides, as well as from the middle plane toward the top and bottom of the fog chamber. With regard to the latter or horizontal symmetry, moreover, the distortion is such that the fog particles must increase in size, from the plane of symmetry down and up.

If the gradation is linear, for instance, with a coefficient, a , so that $d = d_0 - ah$, where d is the diameter of fog particle at a height or a depth, h , from the plane of sight, and s the radius vector from the coronal center to a locus of uniform color, α , the angle of s with the horizontal,

$$s = -(d_0/\sin \alpha) (1 - \sqrt{1 + 2as_0 \sin \alpha/d_0}).$$

These curves are campanulate in outline, passing from closed roundish to open basin-shaped forms, and two examples, a and a' , are shown in figure 7, Chapter I. They all intersect at b and c , and the ends lying outside these lines may obviously here be ignored. As the march from a to a' is one of intensified gradation, the curves eventually becoming flat, it is clear that the horizontal symmetry of figures 2 to 6 is suggested. The latter contain, in addition, the essential gradation from left to right, due to the position of the bulb.

107. Origin of persistent X-ray nuclei.—Admitting that the fog particles are larger from the middle plane toward the top and bottom of the fog chamber, the nuclei must either be large in size toward the top and bottom as well as toward the bulb, or they must be smaller in number. The latter case may be dismissed. It follows, then, that the layers of stagnant, originally dust-free, air within the chamber become more and more rich in relatively large nuclei as they lie nearer the top and bottom and the end. (The corresponding effect toward and from the line of sight will, of course, remain invisible.) These large nuclei capture nearly all the moisture in the parts in question, giving rise to the whirling rains and dense fogs after condensation, whereby the essentially unstable character of this distribution is made manifest.

Hence the case is such as if the persistent nuclei were generated by the impact of the X-rays of sufficient intensity on solid and liquid parts

of the vessel, recalling the way in which similar nuclei are produced by ignition and by high electrical potential, etc. Or one may state that the secondary X-radiation, which plays near the walls of the vessel, is particularly intense near those walls, so that the growth of nuclei in the field of ionized air adjoining is most rapid near those parts. In any case the number of efficient nuclei near the horizontal plane of symmetry is apparently large, because these nuclei are nearly of a size and all are therefore available for condensation. The number of efficient nuclei near the walls is smaller because large and small nuclei are here intermixed, and the former capture nearly all the moisture in those parts. The actual nucleation here must, however, be exceedingly large, and it is because of the relatively great density of the nucleation in question that rapid and pronounced growth of nuclei become possible.

Thus there must be many nuclei which fail of capture in the first exhaustion, and for this reason, finally, the coronas on second (otherwise identical) exhaustion, without fresh nucleation or exposure to the X-rays, are invariably phenomenally large and may correspond to one-third or one-half as many nuclei per cubic centimeter as the first coronas.

108. Order of size of persistent X-ray nuclei.—This may be expressed in terms of the pressure difference needed to produce condensation. Unfortunately the coronas on first exhaustion are apt to be distorted or dense fogs, while as the pressure difference, δp , decreases they become more and more diffuse and equally unsuitable for measurement. I have, therefore, computed the number of particles, N_2 , present on second exhaustion for a given nucleation. These coronas are smaller, but sharp, and the fog particles are condensed on the water nuclei resulting from the first exhaustion. One may estimate roughly that about 10 per cent of the original number of nuclei are condensed in this way. The following is an example of results for 3-minute intervals of exposure to the X-rays (curves 38, 39, Chapter II):

$$N_2 \times 10^{-8} = \begin{matrix} \delta p = 33 & 25 & 17 & 9 & 4 & 17 \\ 15 & 46 & 47 & 28 & 14 & 46 \end{matrix}$$

The passage through a maximum at $\delta p = 16-20$ is capable of a variety of explanations, and therefore of little interest. The important point at issue is the fact that these nuclei require almost no supersaturation for condensation. Filmy coronas are produced by vanishing pressure differences. It follows, then, that these nuclei are about of the size of ordinary dust-like nuclei.

109. Ordinary nuclei.—The persistent nuclei of section 108 were produced by radiation in a medium of damp air, with the specific object of avoiding the introduction of foreign matter into the fog chamber. It is well known, however, that nuclei are producible by any profound method of trituration which may be mechanical, as in the comminution of water by agitation or by the impact of jets. The resources used may be of a more refined physical character like ignition or high electrical potential, or of a chemical character like combustion and the slow oxidation of phosphorus, etc. It is noteworthy that in all these processes not only is ionization present, but that the ionization and the nucleation produced in any definite process are proportional quantities. This important result is demonstrable with phosphorus nuclei by using the condenser and electrometer as usual for the ionization, and the steam jet for the nucleation; or, with water nuclei, by comminuting water by the aid of jets in the fog chamber, determining the nucleation by the coronal method and the ionization by discharging the air laden with water nuclei through a tubular condenser. In both these cases a definite amount of nucleation or ionization is producible, and may be varied under control at pleasure.

The slopes of the lines in the relation between the coulombs per second passing radially in the tubular electrical condenser and the liters per second of air saturated with phosphorus nuclei passing longitudinally through the condenser into the steam tube, differ in different experiments, whereas the colors of the field of the steam tube referred to volumes of charged air per minute are in general agreement; *i. e.*, whereas the nucleation is a fixed quantity, the number of electrons per nucleus varies with the incidentals of the experiment. Inasmuch as the ionization is subject to relatively very rapid decay while the nucleation persists, a result of this kind is to be anticipated; but detailed investigations on the rates at which the ions and the nuclei are severally produced in any given process, and their relations, seem to me to be of great importance, and are now in progress at this laboratory.

110. Ordinary dust-free air an aggregate of nuclei.—The steam jet* shows that nuclei of small relative size, but, nevertheless, large as compared with the molecules of air, must normally be present in dust-free air; for the axial colors may be kept permanent at any stage by fixing the supersaturation. Such nuclei may be called colloidal molecules, even the largest being much smaller than the ions. Moreover, the available nuclei to be reckoned in millions per cubic centimeter increase with enormous rapidity with the supersaturation in

* Cf. Barus: Bulletin U. S. Weather Bureau, No. 12, 1893, Chapter III.

proportion as the molecular dimensions are approached. But even when the yellows of the first order vanish, condensation probably still takes place on the colloidal molecules specified. It is natural to associate these extremely fine nuclei with the existence of a very penetrating radiation, known to be present everywhere. Moreover, the occurrence of many nuclei with but few ions is not contradictory, if the latter are only manifest when the former are made or broken, in the manner suggested above (section 89).

111. The nucleation of filtered air.—If the filtration is moderately slow, and if the pressure difference, δp , continually increases, the angular coronal diameter or its equivalent, s , terminates in a horizontal asymptote, as shown, for instance, in Chapter III, figure 45 *et seq.* Hence the number of efficient nuclei in the exhausted receiver eventually approaches a constant, specific for the given rate of filtration. It is probable, therefore, that extremely small nuclei or colloidal molecules (very small even when compared with ions) pass through the filter; for in such a case more nuclei would enter the fog chamber during the influx of filtered air to replace that removed by exhaustion, in proportion as this exhaustion (δp) is higher. Hence s should be constant in the manner actually observed. The study of the successive groups of nuclei in a scale of decreasing smallness promises to be interesting.

If the current of air through the filter is successively decreased until its velocity all but vanishes, the asymptote in question may be raised enormously until the curve runs upward with a nearly straight sweep. Thus, for extremely slow influx of filtered air to restore the normal pressure after exhaustion, values like the following appear :

$\delta p = 24$	30	33	37	41
$s = \text{rain}$	5.4	5.8	7.2	7.3
$N \times 10^{-8} = 1$	105	143	280	351

data which, from the nature of the work, are inevitably somewhat irregular, but which do not even suggest an asymptote, and from which the character of figure 46 has departed. These nuclei can not come through the filter, for which case $s = \text{const.}$ would be conditional. The fact may also be proved by making observation but once in 24 or 48 hours, in which interval all nuclei originally present would vanish by time loss, unless constantly reestablished as a case of molecular equilibrium, as already suggested. It is possible to filter slowly enough that, *cet. par.*, a specific nucleation may appear for each pressure difference.

Experiments have been in progress in this laboratory since May 9, in which the nucleation of filtered air is examined daily with regard to

its time variation. To guard against errors of interpretation, it was necessary to install two fog chambers side by side, drawing from the same filter and utilizing the same exhaustion system. In spite of the fact that all appurtenances are apparently identical, the two chambers do not show even approximately the same coronas or the same nucleation. Each behaves as if it had its own specific coefficient of radio-activity. Furthermore, the coronas for the same high pressure difference ($\delta p=41.5$) vary in the lapse of time as if some external radiation were involved, though such a conclusion would not as yet be trustworthy. It was shown above that the efficiency of the very penetrating gamma rays in producing nuclei is very marked, but the nuclei here in question are very small in comparison with the cases examined.

112. Nucleation of atmospheric air, not filtered—Dust contents at Providence, R. I.—In the belief that a highly nucleated medium, no matter whence the nuclei may arise, is a medium of special interest, measurements of atmospheric nucleation have been in progress at this laboratory since 1902. Four or more observations were usually made by the coronal method per day, the details of which can not, however, here be instanced.* If the mean of the daily observations be taken, they make up a number of cotemporaneous series, the properties of which are best shown graphically. Apart from details, for which there is no place here, the things noticeable in the curves of successive years are the extremely high winter, as compared with the summer nucleations, the efficiency of rain in depressing the nucleations, and the totally different character of the curves for 1902-3 and 1903-4.

These may be made even clearer by comparing the average monthly nucleations, as are shown by the graphs in figure 103 of Chapter V, in which the ordinates are again the nucleations in thousands per cubic centimeter. (*Cf.* figs. 102, 104.) Here the degree of difference and the similarities of the two curves are strongly brought out. As to the latter, both tend to show sharp maxima near the time of the winter solstice, and flat minima, much subject to rain, at about the time of the summer solstice. It is clear from the enormous difference of nucleation at the maximum and at the minimum that astronomical causes can not be directly involved. The origin of the nucleation must be in large part local, the nuclei themselves being the initially ionized products of combustion. Nucleation is depressed by rain, and possibly also (from the length of the summer day as compared with the winter day) by light pressure.

* *Cf.* Smithsonian Contributions, Vol. XXXIV, 1905.

113. Continued—Dust contents of atmosphere at Providence and at Block Island, R. I., compared.—To interpret the curves in question fully, *i. e.*, to ascertain whether there may not, after all, be a cosmical effect, superimposed on the local effect observed, it is necessary to make a series of observations at a station more remote from the habitations of man. Measurements were therefore made at Block Island, under my direction, by Mr. R. Pierce, jr., simultaneously with my own observations at Providence, by the identical coronal method in question. The stations are sufficiently close together to have nearly the same meteorological elements as to wind and weather, but Block Island lies well out at sea, and is, in the winter at least, nearly free from local effect.

The average daily nucleations for both stations are shown in figure 102, Chapter V, and, as was to be anticipated, those at Providence are much in excess. Leaving these for discussion elsewhere, sufficient may be learned from the average monthly nucleations in the two places, given in figure 104, Chapter V.

In both cases there was an evident tendency in 1904-5 to reproduce the curves of 1902-3 and 1903-4, with the sharp maxima in December, and thereafter a rapid march toward the flat summer minimum. In both cases, however, there is a new effect in February, which, by being superimposed on the local nucleations at Providence, does not appear further than as a determined departure from the curves of the preceding years, but which juts out into striking prominence in the observations at Block Island, where the local effect is relatively negligible. Apart from quantity, the fluctuations of both curves are identical in character.

Finally, as to causes of the usual solstitial maximum and minimum, and of the accessory maximum in February of this year, they may represent the diluted local effects averaged by the sweep of the winds for an enormous extent of territory. But it is quite as reasonable to keep one's mind open to the possibility that the February maximum, at least, may represent an external invasion of the atmosphere on the part of some external nuclei-producing agency.

